AMENDMENTS

CHAPTER 3

Figure 3.5: HA-PRD does also localize in the nucleus, however, this is probably the result passive diffusion as the molecular weight of the recombinant protein is approximately 30 kDa.

Page 113: Expression of the Myc-tagged filamin truncation mutants in yeast was determined by immunoblot of cell lysates using Myc antibodies.

Figure 3.10: Please refer to Figure 3 in the attached Journal of Cell Biology paper for correct alignment of the identifying arrows with the appropriate bands.

CHAPTER 4

Figure 4.1: Discrete co-localization of HA-SHIP-2 and filamin was only observed at the cell membrane although diffuse localization of the two proteins was also observed in the cytosol.

Figure 4.4: The immunoblots presented in this figure are comparable although they are presented in separate panels.

Figure 4.6: The intensity of staining was determined by visual inspection.

CHAPTER 5

Figure 5.1B: In comparison the amount of SHIP-2 antigen immunoblotted in the Triton-soluble of fraction of resting and thrombin-stimulated platelets, only a small proportion of SHIP-2 appears to translocate to the actin cytoskeleton upon platelet activation.

Figure 5.7 and 5.8: The term "patchiness" used to describe areas of co-localization refers to the non-uniform co-localization of the two species.

H2-3451

MONASH UNIVERSITY
THESIS ACCEPTED IN SATISFACTION OF THE
REQUIREMENTS FOR THE DEGREE OF
DOCTOR OF PHILOSOPHY
ON..... 15 April 2003 .....
.....[redacted].....
Sec, Research Graduate School Committee

The SH2-containing inositol polyphosphate 5-phosphatase-2 (SHIP-2) regulates the actin cytoskeleton

Jennifer Maree Dyson B.Sc (Hons)

Department of Biochemistry and Molecular Biology, Monash University, Victoria, Australia.

A thesis submitted for the degree of Doctor of Philosophy, Monash University, December, 2002.

Statement of Originality

The experimental work described in this thesis, was performed by myself, unless otherwise acknowledged, in the Department of Medicine, Box Hill Hospital and Department of Biochemistry and Molecular Biology, Monash University, during the years of 1998-2002, under the supervision of Professor Chrsitina Mitchell.

Jennifer Maree Dyson

Acknowledgments

To my supervisor, Christina Mitchell, I thank you for your guidance, support, enthusiasm and friendship. Your faith in me allowed me to achieve goals I never thought possible. I consider you not only a fantastic supervisor, but also a friend, and look forward to continuing our relationship at a professional and personal level.

To lab members both past and present I thank you all. In particular, to Big Lisa, who introduced me into the world of molecular and cellular biology in Honours, answered all my questions, and participated in helpful discussions. To Raju, a.k.a "Bloody" and "The Guru", your technical assistance was invaluable and your ridiculous jokes made life in the lab more enjoyable. To Adam, who introduced me to platelet isolation and assisted greatly with all things computer-related. To Meagan and Paul, who were a constant source of humour "Price check baby peas" but who were also there to listen and advise through the tougher periods of my PhD. Thanks to Jo, Richie, Ivan, Jelena, Imo, Anne, Fenny and the aforementioned Meagan and Paul who made lunchtime discussions interesting. To Jelena, my partner in crime in the lab who also works on SHIP-2, and to Astle a recent addition, your support is greatly appreciated. To Anne, I thank you for all your help, particularly in the last six months. To Fenny (a.k.a Wiji) thanks for making life at the computer more enjoyable.

To Michael Berndt, I thank you for helpful discussions, although which often resulted in the requirement of more experiments. I am extremely grateful for providing invaluable reagents and expertise.

To Harshal Nandurkar, I thank you (I think) for introducing me to the frustrating Y2H system.

To Susan Brown your advice has been invaluable.

To my family I thank you. In particular, I thank my mum and sister Zoe, who took great interest in my work and progress over the years and who were of great support in latter stressful stages of my PhD.

To my recently wed husband Chris, who has been a tower of strength since day one of my PhD. Thank you for your patience and support, you have certainly made this journey much more enjoyable.

To my close friends, Meags, Tam and Mel (and their partners), I thank you for all your support and encouragement. In particular, Ab and Daz who have shown great interest in my work.

Publications

Publications arising from this thesis:

Dyson, J.M., O'Malley, C.J., Becanovic, J., Munday, A.D., Berndt, M.C., Coghill, I.D., Nandurkar, H.H., Ooms, L.M., and Mitchell, C.A. (2001) The SH2-containing inositol polyphosphate 5-phosphatase, SHIP-2, binds filamin and regulates submembraneous actin. *J Cell Biol*, **155**, 1065-1079.

Dyson, J.M., Munday, A.D., Kong, A.M., Layton, M.J., Nandurkar, H.H., Berndt, M.C., and Mitchell, C.A. (2002) SHIP-2 forms a dynamic tetrameric complex with actin and GPIb-IX-V. Localization of SHIP-2 to the activated platelet actin cytoskeleton. *Blood* (under review).

Other publications:

Mitchell, C.A., Gurung, R., Kong, A.M., **Dyson, J.M.,** Tan, A., and Ooms, L.M. (2002) Inositol polyphosphate 5-phosphatases: lipid phosphatases with flair. *IUBMB life*, **53**, 25-36.

Coghill, I.D., Brown, S., Cottle, D., McGrath, M.J., Robinson, P.A., Nandurkar, H.H., **Dyson, J.M.,** and Mitchell, C.A. (2002) FHL3 is a novel actin-binding protein that regulates alpha-actinin mediated actin bundling. FHL3 localizes to actin stress fibers and enhances cell spreading and fiber disassembly.(In preparation)

Abstracts:

Dyson, J.M., Munday, A.D., O'Malley, C.J., Becanovic, J., Berndt, M.C., and Mitchell, C.A. (2001) The SH2-containing inositol polyphosphate 5-phosphatase, (SHIP-2) complexes with filamin localizes to membrane ruffles. Meeting abstract from 11th international conference, second messengers and phosphoproteins, Melbourne, Victoria, Australia.

Dyson, J.M., O'Malley, C.J., Becanovic, J., Munday, A.D., Berndt, M.C., Coghill, I.D., Nandurkar, H.H., Ooms, L.M., and Mitchell, C.A. (2001) The SH2-containing inositol polyphosphate 5-phosphatase, SHIP-2, binds filamin and regulates submembraneous actin. Meeting abstract from Annual Postgraduate Research Symposium, Monash University, Victoria, Australia.

Summary

Phosphoinositides are lipid second-messengers which are involved in many signaling pathways and regulate multiple cellular processes such as membrane trafficking, apoptosis and cytoskeletal rearrangement. All phosphoinositide signaling molecules are generated from phosphatidylinositol which can be phosphorylated and in turn dephosphorylated at various positions on the inositol ring.

The inositol polyphosphate 5-phosphatases catalyze the removal of the 5'-position phosphate from the inositol ring of the lipid substrates PtdIns(4,5)P_2, PtdIns(3,5)P_2 and PtdIns(3,4,5)P_3 and the water-soluble substrates Ins(1,4,5)P_3 and Ins(1,3,4,5)P_4. To date, ten mammalian and four yeast 5-phosphatases have been identified. SHIP-2 is an SH2-domain containing inositol polyphosphate 5-phosphatase-2 which hydrolyzes PtdIns(4,5)P_2 and PtdIns(3,4,5)P_3 and in some studies has been shown to hydrolyze Ins(1,3,4,5)P_4. SHIP-2 is comprised of an N-terminal SH2 domain, a central catalytic 5-phosphatase domain, and a C-terminal proline-rich domain. SHIP-2 knockout mice have implicated this 5-phosphatase in the regulation of insulin signaling.

Intracellular localization studies revealed that endogenous and recombinant hemagglutinin (HA)- and green fluorescent (GFP)-tagged SHIP-2 localized to membrane ruffles in resting COS-7 cells and epidermal growth factor (EGF)-stimulated COS-7 cells. In resting cells this localization was mediated by the proline-rich domain of SHIP-2 with the Src homology (SH2) domain of SHIP-2 contributing to the plasma membrane localization following prolonged EGF stimulation.

To identify binding partners for SHIP-2, which mediate the localization of SHIP-2 to membrane ruffles, the yeast two-hybrid system was used. Using the proline-rich domain of SHIP-2 as a "bait", a skeletal muscle library was screened, which isolated the actin-binding protein, filamin C as a SHIP-2 interacting partner. Subsequent yeast-two hybrid

assays demonstrated SHIP-2 interacts will all three isoforms of filamin, filamin A, B and C.

Co-immunoprecipitation studies of recombinant and endogenous proteins confirmed an association between SHIP-2 and filmain in COS-7 cells, which was constitutive. Co-localization studies in COS-7 cells and skeletal muscle sections demonstrated these two species co-localize at membrane ruffles in COS-7 cells and to the Z-line in mature muscle. Moreover, the localization of SHIP-2 to membrane ruffles was dependent on filamin expression. Overexpression studies in COS-7 demonstrated SHIP-2 localizes to sites of PtdIns(3,4,5)P_3 production, where the enzyme hydrolyzes PtdIns(3,4,5)P_3 and thereby regulates submembraneous actin.

In highly motile cells such as platelets, SHIP-2 localizes to filopodia, lamellipodia and to the central actin ring. Co-immunoprecipitation studies demonstrated SHIP-2 is part of tetrameric complex with filamin, actin, and the receptor glycoprotein (GP)Ib-IX-V. SHIP-2 dissociates from this complex following thrombin or von Willebrand factor stimulation.

Collectively, these studies demonstrate SHIP-2 localizes to membrane ruffles where this signal modifying enzyme associates with filamin and regulates submembraneous actin.

Abbreviations

ABD	actin-binding domain
ABP	actin-binding protein
Aip	actin-interacting protein
ARAP	ASAP-related protein
ARF	adenosine diphosphate ribosylation factor
ARNO	ARF nucleotide binding site operator
ATP	adenosine triphosphate
BCR	B cell antigen receptor
BMMC	bone marrow-derived mast cells
Btk	Bruton's tyrosine kinase
cDNA	complementary deoxyribonucleic acid
CH	calponin homology
CHO	chinese hamster ovary
dNTPs	deoxyribonucleoside triphosphates
EGF	epidermal growth factor
ER	endoplasmic reticulum
ERK	extracellular signal-related kinase
ERM	exrin/radixin/moesin
F-actin	filamentous-actin
FAK	focal adhesion kinase
FITC	fluorescein isothiocyanate
FLNA/B/C	filamin A/B/C
Gab	Grb2-associated binder
GAP	GTPase activating protein

GDP	guanosine diphosphate
GEF	guanine nucleotide exchange factor
GFP	green fluorescent protein
G-actin	globular-actin
GP	glycoprotein
GPCR	G-protein coupled receptor
Grp	general receptor for phosphoinositides
GST	glutathione-S-transferase
GTP	guanosine triphosphate
H1/2	Hinge 1/2
HA	haemagglutinin
HPLC	high performance liquid chromatography
HRP	horseradish peroxidase
IGF	insulin growth factor
IL	interleukin
$Ins(1,4,5)P_3$	inositol 1,4,5-trisphosphate
$Ins(1,3,4,5)P_4$	inositol 1,3,4,5-tetrakisphosphate
IRS	insulin receptor substrate
ITAM	immunoreceptor tyrosine-based activation motif
ITIM	immunoreceptor tyrosine-based inhibitory motif
kb	kilobases
kDa	kilodaltons
LIMK	LIM kinase
NGF	nerve growth factor
OCRL	oculocerebrorenal syndrome of Lowe

PAK1	p21-activated kinase
PCR	polymerase chain reaction
PDK	phosphoinositide-dependent kinase
PDGF	platelet-derived growth factor
PH	pleckstrin homology
Phox	phox (phagocyte oxidase) homology
PI3-kinase	phosphoinositide 3-kinase
PI4-kinase	phosphatidylinositol 4-kinase
PIPP	proline-rich inositol polyphosphates 5-phosphatase
PLC	phospholipase C
PLD	phospholipase D
PMSF	phenylmethylsulphonyl fluoride
PRD	proline-rich domain
PTB	phosphotyrosine-binding
PTEN	phosphatase and tensin homolog
PtdIns	phosphatidylinositol
PtdIns4P 5-kinase	phosphatidylinositol 4-phosphate 5-kinase
PtdIns(3)P	phosphatidylinositol 3-phosphate
PtdIns(4)P	phosphatidylinositol 4-phosphate
PtdIns(5)P	phosphatidylinositol 5-phosphate
PtdIns(3,4)P_2	phosphatidylinositol 3,4-bisphosphate
PtdIns(3,5)P_2	phosphatidylinositol 3,5-bisphosphate
PtdIns(4,5)P_2	phosphatidylinositol 4,5-bisphosphate
PtdIns(3,4,5)P_3	phosphatidylinositol 3,4,5-trisphosphate
PtdSer	phosphatidylserine

PTEN	phosphatase and tensin homolog deleted on chromosome ten
PVDF	polyvinylidene difluoride
SAM	sterile alpha motif
SDS-PAGE	sodium dodecylsulphate-polyacrylamide gel electrophoresis
SH2/3	src homology 2/3
SHIP	SH2 domain-containing inositol polyphosphate 5-phosphatase
SF	Steel factor
SKIP	skeletal muscle and kidney enriched inositol phosphatase
SNARE	soluble N-ethylmaleimide-sensitive factor (NSF) attachment protein receptor
TNF	tumor necrosis factor
TRAF2	tumor necrosis receptor-associated factor
TLC	thin layer chromatography
TRITC	tetramethylrhodamine isothiocyanate
vWF	von Willebrand factor
WASP	Wiskott-Aldrich syndrome protein

CHAPTER 1: Literature Review

1.1 The actin cytoskeleton

The actin cytoskeleton is a three-dimensional network of protein filaments within the cytoplasm of a cell, consisting of three major types of filaments, microtubules, microfilaments and intermediate filaments (Janmey *et al.*, 1999; Schmidt and Hall, 1998). Microfilaments represent polymers of actin, and taken together with actin-binding proteins and associated proteins constitute the actin cytoskeleton (Schmidt and Hall, 1998)(reviewed by (Winsor and Schiebel, 1997)).

In response to diverse extracellular stimuli, the actin cytoskeleton undergoes rearrangement, including the assembly of actin which involves the addition of monomeric G-actin to free barbed ends of actin-nucleating sites. This process is achieved through the actions of an array of regulatory proteins which nucleate, cap, sever or cross-link actin filaments, or bind to and sequester monomeric actin.

In mammalian cells the actin cytoskeleton is involved in numerous cellular events, one of which is cell motility and cell shape changes. Functionally, cell migration is required for wound healing, immune cell homing and axonal pathfinding (Bear *et al.*, 2001). During cell migration a cell must generate a state of polarity, which occurs in response to external and internal stimuli, directing their movement towards the surface locations where the stimulus has been received (Pruyne and Bretscher, 2000; Stossel *et al.*, 1999). Numerous mechanisms for cell movement have been proposed. One mechanism which is becoming widely accepted is based on the premise that cells contain a peripheral elastic rim (the cell cortex/corticol gel), which is an organelle-excluding substance predominantly composed of actin filaments organized in diverse ways (Stossel *et al.*, 1999). In response to surface stimulation it is thought that the corticol gel weakens, enabling the cell plasma membrane to protrude in the direction of the stimulus, followed by strengthening of the submembrane cortex to stabilize the extension (Stossel *et al.*,

1999). In addition to cortex strengthening, the cell must prevent rapid equilibrium of water pressures throughout the cell, allowing local fluids to contribute to the protrusive activity of the plasma membrane (Stossel *et al.*, 1999). These events are accompanied by rapid actin filament turnover to generate movement, forming two distinct new structures, lamellipodium and filopodium (Carlier *et al.*, 1999; Hartwig, 1992).

Lamellipodium represents a circumferential zone of orthogonally arrayed short actin filaments that act as templates for the growing lamellipodial network; the short filaments originate from the resting actin filaments which are either segmented into shorter pieces or completely disassemble into monomers that are used to generate a new population of short filaments (Hartwig, 1992; Scaife and Langdon, 2000b; Stossel *et al.*, 1999). Following protrusion of lamellipodia, sheet like extensions of the plasma membrane form, "membrane ruffles", often on the cell surface and at the advancing front of a lamellipodium (Cheng *et al.*, 2000; Cheresh *et al.*, 1999b; Scaife and Langdon, 2000b). In contrast to lamellipodia, filopodia are pointed bundles of actin filaments. Within lamellipodia and filopodia are increased concentration of filamentous actin (F-actin), a result of the generation of new barbed ends, by nucleation, or severing and uncapping of existing filaments. These new actin filaments are orientated towards the plasma membrane (Bear *et al.*, 2001; Carlier *et al.*, 1999). At the molecular level, lamellipodia and filopodia have been designated subdomains (Figure 1.1A). A lamellipodium is composed of four subdomains; the tip of lamellipodium, actin meshwork, a region of major disassembly and undegraded filaments that contribute to the cytoplasmic network. A filopodium is composed of two subdomains; the tip of the filopodium and the actin bundle. Contrasting these subdomains is a difference in actin network arrangement and associated proteins. A growing body of evidence indicates that the tips of lamellipodia and filopodia serve an analogous function of localizing and harnessing actin polymerization necessary for cell

Figure 1.1 Schematic representation of the subdomains and associated proteins in lamellipodia and filopodia.

A. Schematic representation of subdomains in lamellipodia and filopodia (modified from Small *et al.*, 2002). B. Schematic representation of selected molecules within the filopodium (orange box), and lamellipodium (blue box) tips, corresponding to those depicted in A (modified from Small *et al.*, 2002).

A

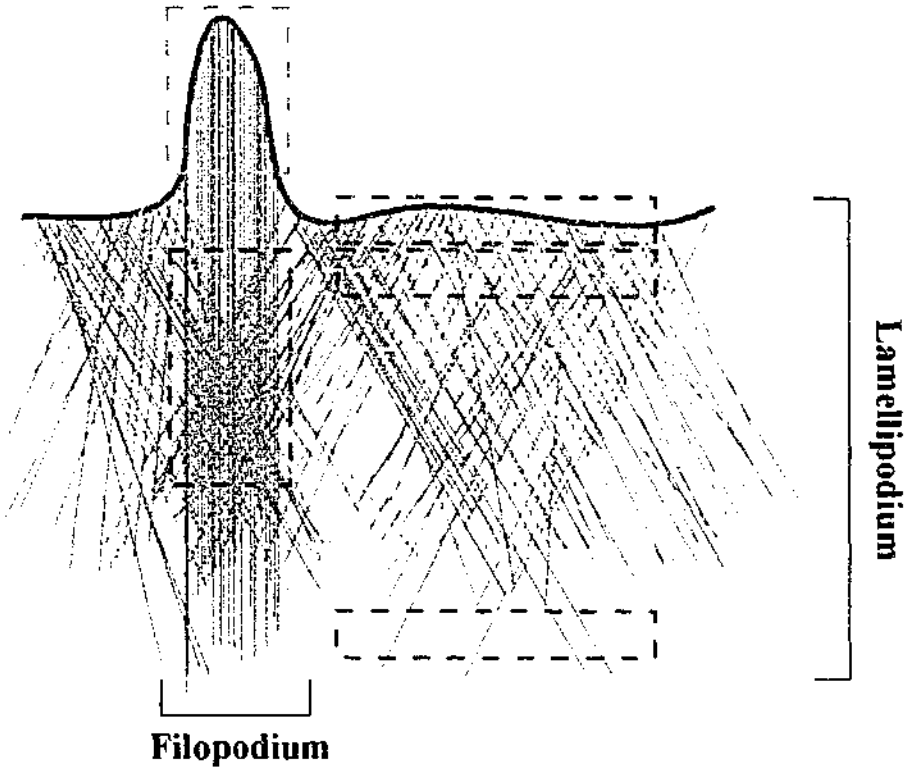

Tip of lamellipodium

Actin meshwork

Region of major disassembly

Undegraded filament that contributes to the cytoplasmic network

Tip of filopodium

Bundle

B

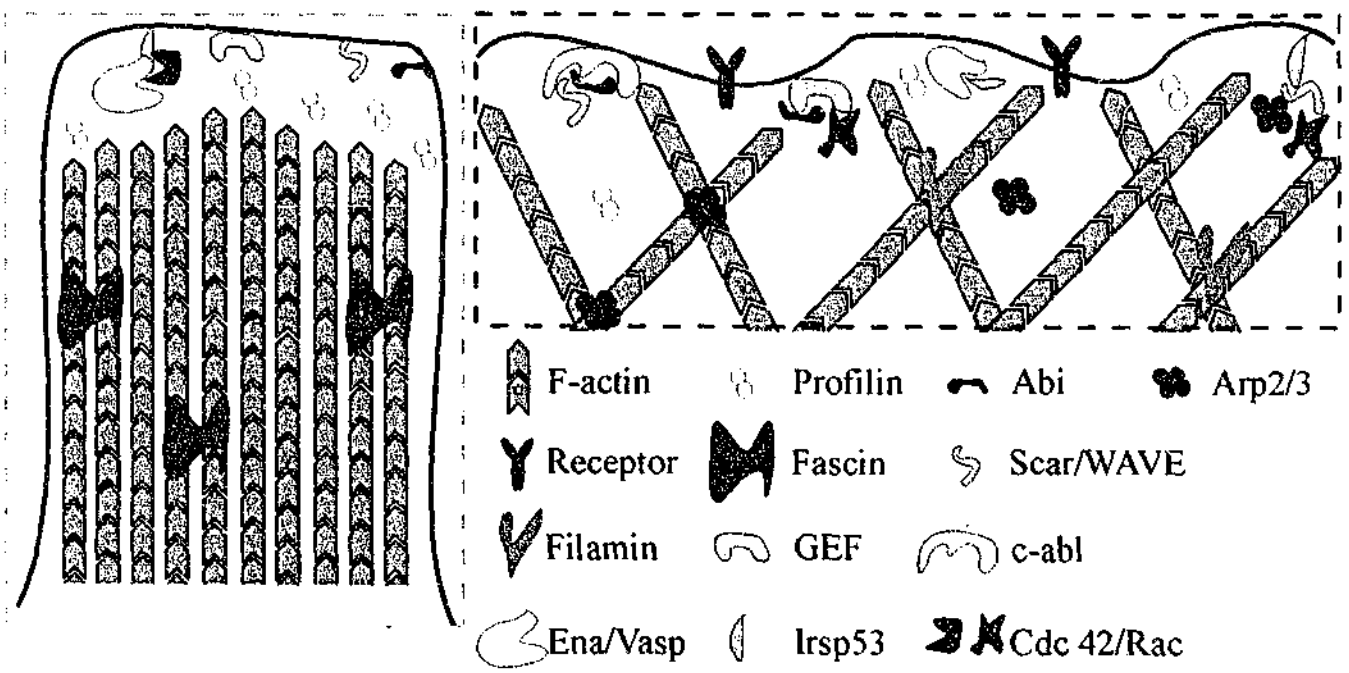

motility. An important feature distinguishing lamellipodia from filopodia is the difference in the complement of proteins at their tips (Small *et al.*, 2002) (Figure 1.1B).

Following actin cytoskeleton reorganization and formation of the leading edge, the cell forms attachment points, focal adhesions, to the substratum, which contain integrins and various cytoplasmic and cytoskeletal proteins, allowing bidirectional signaling between the extracellular matrix and the cytoskeleton (Bear *et al.*, 2001; Schoenwaelder and Burridge, 1999). Once the leading edge has been anchored, the cell slides its body forward by contraction, and then releases substratum attachment points at the rear of the cell (Bear *et al.*, 2001; Stossel *et al.*, 1999)(reviewed by (Critchley, 2000)).

In steadily migrating cells, the lamellipodia remains essentially constant in breadth, indicating a balance between assembly at the front and disassembly at the rear. Protrusion and retraction rates of lamellipodia can be regulated through the recruitment or dissociation of actin assembly regulatory scaffolds (reviewed by (Small *et al.*, 2002)). *In vitro* data suggests disassembly is achieved by proteins of the ADF/Cofilin family and severing proteins such as gelsolin, which co-operate with factors that break filament crosslinks. Based on localization studies of cofilin inhibitory and activating proteins, LIM kinase and actin-interacting protein (Aip1), respectively, it has been suggested depolymerization is not restricted to the rear of lamellipodia (reviewed by (Small *et al.*, 2002)).

Actin cytoskeleton assembly is regulated at multiple levels. Actin-binding proteins regulate actin assembly by controlling filament formation and crosslinking of the actin network (Pollard and Cooper, 1986; Schafer and Cooper, 1995; Stossel, 1993; Welch *et al.*, 1994). The activity of these actin-binding proteins is often modulated by signaling molecules such as phosphorylated phosphoinositides (Janmey, 1994).

1.2 Filamin

Filamin is a phosphoprotein present in the periphery of the cytoplasm where it binds actin filaments, promoting orthogonal branching of actin filaments and thereby cell migration and stability (reviewed by (Stossel *et al.*, 2001)).

Structure

The amino-termini of filamin(s) encode an actin-binding domain (ABD), which is followed by a rod-domain composed of 4-24 100 residue repetitive segments including a carboxyl-terminal dimerization domain (Hock *et al.*, 1990). Interrupting the repeating regions are two hinge domains, H1 and H2 which are located between repeats 15 and 16, and repeats 23 and 24, respectively. Within these hinge regions are calpain-cleavage sites, rendering filamin highly susceptible to proteolysis (Davies *et al.*, 1978)(Figure 1.2A). The filamin dimer is composed of two 280 kDa subunits. Rotary shadowing electron microscopy of filamin isolated from various tissues demonstrated that the dimers are elongated, V-shape flexible structures connected to each other at one end, presumably through the carboxyl-terminal dimerization domain (Gorlin *et al.*, 1990; Tyler *et al.*, 1980).

Isoforms and expression

In humans three filamin genes have been identified, filamin A (FLNA), filamin B (FLNB) and filamin C (FLNC). The three filamin proteins share 70 % homology over their entire sequence, with the exception of two 30 amino acid flexible loops, Hinge 1 (H1) and Hinge 2 (H2). Furthermore, FLNC contains a unique 81 amino acid insertion sequence within repeat 20 (reviewed by (Stossel *et al.*, 2001)).

Alternative poly(A) signals and internal deletions in some domains increases the diversity of the filamin family. The H2 region between repeat 23 and the carboxyl-terminal repeat 24 is present in all human filamin isoforms, however in contrast, the H1 regions between repeats 15 and 16 is absent in some splice variants of human FLNB and FLNC

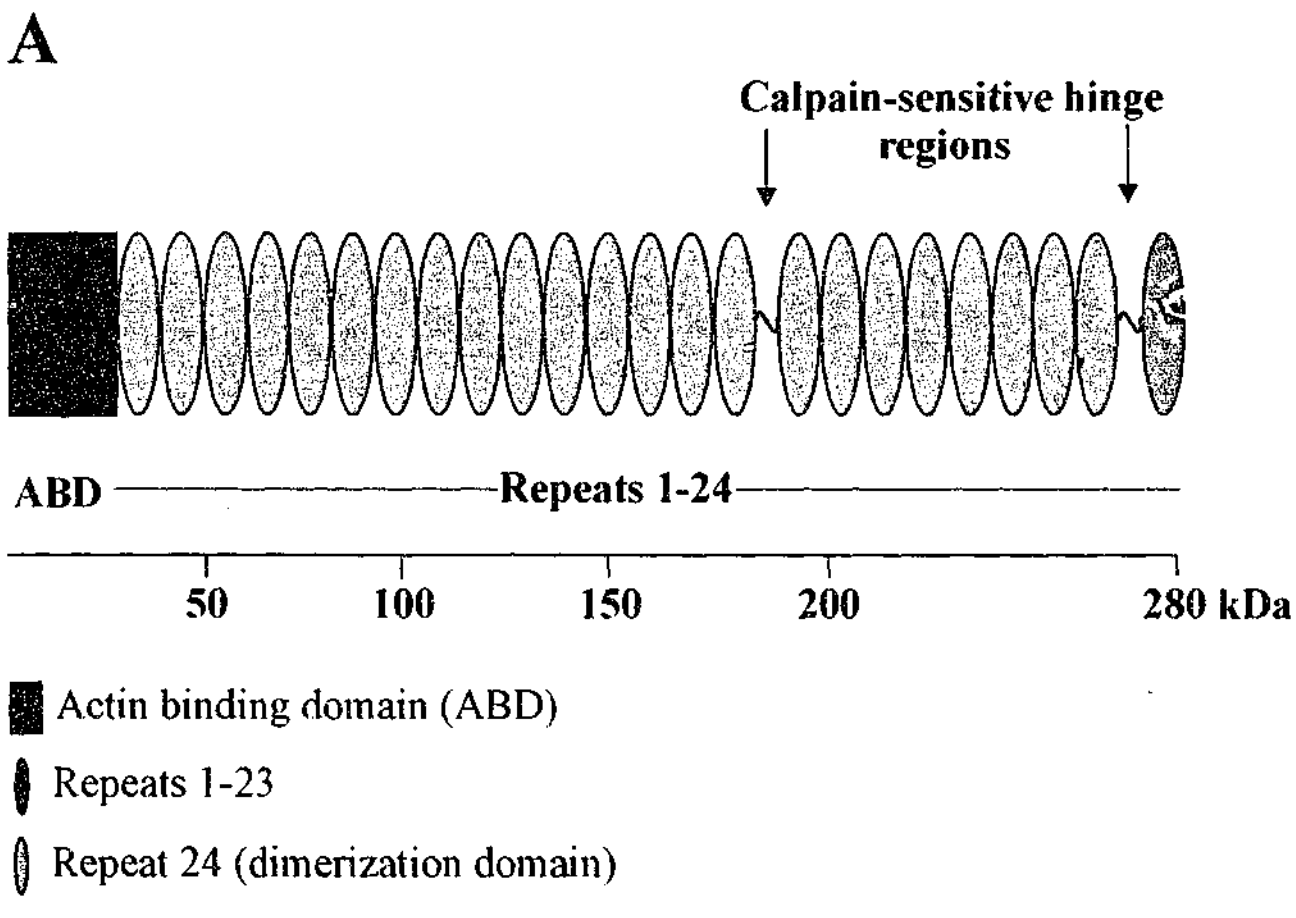

Figure 1.2A Schematic representation of filamin .

Filamin is composed of an N-terminal actin-binding domain (ABD), followed by 24 repeating regions containing the C-terminal dimerization domain.

(Xie *et al.*, 1998; Xu *et al.*, 1998). Furthermore, two widely expressed variants with an internal deletion of 41 amino acids between repeats 19 and 20 of FLNA and FLNB have been detected at low levels, termed $FLNA_{var\text{-}1}$ and $FLNB_{var\text{-}1}$, respectively (van der Flier *et al.*, 2002). Alternative splicing of a region encoding eight amino acids in repeat 15 of FLNA has also been reported (Gorlin *et al.*, 1990). Cardiac tissue-specific filamin isoforms, have also been detected, in which the four carboxyl-terminal repeat domains, including the dimerization domain, are deleted in FLNB (reviewed by (van der Flier and Sonnenberg, 2001)). Most recently, a third FLNB transcript was identified that encodes a variant with a shorter H1 region (van der Flier *et al.*, 2002). The regulation of expression of filamin genes is further complicated in chicken and fruitfly, as alternative promoters have been identified (reviewed by (van der Flier and Sonnenberg, 2001)).

Several studies have revealed overlapping cellular and tissue expression patterns of human FLNA, FLNB and FLNC. FLNA and FLNB are the most ubiquitously expressed isoforms, although interestingly, the expression level of FLNB isoform lacking the H1 region is different is each tissue (Gorlin *et al.*, 1990; Takafuta *et al.*, 1998; Xu *et al.*, 1998). In contrast to FLNA and FLNB, expression of FLNC is largely restricted to skeletal and cardiac muscle where the predominant isoform expressed is FLNC lacking the H1 region (Xie *et al.*, 1998).

The expression of filamin during myogenesis has been most extensively studied however, until recently discrimination of filamin isoforms was not considered. RT-PCR analysis, using specific filamin primers, on total RNA isolated at various time points of the C2C12 cell line myogenic differentiation process, revealed expression of all three murine filamin isoforms, FLNA, FLNB and FLNC. Interestingly, whereas the H1 region is present in FLNA throughout myogenic differentiation, this region is initially present in FLNB and FLNC, however, during the process of myogenesis it is deleted. Immunoblot analysis of

the muscle cell line C2C12 using antibodies specific to the H1 region of FLNB confirmed the RT-PCR data, demonstrating the level of FLNB protein containing the H1 region decreased during differentiation of C2C12 cells. $FLNA_{var-1}$ and $FLNB_{var-1}$ transcripts, which have an internal deletion of 41 amino acids between repeats 19 and 20 were not detected in C2C12 cells (van der Flier *et al.*, 2002). In differentiated myotubes FLNB was shown to localize to Z-lines (van der Flier *et al.*, 2002).

PCR analysis of FLNB transcripts, specifically, $FLNB_{var-1}$ and $FLNB_{var-1}$ lacking the H1 region, $FLNB_{var-1}(\Delta H1)$, revealed expression in a variety of tissues including heart, lung, testis, spleen, thymus and leukocytes (van der Flier *et al.*, 2002).

Role in receptor signaling

Integrins play an important role in regulating cell adhesion, motility and activation. The integrin family are closely related heterodimeric cell surface receptor glycoproteins, composed of an α and β chain, and mediate cell-extracellular matrix and cell-cell interactions (Hynes, 1992). To date, 16 α chains and 8 β chains have been identified, resulting in many heterodimeric combinations. Although both chains are required for ligand binding, association with cytoplasmic proteins is predominantly mediated by the β chain (Loo *et al.*, 1998).

The association of filamin with the cytoplasmic domain of β_{1A} and β_7-integrin was initially demonstrated using affinity chromatography of various cell lysates. Moreover, the β_7-intergrin bound 8.4 times more filamin than β_{1A}-intergrin, isolated using purified recombinant proteins, suggesting filamin acts as a specific link between a subset of integrins and the cytoskeleton (Pfaff *et al.*, 1998). Studies exploiting the yeast two-hybrid system have demonstrated that repeats 20-24 of filamin and all but the most carboxyl-terminal three amino acids of the β_1-integrin, were required for association of the two species (Loo *et al.*, 1998). Recent studies using GST-pulldown assays of FLNB variants,

demonstrated β_1-integrin association only with $FLNB_{var-1}$ and $FLNB_{var-1}(\Delta H1)$, suggesting that deletion of the variant regions of full-length FLNB increases binding to β_1-integrins. Furthermore, β_{1A}-integrin bound more FLNBvar-1 and FLNBvar-1(ΔH1), than the splice variant β_{1D}-integrin (van der Flier *et al.*, 2002).

Functional studies in chinese hamster ovary (CHO) cells using recombinant integrin proteins demonstrated that changing the affinity of filamin for β-integrin cytoplasmic domains can alter initial events required for cell migration, such as membrane protrusion and cell polarization. These studies involved replacing the β_3-integrin tail with the β_7-integrin tail, that binds strongly to filamin, or with the β_{1A}-integrin tail, which binds filamin with an intermediate affinity. In random migration assays across fibrinogen-coated filters, the cells expressing the β_7 chimera manifested profoundly reduced migration relative to those expressing the β_{1A} chimera. Furthermore, expression of the β_7-integrin led to fewer and more peripheral focal adhesions throughout the cell, and an inability to assemble a fibronectin matrix (an integrin-mediated event).

Using an "homology scanning" approach, by making chimeric exchanges between the β_7 and the β_{1D} tails, and affinity chromatography, revealed that residues 35-40 of the β_7-integrin tail, and in particular the isoleucine at positions 36 and 40 confer high levels of filamin binding on β-integrin tails. Introduction of mutations in the β_{1A}-integrin tail which enhances filamin binding, resulted in reduced migration across fibrinogen-coated filters, similar to that observed with cells expressing the β_7 chimera. Additionally, introducing mutations into the β_7-integrin tail, which reduces filamin binding, resulted in increased cell migration levels, as seen for cells expressing the β_{1A} chimera. Fibronectin matrix assembly and focal adhesion formation were not affected in cells expressing integrins containing mutations that alter filamin binding (Calderwood *et al.*, 2001).

The glycoprotein (GP)Ib-IX-V complex contains four polypeptides, GPIbα, GPIbβ, GPIX and GPV, and is the major transmembrane receptor for von Willebrand factor (vWf) on the platelet surface. The GPIb-IX-V complex is involved in mediating several important platelet functions including the initial adhesion of platelets to the subendothelium after vascular damage, the activation of platelets by thrombin, and the regulation of actin polymerization and subsequent platelet shape change (Berndt *et al.*, 1985; Berndt *et al.*, 2001; Williamson *et al.*, 2002) (reviewed by (Jackson *et al.*, 2000)).

Sedimentation assays and studies investigating the effect of Ca^{2+}-dependent proteases on the association of ^{3}H-labeled glycoproteins with the membrane skeleton, indicated actin-binding protein (later named filamin), linked the membrane glycoproteins to actin filaments. Co-immunoprecipitation studies from unactivated platelets demonstrated an association between filamin and GPIb. Furthermore, hydrolysis of filamin, by Ca^{2+}-dependent proteases, resulted in a marked release of GPIb from the membrane skeleton. From these studies it was suggested that filamin links membrane glycoproteins to actin filaments (Fox, 1985).

The exact region of GPIbα that filamin binds is contentious. Peptide-binding assays using GPIbα synthetic peptides demonstrated that residues 536-568 participate in the interaction of the two species (Andrews and Fox, 1992). CHO cell studies, demonstrated residues 570-590 were required for association of GPIb-IX complex with the cytoskeleton and more recently, co-immunoprecipitation studies in these same cells have suggested that residues 557-579 of GPIbα are required for association with filamin (Cunningham *et al.*, 1996; Williamson *et al.*, 2002). The binding site of filamin required for association with GPIbα is less controversial, with repeats 17-19 of filamin defined for association (Meyer *et al.*, 1997; Takafuta *et al.*, 1998).

Association with other proteins

Through its C-terminus, filamin associates with numerous cytosolic proteins, which implicates it in a plethora of cellular pathways (Figure1.2B). Filamin associates with several GTPases of the Ras superfamily, Rho-like GTPases and Trio a guanidine exchange factor RhoA, RhoG and Rac, suggesting that filamin serves as a GTPase docking site and for other regulatory factors for actin dynamics (Bellanger *et al.*, 2000; Ohta *et al.*, 1999).

In muscle, filamin has been implicated in the pathogenesis of muscular dystrophies. Immunohistochemical studies have demonstrated filamin is mislocalized in limb-girdle and Duchenne muscular dystrophies. Moreover, filamin associates with numerous proteins predominantly expressed in skeletal muscle including the dystrophin-glycoprotein complex, which has implicated filamin in the maintenance of muscle membrane integrity (Thompson *et al.*, 2000). Filamin also associates with the muscle specific proteins myozenin and myotilin, the latter known to cause a form of autosomal dominant limb-girdle muscular dystrophy (Takada *et al.*, 2001; van Der Ven *et al.*, 2000).

Apart from association with integrin receptors and the platelet specific receptor GPIb-IX-V, filamin is thought to influence various signaling cascades *via* association with various receptors and their associated proteins. Associations with SEK-1, a dual specificity protein kinase that serves as an intermediate activator of the stress-activated protein kinases (SAPK), and the tumor necrosis receptor-associated factor-2 (TRAF2), have suggested filamin may modulate tumor necrosis factor (TNF)α-mediated signaling (Leonardi *et al.*, 2000; Marti *et al.*, 1997). As well as influencing receptor signaling it has been suggested that filamin may also promote stabilization of receptors at the cell surface. Filamin associates with the Fcγ-R1 immune receptor and the dopamine receptors D2 and D3, and interestingly disruption of association with these receptors results in either receptor internalization or a reduction in both the number and half-life of cell surface

B

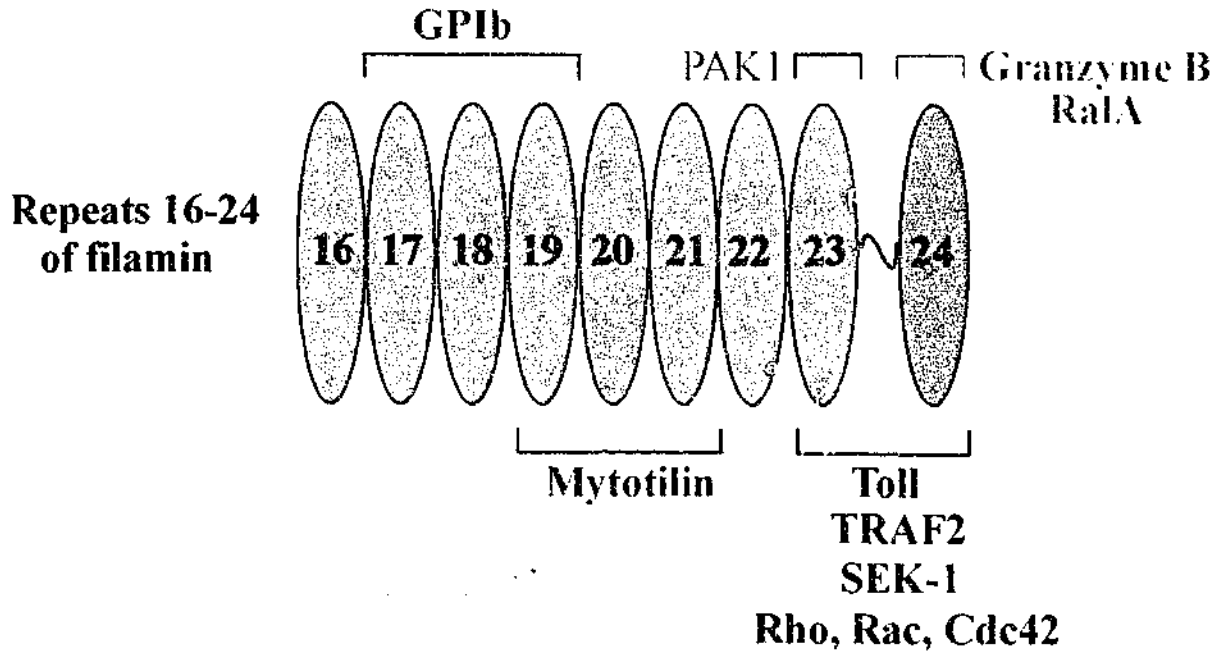

Figure 1.2B Schematic representation of repeats 16-24 of filamin and its binding partners.

Filamin associates with a plethora of proteins through its C-terminus. GPIb, |glycoprotein| Ib-V-IX; PAK1, p21-activated kinase1; TRAF2, tumor necrosis factor receptor-associated factor 2.

receptors, respectively (Harrison *et al.*, 1994; Lin *et al.*, 2002). Filamin has been further implicated in immune cell signaling *via* its association with the adaptor protein Lnk which associates with the T cell receptor (He *et al.*, 2000). In this way it has been proposed that filamin may effect T cell activation.

Filamin has been demonstrated to influence various components of the actin cytoskeleton. Recently it was demonstrated that through association with p21-activated kinase (PAK1), filamin participates and synergizes with LIM kinase in membrane ruffle formation (Vadlamudi *et al.*, 2002). Association of filamin with FAP52, a focal adhesion-associated phosphoprotein, is thought to serve as a link between focal adhesions and the actin cytoskeleton (Nikki *et al.*, 2002).

Role in actin assembly

Filamins are cytoskeletal proteins that organize actin in networks and stress fibers. The ABD of filamin, like all α-actinin-like ABDs, is composed of two calponin-homology (CH) domains, CH1 and CH2. Through these domains filamin binds all actin isoforms (Mejean *et al.*, 1992). The *in vitro* binding affinity of filamin to F-actin and saturation levels are comparable to those found for other actin-binding proteins (Gorlin *et al.*, 1990; Wang and Singer, 1977). *In vitro* filamin is able to generate parallel bundles of actin filaments, or, orthogonal actin networks, depending on the stoichiometry of the two species, and the source of filamin. For instance, filamin isolated from macrophages forms more rigid actin gels than filamin isolated from chicken gizzard. It has recently been speculated that the structure of the filamin variant may affect may effect the organization of the resultant actin filaments. Filamin variants lacking the first hinge region may restrict the flexibility of the filamin rod domains with respect to each other, leading to packed filamin dimers which form rigid actin filaments, as opposed to orthogonal actin networks (reviewed by (van der Flier and Sonnenberg, 2001)).

Recently, filamin has been suggested as a candidate for actin network stabilization at lamellipodia (Flanagan *et al.*, 2001). This proposal is supported by studies using three unrelated human malignant melanoma cell lines which lack actin-binding protein, subsequently named filamin. The human melanoma cells which are deficient for FLNA (M2 cells) display extensive continuous plasma membrane blebbing and impaired locomotion. Reconstitution of the filamin-deficient cells by stable transfection of FLNA (A7 cells), reverts the phenotype of the cells, with cells acquiring greater general asymmetry and shape, focal lamellipodia and increased translocational motility (Cunningham *et al.*, 1992). Recent studies have proposed that FLNA is essential for stabilizing orthogonal actin networks for locomotion (Flanagan *et al.*, 2001). Electron microscopy has demonstrated that the short-lived lamellae of the filamin-deficient cells (M2 cells) contain a dense mat of long actin filaments in contrast to the filamin-replete subline in which the lamellae display a more three-dimensional orthogonal network of actin filaments.

Association with phosphoinositides

Filamin cross-links actin filaments to produce a gel composed of F-actin. It has been reported that the gelating activity of filamin C is regulated by phosphoinositides. The effects of polyphosphoinositides on the gelating activity of filamin C was examined by measuring the low shear viscosity of the F-actin solutions containing filamin and either PtdIns, PtdIns(4)P, or PtdIns(4,5)P_2. It was determined from these studies that micelles of each of the phospholipids bound filamin. Furthermore, PtdIns(4,5)P_2 had the greatest inhibitory effect on filamin C gelating activity, whilst PtdIns(4)P and PtdIns also had an inhibitory effects. The inhibitory effects observed was determined to be the result of a loss of F-actin-binding activity of filamin C (Furuhashi *et al.*, 1992). The effect PtdIns(3,4,5)P_3, or PtdIns(3,5)P_2, on filamin C gelating activity was not investigated.

Recently, a link between filamin and PtdIns(3,4,5)P_3 has been identified (Paranavitane *et al.*, 2002). LL5β is a PH-domain-containing protein which selectively binds PtdIns(3,4,5)P_3 *in vitro* and binds filamin in a PI3-kinase-independent manner (Paranavitane *et al.*, 2002). The effect of this association on the gelating activity of filamin was not investigated.

1.3 Phosphoinositide signaling

Phosphoinositides are ubiquitous components of eukaryotic cell membranes. Although phosphoinositides comprise less than 10 % of the total phospholipids they are important components of intracellular signaling pathways. Phosphatidylinositol (PtdIns) is the precursor for the family of lipid second-messengers, known as phosphoinositides, which differ in the phosphorylation status of their inositol head group (reviewed by (Fruman *et al.*, 1998; Martin, 1998; Zhang and Majerus, 1998)).

PtdIns has five hydroxyl groups on the inositol ring, 2, 3, 4, 5 and 6, which are all potential phosphorylation sites, however, *in vivo* only positions 3, 4 and 5 are known to be phosphorylated (Figure 1.3). Collectively, these phosphoinositides participate in many cellular processes including cell survival and differentiation, vesicular trafficking, and cytoskeletal reorganization (reviewed by (Martin, 1998)).

Monophosphorylated lipids are generated by phosphorylation at the 3, 4 or 5 position of the inositol ring giving rise to PtdIns(3)P (phosphatidylinositol 3-phosphate), PtdIns(4)P (phosphatidylinositol 4-phosphate) or PtdIns(5)P (phosphatidylinositol 5-phosphate), respectively. All monophosphorylated and bisphosphorylated lipids PtdIns(4,5)P_2 (phosphatidylinositol 4,5 bisphosphate), PtdIns(3,5)P_2 (phosphatidylinositol 3,5 bisphosphate) and PtdIns(3,4)P_2 (phosphatidylinositol 3,4 bisphosphate), have been detected *in vivo*. PtdIns(3,4,5)P_3 has also been detected in cells (reviewed by (Fruman *et*

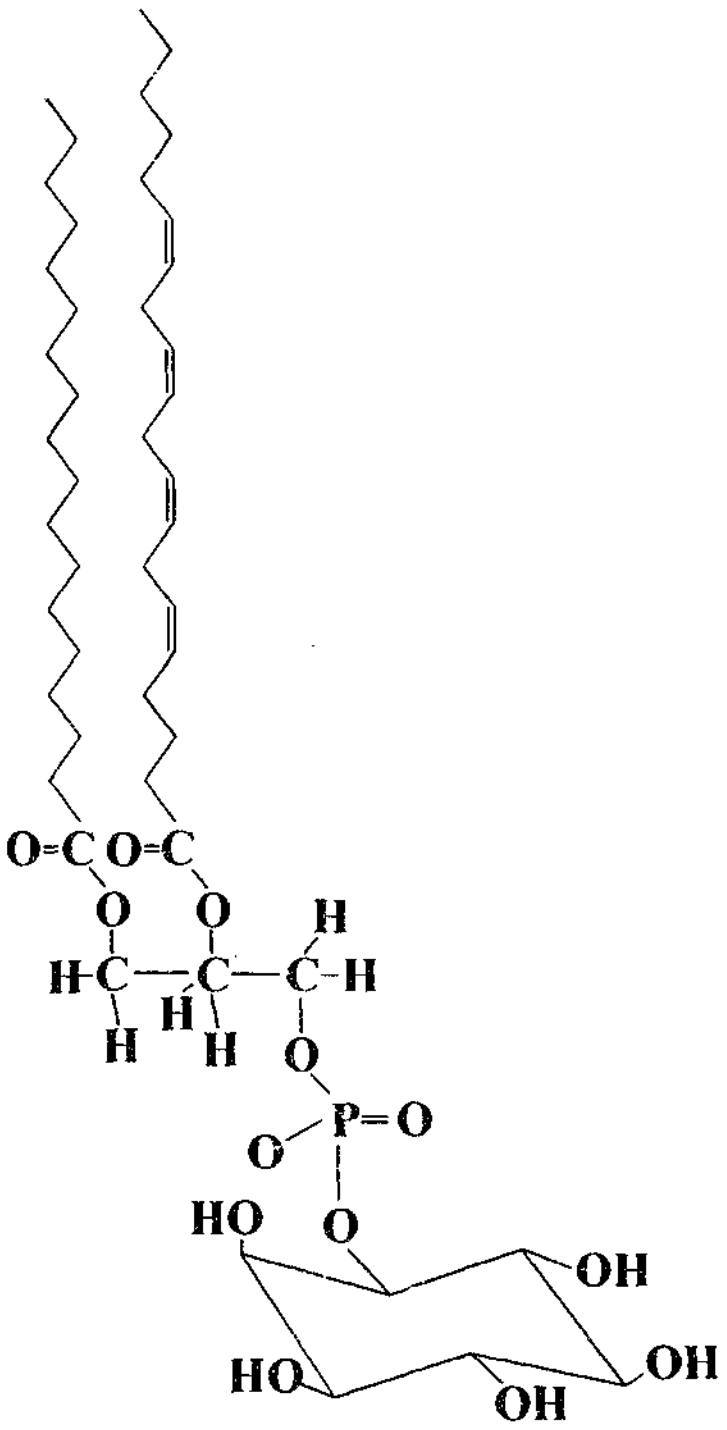

Figure 1.3 Structure of Phosphatidylinositol (PtdIns).

The molecular structure of PtdIns comprises an inositol headgroup coupled to a diacylglycerol backbone via a phosphodiester linkage. The free hydroxyl groups at positions 3', 4', and 5' of the inositol ring can be replaced with phosphate groups by specific lipid kinases to generate various phosphoinositides.

al., 1998; Martin, 1998)). PtdIns constitutes 80 % of total cellular inositol phospholipids whereas PtdIns(4)P and PtdIns(4,5)P_2 represent 90 % of the cellular phosphorylated phosphoinositides. The cellular levels of PtdIns(3,4)P_2 and PtdIns(3,4,5)P_3 are low in resting cells but increase significantly and transiently upon cellular stimulation (Stephens *et al.*, 1991). In addition to serving as substrates for the generation of second messengers, phosphorylated phosphoinositides themselves function as signaling molecules. The ongoing identification of downstream effectors of these phosphoinositides has led to considerable advances being made in the elucidation of their precise cellular role.

1.3.1 PtdIns(4,5)P_2 signaling

PtdIns(4,5)P_2 is the precursor for the second messengers diacylglycerol (DAG), Ins(1,4,5)P_3 and PtdIns(3,4,5)P_3. Although a precursor, PtdIns(4,5)P_2 itself can function as a second messenger and regulate cellular responses including cytoskeletal reorganization and vesicular trafficking. Half of the total cellular PtdIns(4,5)P_2 resides in caveolae, which are small plasma membrane invaginations rich in caveolin, glycosphingolipids and cholesterol, and have been suggested to be the primary sites of agonist-stimulated PtdIns(4,5)P_2 turnover (Pike and Casey, 1996). Cellular levels of PtdIns(4,5)P_2 do not change significantly in response to agonist stimulation and thus local mechanisms are thought to regulate its synthesis (Toker, 1998).

Two pathways have been identified for the synthesis of PtdIns(4,5)P_2 (Figure 1.4). The majority of PtdIns(4,5)P_2 is generated from PtdIns(4)P, which is phosphorylated at the 5' position by PtdIns(4)P 5-kinase, of which three isoforms have been cloned, α, β and γ (Loijens and Anderson, 1996). Alternatively, PtdIns(4,5)P_2 can be generated by 4'position phosphorylation of PtdIns(5)P by either α, β, or γ PtdIns(5)P 4-kinase (Rameh *et al.*, 1997). In addition it has been suggested PtdIns(4,5)P_2 production can be mediated by

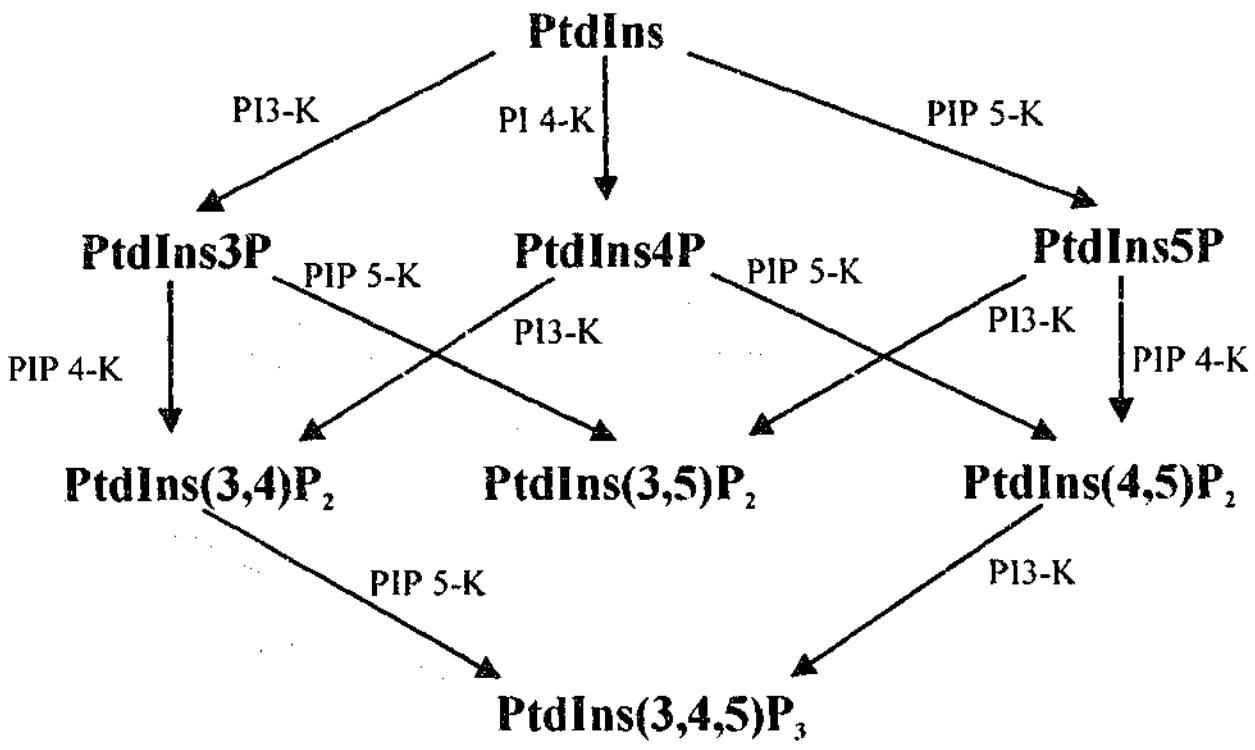

Figure 1.4 Metabolism of phosphoinositides in mammalian cells.

Synthesis of phosphoinositides involves several classes of lipid kinases including phosphoinositide 3-kinases (PI3-K), phosphatidylinositol 4-kinases (PI4-K), phosphatidylinositol 4-phosphate 5-kinases (PIP 5-K) and phosphatidylinositol 5-phosphate 4-kinases (PIP 4-K). Not all of the synthetic pathways depicted have been demonstrated *in vivo*. Inositol polyphosphate 5-phosphatase (5-ptase) activity is represented by the blue arrows. Pathways mediated by other lipid phosphatases are not shown (adapted from Fruman et al., 1998).

dephosphorylation at the 3' position of the trisphosphorylated lipid, PtdIns(3,4,5)P_3, by the tumor suppressor PTEN (Maehama and Dixon, 1998). Although, it appears more likely that PTEN functions as a negative regulator of cellular PtdIns(3,4,5)P_3 levels rather than as a mediator of PtdIns(4,5)P_2 production. Considering the transient nature of PtdIns(3,4,5)P_3 production and the low cellular levels of PtdIns(5)P, it is likely phosphorylation of PtdIns(4)P by PtdIns(4)P 5-kinase is the major pathway for PtdIns(4,5)P_2 production. Although PtdIns(4)P is the preferred substrate, the α and β isoforms of PtdIns(4) 5-kinase can also phosphorylate PtdIns(3)P at the 4' and 5' position to form PtdIns(3,4)P_2, PtdIns(3,5)P_2 and PtdIns(3,4,5)P_3 (Zhang *et al.*, 1997), respectively and PtdIns(5)P from PtdIns (Toker, 1998).

Upon cellular agonist stimulation, phospholipase C (PLC) is activated through heterotrimeric G-proteins or protein tyrosine kinases. Activated PLC hydrolyzes PtdIns(4,5)P_2 to generate the second messengers, diacylglycerol (DAG), which activates protein kinase C (PKC), and Inositol(1,4,5)-trisphosphate (Ins(1,4,5)P_3) which binds to specific receptors on the endoplasmic reticulum, mobilizing intracellular calcium stores and thus influencing a wide range of cellular processes (Berridge, 1993a; Berridge, 1993b; Bootman *et al.*, 2001). Ins(1,4,5)P_3 can be hydrolyzed by specific 5-phosphatases generating Ins(1,4)P_2, which to date has no known function. Dephosphorylation of Ins(1,4,5)P_3 inhibits its ability to mobilize intracellular calcium stores (reviewed by (Mitchell *et al.*, 1996)).

In addition to its role as a second messenger. Ins(1,4,5)P_3 is also a precursor for Inositol(1,3,4,5)-tetrakisphosphate (Ins(1,3,4,5)P_4) production. Ins(1,3,4,5)P_4 has been implicated in facilitating the entry of extracellular calcium across the plasma membrane. One suggested mechanism for Ins(1,3,4,5)P_4 action is through directly activating Ca^{2+} channels on the plasma membrane (Luckhoff and Clapham, 1992; Tsubokawa *et al.*, 1996).

Whole-cell-patch-clamp studies in mast cells has determined Ins(1,3,4,5)P_4 to be an inhibitor of a 5-phosphatase that hydrolyzes Ins(1,4,5)P_3, and thereby facilitates the activation of the store-operated Ca^{2+} current resulting in the mobilization in intracellular calcium (Hermosura *et al.*, 2000).

Four distinct phosphoinositide-binding domains have been identified, pleckstrin homology (PH), FYVE, Phox homology and ENTH domains, each have distinct affinities and specificities for phosphoinositides. The pleckstrin homology (PH) domain is a protein module of approximately 120 amino acids that was originally identified in pleckstrin. To date the only function of PH domains is to bind phosphoinositides (reviewed by (Itoh and Takenawa, 2002)).

PH domains from different proteins display considerable selectivity and affinities for specific phosphoinositides and more recently this property has resulted in exploitation of these domains for investigating cellular functions and localization of specific phosphoinositides (reviewed by (Itoh and Takenawa, 2002)). Employing the PH domain of PLCδ as a probe, the cycle of PtdIns(4,5)P_2 synthesis and hydrolysis was investigated. In resting cells the PH domain of PLCδ, which was fused to GFP, localized to the plasma membrane and was released into the cytosol upon PtdIns(4,5)P_2 hydrolysis and subsequently localized to the Golgi where *de novo* synthesis of PtdIns(4,5)P_2 occurs (Stauffer *et al.*, 1998; Varnai and Balla, 1998).

1.3.2 PtdIns(4,5)P_2 and the actin cytoskeleton

PtdIns(4,5)P_2 has an established role in a number of cellular processes including membrane trafficking specifically vesicle transport, and the regulation of ion channel activity (Baukrowitz *et al.*, 1998; Corvera *et al.*, 1999; De Camilli *et al.*, 1996; Gillooly and Stenmark, 2001; Hilgemann and Ball, 1996). In addition, PtdIns(4,5)P_2, and

PtdIns(3,4,5)P_3, are important mediators of actin cytoskeleton reorganization. It has recently been suggested that due to their specific individual spatial and temporal dynamics these messenger molecules perform distinct roles in the regulation of the actin cytoskeleton. Due to the high concentration and the homogeneous distribution of PtdIns(4,5)P_2, in contrast to PtdIns(3,4,5)P_3, the latter is proposed to act as an instructive signal whilst PtdIns(4,5)P_2 is thought to act permissively, restricting actin polymerization to the cortex (reviewed by (Insall and Weiner, 2001)). Although this model is plausible there are discrepancies within the literature and the role of PtdIns(4,5)P_2 in the regulation of the actin cytoskeleton is not clear-cut.

PtdIns(4,5)P_2 can associate with a variety of actin-regulatory proteins, *via* PH domains, or motifs comprising charged residues. *In vitro* studies have demonstrated PtdIns(4,5)P_2 can affect the function of several actin-associated cytoskeletal proteins by causing dissociation of G-actin from actin-monomer-binding proteins, as well as the uncapping of the actin filament barbed ends. In addition, PtdIns(4,5)P_2 enhances actin filament crosslinking and the linkage of actin filaments to the plasma membrane *via* influencing the activity of actin-regulatory proteins or by inducing a conformational change or regulating their interaction with other cytoskeletal proteins (reviewed by (Sechi and Wehland, 2000)).

Specifically, the association of PtdIns(4,5)P_2 with actin capping proteins has been suggested to influence the direction of actin filament growth. Actin capping proteins bind to the fast growing end of actin filaments and prevent further growth. Through the displacement of capping proteins, such as CapZ, PtdIns(4,5)P_2 is thought to enhance elongation of existing actin filaments. Furthermore, as the growing end of the actin filament is capable of binding PtdIns(4,5)P_2, the phospholipid could bias the orientation of actin filament growth, whereby, it could inhibit capping of newly nucleated actin filaments

if the direction of their growth is toward the plasma membrane (reviewed by (Insall and Weiner, 2001)).

A role for PtdIns(4,5)P_2 in the initiation of new actin filaments has recently been established. The Rho family of GTPases, (including Cdc42, Rho and Rac), may exert their actions in the regulation of the actin cytoskeleton through influencing PtdIns(4,5)P_2 synthesis (Bishop and Hall, 2000; Sechi and Wehland, 2000). ARF6 is a member of the ARF (ADP-ribosylation factor) family of small GTPases which has been implicated with cellular events such as membrane ruffling and cell spreading, processes which require reorganization of the actin cytoskeleton. ARF6 co-localizes with the Rho family GTPase, Rac, at the plasma membrane where PtdIns(4,5)P_2 synthesis is promoted *via* the action of PtdIns(4)P 5-kinase, by GTP-bound ARF6 (Honda *et al.*, 1999). The association of PtdIns(4,5)P_2 with the ERM (ezrin/radixin/moesin) family proteins is thought to activate them by induction of a conformational change inducing their actions as plasma membrane-actin cross-linkers (Bretscher, 1999).

Through a synergistic effect with the Rho family GTPase Cdc42, PtdIns(4,5)P_2 modulates nucleation of actin through its interactions with the WASP (Wiskott-Aldrich syndrome) family proteins. Co-operation between Cdc42 and PtdIns(4,5)P_2 has been suggested based on numerous studies including the observation that the concentration of Cdc42 and PtdIns(4,5)P_2 required for N-WASP activation is reduced by a factor of ten when both ligands are added in combination. Subsequent activation of the Arp2/3 complex leads to nucleation of actin polymerization (Fawcett and Pawson, 2000).

1.3.3 PtdIns(3,5)P_2 signaling

PtdIns(3,5)P_2 was initially detected in yeast where it accumulates in response to hyperosmotic stress (Dove *et al.*, 1997). PtdIns(3,5)P_2 has also been detected in fibroblasts,

platelets, B lymphocytes, COS-7 cells and T cells, however, in the latter two cell types, in contrast to yeast, levels of PtdIns(3,5)P_2 decrease following hyperosmotic stress. In T and B cell lines, IL-2 stimulation leads to increases in PtdIns(3,5)P_2 levels, however, the mechanism for its synthesis in these cells is poorly understood (Dove *et al.*, 1997; Jones *et al.*, 1999).

Phosphate-labelling studies have shown that PtdIns(3,5)P_2 is synthesized from PtdIns3P, by a PtdIns5-kinase, Fab1p in yeast and PIKfyve in mammalian cells (Figure 1.4) (Cooke *et al.*, 1998; Dove *et al.*, 1997; Sbrissa *et al.*, 1999; Whiteford *et al.*, 1997). PIKfyve is highly expressed in insulin-sensitive tissues and localizes predominantly to intracellular vesicles *via* its FYVE domain (Fab1, YGLO23, VPS27 and EEA1), a specialized zinc-finger binding motif specific for PtdIns3P (Shisheva *et al.*, 2000; Stenmark and Aasland, 1999). Insulin stimulation of 3T3L1-adipocytes causes redistribution of PIKfyve from the cytosol to the intracellular membrane fraction, but does not affect its activity. PIKfyve demonstrates protein serine kinase activity in addition to lipid kinase activity (Sbrissa *et al.*, 1999; Shisheva *et al.*, 2000).

In yeast, PtdIns(3,5)P_2 synthesis is required for the sorting of proteins targeted for vacuolar degradation into multivesicular bodies, a prevacuolor compartment which fuses and empties its contents into the vacuole (Odorizzi *et al.*, 2000). The role of PIKfyve in mammalian membrane trafficking is not known, however, pleckstrin-2 and Centurian-β2 bind PtdIns(3,5)P_2 *in vitro*, which supports a role for the lipid in membrane trafficking (Dowler *et al.*, 2000).

1.3.4 Phosphoinositide 3-kinases (PI3-kinase)

Phosphoinositide 3-kinases (PI3-kinase) are important regulatory proteins, involved in many different signaling pathways effecting many cellular functions. PI3-kinases

catalyze the transfer of the γ-phosphate group of ATP to the 3'-position of PtdIns, PtdIns(4)P and PtdIns(4,5)P_2. PI3-kinase enzymes can be divided into three classes on the basis of their *in vitro* lipid substrate specificity and likely mode of regulation. All PI3-kinase catalytic subunits share a homologous region that consists of a catalytic core domain and a C2 domain (reviewed by (Vanhaesebroeck *et al.*, 1997; Vanhaesebroeck and Waterfield, 1999)).

Class I PI3-kinase

Class I PI3-kinases are heterodimers made up of a 110 kDa catalytic subunit (called p110) and an adaptor/regulatory subunit. *In vitro*, class I PI3-kinases can phosphorylate PtdIns, PtdIns(4)P and PtdIns(4,5)P_2. However, *in vivo*, the preferred substrate appears to PtdIns(4,5)P_2. All class I PI3-kinase members bind Ras, however, the physiological relevance of this association is unclear. Class I PI3-kinases are further divided into class IA and IB enzymes, which signal downstream of tyrosine kinases and heterotrimeric G protein-coupled receptors, respectively (reviewed by (Vanhaesebroeck *et al.*, 2001)).

Class IA PI3-kinase

The p110 subunit in this class exists in a complex with an adaptor subunit that that has two SH2 domains, which binds to phosphorylated tyrosine residues, and thought to allows translocation of the cytosolic PI3-kinase to the membrane, the site of their lipid substrates and Ras. Mammals have three class IA p110 isoforms, encoded by three separate genes, which are differentially expressed, however, all mammalian cells express are least one type of class IA PI3-kinase. Stimulation of almost any receptor can lead to class IA PI3-kinase activation, additionally, activation can be mediated by receptors with intrinsic kinase activity or non-receptor tyrosine kinases (reviewed by (Fry, 1994; Stephens *et al.*, 1993; Wymann and Pirola, 1998)). There are at least seven adaptor subunits with

which the p110 subunit can form functional complexes (reviewed by (Vanhaesebroeck *et al.*, 1997)).

Class IB PI3-kinase

To date only one class IB PI3-kinase has been identified, which is composed of a p110 catalytic subunit complexed with a 101 kDa regulatory protein. Unlike class IA, class IB PI3-kinase is only expressed in white blood cells. Several studies have reported that class IB PI3-kinase is activated by either ligands that activate G-protein-coupled receptors, or by interaction with GTP-bound Ras (reviewed by (Vanhaesebroeck and Waterfield, 1999)).

Class II PI3-kinase

Class II PI3-kinases are approximately 170 kDa. Structurally, these enzymes contain an N-terminal Ras binding domain fold, however, there are no reports of these PI3-kinases binding to Ras or adaptor subunits, and a C-terminal C2 domain which *in vitro* binds phospholipids in a Ca^{2+}-independent manner (Arcaro *et al.*, 1998; MacDougall *et al.*, 1995). *In vivo* it has not been established which lipids are generated by this class of PI3-kinase, however, *in vitro* PtdIns, PtdIns(4)P and PtdIns(4,5)P_2 can be used as substrates with a strong preference for PtdIns. Interestingly, *in vitro*, the lipid kinase activity of the class II PI3-kinase toward phosphorylated inositide substrates is increased upon binding of clathrin (Gaidarov *et al.*, 2001). Although the mechanism is not clear, class II PI3-kinase activity is increased in response to stimuli such as epidermal growth factor (EGF), platelet-derived growth factor (PDGF), insulin, integrin ligation, and the chemokine MCP-1 (Arcaro, 1998; Brown *et al.*, 1999; Turner *et al.*, 1998; Zhang *et al.*, 1998a). Mammals express three class II isoforms of which two are ubiquitously expressed and one mainly expressed in liver. They are predominantly associated with the membrane fraction of cells,

and deletion of the lipid-binding C2 domain does not alter their subcellular localization (Arcaro *et al.*, 1998; Domin *et al.*, 2000; Prior and Clague, 1999).

Class III PI3-kinase

This class of PI3-kinases are the homologs of the yeast vesicular-protein-sorting-protein Vps34p (reviewed by (Herman and Emr, 1990; Odorizzi *et al.*, 2000)). Class III PI3-kinases can only utilize PtdIns as a substrate *in vitro*, and is likely to be responsible for the production of most of the PtdIns(3)P in cells. The cellular levels of this mono-phosphorylated lipid does not alter significantly in cells, suggesting that the intracellular trafficking processes in which class III PI3-kinases are likely to be involved are not triggered by cellular stimulation (reviewed by (Vanhaesebroeck and Waterfield, 1999)).

A single class PI3-kinase catalytic subunit has been identified in all eukaryotic species. In yeast and mammals, the catalytic subunit complexes with a serine/threonine kinase, Vps15p (vacuolar protein sorting) and p150, respectively. Yeast studies have demonstrated that Vps15p is responsible for targeting Vps34p to membranes, and it has been suggested that p150 will play the same role in mammalian cells (Panaretou *et al.*, 1997)(reviewed by (Fruman *et al.*, 1998)).

Role of PI3-kinase and insulin signaling

Activation of PI3-kinase is an essential step for insulin-mediated signaling in adipose and skeletal muscle tissue. Insulin-mediated activation of PI3-kinase in muscle cells and adipocytes results in plasma membrane recruitment of the glucose transporter, GLUT4 which facilitates glucose uptake (Cheatham *et al.*, 1994; Kotani *et al.*, 1995). The p85 subunit of PI3-kinase rapidly associates with GLUT4-containing membranes in insulin-stimulated 3T3-L1 adipocytes (Heller-Harrison *et al.*, 1996). Targeted disruption of the p85α regulatory subunit of PI3-kinase results in a hypoglycemic phenotype and

increased insulin sensitivity, due to increased glucose transport in skeletal muscle and adipocytes, which was mediated by a splice variant regulatory subunit p50α. This isoform switch was associated with an increase in insulin-induced generation of PtdIns(3,4,5)P_3 in the p85-/- adipocytes which facilitated GLUT4 translocation to the plasma membrane (Terauchi *et al.*, 1999).

The actin cytoskeleton has been implicated in insulin-mediated events. Disruption of actin polymerization inhibits insulin-dependent association of p85 with GLUT4-containing membranes, and recruitment of GLUT4-containing vesicles to the plasma membrane in both 3T3-L1 adipocytes and L6 skeletal muscle cells (Tsakiridis *et al.*, 1995). A model based on microscopy studies performed on L6 myotubes assessing changes in actin, PI3-kinase and GLUT4 localization following insulin stimulation, suggests activated PI3-kinases influence actin remodeling, followed by recruitment of GLUT4 vesicles to the plasma membrane. Activation of downstream effectors of PI3-kinase such as Akt are thought to be involved in promoting the enrichment of GLUT4 on the plasma membrane (Khayat *et al.*, 2000). However, inhibition of PI3-kinase in adipocytes blocks exocytosis, but not endocytosis of the transferrin receptor, suggesting a wider role for PI3-kinase in trafficking that is not restricted to GLUT4 vesicle translocation (Jess *et al.*, 1996; Shepherd *et al.*, 1998).

1.3.5 PtdIns(3,4)P_2 and PtdIns(3,4,5)P_3 signaling

The absence of PtdIns(3,4)P_2 and PtdIns(3,4,5)P_3 in lower eukaryotes such as yeast suggests that these lipids have evolved to participate in more complex signaling pathways in higher eukaryotes (reviewed by (Toker and Cantley, 1997)). Although virtually undetectable in unstimulated cells, these lipids rapidly accumulate in response to a variety of stimuli (reviewed by (Hinchliffe, 2001)). The generation of these second messengers at

the membrane results in recruitment of specific binding proteins to the membrane and initiation of various signaling cascades, which may also feed, through effectors of the lipids, into other signaling cascades (Figure 1.5) (reviewed by (Cantrell, 2001; Hinchliffe, 2001; Rameh and Cantley, 1999; Toker and Cantley, 1997)).

In response to agonist stimulation, PtdIns(3,4,5)P_3 is generated from PtdIns(4,5)P_2 by the actions of class I PI3-kinases. Class I PI3-kinases are recruited to membranes by activated tyrosine kinases, heterotrimeric G-proteins, or GTP-bound Ras (reviewed by (Rameh and Cantley, 1999; Vanhaesebroeck *et al.*, 2001)). In addition to class I PI3-kinases, a distinct family of proteins which lack any discernible sequence homology with the PI3-kinases, phosphatidylinositol phosphate kinases (PIP kinases), are involved in PtdIns(3,4,5)P_3 synthesis (Zhang *et al.*, 1997). In this way, PtdIns(3,4,5)P_3 synthesis is mediated by 4'- and 5'-phosphorylation of PtdIns(3)P.

Kinetic analysis of the appearance of PtdIns(3,4)P_2 in cells suggests that PtdIns(3,4)P_2 is produced by dephosphorylation of PtdIns(3,4,5)P_3. However, PtdIns(3,4)P_2 can be produced independently of PtdIns(3,4,5)P_3 generation. These studies include the observed production of PtdIns(3,4)P_2 in platelets by 4'-phosphorylation of PtdIns(3)P (Banfic *et al.*, 1998). In addition, it has been demonstrated that class II PI3-kinases can phosphorylate PtdIns(4)P (reviewed by (Vanhaesebroeck *et al.*, 2001)). It is not clear what the relative contributions of these pathways are to cellular PtdIns(3,4)P_2 levels.

PtdIns(3,4)P_2 and PtdIns(3,4,5)P_3 are both capable of binding PH domain-containing proteins with different degrees of affinity and thereby modulating a variety of signaling pathways including the regulation of serine/threonine kinases such as Akt (also known as PKB) and PKC. These lipids can associate with several exchange factors and GTPase-activating proteins for small GTPases.

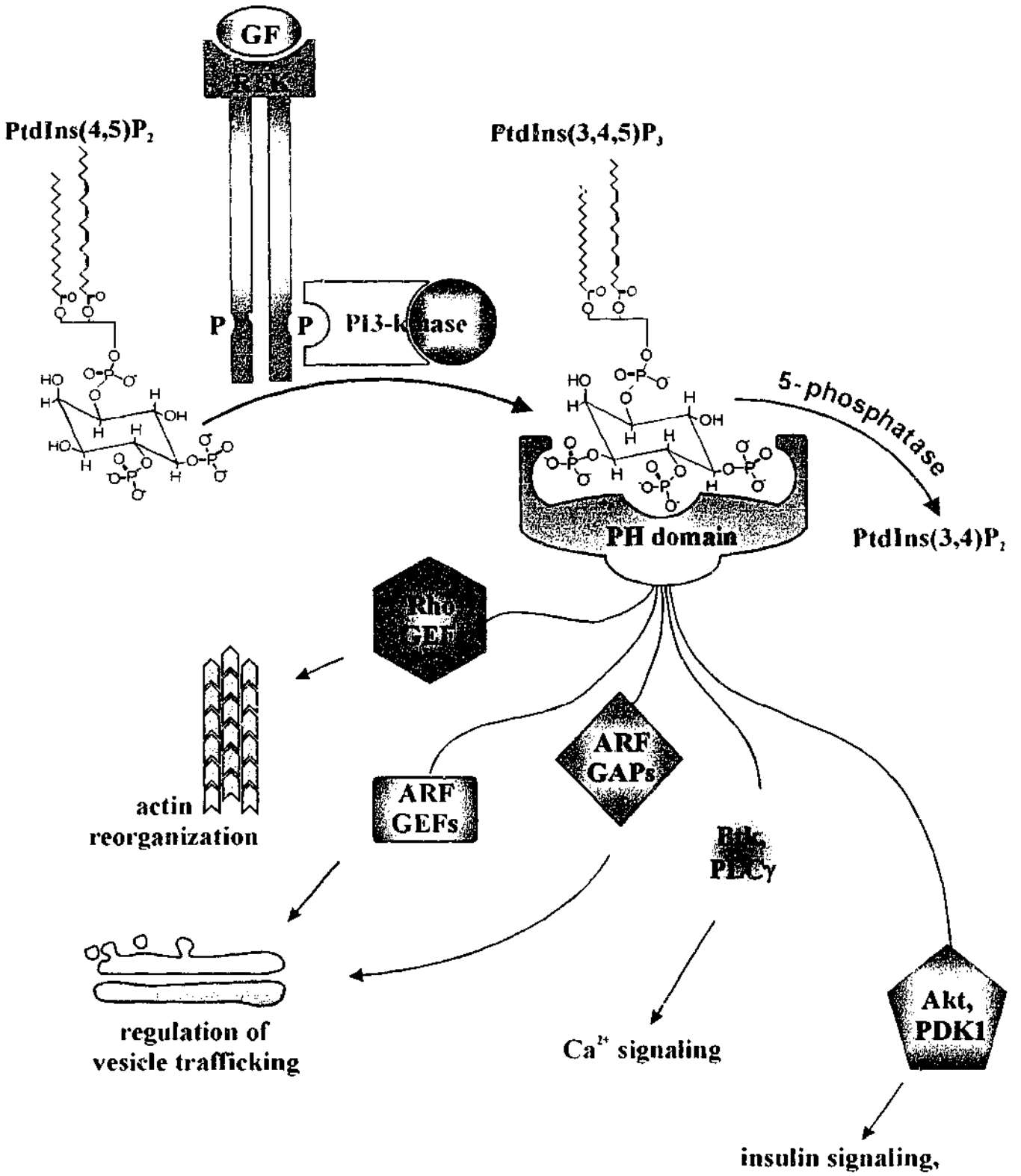

Figure 1.5 PtdIns(3,4,5)P_3 signaling pathways.

Growth factor (GF)-mediated activation of receptor tyrosine kinases (RTKs) leads to the activation of phosphoinositide 3-kinase (PI3-kinase) resulting in the synthesis of PtdIns(3,4,5)P_3 from PtdIns(4,5)P_2. PtdIns(3,4,5)P_3 interacts with and modulates the activities and localizations of a number of PH domain-containing proteins, which regulate anti-apoptotic, B-cell proliferation, insulin signaling, membrane trafficking, and actin reorganization. ARF, adenosine diphosphate ribosylation factor; Btk, Bruton's tyrosine kinase; GAP, GTPase activating protein; GEF, guanine nucleotide exchange factor; PDK1, phosphoinositide-dependent kinase-1; PH, pleckstrin homology; PLC, phosholipase C.

Downstream targets

The serine/threonine kinase Akt, is one of the most well characterized targets of PtdIns(3,4,5)P_3 and PtdIns(3,4)P_2. By virtue of association of its PH domain with these lipids, Akt translocates from the cytosol to the plasma membrane in a PI3-kinase-dependent manner, where it becomes activated. Active Akt then appears to detach from the plasma membrane, and by an unknown mechanism, translocates through the cytosol to the nucleus (Andjelkovic *et al.*, 1997; Meier *et al.*, 1997). The relative importance of PtdIns(3,4,5)P_3 and PtdIns(3,4)P_2 for Akt activation *in vivo* remains unclear. *In vitro*, the PH domain of Akt displays greater affinity for the PtdIns(3,4)P_2 than PtdIns(3,4,5)P_3. *In vitro* PtdIns(3,4)P_2 causes a 3-5-fold increase in Akt activity and *in vivo* the generation of this lipid correlates well with Akt activation (Franke *et al.*, 1997). However, in thrombin-stimulated platelets, both PtdIns(3,4)P_2 and PtdIns(3,4,5)P_3 are required to initiate pre- and post-aggregation-dependent signaling by Akt (Banfic *et al.*, 1998).

Complete activation of Akt requires phosphorylation at two of its residues, Thr308 and Ser373 (Alessi *et al.*, 1996). *In vitro* PDK1 (phosphoinositide-dependent kinase-1) can phosphorylate Akt at the Thr308, however, as the name suggests, binding of PtdIns(3,4)P_2 and PtdIns(3,4,5)P_3 are absolutely required for this event (Alessi *et al.*, 1997). The kinase responsible for phosphorylation of Akt at Ser373 has not been defined. As purified PDK1 can only phosphorylate Akt at Thr308, it was assumed a distinct kinase (termed PDK2) would phosphorylate Akt at Ser373. However, kinase assays performed on PDK1 immunoprecipitates from brain extracts suggests that PDK1 in complex with another protein(s), may mediate phosphorylation of Akt at Ser373.

Activation of Akt leads directly or indirectly to increased phosphorylation of several substrates which activate metabolic and cell survival pathways. Akt plays a role in protecting cells from apoptosis and promoting cell survival, and more recently has been

implicated in insulin signaling (Chong *et al.*, 1994; Franke *et al.*, 1997; Klippel *et al.*, 1997).

Grp1 (general receptor for phosphoinositides) functions as an adenosine diphosphate ribosylation factor (ARF) guanine nucleotide exchange factor (GEF) thereby promoting formation of active GTP-bound ARF. *In vitro* studies have demonstrated the PH domain of Grp1 is selective for PtdIns(3,4,5)P_3 which mediates recruitment of Grp1 to the plasma membrane to regulate vesicle trafficking (Klarlund *et al.*, 1997). ARNO (ARF nucleotide binding site operator), a functional homolog of Grp1, translocates to the plasma membrane upon insulin stimulation in 3T3-L1 adipocytes and binds PtdIns(3,4,5)P_3 *in vivo* (Venkateswarlu *et al.*, 1998). Both PtdIns(3,4,5)P_3 and PtdIns(3,4)P_2 can interact with the PH domain of Vav and stimulate its nucleotide activity towards the Rho GTPases leading to cytoskeletal effects (Han *et al.*, 1998). Recently, ARAP-1 has been demonstrated to be an effector of PtdIns(3,4,5)P_3. ARAP-1, an ASAP-related protein, has ARF GTPase activating protein (GAP) and Rho GAP activity, an Ankryin repeat, Ras-associating, and five PH domains, further implicating PtdIns(3,4,5)P_3 in numerous signaling pathways. These studies demonstrated ARAP-1 contains PtdIns(3,4,5)P_3-dependent ARF GAP activity that regulates Golgi structures and induces filopodia (Miura *et al.*, 2002).

1.3.6 PtdIns(3,4,5)P_3 and the actin cytoskeleton

Historically, PtdIns(4,5)P_2 was thought to be the major phospholipid involved in the regulation of the cytoskeleton, however, a role for PI3-kinase and its lipid product PtdIns(3,4,5)P_3, is emerging. Unlike PtdIns(4,5)P_2, the kinetics of PtdIns(3,4,5)P_3 production correlate well with stimulus-induced actin polymerization (reviewed by (Insall and Weiner, 2001)). Studies using pharmacological inhibitors of PtdIns(3,4,5)P_3 generation, dominant-negative proteins, and mutant receptors unable to activate PI3-

kinase, have, in a variety of cell types, been demonstrated to interfere with stimulus-induced actin polymerization (Funamoto *et al.*, 2001; Niggli and Keller, 1997; Wennstrom *et al.*, 1994a).

The levels of PtdIns(3,4,5)P_3 in unstimulated neutrophils are very low and rapidly rise within 10 seconds of stimulation with chemoattractant (Stephens *et al.*, 1991). Studies in neutrophils using a potent inhibitor of PI3-kinase, wortmannin, which binds irreversibly to the catalytic subunit of the enzyme and prevents production of D3-phosphorylated lipid products of the enzyme, markedly attenuated chemotactic peptide-induced development of polarity and cell motility, which correlated well with the inhibition of PtdIns(3,4,5)P_3 production. Furthermore, extension of these studies suggested inhibition of PI3-kinase effects F-actin (Niggli and Keller, 1997).

More specifically the role of PI3-kinase γ in chemotaxis has been investigated in regulating leukocyte motility. Chemoattractant-mediated recruitment of leukocytes is a pivotal step in the acute and chronic inflammation response (Hirsch *et al.*, 2000b). Leukocytes express all four known class I PI3-kinase isoforms α, β, γ and δ. Using homologous recombination PI3-kinase γ-deficient mice have been generated. *In vitro* chemotaxis assays, using a variety of chemoattractants, demonstrated the chemotaxis of PI3-kinase γ-null macrophages was reduced by up to 85 %. A defect in chemotaxis was also observed in PI3-kinase γ-null polymorphonuclear neutrophils. The *in vivo* implications of the defective chemotaxis observed in PI3-kinase γ-null neutrophils and macrophages has been investigated. Induction of septic peritonitis, in PI3-kinase γ-null mice by injection of Gram-positive and Gram-negative bacteria, resulted in an impaired inflammatory response. FACS analysis of the elicited cell populations indicated a reduction in the recruitment of neutrophils and macrophages, presumably due to the defect in chemotaxis of these leukocytes (Hirsch *et al.*, 2000b).

The addition of membrane-permeant esters of PtdIns(3,4,5)P_3, a product of PI3-kinase, has further implicated this signaling pathway in the regulation of the cytoskeleton and cell motility. The development of cell polarity, which occurs in response to external and internal stimuli, is a prerequisite for the process of cell migration. Incubation of human neutrophils with a membrane-permeant ester of PtdIns(3,4,5)P_3, resulted in a significant increase in the number of polarized neutrophils. Furthermore, pre-treatment of neutrophils with this same ester increased migration and speeds, comparative to cells stimulated with chemotactic peptide. At the molecular level, neutrophils treated with the membrane-permeant ester of PtdIns(3,4,5)P_3, had a marked increase of F-actin in the leading lamellae (Niggli, 2000).

The role of PI3-kinase signaling in chemotaxis is not restricted to cells of hematopoietic origin. Activation of platelet PDGF β-receptors expressed in cultured porcine aortic endothelial cells elicits motility responses such as the formation of membrane ruffles and chemotaxis. Porcine aortic endothelial cells expressing the PDGF β-receptor, migrate efficiently towards a concentration gradient of the appropriate stimulus, and exhibit pronounced membrane ruffling. However, expression of mutant receptors, in which the binding site for PI3-kinase is destroyed, results in a failure of motility responses, such as membrane ruffling and chemotaxis (Wennstrom *et al.*, 1994b). Addition of a synthetic form of PtdIns(3,4,5)P_3 stimulated membrane ruffling responses to the same extent as PDGF stimulation, in contrast, the addition of a synthetic form of PtdIns(4,5)P_2 had no effect (Derman *et al.*, 1997). The apparent requirement of PI3-kinase for cell motility responses was confirmed in subsequent studies, whereby overexpression of a mutant p85 PI3-kinase regulatory subunit, to which the catalytic kinase cannot bind, resulted in the same cellular phenotype (Wennstrom *et al.*, 1994a).

The downstream targets of PI3-kinase, and more specifically PtdIns(3,4,5)P_3 targets, involved in cell motility and cytoskeletal regulation are being identified. Several studies have been performed in a variety of cell types in an attempt to identify the signaling pathways, however, the specific effector proteins involved in this process is contentious, with supportive data implicating a variety of signaling pathways (reviewed by (Insall and Weiner, 2001; Small *et al.*, 2002)).

As one of the processes involved in cell motility is cell polarization, and, morphological polarity directly reflects local increases in F-actin at the leading edge of the cell, it has been suggested that some of the key signaling pathways involved regulate actin assembly and polymerization (Rickert *et al.*, 2000). The Rho GTPases, Rac and Cdc42, are considered prime candidates for relaying signals to the actin cytoskeleton.

It is clear from several studies that PtdIns(3,4,5)P_3 is required for activation of the Rho GTPases, Rac1, Rho and Cdc42, although the underlying molecular mechanisms are not well understood (Akasaki *et al.*, 1999; Benard *et al.*, 1999a; Rickert *et al.*, 2000). The activity of the RhoGTPases is regulated by GEFs such as Vav, Sos1, and Tiam-1, and by GAPs (Maghazachi, 2000; Zheng, 2001). Rho GTPases have two interconvertible forms, a GDP-bound inactive state, and, a GTP-bound active state, regulated by the GAPs and GEFs, respectively (Bourne *et al.*, 1990). A proposed mechanism for GEF activation is by their association with PtdIns(3,4,5)P_3, or, by cytosolic kinases which indirectly or directly associate with and are subsequently activated by PtdIns(3,4,5)P_3.

Four distinct phosphoinositide-binding domains have been identified, however, PH domains are the most abundant of the phosphoinositide-binding domains, and bind phospholipids specifically phosphorylated at the D3-position (Itoh and Takenawa, 2002; Lemmon *et al.*, 2002). Vav, Sos1, and Tiam-1 contain PH domains. Recent studies have suggested that association of the PH domains of Vav, Sos1 and Tiam-1 with

PtdIns(3,4,5)P_3 is required for their activation, and thus, subsequent activation of the RhoGTPases (Fleming *et al.*, 2000; Han *et al.*, 1998; Nimnual *et al.*, 1998). *In vitro*, the PI3-kinase lipid product, PtdIns(3,4,5)P_3 greatly increases the GEF activity of Vav, thereby activating the RhoGTPases. Moreover, PI3-kinase has been shown to activate Tiam-1 (Fleming *et al.*, 2000). PI3-kinase has been demonstrated to influence the activity of the GEF effectors, specifically Rac2, the predominant neutrophil form of the RhoGTPases, Rac1. In human leukocytes, pharmacological inhibition of PI3-kinase blocks Rac2 activation (Akasaki *et al.*, 1999).

A role for the RhoGTPases in cell motility and its associated processes has been strengthened from studies where mutational inactivation of Rac2 or dominant-negative forms of Rac1 or Cdc42, impairs chemoattractant-induced cell migration, F-actin polymerization and development of polarity in neutrophils and leukocytes (Ambruso *et al.*, 2000; Roberts *et al.*, 1999). More specifically, studies using pharmacological inhibitors or dominant-negative mutants of PI3-kinase, has directly suggested a link between PI3-kinase, RhoGTPase activity, and cell motility processes. In neutrophils, inhibition of PI3-kinase either by pharmacological inhibition, or the use of dominant-negative mutant PI3-kinase, decreases the fraction of neutrophils that are polarized in response to chemoattractant, and attenuates chemoattractant-induced activation of Rac and Cdc42 (Akasaki *et al.*, 1999; Benard *et al.*, 1999a). Similar studies performed using cultured cell lines, expressing recombinant chemoattractant receptors, demonstrated a reduction in Rac- and Cdc42-dependent remodeling of actin assemblies (Belisle and Abo, 2000; Ma *et al.*, 1998). Furthermore, in fibroblasts, PI3-kinase-dependent actin rearrangements are dependent on Rac activation (Benard *et al.*, 1999b; Hawkins *et al.*, 1995). Quite a striking similarity is the phenotype of the PI3-kinase γ-deficient mice with that of the Rac2-deficient mice, both displaying common defects including leukocyte migration. The

overlap in the phenotypes of these two animals and additional *in vitro* studies, has suggested PI3-kinase γ and Rac may be in the same signaling pathway, the latter downstream of PI3-kinase (Dekker and Segal, 2000; Ma *et al.*, 1998; Roberts *et al.*, 1999).

Recent studies have proposed a positive feedback loop between PtdIns(3,4,5)P_3, the RhoGTPases and polymerized actin (Wang *et al.*, 2002; Weiner *et al.*, 2002). Using high concentrations of a pharmacological inhibitor of PI3-kinase completely blocks chemoattractant-induced polarity and migration in HL-60 cells. However, using intermediate concentrations (30-50 nm wortmannin) results in reduction of membrane recruitment of PH-Akt-GFP, which binds PtdIns(3,4,5)P_3, and an accumulation of F-actin and phosphorylation of Akt was observed. Actin assemblies at the leading edge of the cell (lamellipodia) were markedly less prominent, and 30 % of cells displayed diffuse actin staining. In untreated cells, chemoattractant-treated cells rapidly polarize and asymmetrically accumulate PH-Akt-GFP and PtdIns(3,4,5)P_3 at the leading edge which persists for many minutes. However, in cells treated with latrunculin, which inhibits actin polymerization, the chemoattractant causes a transient translocation of PH-Akt-GFP from the cytoplasm to the plasma membrane in a symmetric distribution and returns to the cytoplasm within two minutes (Wang *et al.*, 2002). Pretreating cells with toxB, which inhibits RhoGTPases, prevented PH-Akt-GFP translocation to the plasma membrane. In addition, using a cationic lipid shuttling system, delivering exogenous PtdIns(3,4,5)P_3 to neutrophils, elicits an accumulation of endogenous PtdIns(3,4,5)P_3 and localization of PH-Akt-GFP to the plasma membrane (Weiner *et al.*, 2002). Collectively, these studies suggest that the actin cytoskeleton and the RhoGTPases are important in stabilizing the accumulation of PtdIns(3,4,5)P_3 at the plasma membrane. The proposed model suggests that PtdIns(3,4,5)P_3 at the leading edge of the cell stimulates its own accumulation by activating the RhoGTPases, which in turn increases PtdIns(3,4,5)P_3 accumulation.

Moreover, accumulation of PtdIns(3,4,5)P_3 is dependent on actin polymerization, and thus, reciprocal interplay exists between PtdIns(3,4,5)P_3 and polymerized actin which initiates intracellular signals responsible for cell polarity and directed motility (Wang *et al.*, 2002; Weiner *et al.*, 2002).

Parallel studies in neutrophils, leukocytes and *Dictyostelium discoideum* (*D.discoideum*) have identified the serine-threonine kinase Akt/PKB as an effector of PI3-kinase and subsequent studies in *D.discoideum* have implicated PAKa, a structural homolog of mammalian PAKs (p21-activated kinase), as an essential effector of Akt/PKB. It has been demonstrated that both Akt/PKB and PAK are required for proper cell polarity, chemotaxis and cytokinesis (Chung and Firtel, 1999; Hirsch *et al.*, 2000a; Meili *et al.*, 1999). Extension of this signaling pathway implicates the Rho family of GTPases. The catalytic activity of many PAKs is regulated by its association with $Rac1^{GTP}$ or $Cdc42^{GTP}$, which itself can phosphorylate and subsequently activate LIM kinase. Recently, it has been demonstrated that filamin associates with, and is a substrate for PAK1, which is required for PAK1-mediated actin assembly, including lamellipodia formation. In addition, filamin stimulates both the autophosphorylation and the kinase activity of PAK1 in response to growth factor stimulation (Vadlamudi *et al.*, 2002). Activated LIM kinase then indirectly effects actin structures by inactivating cofilin, inhibiting its actin depolymerization and severing activity, leading to membrane protrusion, membrane ruffle formation, and chemotaxis.

In leukocytes G-protein coupled receptor activation leads to activation of the Ras family of proteins which activates PI3-kinase resulting in the generation of PtdIns(3,4,5)P_3. PtdIns(3,4,5)P_3 both interacts with the PH domain of Vav, and stimulates its nucleotide exchange activity towards the Rho GTPases and thus subsequently activates the GTPases, Rac1 and Cdc42. Through association of the Rho family of GTPases either directly or

indirectly with the Wiskott-Aldrich Syndrome family of proteins (WASP), the Arp2/3 complex is activated directly effecting F-actin organization, resulting in protrusion of the leading edge (lamellipodia) and finally chemotaxis (Chung *et al.*, 2001) (Figure 1.6).

1.3.7 PTEN

PTEN (phosphatase and tensin homolog deleted from chromosome 10), also known as MMAC-1 (mutated in multiple advanced cancers) or TEP-1 (TGF-β-regulated and epithelial cell-enriched phosphatase), is a widely expressed product of a tumor suppressor gene located on chromosome 10q23, a region deleted at very high frequency in many tumor types (Li and Sun, 1997; Li *et al.*, 1997; Steck *et al.*, 1997). Human germline mutations of PTEN are associated with the rare autosomal dominant hamartomatous syndromes, Cowden Disease and Bannayan-Riley-Ruvalcaba syndrome.

The structure of PTEN includes several unique features not seen in related protein phosphatases. In its amino-terminus, PTEN contains a phosphatase domain and a C2 domain, the latter shown to bind lipid vesicles *in vitro* (Li *et al.*, 1997; Steck *et al.*, 1997). The C-terminus of PTEN contains a binding motif for a class of PDZ protein-protein interaction domains, several phosphorylation sites and two putative PEST sequences (Adey *et al.*, 2000; Lee *et al.*, 1999; Wu *et al.*, 2000a; Wu *et al.*, 2000b). In addition to its protein phosphatase activity, *in vitro* PTEN dephosphorylates several phosphoinositides, specifically removing the 3'-position phosphate from PtdIns(3,4,5)P_3 and PtdIns(3,4)P_2 and much less efficiently from Ins(1,3,4,5)P_4, PtdIns(3)P and PtdIns(3,5)P_2 (Maehama and Dixon, 1998; Myers *et al.*, 1998; Wu *et al.*, 2001).

Many studies have shown that inactivation or deletion of the tumor suppressor gene PTEN results in defects in chemotaxis and cell motility (Funamoto *et al.*, 2002; Iijima *et al.*, 2002; Liliental *et al.*, 2000; Tamura *et al.*, 1999). The molecular mechanisms

Figure 1.6 Model of pathways regulating co-orodinate control of chemotaxis *via* G-protein coupled receptors (GPCRs).

The diagram shows the signaling pathways which regulate chemotaxis by GPCRs. Phosphoinositide 3-kinase (PI3-kinase) is essential for chemotaxis in leukocytes. G-protein coupled receptor activation leads to activation of Rac1 and Cdc42, which activates PAK1 and the WASP family of proteins, leading to F-actin organization, protrusion of the leading edge, and chemotaxis. Blocked arrow denotes inhibition (modified from Small *et al.*, 2002). GEF, guanine nucleotide exchange factor; PAK1, p21-activated kinase; WASP, Whiskott-Aldrich syndrome proteins; LIMK, LIM kinase.

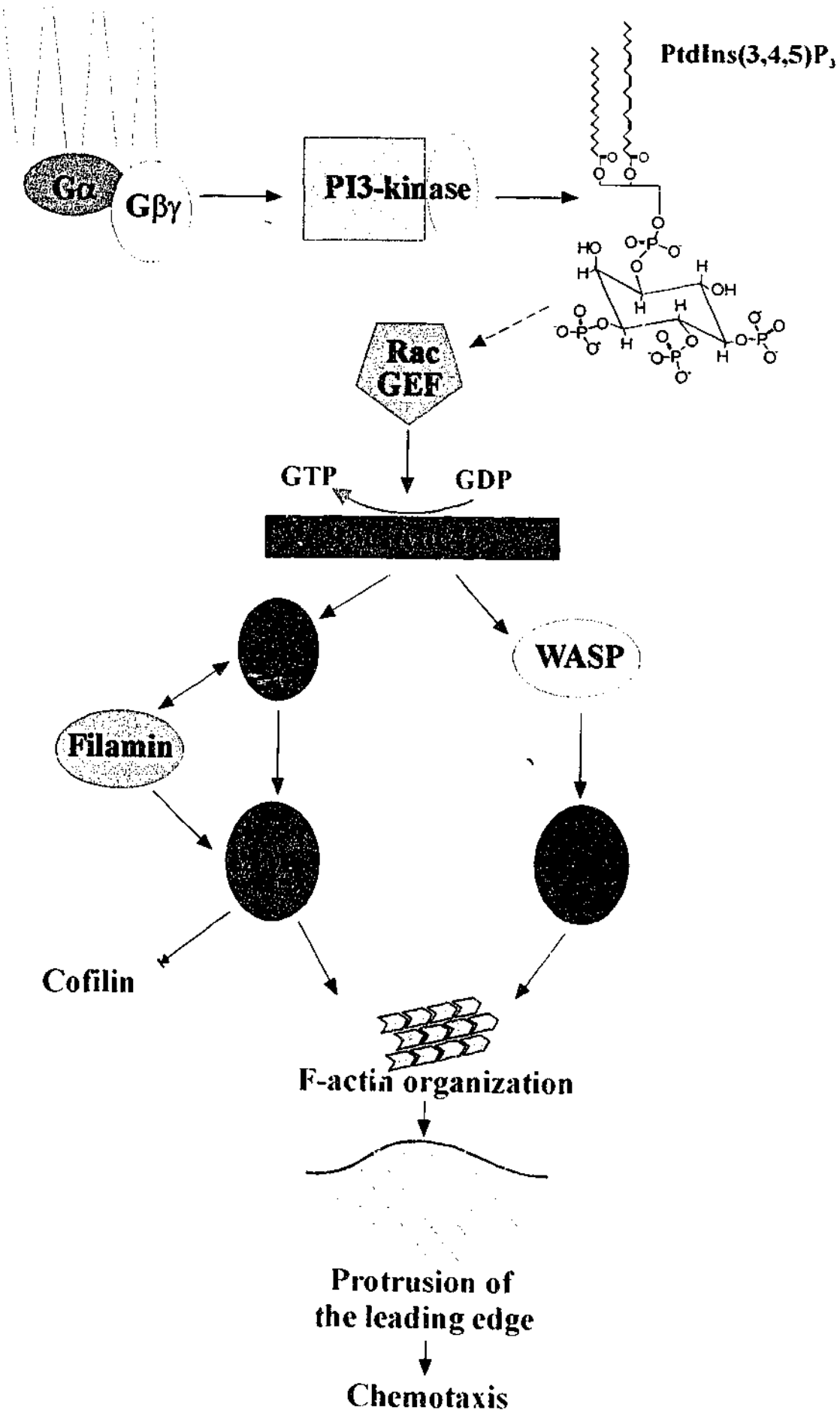
PtdIns(3,4,5)P3
Gα
Gβγ
PI3-kinase
Rac
GEF
GTP
GDP
WASP
Filamin
Cofilin
F-actin organization
Protrusion of
the leading edge
Chemotaxis

underlying PTEN's involvement in the inhibition of cell migration is contentious, with some studies emphasizing the role of the lipid phosphatase activity and other reports suggesting the importance of the protein phosphatase activity of PTEN (Liliental *et al.*, 2000; Tamura *et al.*, 1998; Tamura *et al.*, 1999).

A G129E mutant of PTEN, which retains it protein phosphatase activity but lacks its lipid phosphatase activity inhibits integrin-mediated cell migration, focal adhesions and cell spreading. However, the C124A mutant of PTEN, which lacks its protein phosphatase activity, cannot inhibit cell migration, this study suggesting the importance of the protein phosphatase activity of PTEN for its function (Tamura *et al.*, 1999). Additional studies reported by this group, has led to the identification of two distinct additive pathways regulating cell migration that are downregulated by PTEN. One involved in random migration identifies Shc and MAP kinase as key components, and the second involves FAK and $p130^{Cas}$ and more extensive cytoskeletal organization and directional cell motility (Gu *et al.*, 1999).

However, more recent studies have suggested the importance of the lipid phosphatase activity of PTEN and PtdIns(3,4,5)P_3 in cell migration (Liliental *et al.*, 2000; Wu *et al.*, 1998). Genetic deletion of PTEN in mouse fibroblasts leads to an increase in cell motility, as determined by "wound healing" assays, and elevated levels of PtdIns(3,4,5)P_3. In contrast to the aforementioned study, FAK and MAP kinase were not effected in PTEN-deficient cells. Reintroduction of wild-type and various mutants of PTEN suggested the enhanced motility observed in the PTEN-deficient cells is the result of the loss of PTEN phosphatase activity, particularly its lipid phosphatase activity. The PtdIns(3,4,5)P_3 effectors, Rac1 and Cdc42 and their associated activities in PTEN-deficient cells were assessed. In PTEN-deficient cells elevated levels of GTP-bound Rac1 and Cdc42 were observed. Moreover, pharmacological inhibition of PI3-kinase in these same cells resulted

in a decrease in the active forms of the RhoGTPases, Rac and Cdc42. Strikingly, retroviral infection of PTEN-deficient cells with dominant-negative forms of Rac1 and Cdc42 could reverse the cell migration phenotype by 100 % and 50 %, respectively (Liliental *et al.*, 2000).

Recent studies in *D.discoideum* have demonstrated that disruption of PTEN in the slime mould resulted in a dramatically broadened front, chemotaxis defects and prolonged actin polymerization responses to chemoattractants (Iijima and Devreotes, 2002). In *D.discoideum*, PTEN-knock in cells exhibit a decrease in the rate of chemotaxis and cell polarity (Funamoto *et al.*, 2002). Through a variety of localization studies in *D.discoideum* including, uniformly localizing PI3-kinase along the plasma membrane, and studies demonstrating that chemotaxis signaling pathways are activated along the lateral sides of the cells which can initiate pseudopod formation, a direct link for an instructional role of PI3-kinase in leading edge formation has been proposed.

Recently a second PTEN isoform has been identified, PTEN2, which displays similar enzyme activity to PTEN with a preference for PtdIns(3,5)P_2. Expression of PTEN2 is restricted to testis with Golgi membrane localization (Wu *et al.*, 2001).

1.4 Inositol polyphosphate 5-phosphatases

Phosphoinositide metabolism encompasses an array of specific kinase and phosphatase activities, one of which is provided by inositol polyphosphate-5-phosphatases (5-phosphatases). The 5-phosphatases are a family of enzymes which specifically remove the 5-position phosphate of the inositol ring of inositol polyphosphates and phosphoinositides (Erneux *et al.*, 1998; Majerus *et al.*, 1999). Historically, 5-phosphatases have been regarded as signal-terminating enzymes, however, some 5-phosphatase isoforms convert PtdIns(3,4,5)P_3 to PtdIns(3,4)P_2, which itself acts a signaling molecule. This has

led to the reclassification of 5-phosphatases as signal-modifying enzymes (Chan *et al.*, 1999; Majerus *et al.*, 1999).

Common to all 5-phosphatases, irrespective of substrate specificity, is a conserved domain of approximately 300 amino acids designated the "5-phosphatase domain" (reviewed by (Mitchell *et al.*, 1996)). Although six substrates have been identified as targets for 5-phosphatases, a particular enzyme may exhibit activity towards all, or only a subset of these inositol signaling molecules (reviewed by (Mitchell *et al.*, 1996)). Although the molecular basis of this substrate specificity is not known, elegant studies performed by Tsujishita *et al.*, and Whisstock *et al.*, have delineated a catalytic mechanism for 5-phosphatase substrate hydrolysis (Tsujishita *et al.*, 2001; Whisstock *et al.*, 2000).

In addition to the 5-phosphatase domain, most 5-phosphatase family members contain regulatory motifs or domains. These include, proline-rich domains (PRDs), Src-homology (SH2) domains and Sac1 domains, which mediate intracellular localization, phosphoinositide metabolism, and associations with other signaling or structural proteins (Figure 1.7). Due to the overlapping substrate activities of some 5-phosphatases, these regulatory domains must be important for defining the cellular role of specific 5-phosphatases.

1.4.1 SHIP-1

Structure

SHIP-1 was initially observed as a tyrosine-phosphorylated protein after stimulation of blood cells with a variety of growth factors and cytokines. The 145 kDa protein was named SH2-containing inositol phosphatase following cloning of the SHIP-1 cDNA (Damen *et al.*, 1996).

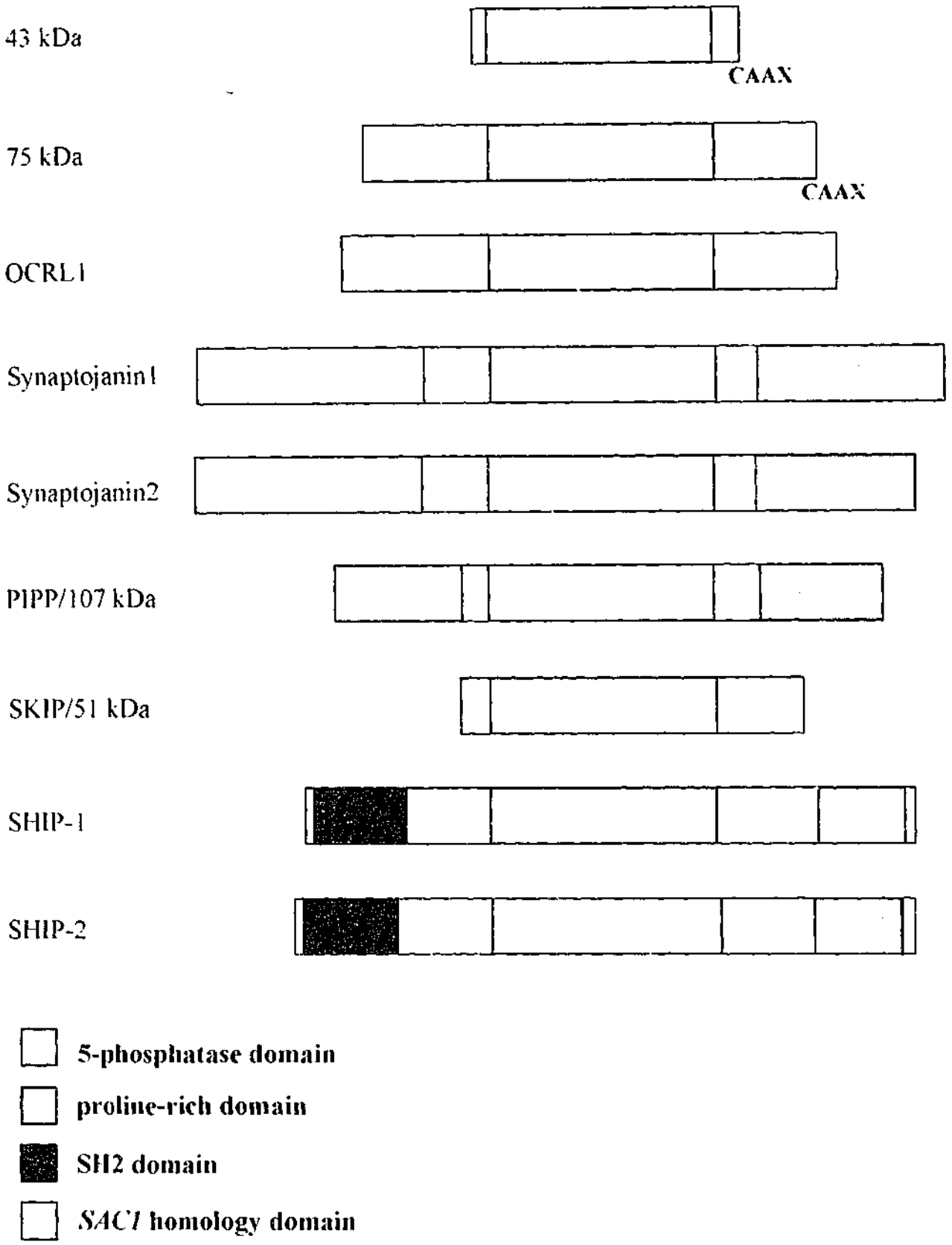

Figure 1.7 Domain structures of the mammalian inositol polyphosphate 5-phosphate 5-phosphatases.

Schematic representation of catalytic domains (5-phosphatase and SAC1 homology) and known structural motifs or signaling motifs (SH2, proline-rich and CAAX) identified within mammalian members of the 5-phosphatase family.

SHIP-1 is encoded by 1190 amino acids and contains several identifiable protein-protein interaction motifs. The primary structure of SHIP-1 comprises an SH2 at the N-terminus, a central conserved 5-phosphatase homology region, and an extensive carboxyl-terminal proline-rich domain. Within the carboxyl-terminal proline-rich domain of SHIP-1 lies two NPXY motifs, which undergo tyrosine phosphorylation and have potential for binding phosphotyrosine-binding (PTB)-domain-containing proteins, or possibly SH2 domain-containing proteins. The remainder of the carboxyl-terminal proline-rich domain has five potential polyproline motifs (PXXP) for binding SH3 domain-containing proteins. Three of the polyproline-rich motifs show very good consensus for SH3 domain binding, whilst the two other polyproline motifs have weaker homology (reviewed by (Rohrschneider *et al.*, 2000)). It is evident from the numerous protein-protein interaction motifs, that the functional significance of SHIP-1 will be dependent upon its protein interactions.

Isoforms

The cDNA encoding SHIP-1 was cloned in several laboratories using various methods, and a number of isoforms have been reported. Although the isolated cDNAs encoding for SHIP-1 have a calculated molecular weight of 133 kDa, endogenous SHIP-1 usually is detected as multiple polypeptides, with the 145 kDa form as the most abundant isoform (Geier *et al.*, 1997).

The multiple isoforms of SHIP-1 can arise from alternative transcriptional or translational initiation, proteolytic processing, alternative splicing, posttranslational modifications or a combination of these events. The resultant isoforms of SHIP-1 include isoforms lacking the amino-terminal SH2 domain, internal deletions and one isoform with 41 unique amino acids at its carboxyl terminus. For instance, a murine cDNA encoding SHIP-1 with deletion of 61 amino acids between the two PTB targets has been cloned from

the WEHI-3 myeloid cell line. This isoform is generated by alternative mRNA splicing (Lucas and Rohrschneider, 1999). Immunoblot analysis of the murine hemopoietic cell line DA-ER using several distinct SHIP-1 antibodies suggests the presence of C-terminal truncations of the full-length SHIP-1. Immunoblotting of the DA-ER cell line using a SHIP-1 antibody showed the presence of 145-, 135-, 125- and 110 kDa bands, however, only the 145- and 135 kDa polypeptides could be detected when immunoblotting with a C-terminal SHIP-1 antibody (Damen *et al.*, 1998).

In a search evaluating expression of the SHIP-1 gene, it was recently identified that embryonic stem cells express SHIP-1 mRNA. These studies demonstrated that transcription from an internal site within the SHIP-1 gene promotes expression of s-SHIP-1, which lacks the SH2 domain, in totipotent embryonic stem cells and hematopoietic stem cells, but not in mature hematopoietic cells (Tu *et al.*, 2001).

Expression

The expression of SHIP-1 is mostly restricted to hematopoietic cells, with protein detected in all cell lineages of bone marrow and blood. Northern blot analysis has detected SHIP-1 mRNA expression at the earliest stages of hematopoietic cell development in mouse embryos, and protein expression has been observed in all blood cell lineages (Geier *et al.*, 1997; Liu *et al.*, 1998b). Furthermore, expression of SHIP-1 is developmentally regulated in T cell maturation, but remains constant in B cells (Liu *et al.*, 1998b). The expression pattern of different SHIP-1 isoforms is developmentally regulated during hemopoiesis with levels of larger isoforms increasing with cell maturation (Geier *et al.*, 1997). Apart from hemopoietic cells, SHIP-1 expression has been detected in histochemically in testis, specifically at the membranes of spermatids, however the role of SHIP-1 in spermatogenesis has not been established (Liu *et al.*, 1998b).

Several reports have demonstrated SHIP-1 mRNA expression in tissues such as spleen, testis, liver, lung, and brain. However, it is possible that these tissues were contaminated with blood cells and expression should be confirmed with histochemical detection (reviewed by (Rohrschneider *et al.*, 2000)).

Enzymatic activity

The central catalytic domain of murine and human SHIP-1 is tightly conserved, with 96 % identity between the two (Ware *et al.*, 1996). SHIP-1's enzyme activity removes the 5' position phosphate group from the inositol ring of not only the 3' position phosphorylated lipids, PtdIns(3,4,5)P_3, Ins(1,3,4,5)P_4, but in addition PtdIns(4,5)P_2 (Damen *et al.*, 1996; Lioubin *et al.*, 1996). The enzymatic activity of SHIP-1 is not affected by its association with adaptor proteins or by cytokine stimulation, however, there are conflicting reports as to whether the tyrosine phosphorylation status of SHIP-1 may be an influencing catalyst to its activity (Damen *et al.*, 1996; Giuriato *et al.*, 1997; Jefferson *et al.*, 1997; Osborne *et al.*, 1996). However, it has been suggested SHIP-1's enzymatic activity is affected by its localization (Phee *et al.*, 2000). Upon cell stimulation with a growth factor, cytoplasmic SHIP-1 is transported to sites near the lipid substrates at the plasma membrane. SHIP-1 5-phosphatase activity was only detected in Shc immunoprecipitates from IL-3-stimulated hemopoietic cells, but not from unstimulated cells, suggesting a cytokine-induced change in the localization of SHIP-1. Furthermore, tyrosine phosphorylation of SHIP-1 in thrombin-stimulated platelets did not alter enzyme activity of SHIP-1, but was found to induce translocation of the enzyme to the actin cytoskeleton (Giuriato *et al.*, 1997).

Interactions with proteins

The protein structure of SHIP-1 contains numerous protein-protein interaction motifs, such as, SH3 binding motifs, PTB and SH2 binding motifs, as well as a SH2

domain for binding to phosphorylated motifs (reviewed by (Rohrschneider *et al.*, 2000)). The biological function of SHIP-1 probably depends on its interactions with upstream and downstream proteins.

Interaction with Shc and Grb2

Shc and Grb2 are widely expressed adaptor proteins involved in mitogenic signaling through the Ras/MAPK pathway (Luttrell *et al.*, 1999). Grb2 contains two SH3 domains and one SH2 domain, whilst Shc contains an SH2 domain and a PTB domain. Through these protein-binding modules Grb2 and Shc associate with various cellular proteins and bring these associated proteins into close proximity to sites of receptor activation (Lewis *et al.*, 1998). *In vitro* and *in vivo* immunoprecipitation studies have shown the proline-rich motifs of SHIP-1 bind to the SH3 domain of Grb2. SHIP-1s association with Shc occurs *via* its PTB domain and the phosphorylated-NPXY motifs of SHIP-1. The role of SHIP-1's SH2 domain mediating this interaction is contentious.

The exact mechanism for association between SHIP-1 and Grb2 is as contentious as that for the SHIP-1 and Shc association. Early *in vivo* and *in vitro* studies investigating the association of SHIP-1 and Grb2 found SHIP-1 binds to the SH3 domain of Grb2 (Damen *et al.*, 1996; Jefferson *et al.*, 1997; Kavanaugh *et al.*, 1996). However, more recent studies have suggested the association is mediated by the SH2 domain of Grb2 binding to a phosphotyrosine residue N-terminal of 5-phosphatase domain of SHIP-1 (Huber *et al.*, 1999).

The association of SHIP-1 with Shc and Grb2, raises the question whether Grb2 is essential for efficient binding of Shc and SHIP-1, analogous to the Sos/Shc/Grb2 heterotrimeric complex. Analysis of the association between SHIP-1 and Shc in a Grb2-deficient cell line suggests that indeed Grb2 is necessary for efficient association of the two species (Harmer and DeFranco, 1999). The Sos/Shc/Grb2 are involved in the Ras/MAPK

pathway and therefore association of SHIP-1 with Shc and Grb2 may block or interfere with the Sos/Shc/Grb2 complex and subsequently block activation of the Ras pathway.

Role in receptor signaling

Antigen-induced aggregation of the B-cell receptor (BCR) on the surface of B lymphocytes initiates a series of activating pathways including the Ras signaling pathway. The Ras signaling pathway is activated following signal transduction *via* the immunoreceptor tyrosine-based activation motif (ITAM) located on the cytoplasmic tail of the BCR. Negative signaling in B cells is mediated by the FcγRIIB receptor. Association of SHIP-1 with the immunoreceptor tyrosine-based inhibitory motif (ITIM) in B cells and studies demonstrating the association of SHIP-1 and Shc is promoted under negative signaling conditions, suggests SHIP-1 could negatively regulate growth factor-induced signaling in immune cells (Ono *et al.*, 1996).

A current model proposes that upon co-ligation of FcγRIIB and the BCR, SHIP-1 is recruited *via* its SH2 domain to the phosphorylated ITIM, where it is itself phosphorylated (Figure 1.8) (Kiener *et al.*, 1997; Ravetch and Lanier, 2000; Tridandapani *et al.*, 1997; Vely *et al.*, 1997). The kinase responsible for this phosphorylation event has not yet been identified, however, SHIP-1 can be phosphorylated by the Src family of kinases *in vitro* and *in vivo* (Phee *et al.*, 2000). Following tyrosine phosphorylation of SHIP-1, Shc associates *via* its PTB domain with SHIP-1, and promotes Shc phosphorylation (Ingham *et al.*, 1999). Kinetic analyses, performed in stimulated murine B cells, by immunoprecipitation of SHIP-1 and immunoblotting to detect FcγRIIB and Shc demonstrated the association of SHIP-1 with the FcγRIIB was more rapid than association with Shc. Affinity analysis using the recombinant SH2 domain of SHIP-1 and phosphopeptides corresponding to phospho-Shc and FcγRIIB-ITIM demonstrated the affinity of SHIP-1 for the latter phosphopeptide was lower, because of a greater

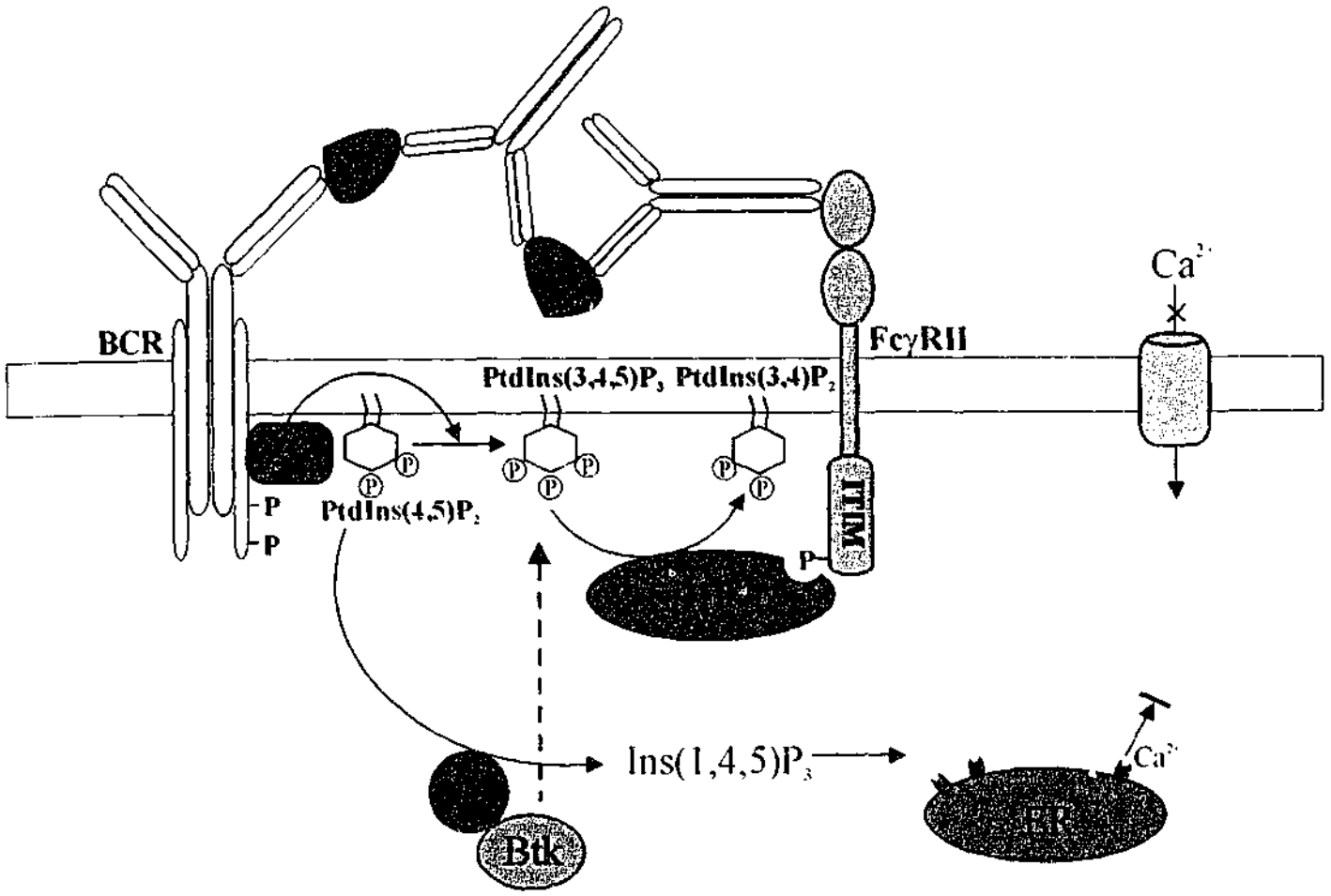

Figure 1.8 SHIP-1-mediated inhibition of B cell activation.

Recruitment of phosphoinositide 3-kinase (PI3-K) by activated immunoreceptors such as the B cell antigen receptor (BCR) leads to production of PtdIns(3,4,5)P_3 which can bind to various PH-domain-containing proteins such as phospholipase Cγ (PLCγ) and Bruton's tyrosine kinase (Btk). Co-ligation of the inhibitory FcγRIIB receptor with the BCR by soluble antibody leads to phosphorylation of the ITIM (immunoreactive tyrosine based inhibitory motif) sequence of FcγRIIB resulting in recruitment of SHIP-1. SHIP-1-mediated hydrolysis of PtdIns(3,4,5)P_3-dependent responses such as sustained calcium signaling by inhibition of PLCγ-mediated production of Ins(1,4,5)P_3 from PtdIns(4,5)P_2 (adapted from Ravetch and Lanier, 2000).

dissociation rate (Ingham *et al.*, 1999; Tridandapani *et al.*, 1999). Collectively, these observations support a model that SHIP-1, following association with FcγRIIB, competes with Grb2 for binding to Shc, leading to downregulation of the Ras signaling pathway.

Negative signaling in mast cells is induced by crosslinking of the FcγRIIB with FcεRI and FcγRIII leading to inhibition of calcium mobilization and degranulation. As in B cells, SHIP-1 is able to bind to the phosphorylated ITIM sequence of the FcγRIIB. Under negative signaling conditions SHIP-1 is also able to bind to the ITAM sequence of the FcεRI (Kimura *et al.*, 1997; Ono *et al.*, 1996; Osborne *et al.*, 1996). SHIP-1 *via* its SH2 domain has been demonstrated to associate with SHP-2 in IL-3 stimulated mast cells, implicating this phosphatase in the dephosphorylation of SHIP-1. A recent report using SHIP-1-/- bone marrow derived mast cells has demonstrated that SHIP-1 represses IL-6 mRNA levels (Kalesnikoff *et al.*, 2002).

SHIP-1 has been shown to bind to ITIM sequences of a number of receptors, such as, the gp49B1 in mast cells and PECAM-1/CD3 in platelets (Kuroiwa *et al.*, 1998; Pumphrey *et al.*, 1999). *In vitro* interactions of SHIP-1 with ITAM-containing receptors has also been reported in monocytes and T cells. However, the role of SHIP-1 in ITAM-mediated signaling is not clear (reviewed by (Rohrschneider *et al.*, 2000)).

Association with other proteins

SHIP-1 has been shown to interact with a number of other proteins, apart from Shc and Grb2, however the association with some of these proteins is not as well characterized.

The protein tyrosine phosphatase, SHP-2, has been shown to co-precipitate with the SHIP-1. More specifically, the SH2 domain of SHIP-1 was able to mediate the co-precipitation from cell lysates, although a direct association of SHIP-1 and SHP-2 has not been described. Potentially, the SHIP-1-SHP-2 interaction may be responsible for the

observed dephosphorylation of SHIP-1 or a protein associated with SHIP-1 (Sattler *et al.*, 1997).

The Gab family of proteins are scaffolding proteins that participate in many signaling pathways activated by various cytokines and growth factors. Direct association of the Gab family of proteins with Grb2, the p85 subunit of the PI3-kinase and the tyrosine phosphatase SHP-2 have been identified. SHIP-1 has been shown to associate with the Gab (Grb2-associated binder) family of proteins, in particular tyrosine phosphorylated Gab-1 and Gab-2. It is presumed that association is mediated by the SH2 domain of SHIP-1, however, direct association between SHIP-1 and Gab-1 or Gab-2 has not been confirmed (Lecoq-Lafon *et al.*, 1999; Liu *et al.*, 2001).

The p85 subunit of the PI3-kinase contains two SH2 domains which have similar binding specificities that are present in SHIP-1. Using GST-p85 SH2 fusion proteins with SHIP-1 and phosphotyrosine antibodies, have demonstrated a direct association between the SH2 domain of the p85 subunit of the PI3-kinase and SHIP-1, but not tyrosine-phosphorylated SHIP-1. Alteration of the p85 SH2 domain-binding motif in SHIP-1, as seen in the SHIP-1β isoform, reduces association between the two species. To date, this association has only been demonstrated with murine proteins (Gupta *et al.*, 1999; Lucas and Rohrschneider, 1999).

The association of the carboxyl terminus of non-phosphorylated SHIP-1 and a protein inhibitor of STAT1 called PIAS1 (for protein inhibitor of activated STAT1) has also been demonstrated (reviewed by (Rohrschneider *et al.*, 2000)). *In vitro* studies have also shown binding of SHIP-1 to the neuronal protein disabled 1 (Dab-1) (Howell *et al.*, 1999).

SHIP-1 knockout mice

Targeted disruption of SHIP-1, generated by homologous recombination, results in mice that are viable and fertile, but the life span of the homozygous-null animals is decreased due to myeloid infiltration of the lungs. SHIP-1-deficient mice exhibit marked increases in the numbers of granulocyte-macrophage progenitors in the bone marrow and spleen, probably the result of the enhanced sensitivity observed in SHIP-$1^{-/-}$ granulocyte-macrophage progenitors to multiple cytokines including IL-3, GM-CSF, M-CSF and Steel factor (SF) (Helgason *et al.*, 1998).

There are several signal transduction pathways that may be involved in the abnormal proliferation and differentiation patterns of certain hemopoietic cell populations in SHIP-1 null mice, including aberrant Ras activation resulting from deregulated Shc and SHP-2 activities, or increased Akt activation. Alternatively, the loss of the 5-phosphatase enzyme activity may contribute or be responsible for the enhanced proliferative potential of the SHIP-1 null granulocyte-macrophage progenitors as PtdIns(3,4,5)P_3 is capable of stimulating PKC, as well as modulating Akt activity. In an attempt to identify the signaling pathways involved, further characterization has been performed on isolated lymphocytes and myeloid cells from SHIP-1 -/- mice.

Isolation of bone marrow-derived mast cells (BMMCs) from SHIP-1 -/- and subsequent treatment with SF and IgE resulted in massive degranulation which was not observed in SHIP-1 +/+ and +/- cells (Huber *et al.*, 1998a; Huber *et al.*, 1998b). This increase in degranulation from SHIP-1 -/- BMMCs was not due to increased expression of the SF receptor and c-kit as analyzed by immunoblotting and FACS, but was associated with substantially higher PtdIns(3,4,5)P_3 levels which enhanced extracellular calcium release preceded by intracellular calcium release (Huber *et al.*, 1998b). Introduction of wild-type SHIP-1 into SHIP-1 -/- mast cells inhibited SF-induced increases in

PtdIns(3,4,5)P_3, calcium levels and degranulation confirming the absence of SHIP-1 was responsible for these responses. Recent studies comparing cytokine production by mast cells from SHIP-1 -/- and SHIP-1 +/+ littermates demonstrated that SHIP-1 negatively regulates IL-6 mRNA and protein levels in IgE+Ag-stimulated mast cells. Furthermore, the 5-phosphatase activity of SHIP-1 and a reduction in activity of Akt, PKC, p38 and extracellular signal-related kinase (ERK) was essential for this negative effect (Brauweiler *et al.*, 2001; Liu *et al.*, 1999).

In B cells, coligation of the BCR and the FcγRIIB leads to the inhibition of calcium influx, resulting in a reduction of BCR signaling. Deletion of SHIP-1 in B cells abrogates FcγRIIB-mediated inhibition of calcium influx, confirming the role of SHIP-1 in B cell signaling. Recent studies, however, have demonstrated that lipopolysaccharide (LPS)-activated B cells from SHIP-1-deficient mice exhibit significant FcγRIIB-mediated inhibition of calcium mobilization and Ins(1,4,5)P_3 production, in addition to ERK and Akt phosphorylation (Brauweiler *et al.*, 2001). Less pronounced changes were detected in SHIP-1 -/- T cells suggesting a minor role for SHIP-1 in T cell receptor signaling (Liu *et al.*, 1998a).

Recently, some compelling studies analyzing the bones of SHIP-1-deficient mice has suggested a role for SHIP-1 in osteoclast formation and function. Moreover, the loss of SHIP-1 results in severe osteoporosis. SHIP-1 -/- mice have elevated numbers of osteoclast-precursor cells (macrophages) and a 2-fold increase in the number of osteoclasts which is due to the prolonged life span of these cells and the hypersensitivity of the precursors to their differentiating factors, M-CSF and nuclear factor-kappa B ligand (RANKL). The osteoclasts from SHIP-1-deficient mice are reminiscent of Pagetic osteoclasts, enlarged, containing more than 100 nuclei and display enhanced resorptive activity. Moreover, SHIP-1 -/- mice exhibit numerous characteristics consistent with

accelerated osteoclast resorptive activity, resulting in a 22 % loss of bone-mineral density, and a 49 % decrease in fracture energy, resulting in severe osteoporosis (Takeshita *et al.*, 2002).

1.4.2 SHIP-2

Cloning and Structure

INPPL-1 (inositol polyphosphate-like protein 1) was inadvertantly cloned in a search for genes that correct one of the *in vitro* defects of Fanconi anaemia group A cells. The complete cDNA sequence, 4657 nucleotides, defines an open reading frame of 3441 nucleotides, encoding for a protein with a predicted molecular weight of 126 kDa. The C-terminal region of INPPL-1 is proline-rich. Northern blot analysis revealed widespread distribution in tissues such as, kidney, skeletal muscle, lung, pancreas, placenta, heart, liver and brain (Hejna *et al.*, 1995).

Human SHIP-2 (SH2-containing inositol polyphosphate 5-phosphatase-2) was cloned using primers designed to highly conserved amino acid regions that is shared between 5-phosphatases (Pesesse *et al.*, 1997). The SHIP-2 cDNA was 99 % identical to INPPL-1, however, the sequence differs from INPPL-1 at both the N- and C-terminal ends. SHIP-2 probably represents the same gene as INPPL-1, with sequence differences possible representing sequencing of an unspliced intron upstream of the catalytic domain, and an artificial frameshift downstream, in the INPPL-1 sequence. The translated sequence for SHIP-2 encodes a 1258 amino acid protein with a predicted molecular mass of 142 kDa. The deduced N-terminal sequence of SHIP-2 suggested an SH2 domain. Alignment of the amino acid of SHIP-2 with SHIP-1 revealed similar structural domains, an N-terminal SH2 domain, a central catalytic 5-phosphatase domain and a C-terminal proline-rich domain (PRD). In addition, a high degree of identity was observed between the SH2 domains and

catalytic 5-phosphatase domains of SHIP-2 and SHIP-1, 54 % and 64 %, respectively. However, although the PRDs of SHIP-2 and SHIP-1 contain numerous PXXP motifs and NPXY motif(s), for binding SH3 domain containing proteins, and SH2 or PTB-domain containing proteins respectively, no significant homology is observed between the PRDs of SHIP-2 and SHIP-1. The uniqueness of the PRDs suggests that this region may interact with different proteins, regulating distinct biological functions and signaling pathways. Unlike SHIP-1, SHIP-2 also contains a sterile alpha motif (SAM) within its PRD which acts as a protein interaction module through the ability to homo- and hetero-oligomerize with other SAM domain-containing proteins (Pesesse *et al.*, 1997; Schurmans *et al.*, 1999).

Murine SHIP-2 was assembled following screening of mouse thyroid and mouse brain cDNA libraries, using a human SHIP-2 cDNA probe. Rat SHIP-2 was cloned using a direct PCR-based cloning strategy. Murine SHIP-2 shares 95 % identity with human SHIP-2, whereas rat SHIP-2 shares 92 % identity. Overall the structural domains are conserved amongst the three species. However, a rat SHIP-2 cDNA, thought to be a splice variant, has been isolated from skeletal muscle, which is 74 amino acids shorter than human SHIP-2, and lacks the SAM domain (Ishihara *et al.*, 1999; Schurmans *et al.*, 1999).

Expression

In contrast to SHIP-1, where expression is mainly limited to cells of hemopoietic origin, SHIP-2 expression is widespread including fibroblasts and non-hemopoietic tumor cell lines. Northern blot analysis has demonstrated particularly high expression of SHIP-2 in heart, skeletal muscle and placenta. Immunoblot analysis of SHIP-2 expression has confirmed the Northern blot data, with expression also noted in lung, thymus, brain and spleen tissues. Mechanical dissociation of spleen cells into T-cell enriched spleen cells and B-cell enriched spleen cells and immunoblotting these fractions with a SHIP-2 specific antibody, suggested expression of SHIP-2 in B cells (Muraille *et al.*, 1999).

Consistent with human SHIP-2 expression, murine SHIP-2 is widely expressed. In the developing embryo, E15.5, expression of murine SHIP-2 was detected in a multitude of tissues with highest expression observed in liver, brain and thymus. In the adult mice, murine SHIP-2 was again detect in every tissue tested however, highest expression was observed in brain and thymus (Muraille *et al.*, 2001).

Although the predicted molecular weight of human SHIP-2 is 142 kDa, several studies have detected 150-160 kDa polypeptides using SHIP-2 specific antibodies (Muraille *et al.*, 1999; Pesesse *et al.*, 2001; Wisniewski *et al.*, 1999). This increased molecular mass of SHIP-2 observed could be due to post-translation modification such as phosphorylation.

Enzymatic activity

The catalytic 5-phosphatase domain of SHIP-2 and SHIP-1 share 64 % identity at the amino acid level. The catalytic activity of these two enzymes does overlap, however hydrolysis of Ins(1,3,4,5)P_4 by SHIP-2 is contentious. Lysates from M07 and K562 cells were immunoprecipitated with anti-SHIP-2 antibodies in the presence or absence of antigenic peptide and the immunoprecipitates were assessed for Ins(1,3,4,5)P_4 and PtdIns(3,4,5)P_3 activity. Immunoprecipitates of SHIP-2, like SHIP-1, hydrolyzed the 5' phosphate from the PtdIns(3,4,5)P_3, but not in the presence of the antigenic peptide. SHIP-2 immunoprecipitates did not hydrolyze Ins(1,3,4,5)P_4 (Wisniewski *et al.*, 1999). In contrast, expression of recombinant SHIP-2 in bacteria, expressing the SH2 domain and catalytic domain of SHIP-2, was demonstrated to hydrolyze Ins(1,3,4,5)P_4 (Pesesse *et al.*, 1998).

In vivo studies have confirmed the PtdIns(3,4,5)P_3 enzymatic activity of SHIP-2. Transfection of 3T3-L1 adipocytes with wild-type SHIP-2 or 5-phosphatase defective SHIP-2 and analysis by HPLC of the extracted lipids confirmed the PtdIns(3,4,5)P_3 5-

phosphatase activity (Wada *et al.*, 2001). *In vitro* studies have investigated the role of various domains/motifs of SHIP-2 in regulating PtdIns(3,4,5)P_3 5-phoshatase activity. Overexpression in U87-MG cells of wild-type SHIP-2, or mutated forms of SHIP-2, which have either mutations in the conserved FLVR motif within the SH2 domain, or the C-terminal tyrosine phosphorylation site (NPXY) were subsequently immunoprecipitated, purified, and were tested for their ability to hydrolyze PtdIns(3,4,5)P_3. Wild-type SHIP-2 and the SHIP-2 mutants were all able to dephosphorylate PtdIns(3,4,5)P_3 to produce PtdIns(3,4)P_2, suggesting that at least *in vitro* these motifs are not essential for 5-phosphatase activity (Pesesse *et al.*, 2001; Taylor *et al.*, 2000).

Overexpression of SHIP-2 in U87-MG cells using adenoviruses has demonstrated a reduction in PtdIns(4,5)P_2 levels in a time-dependent manner, suggesting that SHIP-2 may also hydrolyze this phospholipid (Taylor *et al.*, 2000). Expression of SHIP-2 recombinant protein and 5-phosphatase assays has demonstrated that SHIP-2 does not hydrolyze Ins(1,4,5)P_3 (Pesesse *et al.*, 1998).

Interaction with proteins

SHIP-1 and SHIP-2 share major structural similarities, overlapping substrates and expression. The overall amino acid identity between the two enzymes is 38 %, with the highest identity occurring in the 5-phosphatase and SH2 domains, 64 % and 54 %, respectively (Pesesse *et al.*, 1998). Within the C-terminal PRDs of SHIP-1 and SHIP-2 there is no significant homology, suggesting that this region may be important for defining their distinct biological roles, through protein-protein interactions. The C-terminal PRD of SHIP-2 contains numerous SH3 domain containing protein binding sites, a PTB binding site (NPXY) for interaction with PTB domain containing proteins and a SAM domain, which may mediate hetero- or homo-dimerization. Literature describing association of SHIP-2 with other proteins is only just emerging.

Association with Shc

Due to the structural similarities between SHIP-2 and SHIP-1, several groups have investigated whether SHIP-2, like SHIP-1, is tyrosine phosphorylated and associated with Shc following growth factor stimulation. Immunoprecipitation of SHIP-2 from growth factor-stimulated SH-SY5Y, PC12 cells and 3T3-L1 adipocytes with a SHIP-2 specific antibody and immunoblotting these immunoprecipitates with an anti-phosphotyrosine antibody revealed that SHIP-2 is tyrosine phosphorylated in response to EGF and PDGF with maximal phosphorylation noted at 5-10 minutes post-stimulation, returning to control levels after 20 minutes stimulation. In contrast, IGF-1, insulin, and NGF induced long term tyrosine phosphorylation of SHIP-2 with 40-80 % maximal levels maintained for up to 2 hours following stimulation. In some SHIP-2 immunoprecipitates, 52- and 66-kDa tyrosine phosphorylated proteins were detected. The identity of these were confirmed as Shc, however, interestingly the association of Shc with SHIP-2 was only observed in response to EGF, PDGF and NGF (Habib *et al.*, 1998).

Investigation of hematopoietic growth factor-dependent cell lines, where SHIP-1 is also expressed, demonstrated Stem cell factor, IL-3 and GM-CSF also induced tyrosine phosphorylation of SHIP-2, and association with Shc. Constitutive tyrosine phosphorylation of SHIP-2 was observed in SHIP-2 immunoprecipitates of chronic myelogenous leukemia progenitor cells. Immunoprecipitates of Shc from K562 lysates demonstrated co-precipitation with SHIP-2 and the $p210^{bcr/abl}$ tyrosine kinase. GST-fusion-protein pull-down assays from the $p210^{bcr/abl}$ expressing cell line $R10^{+}$, demonstrated phosphorylated SHIP-2 selectively binds the to the PTB domain of Shc and the SH3 domain of Abl (Wisniewski *et al.*, 1999). Furthermore, immunoprecipitation of the EGF receptor from COS-7 cells demonstrated co-precipitation of SHIP-2 and Shc, however, a direct association between SHIP-2 and the EGF receptor has not been demonstrated

(Pesesse *et al.*, 2001). Extension of these studies has demonstrated that tyrosine phosphorylation of SHIP-2 does not effect its enzyme activity (Pesesse *et al.*, 2001). Furthermore, SHIP-2-dependent inhibition of Akt activity has been demonstrated in COS-7 and U87-MG glioblastoma cells, and like PTEN, in the latter cell line, SHIP-2 was demonstrated to effect cell cycle progression (Pesesse *et al.*, 2001; Taylor *et al.*, 2000).

A role for SHIP-2 regulating cell adhesion and spreading has recently been suggested (Prasad *et al.*, 2001). Immunoprecipitation of SHIP-2 from HeLa cell lysates and immunoblotting of these immunoprecipitates with an anti-phosphotyrosine antibody revealed the presence of 105, 110 and 120 kDa polypeptides, which were identified as $p130^{cas}$, an adaptor protein that mediates actin cytoskeletal reorganization. GST pull-down assays from 293T cell lysates identified the SH2 domain of SHIP-2 as the domain mediating the adhesion-dependent interaction with phosphorylated $p130^{cas}$. Intracellular localization studies of SHIP-2 in adherent HeLa cells revealed localization to peripheral membrane protrusions, lamellipodia and diffuse perinuclear cytoplasmic staining. However, when HeLa cells were plated onto collagen-coated coverslips, SHIP-2 localized primarily to focal adhesions in the initial stages of cell spreading and at later stages to lamellipodia. Transfection of HeLa cells with truncation mutants of SHIP-2, which lacked the catalytic domain or had a single residue mutation within the SH2 domain rendering the SH2 domain defective, suggested the requirement of the SH2 domain for peripheral membrane localization (Prasad *et al.*, 2001).

The cellular significance on adhesion was investigated. Transient overexpression of wild type SHIP-2 in HeLa cells stimulated a two- to three-fold increase in the number of adherent cells compared to control groups. Deletion of the catalytic domain promoted adhesion to a lesser extent than wild-type SHIP-2, however the SH2-defective mutant was inactive, suggesting SHIP-2 SH2 domain interactions were important for this effect. Wild-

type SHIP-2 promoted cell spreading, whilst the catalytically inactive mutant of SHIP-2 had a lesser effect. Overexpression of the SH2 domain defective SHIP-2 had no effect on cell spreading (Prasad *et al.*, 2001).

Role in insulin signaling

A significant role for SHIP-2 has emerged in signaling pathways downstream of insulin receptor activation. Insulin-induced Akt activation and translocation of the glucose reporter GLUT4 in skeletal muscle and adipocytes is largely dependent on PI 3-kinase activation and the production of PtdIns(3,4,5)P_3 and PtdIns(3,4)P_2 (Cheatham *et al.*, 1994; Kotani *et al.*, 1995). Unlike SHIP-1, SHIP-2 has been detected in adipose tissue, and recent studies have investigated the role of SHIP-2 in insulin signaling.

Insulin treatment induces autophosphorylation and activation of the insulin receptor β-subunit, leading to phosphorylation of various substrates including insulin receptor substrate, IRS-1 and Shc, to propagate the insulin signal downstream. In insulin-stimulated Rat1 fibroblasts, expressing insulin receptors, endogenous SHIP-2 was tyrosine-phosphorylated within 1 minute, persisting for greater than 15 minutes. Stable overexpression of SHIP-2 in these cells, resulted in greater and faster phosphorylation of SHIP-2 in response to insulin. Overexpression of SHIP-2 did not effect tyrosine-phosphorylation of the insulin receptor β-subunit, IRS-1 or Shc, indicating SHIP-2 does not interfere with the most proximate events in the insulin signaling pathway. However, overexpression of SHIP-2 did interfere with association of Shc with Grb2, resulting in attenuation of signaling through the Ras pathway, reducing MAP kinase activation (Ishihara *et al.*, 2002).

Overexpression of SHIP-2 did not effect insulin-mediated IRS-1 association with p85, indicating SHIP-2 does not act upstream of insulin-induced PI 3-kinase activation. However, insulin-mediated Akt activation, a downstream effector of PI 3-kinase, was

inhibited by overexpression of SHIP-2. These same studies demonstrated overexpression of SHIP-2 arrested insulin-induced mitogenesis (Ishihara *et al.*, 1999), findings consistent with more recent studies in which overexpression of SHIP-2 inhibited Akt activity and induced cell cycle arrest in glioblastoma cells (Taylor *et al.*, 2000). Studies in CHO cells, expressing the insulin receptor (CHO-IR cells), has confirmed the previous observations that overexpression of SHIP-2 results in aberrant MAP kinase and Akt signaling in response to insulin. The catalytic activity of SHIP-2 was essential for maximal inhibition of Akt, but not MAP kinase (Blero *et al.*, 2001). Studies performed in L6 myotubes, have demonstrated overexpression of SHIP-2 reduces insulin-induced phosphorylation of glycogen synthase kinase GSKβ, an important mediator of insulin-induced glycogen synthesis, and consequently, SHIP-2 negatively regulates glycogen synthase activity and thus, glycogen synthesis. The catalytic activity of SHIP-2 was essential for these events (Sasaoka *et al.*, 2001).

The generation of SHIP-2-deficient mice has further cemented a role for SHIP-2 as an essential negative regulator of insulin signaling events *in vivo* (Clement *et al.*, 2001). At birth SHIP-2 -/- mice were phenotypically indistinguishable from their littermates, although progressive decreased feeding, lethargy and paleness was noted, phenotypes often associated with hypoglycemia. Although no difference was observed 2 to 8 hours post delivery, by 10 to 15 hours postpartum, the blood glucose concentration in SHIP-2 -/- mice compared to SHIP-2 +/- and +/+ mice was significantly lower. SHIP-2 -/- mice could be transiently rescued by injection with D-glucose within 24 hours postpartum. Prolonged survival could be induced by injection with a neutralizing antibody to insulin, within one hour of birth. Pancreatic islets were normal in these animals as were insulin levels suggesting hypoglycemia in SHIP-2 -/- mice is not caused by an increase in the production of insulin, but rather results from an increased sensitivity to insulin. Moreover, the absence

of SHIP-2 led to a decrease in several gluceogenic enzymes, further contributing to the hypoglycemia.

Adult SHIP-2 +/- mice demonstrated an increase in the translocation of the GLUT4 glucose transporter to the cell surface (Clement *et al.*, 2001). After overnight fasting, the amount of GLUT4 in the myocyte membrane was low, but similar in SHIP-2 +/+ and SHIP-2 +/- mice. However, when SHIP-2 +/+ and SHIP-2 +/- mice were loaded with insulin, the plasma membrane GLUT4 levels were higher in the heterozygous mice skeletal muscles. The loss of a SHIP-2 allele also affected glycogen synthesis. In the presence of physiological concentrations of insulin, 0.1 and 0.3 mM, glycogen synthesis in SHIP-2 +/- muscles compared to SHIP-2 +/+ muscles was increased 3.6-fold and 1.5-fold, respectively. Taken together this data indicates that insulin sensitivity is significantly increased in skeletal muscles from heterozygous SHIP-2 +/- mice.

Histological analysis of various organs, hematopoietic cell analysis and lack of tumors in SHIP-2 +/- and SHIP-2 +/+ mice showed *in vivo* SHIP-2's major role appears downstream of insulin signaling (Clement *et al.*, 2001).

Collectively, these studies demonstrate SHIP-2 as a critical negative regulator of insulin signaling and identify SHIP-2 as a potential therapeutic target for the treatment of type II diabetes (Clement *et al.*, 2001).

1.4.3 43 kDa 5-phosphatase

The 43 kDa 5-phosphatase specifically dephosphorylates $Ins(1,4,5)P_3$ and $Ins(1,3,4,5)P_4$ and functions as a negative regulator of $Ins(1,4,5)P_3$-induced Ca^{2+} release (Erneux *et al.*, 1998). Purification of the 43 kDa 5-phosphatase from platelets proposed the 5-phosphatase was phosphorylated by protein kinase C, resulting in an increase in enzymatic activity (Connolly *et al.*, 1986), although studies using recombinant 43 kDa 5-

phosphatase could not demonstrate phosphorylation by protein kinase C (Erneux *et al.*, 1995). However, co-immunoprecipitation of the 43 kDa from platelets demonstrated association with the kinase substrate, pleckstrin, which when in its phosphorylated form can associated with the 43 kDa 5-phosphatase and stimulate its activity (Auethavekiat *et al.*, 1997). Furthermore, complex formation has been demonstrated between the 5-phosphatase and the adaptor proteins 14-3-3, also resulting in activation of the 43 kDa 5-phosphatase (Campbell *et al.*, 1997).

The 43 kDa 5-phosphatase is located in the soluble and particulate fraction of cells with the majority of enzyme activity associated with the latter fraction. In COS-7 cells the 43 kDa 5-phosphatase localises to the plasma membrane as well as the Golgi and endoplasmic reticulum. The subcellular distribution of the 43 kDa 5-phosphatase is thought to be mediated by the C-terminal CAAX motif (where A is an aliphatic amino acid and X is any amino acid), as mutant enzymes with nonfunctional CAAX motifs localized diffusely throughout the cytosol, and resulted in a redistribution of enzyme activity to the soluble fraction (De Smedt *et al.*, 1996).

The 43 kDa 5-phosphatase has bee implicated in regulation of cell growth and cellular transformation *via* Ca^{2+}-dependent signaling events. Underexpression of the 43 kDa 5-phosphatase results in elevated basal levels of its inositol substrates, and intracellular Ca^{2+} consequently resulting in increased cell growth rates which formed tumors in nude mice (Speed *et al.*, 1996).

1.4.4 75 kDa 5-phosphatase

The 75 kDa 5-phosphatase was initially purified from human platelets and dephosphorylates Ins(1,4,5)P_3 and Ins(1,3,4,5)P_4, although less efficiently than the 43 kDa 5-phosphatase (Matzaris *et al.*, 1994). The enzyme has subsequently been shown to

hydrolyze the lipid substrates PtdIns(4,5)P_2 (Matzaris *et al.*, 1998) and PtdIns(3,4,5)P_3 (Jackson *et al.*, 1995). Although the enzyme has widespread distribution (Janne *et al.*, 1998; Matzaris *et al.*, 1998) it plays a significant role in platelet phosphoinositide homeostasis as 90 % of PtdIns(4,5)P_2 5-phosphatase activity can be detected in immunoprecipitates of the 75 kDa 5-phosphatase (Speed *et al.*, 1995). As with the 43 kDa 5-phosphatase, the 75 kDa 5-phosphatase contains a C-terminal CAAX motif, which when mutated results in an increase of soluble 75 kDa 5-phosphatase protein levels. The redistribution of protein to the soluble fraction resulted in a decrease in activity towards its bisphosphorylated substrate (Jefferson and Majerus, 1995).

Several isoforms of the 75 kDa 5-phosphatase have been observed, and are thought to arise from alternative splicing and proteolytic processing. At least in mice, the 75 kDa 5-phosphatase appears to have somewhat of a redundant role. Mice with a deletion of the gene encoding the 75 kDa 5-phosphatase are viable and fertile, with only a minor abnormality in testis function (Janne *et al.*, 1998).

1.4.5 OCRL1 protein

Lowe's oculocerebrorenal (OCRL) is a rare X-linked developmental disorder characterized by congenital cataracts, mental retardation, and renal tubular dysfunction. The gene locus disrupted in this syndrome was mapped to Xq25-q26 and found to code for a putative inositol polyphosphate 5-phosphatase of 968 amino acids with a predicted molecular weight of 112 kDa. Northern and Western blot analysis revealed widespread tissue distribution. Recombinant OCRL preferentially hydrolyzes the lipid substrate PtdIns(4,5)P_2 but activity towards PtdIns(3,4,5)P_3, Ins(1,4,5)P_3 and Ins(1,3,4,5)P_4 has also been demonstrated (Zhang *et al.*, 1995). Analysis of cell lines derived from kidney proximal tubules of Lowe syndrome patients found reduced levels of PtdIns(3,4,5)P_3,

$Ins(1,4,5)P_3$ and $Ins(1,3,4,5)P_4$ whereas $PtdIns(4,5)P_2$ 5-phosphatase activity was negligible (Zhang *et al.*, 1998b). A mouse model was developed for Lowe's syndrome in an attempt to further understand the pathogenesis of the disease, however, the phenotype of mice lacking the Ocrl1 protein was normal, possibly due to complementation by another 5-phosphatase namely the 75 kDa 5-phosphatase with which it shares greatest homology. Targeted disruption of both genes was found to be lethal, suggesting functional overlap between these two 5-phosphatases (Janne *et al.*, 1998).

Immunoflourescence studies of human fibroblasts indicated Golgi localization of the Ocrl1 protein. Moreover, a yeast two-hybrid screen with full-length Ocrl1 as bait isolated a Golgi integral membrane protein called Golgin-84, furthermore, indirect immunoflourescence, sub-cellular fractionation and Golgi perturbation studies provided further evidence for Golgi localization of this enzyme (Dressman *et al.*, 2000).

1.4.6 Synaptojanin 1

Synaptojanin 1 was initially purified as a Grb2-binding protein from rat brain synaptic vesicles. Synaptojanin was so named based on initial observations that it is enriched in nerve terminals and that it contained two distinct domains which were potentially involved in phosphoinositide metabolism. The primary sequence of synaptojanin is comprised of an N-terminal region with significant homology to the cytosplasmic portion of the yeast Sac1 protein, a central 5-phosphatase domain, and a C-terminal proline-rich domain.

Several isoforms of synaptojanin 1 have been identified. Molecular cloning of the synaptojanin DNA, and PCR analysis of genomic DNA, revealed two transcripts are generated through alternative use of an exon containing an inframe stop codon (Ramjaun and McPherson, 1996). A further two transcripts have also been described where one

contains a 16 amino acid insert in its C-terminus and another in which the N-terminal Sac1 domain is absent (Woscholski *et al.*, 1998; Woscholski *et al.*, 1997).

Synaptojanin 1 hydrolyzes lipid and inositol phosphate substrates, Ins(1,4,5)P_3, Ins(1,3,4,5)P_4, PtdIns(4,5)P_2 and PtdIns(3,4,5)P_3 (McPherson *et al.*, 1996; Woscholski *et al.*, 1997). The SAC1 homology region of synaptojanin 1 has intrinsic phosphoinositide phosphatase activity and is able to dephosphorylate PtdIns(3)P, PtdIns(4)P and PtdIns(3,5)P_2 to PtdIns (Guo *et al.*, 1999).

Several lines of evidence exist implicating synaptojanin in the regulation of clathrin-mediated endocytosis, particularly in synaptic vesicle recycling. In mice gene-targeted disruption of synaptojanin 1 results in neurological defects in which there is an increase in PtdIns(3,4,5)P_3 and PtdIns(4,5)P_2 levels, an accumulation of clathrin-coated vesicles and a defect in synaptic vesicle recycling (Cremona *et al.*, 1999). In *Caenorhabditis elegans* gene-targeted disruption of *unc*-26, the synaptojanin 1 ortholog, results in a trafficking defect not restricted to neuronal tissue (Harris *et al.*, 2000). In addition, synaptojanin 1 has been demonstrated to associate with a host of proteins including Eps15, a clathrin-associated protein, clathrin, and a the clathrin adaptor AP-2 (Haffner *et al.*, 2000; Haffner *et al.*, 1997).

A role for synaptojanin 1 in actin regulation of the cytoskeleton has also been investigated. COS-7 cells overexpressing synaptojanin display abnormal actin stress fiber formation and are multinuclear (Qualmann *et al.*, 1999). It is suggested that *via* hydrolysis of PtdIns(4,5)P_2, synaptojanin 1 can influence actin-regulatory proteins which bind the bisphosphorylated lipid PtdIns(4,5)P_2 (Sakisaka *et al.*, 1997).

1.4.7 Synaptojanin 2

Synaptojanin 2 shares the same domain structure of Synaptojanin 1, although their C-termini bear little homology, suggesting this region may direct different physiological functions. Like synaptojanin 1, synaptojanin 2 undergoes alternative splicing generating 140 kDa (synaptojanin 2A) and 170 kDa (synaptojanin 2B) isoforms, which are differentially expressed, with the smaller isoform predominantly in brain and the larger expressed in peripheral tissues (Khvotchev and Sudhof, 1998).

The C-terminal regions of synaptojanin 1 and synaptojanin 2 associate with Grb2. OMP25, a novel mitochondrial protein can specifically interact with synaptojanin 2A and recruit cytoplasmic synaptojanin 2A to mitochondria. Specific targeting of synaptojanin 2A to the mitochondria results in pronounced changes in the distribution and morphology of mitochondria, a phenotype also observed in cells co-expressing OMP25 and synaptojanin 2A, suggesting a role for phosphoinositides in the regulation of mitochondria distribution (Nemoto and De Camilli, 1999).

The activated form of the GTPase Rac1, which inhibits endocytosis of growth factor receptors, has also been identified as binding partner for synaptojanin 2 (Malecz *et al.*, 2000). In the presence of activated Rac1 synaptojanin 2 translocates from the cytosol to the plasma membrane. Catalytically active synaptojanin 2 targeted to the plasma membrane also inhibits endocytosis of the EGF receptor, suggesting synaptojanin 2 mediates the inhibitory effect of Rac1 on endocytosis. However, membrane-targeted synaptojanin 2 did not influence lamellipodia formation, which is thought to be mediated by Rac1 activity and phosphoinositides.

Six additional splice variants of synaptojanin 2 have been reported, which differ at their N-terminal and C-terminal ends, suggesting additional splice sites at the 5' and 3' ends of the synaptojanin 2 gene (Seet *et al.*, 1998).

1.4.8 PIPP/107 kDa 5-phosphatase

PIPP (proline-rich inositol polyphosphate 5-phosphatase) was originally identified from a rat brain cDNA library and was so named after the identification of N- and C-termini proline-rich domains. PIPP is widely expressed and recombinant PIPP displays 5-phosphatase activity towards Ins(1,4,5)P_3, Ins(1,3,4,5)P_4, and PtdIns(4,5)P_2, although it is not known whether PIPP can hydrolyze PtdIns(3,4,5)P_3. PIPP is localized to membrane ruffles which is mediated through both proline-rich domains, suggesting recruitment by association with plasma membrane proteins (Mochizuki and Takenawa, 1999).

1.4.9 SKIP/51 kDa 5-phosphatase

SKIP (skeletal muscle and kidney enriched inositol phosphatase) is a recently identified 5-phosphatase cloned from human testis cDNA library, with activity towards Ins(1,4,5)P_3, Ins(1,3,4,5)P_4, PtdIns(4,5)P_2, and PtdIns(3,4,5)P_3. Recombinant and native SKIP localizes throughout the cytosol and is concentrated in perinuclear regions. Co-localization of recombinant SKIP with polymerized actin in COS-7 cells demonstrated areas in which SKIP was detected, a reduction in stress fiber formation was observed, implicating SKIP in the regulation of the actin cytoskeletal architecture (Ijuin *et al.*, 2000).

1.4.10 Type IV 5-phosphatase

The Type IV 5-phosphatase was originally identified searching the human expressed sequence tag (EST) database for 5-phosphatase consensus sequences. One clone was identified, and using the EST cDNA, the full-length sequence of the Type IV 5-phosphatse was isolated by screening a human fetal brain library. Northern blot analysis revealed widespread distribution with highest expression noted in brain, heart, spleen, pancreas and testis. Uniquely, the Type IV 5-phosphatase displays activity only towards

the lipid substrates, PtdIns(4,5)P_2 and PtdIns(3,4,5)P_3 (Kisseleva *et al.*, 2000). Sequence analysis of the Type IV 5-phosphatase suggests an N-terminal proline-rich region, a C-terminal isoprenylation signal (CAAX motif), and a putative immunoreceptor activation motif (ITAM).

Recent studies have demonstrated by stable overexpression of the Type IV 5-phosphatase in human embryonic kidney cells that through hydrolysis of PtdIns(3,4,5)P_3, the Type IV 5-phosphatase leads to the inhibition of Akt and makes the cells highly susceptible to apoptosis (Kisseleva *et al.*, 2002).

1.4.11 Pharbin/72 kDa 5-phosphatase

In an attempt to identify proteins interacting with M-Ras, a small GTPase, Pharbin was isolated from a rat brain cDNA library. Pharbin is structurally similar to the human Type IV 5-phosphatase, containing an N-terminal proline-rich domain, a C-terminal CAAX motif and a putative ITAM. Recombinant Pharbin displays 5-phosphatase activity towards Ins(1,4,5)P_3, Ins(1,3,4,5)P_4, and PtdIns(4,5)P_2. Recombinant Pharbin expressed in C3H/10T1/2 fibroblasts localized to membrane ruffles independent of the CAAX motif, and furthermore, induced arborization of dendritic cells (Asano *et al.*, 1999). An association between Pharbin and M-Ras has not been demonstrated.

A mouse homolog of Pharbin has been identified and termed, in accordance with its molecular weight, the 72 kDa 5-phosphatase. Structurally, like the Type IV 5-phosphatase and Pharbin, the 72 kDa 5-phosphatase has an N-terminal proline-rich domain, a C-terminal CAAX motif, and a putative ITAM. Northern blot analysis revealed restricted distribution with abundant expression in testis and brain. Indirect immunofluoresence in Tera-1 cells, a testis carcinoma cell line, demonstrated the 72 kDa 5-phosphatase is predominantly localized to the Golgi. Expression of recombinant 72 kDa 5-phosphatase in

COS-7 cells confirmed the Golgi localization of this enzyme, which is mediated by the N-terminal proline-rich domain. Immunoprecipitated recombinant 72 kDa 5-phosphatase displayed 5-phosphatase activity towards PtdIns(3,4,5)P_3 and PtdIns(3,5)P_2 (Kong *et al.*, 2000). It is possible that the Type IV 5-phosphatase is the human homolog of Pharbin and the 72 kDa 5-phosphatase, although this has not been established in the literature.

1.4.12 hSac2

Numerous SAC1-like domain-containing proteins have been identified in mammals and yeast (Hughes *et al.*, 2000a). The primary sequence of the human Sac domain-containing protein, hSac1, is highly homologous to that of the yeast and rat Sac1p proteins which display phosphoinositide activity towards the lipid substrates PtdIns(3)P, PtdIns(4)P and PtdIns(3,5)P_2 (Nemoto *et al.*, 2000). A homolog of hSac1 has been identified, hSac2, which has been reported to have 5-phosphatase activity towards PtdIns(4,5)P_2 and PtdIns(3,4,5)P_3 (Minagawa *et al.*, 2001). Sequence analysis indicates there is no homolog for hSac2 in yeast.

1.4.13 Yeast 5-phosphatases

Sequencing of the *Saccharomyces cerevisiae* genome has identified the presence of four genes coding for inositol 5-phosphatase domain-containing proteins. The products of three of these genes, Inp51p, Inp52p and Inp53p are structurally similar to synaptojanin, with an N-terminal SAC1 homology domain, a central 5-phosphatase domain, a C-terminal proline-rich domain, with respective molecular weights of 108 kDa, 136 kDa and 124 kDa (Srinivasan *et al.*, 1997; Stolz *et al.*, 1998a). Inp54p is considerably smaller with a molecular weight of 44 kDa and is comprised of a central 5-phosphatase domain and a C-terminal leucine-rich tail (Wiradjaja *et al.*, 2000).

All of the yeast 5-phosphatases display Mg^{2+}-independent 5-phosphatase activity towards PtdIns(4,5)P_2, but are unable to hydrolyze soluble inositol phosphates (Raucher *et al.*, 2000; Stolz *et al.*, 1998a; Stolz *et al.*, 1998b). It has also been reported that recombinant Inp52p lacking the SAC1 homology domain is able hydrolyze PtdIns(3,5)P_2 (Ooms *et al.*, 2000). Like synaptojanin, the SAC-1 homology domain of Inp52p, Inp53p and the SAC1p protein possess intrinsic Mg^{2+}-independent polyphosphoinositide activity converting PtdIns(3)P, PtdIns(4)P, and PtdIns(3,5)P_2 to PtdIns (Guo *et al.*, 1999; Hughes *et al.*, 2000b).

Mutant strains in which single and double disruptions of Inp51p, Inp52p, Inp53p and Inp54p have implicated Inp53p in clathrin-dependent vesicle trafficking from the *trans*-Golgi network, and Inp54p in the regulation of secretion (Bensen *et al.*, 2000; Wiradjaja *et al.*, 2000). Actin cytoskeletal and cell wall defects have been observed to varying degrees in most of the yeast 5-phosphatase null mutants (Singer-Kruger *et al.*, 1998; Srinivasan *et al.*, 1997).

1.5 Conclusions

Phosphoinositides are important regulators of various signaling pathways which participate in a variety of cellular functions including apoptosis, membrane trafficking and actin reorganization. The levels of distinct phosphoinositides are dependent on the activity of various lipid kinases and phosphatases for which multiple regulatory mechanisms exist and are only partially understood. The inositol polyphosphate 5-phosphatases are a diverse group of enzymes which can selectively modulate the activity of the phosphoinositides. Further characterization of the 5-phosphatases, specifically the identification of binding

partners, will assist with elucidation of the signaling pathways and cellular effects the 5-phosphatases modulate

CHAPTER 2: Materials and Methods

2.1 Materials

2.1.1 Cloning reagents and kits

Big Dye Terminator Cycle Sequencing kit	PE Applied Biosystems, USA.
Calf intestinal alkaline phosphatase	New England Biolabs, USA.
dNTPs	Amersham, UK.
Plasmid MIDI kit	Qiagen, Germany.
Qiaprep spin miniprep kit	Qiagen, Germany.
Prime-a-Gene labelling system	Primage, USA.
Restriction endonucleases	New England Biolabs, USA.
T4 DNA ligase	New England Biolabs, USA.
UltraClean DNA purification kit	Geneworks, Australia.
Vent DNA polymerase	New England Biolabs, USA.
λ DNA	Promega, USA.
100 bp ladder DNA	Gibco BRL, U.S.A.

2.1.2 Oligonucleotides

Synthetic oligonucleotides were obtained from Geneworks, Australia or Department of Microbiology, Monash University. All sequences are written in 5' to 3' direction.

General primers

T3	ttaaccctcactaaaggg
T7	aatacgactcactataggg
M13 Universal	taaaacgacggccag
M13 Reverse	aggaaacagctatgac
GFP5'	agtccgccctgagcaaagac
CGN5'	agcgccttgtagaagc

2.1.3 Plasmids

pCGN	Dr Tony Tiganis, Monash University, Australia.
pCR-Blunt	Invitrogen, the Netherlands.
pEFBOS-Flag	Dr. Tracey Wilson, Walter and Eliza Hall Institute of Medical Research, Australia.
pEFBOS-Myc	Dr. Tracey Wilson, Walter and Eliza Hall Institute of Medical Research, Australia.
pEGFP-C2	Clontech Laboratories, USA.
pEGFP-C2-PH/ARNO	Dr. Tamas Bella, National Institute of Health, USA. .
pGBKT7	Clontech Laboratories, USA.
pGADT7	Clontech Laboratories, USA.
pGADT7-filamin A	Dr. Joe Tripani and Kylie Brown, Peter MacCallum Cancer Institute, Australia.
pGADT7-filamin B	Dr. Joe Tripani and Kylie Brown, Peter MacCallum Cancer Institute, Australia.

2.1.4 Bacteria

Escherichia coli, strain TOP10	Invitrogen, The Netherlands.

2.1.5 Yeast

Saccharomyces cerevisiae, strain AH109	Clontech Laboratories, USA.

2.1.6 Antibodies

Anti-actin	Santa Cruz, Australia.
Anti-α-actinin	Sigma-Aldrich, USA.
Anti-β-actin, monoclonal	Sigma-Aldrich, USA.
Anti-filamin, monoclonal	Chemicon, USA.
Anti-filamin, goat polyclonal	Sigma-Aldrich, USA.
Anti-filamin B, polyclonal	Dr. Dominic Chung, University of Washington, School of Medicine, USA.
Anti-FLAG, monoclonal	Sigma-Aldrich, USA.
Anti-green fluorescent protein (GFP),	Roche Diagnostics, Germany.
Anti-glycocalicin, polyclonal (raised to a soluble fragment of GPIbα)	Dr. Michael Berndt, Monash University, Australia.
Anti-GPIbβ_p, polyclonal (raised to phosphorylated β-chain of GPIb)	Dr. Michael Berndt, Monash University, Australia.
Anti-haemagglutinin (HA), monoclonal	Berkeley Antibody, USA.
Anti-haemagglutinin (HA), polyclonal	Berkeley Antibody, USA.
Anti-myc, monoclonal	Dr. Tracey Wilson, Walter and Eliza Hall Institute of Medical Research, Australia.
Anti-p85, polyclonal (raised to p85 subunit of PI3-kinase)	Upstate Biotechnology, USA.
Anti-rabbit/goat/mouse immunoglobulin, affinity-isolated, horseradish peroxidase/ FITC/TRITC-conjugated	Silenus Laboratories, Australia.

Alexa Fluor 546 goat anti-mouse immunoglobulin conjugate	Molecular Probes, USA.
N-^{1}MASACGA^{7,1251}DTLQLSK^{1258}-C	Chiron Technologies, Australia.
N-^{1019}ITVPAPQLGHHRH^{1030}-C	Chiron Technologies, Australia
peptides for raising antibodies against the SHIP-2 5-phosphatase	
Freund's complete adjuvant	Sigma-Aldrich, USA.
Freund's incomplete adjuvant	Sigma-Aldrich, USA.
New Zealand White rabbits	Animal House, Monash University.

2.1.7 Phosphoinositides and inositol phosphates

L-α-Phosphatidyl-L-serine	Sigma-Aldrich, USA.
D-α-Phosphatidylinositol 4,5-bisphosphate	Sigma-Aldrich, USA.
L-α-Phosphatidylinositol 4-phosphate	Sigma-Aldrich, USA.

2.1.8 Radiolabelled compounds

[γ^{32}P] Adenosine 5'-triphosphate	NEN Life Science, USA.
[α^{32}P] Deoxycytidine 5'-triphosphate	NEN Life Science, USA.

2.1.9 Tissue culture

DMEM without L-glutamine	ICN Biomedicals, USA.
G418 Sulphate	A.G. Scientific, USA.
Human melanoma cell line (M2)	Dr. Thomas Stossel, Brigham and Women's Hospital, USA.
Human melanoma cell line stably transfected with filamin A (A7)	Dr. Thomas Stossel, Brigham and Women's Hospital, USA.

Foetal calf serum	Gibco BRL, U.S.A.
L-Glutamine	ICN Biomedicals, USA.
M199	Trace Bioscientific, Australia.
Monkey kidney cell line (COS-7)	American Type Culture Collection.
Penicillin/Streptomycin	ICN Biomedicals, USA.
Trypsin/EDTA	ICN Biomedicals, USA.
SlowFade	Molecular Probes, USA.

2.1.10 Yeast two-hybrid

Yeast two-hybrid system Matchmaker III	Clontech Laboratories, USA.
Complete synthetic media - Trp	BIO 101, USA.
Complete synthetic media - Ade, -His, -Leu, -Trp	BIO 101, USA.
L-Histidine HCl monohydrate	Sigma-Aldrich, USA.
L-Adenine hemisulphate salt	Sigma-Aldrich, USA.
Lithium acetate	Sigma-Aldrich, USA.
Polyethylene glycol, 3350	Sigma-Aldrich, USA.
Salmon sperm DNA	Sigma-Aldrich, USA.
X-α-gal	Clontech Laboratories, USA.

2.1.11 General reagents

Acetic acid	BDH Chemicals, UK.
Acrylamide	Bio-Rad Laboratories, USA.
Agarose	Promega, USA.
Ammonium persulfate	Bio-Rad Laboratories, USA.
Ampicillin	Sigma-Aldrich, USA.
Aprotinin	Sigma-Aldrich, USA.

Bacteriological agar	Oxoid, UK.
Benzamidine	Sigma-Aldrich, USA.
Bis-acrylamide	Bio-Rad Laboratories, USA.
Boric acid	BDH Chemicals, UK.
Botrocetin	Dr. Michael Berndt, Monash University, Australia.
Bromophenol Blue	BDH Chemicals, UK.
BSA (bovine serum albumin)	Sigma-Aldrich, USA.
Butan-1-ol	BDH Chemicals, UK.
Calcium chloride	BDH Chemicals, UK.
Citric acid	BDH Chemicals, UK.
Chloroform	BDH Chemicals, UK.
Chloroquine	Sigma-Aldrich, USA.
DEAE Dextran	Sigma-Aldrich, USA.
Dextrose (glucose)	ICN Biochemicals, USA.
Dimethyl sulfoxide	Sigma-Aldrich, USA.
Dimethyl formamide	Sigma-Aldrich, USA.
Dipotassium hydrogen orthophosphate	BDH Chemicals, UK.
Disodium hydrogen orthophosphate	BDH Chemicals, UK.
EDTA (ethylenediaminetetraacetic acid)	Sigma-Aldrich, USA.
EGTA (ethylene glycol tetraacetic acid)	Sigma-Aldrich, USA.
Epidermal growth factor (EGF)	BD Biosciences, USA.
Ethanol	BDH Chemicals, UK.
Ethidium bromide	Sigma-Aldrich, USA.
Ficoll	Sigma-Aldrich, USA.

Formaldehyde	Sigma-Aldrich, USA.
Formamide	Sigma-Aldrich, USA.
Glass beads (0.44 mm diameter)	Sigma-Aldrich, USA.
Glycerol	BDH Chemicals, UK.
Glycine	BDH Chemicals, UK.
HEPES (N-[2-hydroxyethyl] piperazine-N'-[2-ethanesulphonic acid])	BDH Chemicals, UK.
Horse serum	CSL Biosciences, Australia.
Hydrochloric acid	BDH Chemicals, UK.
Iodine	Sigma-Aldrich, USA.
Isoamyl alcohol	BDH Chemicals, UK.
Kanamycin	Sigma-Aldrich, USA.
Leupeptin	Sigma-Aldrich, USA.
Magnesium chloride	Sigma-Aldrich, USA.
Manganese chloride	BDH Chemicals, UK.
2-Mercaptoethanol	BDH Chemicals, UK.
Methanol	BDH Chemicals, UK.
MOPS (3-[N-morpholino]ethanesulphonic acid)	Sigma-Aldrich, USA.
Nonident P-40	BDH Chemical, UK.
OCT (optimal cutting temperature) compound	Tissue-Tek, USA.
Phalloidin, Texas Red-conjugated	
Phenol	Sigma-Aldrich, USA.
PMSF (phenylmethylsulphonyl fluoride)	Sigma-Aldrich, USA.
Polyvinylpyrrolidone	Sigma-Aldrich, USA.
Potassium acetate	BDH Chemicals, UK.

Potassium chloride	BDH Chemicals, UK.
Potassium oxalate	BDH Chemicals, UK.
RNase A	Roche Diagnostics, Germany.
Rubidium chloride	BDH Chemicals, UK.
SDS (sodium dodecylsulphate)	BDH Chemicals, UK.
SDS-PAGE protein molecular weight markers	New England Biolabs, USA. Gibco BRL, U.S.A.
Skim milk powder	Safeway, Australia.
Sodium acetate	BDH Chemicals, UK.
Sodium azide	Sigma-Aldrich, USA.
Sodium hydrogen carbonate	BDH Chemicals, UK.
Sodium chloride	BDH Chemicals, UK.
Sodium dihydrogen orthophosphate	BDH Chemicals, UK.
Sodium hydroxide	BDH Chemicals, UK.
TEMED (N,N,N',N'-tetramethylethylene-diamine)	Bio-Rad Laboratories, USA.
Theophylline	Sigma-Aldrich, USA.
Thrombin	Dr. Michael Berndt, Monash University, Australia.
Tris (tris(hydroxymethyl)aminomethane)	Progen Industries, Australia.
Trisodium citrate	BDH Chemicals, UK.
Triton X-100 (octylphenoxypolyethanoxyethanol)	Sigma-Aldrich, USA.
Tryptone	Oxoid, U.K.
vonWillebrand Factor (vWF)	Dr. Michael Berndt, Monash University, Australia.

Xylene cyanol	BDH Chemicals, UK.
Yeast extract	Oxoid, U.K.
Yeast nitrogen base (without amino acids)	Difco Laboratories, UK.

2.1.12 Miscellaneous

Affinity-purified recombinant PI3-kinase	Dr Meredith Layton, Ludwig Institute for Cancer Research, Australia.
Bio-Rad protein assay reagent	Bio-Rad Laboratories, USA.
Enhanced chemiluminescence system (ECL)	NEN Life Science, USA.
Filter paper	Whatman, UK.
Filters (0.22 μm)	Millipore Corp, USA.
Guanosine 5'-O-(3-thiotriphosphate) (GTPγS)	Sigma-Aldrich, USA.
Polyvinylidene fluoride (PVDF) membrane	Millipore Corp, USA.
X-ray film	Fuji Photofilm, Japan.

2.2 Buffers and solutions

100 × Denhardt's solution

2 % bovine serum albumin, 2 % ficoll, 2 % polyvinylpyrrolidone in distilled water.

20 × SSC (sodium chloride, sodium citrate)

3 M NaCl, 0.3 M trisodium citrate in distilled water.

20 × SSPE (sodium chloride, sodium phosphate, EDTA)

3.6 M NaCl, 0.2 M NaH_2PO_4, 0.02 M EDTA pH 7.4 in distilled water.

20 x assay buffer

1 M Tris, pH 7.2 and 100 mM $MgCl_2$

Acrylamide solution for SDS-PAGE

acrylamide:bis-acrylamide at 29:1, 30 % in distilled water.

Anticoagulant

90 mM trisodium citrate, 7 mM citric acid pH 4.6, 140 mM glucose, 70 mM theophylline in MilliQ water.

DEAE Dextran Chloroquine

1 % DEAE Dextran, 2.5 mM Chloroquine in MilliQ water. Filter sterilized.

DNA loading buffer for agarose gel electrophoresis

10 mM Tris pH 7.4, 50 mM EDTA, 10 % glycerol, 0.2 % SDS, 0.02 % xylene cyanol, 0.02 % bromophenol blue in distilled water.

Formaldehyde fix and permeabilisation solution

10 % formaldehyde (37 %), 0.1 % Triton X-100 in PBS.

Kinase assay buffer

20 mM HEPES pH 7.5, 5 mM $MgCl_2$, 1 mM EGTA in distilled water.

LB (Luria-Bertani medium)

1 % bacto-tryptone, 0.5 % bacto-yeast extract, 1 % NaCl in distilled water.

LB agar

1 % bacto-tryptone, 0.5 % bacto-yeast extract, 1 % NaCl, 1.5 % agar in distilled water.

Lipid resuspension buffer

20 mM HEPES pH 7.5, 1 mM $MgCl_2$, 1 mM EGTA in distilled water.

Oxalate dip for TLC plates

1 % potassium oxalate, 2 mM EDTA, 50 % ethanol in distilled water.

Phenol/chloroform

Tris-saturated phenol:isoamyl alcohol:chloroform at 25:1:24.

Phosphate-buffered saline (PBS)

8 mM Na_2HPO_4, 17.5 mM K_2HPO_4, 2.7 mM KCl, 137 mM NaCl in distilled water; pH 7.4.

Platelet lysis buffer (10 x)

200 mM Tris, pH 7.4, 50 mM EGTA, 10 % Triton X-100, 4 mM leuptptin, 4 mM aprotinin, 2.5 mg/ml PMSF in distilled water.

Platelet resuspension buffer

12 mM $NaHCO_3$, 10 mM HEPES, 137 mM NaCl, 2.7 mM KCl, 5.5 mM glucose in distilled water; pH 7.5.

Platelet wash buffer

4.3 mM Na_2HPO_4, 24.3 mM $NaH_2PO_4.2H_2O$, 4.3 mM K_2HPO_4, 113 mM NaCl, 5.5 mM glucose, 0.5 % bovine serum albumin, 10 mM theophylline in distilled water; pH 6.5

Prehybridisation solution

50 % formamide, 5 × SSPE, 5 × Denhardt's solution, 0.5 % SDS in distilled water.

RIPA-buffer

10 mM NaH_2PO_4, pH 7.0, 150 mM NaCl, 2 mM EDTA, 250 µg/ml PMSF, 400 µM leupeptin, 400 µM aprotinin, 1 % Nonidet P-40, 1 % sodium deoxycholate, 0.1 % SDS

SC-Trp dropout agar

6.7 g Yeast nitrogen base, 0.74 g CSM-Trp, 1 % bacto-agar in 900 ml MilliQ water. Autoclaved. Sterile dextrose was added to 2 %.

SC-Trp droput media

6.7 g Yeast nitrogen base (without amino acids), 0.74 g CSM-Trp in 900 ml MilliQ water. Autoclaved. Sterile dextrose was added to 2 %.

SC-Trp-Leu droput agar

6.7 g Yeast nitrogen base (without amino acids), 0.61 g of -Ade, -His, -Leu, -Trp droput mix, 1 % bacto-agar in 900 ml MilliQ water. 200 mg of L-Adenine hemisulphate salt and L-Histidine HCl monohydrate were added back. Autoclaved. Sterile dextrose was added to 2 %.

SC-Trp-Leu-His-Ade dropout agar

6.7 g Yeast nitrogen base (without amino acids), 0.61 g of -Ade, -His, -Leu, -Trp dropout mix, 1 % bacto-agar in 900 ml MilliQ water. Autoclaved. Sterile dextrose was added to 2 %.

SDS-PAGE blocking buffer

5 % skim milk powder in Tris-buffered saline.

SDS-PAGE reducing buffer

40 mM Tris pH 6.8, 4 % SDS, 20 % glycerol, 0.002 % bromophenol blue, 10 % 2-mercaptoethanol in distilled water.

SDS-PAGE tank buffer

125 mM Tris pH 8.3, 190 mM glycine, 0.1 % SDS in distilled water.

SDS-PAGE transfer buffer

125 mM Tris pH 8.3, 190 mM glycine, 20 % methanol in distilled water.

Solution I for isolation of plasmid DNA

50 mM glucose, 25 mM Tris pH 8.0, 10 mM EDTA in distilled water.

Solution II for isolation of plasmid DNA

200 mM NaOH, 1 % SDS in distilled water.

Solution III for isolation of plasmid DNA

160 μM potassium acetate, 11.5 % glacial acetic acid in distilled water.

Stripping buffer for PVDF membranes

62.5 mM Tris pH 6.7, 2 % SDS, 70 mM 2-mercaptoethanol in distilled water.

TLC tank buffer for PtdIns(3,4,5)P_3

2 M acetic acid:butanol at 7:13 (v/v).

Transformation buffer I for preparation of competent bacteria

30 mM potassium acetate pH 5.8, 100 mM rubidium chloride, 10 mM $CaCl_2$, 50 mM manganese chloride, 15 % glycerol in distilled water. Filter sterilized.

Transformation buffer II for preparation of competent bacteria

10 mM MOPS pH 6.5, 75 mM $CaCl_2$, 10 mM rubidium chloride, 15 % glycerol in distilled water. Filter sterilized.

Tris-Borate EDTA (TBE)

10 mM Tris, 10 mM boric acid, 1 mM EDTA in distilled water.

Tris-EDTA (TE)

10 mM Tris pH 7.5, 1 mM EDTA in distilled water.

Tris-buffered saline (TBS)

20 mM Tris pH 7.4, 150 mM NaCl in distilled water.

Triton extraction buffer

50 mM Tris pH 8.0, 150 mM NaCl, 2 mM EDTA, 1 % Triton X-100, 1 mM benzamidine, 2 mM phenylmethylsulfonylfluoride, 2 μg/ml aprotinin, 2 μg/ml leupeptin in distilled water.

Yeast resuspension buffer

100 mM NaCl, 10 mM Tris pH 8.0, 1 mM EDTA, 0.1 % SDS in distilled water.

YPAD media

1 % yeast extract, 2 % peptone in distilled water. Autoclaved. Sterile dextrose was added to 2 % and sterile adenine was added to 0.003 %.

X-α-gal

X-α-gal powder was resuspended in dimethyl formamide to a working concentration of 2mg/ml.

2.3 Methods

2.3.1 Radiolabelling cDNA probes

cDNA probes were labelled with α^{32}P-dCTP using the Prime-a-Gene labelling kit (Promega). Approximately 25 ng of the probe in 15 μl volume was denatured by heating at 100 °C for 5 minutes and allowed to chill completely on ice. To the DNA, 5 μl of 5× labelling buffer containing random hexadeoxyribonucleotides, 1 μl of 1.5 mM dNTP mix (dATP, dGTP, dTTP), 1 μl BSA (bovine serum albumin), 5 μl α^{32}P-dCTP and 2.5 units of DNA polymerase (Klenow fragment) were added. Following incubation of the mixture for

one hour at room temperature, 1 µl of the sample was loaded onto a cellulose-coated plastic strip (pei-cellulose) to assess by thin layer chromatography (TLC) the incorporation of α^{32}P-dCTP in the probe. The incorporation ranged from 65-90 %.

2.3.2 DNA sequencing and analysis

Automated sequencing of plasmid DNA samples was undertaken at the Department of Microbiology, Monash University.

Template-DNA was prepared using the Qiaprep spin miniprep kit (Qiagen). Approximately 500 ng of template was mixed with 10 pmol of the sequencing primer and 2 µl of the 'BigDye terminator reaction mixture' (PE Applied Biosystems) in a 10 µl reaction volume. The reaction conditions were as follows: 28 cycles of PCR with 95 °C for 30 seconds, 50 °C for 15 seconds and 60 °C for 4 minutes. The products were ethanol precipitated and dried before being submitted for sequencing.

Sequences were analysed using the online programmes available from the National Center for Biotechnology Information (www.ncbi.nlm.nih.gov) and the ExPASy Molecular Biology Server (www.expasy.ch).

2.3.3 Polymerase chain reaction (PCR)

PCR reactions, unless otherwise stated, were carried out with approximately 40 ng of template DNA in the presence of 0.8 mM dNTPs, 20 pmol of each primer and 2 mM $MgSO_4$ using Vent DNA polymerase. A 90 second denaturation at 95 °C was followed by one minute of annealing at 50-60 °C and product length-dependent polymerisation at 72 °C, with the cycle repeated 30 times. The PCR product was visualised by agarose gel electrophoresis and was ligated directly into the cloning vector pCR-Blunt.

2.3.4 Preparation and transformation of competent *Escherichia coli*

Escherichia coli strain TOP10 was used for general subcloning. For the preparation of chemically competent bacteria, an overnight culture was diluted one in 100 in LB medium and grown for 2 hours at 37 °C. This culture was further diluted twenty-fold (final volume 50 ml) and grown at 37 °C until the OD_{550} was 0.6. The cells were then pelleted by centrifugation at 3,000 × g for 15 minutes and resuspended in 20 ml of transformation buffer I (30 mM potassium acetate pH 5.8, 100 mM rubidium chloride, 10 mM $CaCl_2$, 50 mM manganese chloride, 15 % glycerol). They were centrifuged again after incubation on ice for 5 minutes. The bacteria were resuspended in 2 ml of transformation buffer II (10 mM MOPS pH 6.5, 75 mM $CaCl_2$, 10 mM rubidium chloride, 15 % glycerol) and chilled on ice for 15 minutes. 50 µl aliquots were transferred to pre-chilled tubes and stored at –70 °C.

For transformation of bacteria with plasmid DNA, DNA to be transformed was incubated with the thawed competent cells for 30 minutes on ice. The cells were then heat-shocked at 42 °C for 90 seconds. 800 µl of LB media was added to the transformation mixture, which was then incubated at 37 °C for 45 minutes with shaking. The cells were plated on LB agar plates containing the appropriate antibiotic and incubated at 37 °C overnight.

2.3.5 Transformation of yeast strain AH109 (yeast two-hybrid)

The yeast two-hybrid Matchmaker III system was used for all yeast two-hybrid work. Yeast cells were transformed using a Polyethylene glycol (PEG)/Lithium acetate (LiAc) method, according to manufacturers instructions with minor modifications.

Small-scale yeast transformations were used for the initial transformation of the "bait" plasmid in the yeast strain AH109 and for appropriate controls.

Day 1

Yeast strain, AH109 was innoculated into 25 ml of YPAD media and incubated overnight at 30 °C shaking at 200 rpm.

Day 2

The cell titre of the overnight culture was determined *via* OD_{600}, where an OD_{600} of 1.0 corresponds to approximately 3 x 10^7 cells/ml. An aliquot of the culture which contains approximately 2.5 x 10^8 cells was centrifuged at 1000 x g for 5 minutes. The pelleted yeast cells were resuspended in 50 ml of YPAD media (prewarmed to 30 °C), resulting in a starting culture of approximately 5 x 10^6 cells/ml. The culture was incubated at 30 °C shaking at 200 rpm until the yeast cells have undergone two cell divisions. Once the OD_{600} of the culture had reached 0.66 the cells were harvested by centrifugation at 1000 x g for 5 minutes at room temperature. The yeast cell pellet was washed once with 25 ml of sterile MilliQ water and finally resuspended in 900 µl of sterile MilliQ water and transferred to an eppendorf tube. The yeast cells were pelleted by centrifugation at 13,000 x g for 5 minutes at room temperature, resuspended in 700 µl of 100 mM LiAc, and incubated at 30 °C for 10 minutes. For each transformation reaction a 100 µl aliquot of the LiAc cell suspension was transferred to a sterile eppendorf tube centrifuged at 13,000 x g for 1 minute at room temperature, the supernatant aspirated, and the following reagents were added to the cell pellet in a specific order of specific volumes; 240 µl of 50 % PEG, 36 µl of 1.0 M LiAc, 50 µl of single stranded-salmon sperm DNA (2 mg/ml), X µl of plasmid DNA and 34 µl - X µl of sterile MilliQ water. The final volume of the plasmid DNA and sterile MilliQ water was 34 µl. For small-scale transformations approximately 500 ng of plasmid DNA was used. The transformation mix was vortexed vigorously until the cell pellet was fully resuspended. The transformation mix was then incubated at 30 °C for 30 minutes. The transformation mix was then heat-shocked at 42 °C for 30 minutes and inverted gently

several times at 5 minute intervals. Following this, the transformation mix was centrifuged at 13,000 x g for 1 minute, the supernatant removed, and the cell pellet gently resuspended in 1 ml of sterile MilliQ water. The transformants were then plated onto appropriate SC-dropout plates. Where X-α-gal was used (a chromogenic substrate for LacZ) 10 cm agar plates were pre-spread with 100 µl of 2 mg/ml X-α-gal 1 hour prior to cell plating. The agar plates were incubated at 30 °C for 4-5 days.

For library screening the above transformation procedure was used, however minor modifications were made. Day 1 inoculation of the yeast was into 25 ml of -Trp media rather than YPAD media. Secondly, rather than using a 100 µl aliquot of the LiAc yeast cell suspension, the entire yeast cell pellet was used. Finally, each of the components added to the yeast cell pellet and the final resuspension volume was increased ten times. Approximately 10 µg of library plasmid DNA was used for screening.

2.3.6 Yeast plasmid extraction

Yeast cells from an overnight culture were pelleted *via* centrifugation at 13, 000 x g for 1 minute and resuspended in 200 µl in yeast resuspension buffer (100 mM NaCl, 10 mM Tris pH 8.0, 1 mM EDTA, 0.1 % SDS). Sterile glass beads (0.45 mm diameter) were added until just below the level of the liquid, mixed vigorously on a vortex mixer for 1 minute. 200 µl of chloroform was added, mixed by vortexing for 1 minute, and centrifuged at 13,000 x g for 2 minutes. The aqueous layer was transferred to a new microfuge and extracted a second time. Following extraction, a 3 times volume of Ultra Salt and 10 µl of Ultra bind was added. The DNA bound to the resin was briefly pelleted and washed with 500 µl of UltraWash solution. To elute the DNA from the resin the pellet was resuspended in water and incubated for 5 minutes at 55 °C before centrifugation at 13,000 × g for 1 minute. The supernatant was transferred to another tube and the DNA precipitated at -20

°C for 30 minutes using 3 mM sodium acetate and 40 µl of 100 % ethanol. Following incubation, the DNA solution was centrifuged at 13,000 x *g* for 10 minutes. The resultant pellet was washed in 80 % ethanol. The dried DNA pellet was resuspended in 50 µl of TE buffer. An aliquot was subjected to agarose gel electrophoresis to confirm the DNA had been purified.

2.3.7 Preparation of competent *Escherichia coli* for transformation with yeast plasmids

Escherichia coli strain TOP10 was used for transformation of yeast plasmids *via* electroporation. For the preparation of competent bacteria for electroporation, an overnight culture was diluted one in 100 in half salt LB medium and grown for 2 hours at 37 °C. This culture was further diluted twenty-fold (final volume 50 ml) and grown at 37 °C until the OD_{600} was 0.8. The cells were then pelleted by centrifugation at 3,000 × g for 15 minutes at 4 °C and washed 4 times in 100 ml of ice-cold sterile Milli Q. After the final wash, the cells were resuspended in 10 % glycerol and 50 µl aliquots were transferred to pre-chilled tubes and stored at –70 °C.

2.3.8 Plasmid DNA extraction from bacterial cultures

Plasmid DNA extraction from bacterial cultures was carried out according to standard protocols (Sambrook *et al.*, 1989). Cells grown in overnight culture were pelleted and resuspended in solution I (50 mM glucose, 25 mM Tris pH 8.0, 10 mM EDTA). After incubations with solutions II (200 mM NaOH, 1 % SDS) and III (160 µM potassium acetate, 11.5 % glacial acetic acid), the supernatant was treated with RNase A (20 µg/ml) and extracted with phenol/chloroform. The aqueous layer was ethanol precipitated and the pellet was resuspended in water or TE. The DNA concentration was determined by

measuring optical density of samples at 260 nm in a spectrophotometer. An OD_{260} of 1 corresponds to 50 µg/ml of double stranded DNA.

Preparation of sequence grade DNA was carried out using the plasmid miniprep kit according to the manufacturer's protocols. The plasmid midiprep kit was used to prepare DNA for transient transfection of COS-7 cells.

2.3.9 Restriction endonuclease digestion

Plasmid DNA was digested using the appropriate restriction endonuclease and buffer at the recommended temperature. The incubation was for a minimum of 2 hours and the digested DNA was analysed by agarose gel electrophoresis.

For ligation of restriction-digested DNA fragments into a particular vector, the vector DNA was treated with calf intestinal alkaline phosphatase following digestion, to prevent recircularisation during ligation. The phosphatase treatment was carried out at 37 °C for one hour on ethanol-precipitated DNA. An approximately ten-fold molar excess of insert DNA relative to the vector DNA was used in the ligation reaction. Ligations were performed at 14 °C with 1 µl of T4 DNA ligase and 1 µl of 10 × ligation buffer in a total volume of 10 µl for at least 4 hours, except for ligations of PCR products into pCR-Blunt, which were incubated for one hour.

2.3.10 Agarose gel electrophoresis

Agarose gels were prepared by dissolving agarose in 0.5 × TBE buffer by heating. The molten agarose was allowed to cool to below 50 °C before addition of ethidium bromide (0.5 µg/ml). The agarose solution was poured into a gel tray, on which combs had been fixed into position, and allowed to solidify. The DNA samples were mixed with DNA loading buffer, before loading into the wells. Electrophoresis was carried out in a

horizontal minigel tank using 0.5 × TBE buffer at 110 V (~90 mA) for 45 minutes. λ DNA digested with *Hind*III and *Eco*RI, or 100 base-pair ladder DNA was used as the size-standard markers. DNA bands were visualised using a UV transilluminator and photographed with a video copy processor.

2.3.11 DNA isolation from agarose gels

DNA was recovered from agarose gels using the 'UltraClean DNA purification kit'. The portion of the agarose gel containing the required DNA fragment was excised and its volume was estimated. 0.5 volume of TBEMelt solution and 4.5 volumes of UltraSalt solution were added to the gel fragment which was then melted at 55 °C for 5 minutes. The DNA-containing solution was incubated with UltraBind at room temperature for 5 minutes. The amount of UltraBind resin used was 5 µl plus 1 µl for each 1 µg of DNA to be purified. The DNA bound to the resin was briefly pelleted and washed with 500 µl of UltraWash solution. To elute the DNA from the resin the pellet was resuspended in water and incubated for 5 minutes at 55 °C before centrifugation at 13,000 × g for 1 minute. The supernatant was transferred to another tube and an aliquot was subjected to agarose gel electrophoresis to confirm the DNA had been purified.

2.3.12 Northern blot analysis

A membrane containing poly(A) RNA from various cell lines was probed with a [^{32}P]-labelled 966 bp cDNA fragment encoding the proline-rich domain of SHIP-2. The open reading frame was obtained by PCR amplification and subcloning into the pCR-Blunt vector. Following incubation of the membrane at 42 °C for 2 hours in prehybridisation solution, the [^{32}P]-labelled probe was added to the prehybridisation solution and hybridised at the same temperature overnight. The membranes were then washed in 2 × SSC, 0.1 %

SDS for 20 minutes at 42 °C three times, followed by two washes in 0.1 × SSC, 0.1 % SDS for 20 minutes at 50 °C. The signals were detected by autoradiography following exposure to film for 2 days at –70 °C. The membranes were allowed to decay and were subsequently hybridised with an actin probe.

2.3.13 Generation of anti-peptide antibodies

Anti-peptide antibodies were generated to a synthetic fusion peptide, comprising the NH_2-terminal seven amino acids of SHIP-2 fused to the COOH-terminal seven amino acids of SHIP-2 (MASACGADTLQSK-human sequence), conjugated to diphtheria toxoid. The diphtheria toxoid-conjugated peptide was injected subcutaneously into two New Zealand White rabbits. The first injection was 1 mg of the peptide with Freund's complete adjuvant and the subsequent injections were 0.5 mg of the peptide with incomplete adjuvant every two weeks. Each rabbit was subjected to a total of six injections. Bleeds were collected every two weeks following the third injection, and affinity-purified antibodies were obtained by chromatography using thiopropyl-Sepharose resin coupled to the same peptide. Serum was mixed with the resin overnight at 4 °C and the bound antibodies were eluted with 0.1 M glycine-HCl, pH 2.5 and 0.1 M glycine-NaOH, pH 11.5. Aliquots of affinity-purified antibody were stored at -70 °C with 0.1 % sodium azide.

2.3.14 Generation of SHIP-2 constructs for production of recombinant protein

The 3.726 kb sequence encoding the complete open reading frame of the human SHIP-2 5-phosphatase (nucleotides 48-3774) was amplified by PCR and cloned in frame into the *Eco*RI and *Xba*I site of the mammalian expression vectors, pEGFP-C2 and pCGN, respectively (provided by Dr. Cindy O'Malley). Recombinant proteins expressed from

these vectors respectively contain green fluorescent protein (GFP) and haemagglutinin (HA) tags fused to the N-terminus of the cloned sequence.

Three truncation mutants of SHIP-2 were generated by amplifying the desired region by PCR and subcloning the products into pCR-Blunt. The inserts were completely sequenced in this vector before they were ligated into the *Xba*I site of the mammalian expression vector, pCGN. The truncated constructs were produced by amplifying the following regions of the human SHIP-2 cDNA:

Name of Construct	**5' oligonucleotide**	**3' oligonucleotide**	**SHIP-2 polypeptide expressed**
HA-SHIP-2ΔSH2	5'-tattctagagagggt gagcgagagccg-3'	5'-atatctagatcaatga tgatgatgatgatgcttgct gagctgcagggt-3'	5-phosphatase domain and proline-rich domain (aa 118-1,258 with COOH-terminal hexa HisTag)
HA-SHIP-2ΔPRD	5'-gtctagaagccaggc cccctcctgg-3'	5'-tctagatcatggttctt caaataacctgg-3'	SH2 domain and 5-phosphatase domain (aa 16-936)
HA-PRD	5'-gtctagagagaaacc gccaccaacgggg-3'	5'-tctagatcatggttctt caaataacctgg-3'	Proline-rich domain (aa 936-1,258)

2.3.15 Generation of filamin C (FLNC) constructs for production of recombinant protein

Seven truncation mutants of filamin C (FLNC) were generated by amplifying the desired region by PCR and subcloning the products into pCR-Blunt. The inserts were completely sequenced in this vector before they were ligated into the *Eco*RI site of the yeast expression vector, pGADT7. The recombinant proteins expressed in this vector contain HA- and GAL4-tags fused to the N-terminus of the cloned sequence. In addition, using the above strategy, the partial filamin C clone (nucleotides 7,302 to 8,115) isolated from yeast two-hybrid assays, was ligated into the *Mlu*I site of the mammalian expression vector, pEFBOS-Myc. The recombinant protein expressed in this vector contains a Myc-tag fused to the N-terminus of the cloned sequence. The constructs were produced by amplifying the following regions of the FLNC cDNA:

Name of Construct	**5' oligonucleotide**	**3' oligonucleotide**	**FLNC polypeptide expressed**
PFLNCΔ24	5'-cgaattctgctacgtct ctgagctg-3'	5'-cgaattctcaggcatc tgaggagaactt-3'	aa 2,434-2,476 of repeat 22, repeat 23 and Hinge II region; aa 2,434-2,614
PFLNCΔH2ΔR24	5'-cgaattctgctacgtct ctgagctg-3'	5'-cgaattctcacagcc tcggaccagtgac-3'	aa 2,434-2,476 of repeat 22 and repeat 23; aa 2,434-2,578

Name of Construct	5' oligonucleotide	3' oligonucleotide	FLNC polypeptide expressed
pFLNCR23H2	5'-cgaattcatgcccttc aagatccgcgttg-3'	5'-cgaattctcaggcatc tgaggagaactt-3'	Repeat 23 and Hinge II region; aa 2,471-2,614
pFLNCR22 alone	5'-cgaattctgctacgtct ctgagctg-3'	5'-gaattctcaagcctgg ctctgctcccc-3'	aa 2,434-2,476 of repeat 22; aa 2,434-2,481
pFLNCR23 alone	5'-cgaattcatgcccttc aagatccgcgttg-3'	5'-cgaattctcacagcct cggaccagtgac-3'	Repeat 23; aa 2,471-2,577
pFLNCR24 alone	5'-cgaattcatgagctac agctccatcccc-3'	5'-cgaattctcaaaggg accttgactttg-3'	Repeat 24; aa 2,602-2,705
Myc-filamin	5'-cacgcgtatgccgtc cacggagaaggac-3'	5'-cgcgcgttcaaggga ccttgactttgaag-3'	aa 2,434-2,476 of repeat 22, repeat 23, Hinge II region and repeat 24 aa 2,434-2,705

2.3.16 Transient transfection of COS-7 cells (DEAE-Dextran chloroquine method)

COS-7 cells were maintained in Dulbecco's modified Eagle medium (DMEM) supplemented with 10 % foetal calf serum, 2 mM L-glutamine, 100 units/ml penicillin and 0.1 % streptomycin under 5 % CO_2 in a humidified 37 °C incubator.

For immunofluorescence studies transient transfections of COS-7 cells were carried out using the DEAE-Dextran chloroquine method. COS-7 cells were maintained in 10 cm

dishes as described above until a confluency of 70 % was attained. The cells were trypsinised and subcultured at 1 in 2 dilution for 4 hours as described above. Once the cells had firmly attached to the plate, the DMEM was removed, cells were washed with PBS and 5 ml of serum-free M199 was added. To this, 200 µl of DEAE-dextran chloroquine reagent (1 % DEAE Dextran, 2.5 mM Chloroquine), and 5 µg of DNA was added. Cells were incubated as described above for 4 hours, after which cells were washed with PBS and treated with 10 % dimethylsulphoxide (DMSO) in PBS. Cells were cultured for 48 hours in DMEM containing 10 % foetal calf serum and harvested. In some instances, COS-7 cells were treated with epidermal growth factor (EGF). For this, 36 hours after transfection, cells were washed with PBS and placed in DMEM containing 0.1 % foetal calf serum, 2 mM L-Glutamine, 250 IU/ml penicillin, 250 µg/ml streptomycin for a period of 16 hours. Following this, cells were treated with EGF at a final concentration of 0.1 µg/ml.

2.3.17 Transient transfection of COS-7 cells (electroporation method)

COS-7 were maintained as described in section 2.3.16 For immunoprecipitation studies COS-7 cells were transiently transfected *via* electroporation (Sambrook *et al.*, 1989). COS-7 cells were maintained until a confluency of 90 % was attained. The cells were trypsinised and centrifuged at 800 x g for 5 minutes. The pelleted cells were resuspended in PBS and transferred to an electroporation cuvette. 5 µg of DNA was added to the cuvette containing the cells, and gently mixed. The cells were electroporated using Bio-Rad gene pulser II at a capacitance of 0.975 (µf x 1000) and a voltage of 0.20 (kV). Following this, an equal volume of DMEM containing 10 % foetal calf serum was immediately added to the cells and were subcultured at a 1 in 2 dilution. Cells were

cultured in DMEM containing 10 % foetal calf serum for a period of 48 hours post-transfection. In some instances, cells were treated with EGF as described in section 2.3.16.

2.3.18 Intracellular localization of endogenous SHIP-2 in COS-7 cells

COS-7 cells were maintained as described in section 2.3.16. Endogenous SHIP-2 was co-localized with a specific actin marker, phalloidin, and Myc-tagged partial filamin (amino acids 2,434 to 2,705).

For indirect immunofluorescence, COS-7 cells grown on glass coverslips (25 mm × 25 mm) were washed twice with PBS and then fixed and permeabilized for 10 minutes in PBS containing 3.7 % formaldehyde and 0.2 % Triton X-100. The cells were incubated for at least 10 minutes at room temperature in blocking buffer (1 % bovine serum albumin in PBS, w/v). Pre-immune or affinity-purified polyclonal SHIP-2 (neat) antibodies were incubated with the cells for 30 minutes at room temperature. The cells were washed three times with PBS and incubated with fluoroscein isothiocyanate (FITC)-conjugated sheep anti-rabbit IgG antibody (diluted 1:400 in PBS), for 30 minutes at room temperature. Coverslips were then washed with PBS three times, mounted onto glass slides using SlowFade reagent, and visualized using confocal microscopy using a Leica TCS-NT confocal ArKr triple line laser microscope.

Co-localization of SHIP-2 with a specific actin marker was performed using Texas-Red-conjugated phalloidin, which stains polymerized actin. For this, Texas-Red-conjugated phalloidin was diluted 1:2000 in PBS in the affinity-purified SHIP-2 antibodies and incubated with the cells for 30 minutes at room temperature. Coverslips were washed and stained as above, mounted onto glass slides with SlowFade reagent and examined by confocal microscopy.

Endogenous SHIP-2 was co-localized with a Myc-tagged partial filamin (aa 2,434 to 2,705) recombinant protein (Myc-filamin). COS-7 cells transiently transfected with Myc-filamin (as described in section 2.3.17) were stained for endogenous SHIP-2 and Myc-filamin using affinity-purified SHIP-2 antibodies as described above. Monoclonal myc antibodies were diluted 1:1000 in the affinity-purified SHIP-2 antibodies. SHIP-2 and Myc-filamin were detected using FITC-conjugated sheep anti-rabbit IgG antibody (diluted 1:400 in PBS) and TRITC-conjugated goat anti-mouse IgG antibody (diluted 1:700 in PBS), respectively. Coverslips were mounted onto glass slides using SlowFade reagent and visualized by confocal microscopy.

2.3.19 Intracellular localization of endogenous SHIP-2 in A7 and M2 cells

A7 and M2 cells were maintained in Dulbecco's modified Eagle medium (DMEM) supplemented with 10 % foetal calf serum, 2 mM L-glutamine, 100 units/ml penicillin and 0.1 % streptomycin under 5 % CO_2 in a humidified 37 °C incubator. For A7 cells media was also supplemented with 1 mg/ml G418.

For indirect immunofluorescence, A7 and M2 cells were stained with pre-immune and affinity-purified polyclonal SHIP-2 antibodies as described in section 2.3.18

2.3.20 Intracellular localization of recombinant SHIP-2 in COS-7 cells

COS-7 cells were maintained and transiently transfected as described in sections 2.3.16 and 2.3.17 respectively.

Two days after transient transfection of COS-7 cells, cells were washed, fixed and permeabilized as described in section 2.3.18. After incubation in blocking buffer (1 % bovine serum albumin in PBS, w/v) for 10 minutes at room temperature, expression of HA-tagged proteins were detected using anti-HA monoclonal antibodies (diluted 1:1000 in

PBS) incubated with cells for 30 minutes at room temperature. Following this cells were washed three times with PBS, stained with FITC-conjugated sheep anti-mouse IgG antibody (diluted 1:400 in PBS) and washed three times with PBS. Coverlips were mounted onto glass slides using SlowFade reagent and visualized by confocal microscopy.

Co-localization of HA-tagged proteins was performed with specific actin markers, β-actin monoclonal antibodies or Texas-Red-conjugated phalloidin. For this, coverlsips were stained with anti-HA polyclonal antibodies (diluted 1:1000 in PBS) and detected with FITC-conjugated sheep anti-rabbit IgG antibodies (diluted 1:400 in PBS).

Co-localization of HA-tagged proteins with β-actin was performed as described above. β-actin monoclonal antibodies were diluted 1:1000 in PBS, and detected using secondary TRITC-conjugated sheep anti-mouse IgG antibody (diluted 1:700 in PBS).

Co-localization of HA-tagged proteins with phalloidin was performed as described above. Texas-Red-conjugated phalloidin was diluted 1:2000 in PBS.

HA-tagged SHIP-2 recombinant proteins were also co-localized with GFP-tagged recombinant proteins, specifically GFP-PH/ARNO. Co-localization of GFP- and HA-tagged proteins was performed as described above, using monoclonal HA antibodies, diluted 1:1000 in PBS, and detected with TRITC-conjugated sheep anti-mouse IgG antibody (diluted 1:700 in PBS).

2.3.21 Localization of SHIP-2 and filamin in murine heart and soleus muscle

Mice were killed humanely following National Health and Medical Research Council guidelines, Monash University animal ethics number BAM/B/2000/17. Murine heart and soleus were dissected from 12-week-old male mice, C57B/6. Organs were snap frozen in isopentane chilled with liquid nitrogen and blocked in Optimal Cutting Temperature (OCT) compound (10.24 % wt/wt polyvinyl alcohol, 4.26 % wt/wt

polyethylene glycol, 85.5 % nonreactive ingredients) and stored at -70 °C until use. Blocks were equilibrated to -20 °C before sectioning. Cross-sections and longitudinal sections were cut 7 μm thick and placed on superfrost plus slides before staining. Sections were then fixed with 4 % formaldehyde in PBS for 5 minutes at room temperature and washed with PBS, followed by blocking and permeabilization with 10 % horse serum and 0.1 % Triton X-100 in PBS for 15 minutes at room temperature. Slides were then washed with PBS and stained with affinity-purified polyclonal SHIP-2 antibodies (neat, 5 μg/ml), or co-stained with affinity-purified polyclonal SHIP-2 (neat, 5 μg/ml) and monoclonal filamin antibodies (diluted 1:1000 in PBS), or affinity-purified polyclonal SHIP-2 antibodies (5 μg/ml) and monoclonal α-actinin antibodies (diluted 1:800 in PBS) overnight at 4 °C. The following day, sections were washed with PBS and stained with the appropriate secondary antibodies overnight at 4 °C. For detection of SHIP-2, FITC-conjugated sheep anti-rabbit IgG antibodies (diluted 1:400 in PBS) were used, whereas, filamin and α-actinin were detected using TRITC-conjugated sheep anti-mouse IgG antibodies (diluted 1:700 in PBS). Following this, the slides were washed with PBS and coverslips were mounted on to glass slides using SlowFade reagent, and visualized by confocal microscopy.

2.3.22 Preparation of A7, M2 and COS-7 cell lysates for immunoblotting

To confirm the synthesis of recombinant GFP- and HA-tagged proteins in transfected cells or the presence of endogenous proteins, cells were washed briefly with PBS and scraped from the plate in 1 ml of lysis buffer (50 mM Tris, pH 8.0, 150 mM NaCl, 1 % Triton X-100, 2 mM EDTA, 1 mM benzamidine, 2 mM phenylmethylsulfonylfluoride, 2 μg/ml leupeptin, and 2 μg/ml aprotinin) and transferred to a microcentrifuge tube. The cells were extracted for 2 hours at 4 °C, and centrifuged at 13,000 x g for 10 minutes at 4 °C. The supernatant, which represents the Triton-soluble

fraction, was collected and 100 µl was subjected to SDS-PAGE and immunoblotted with the appropriate antibody. Anti-GFP, HA and filamin monoclonal antibodies were diluted 1:1000 in Tris-buffered saline. Affinity-purified polyclonal anti-SHIP-2 antibodies were used neat (5 µg/ml). Appropriate HRP-conjugated sheep anti-mouse/rabbit IgG antibodies diluted 1:10,000 in Tris-buffered saline was used for detection.

2.3.23 Immunoprecipitation of recombinant and endogenous proteins from COS-7 cells

COS-7 cells were maintained and transfected as described in sections 2.3.16 and 2.3.17 respectively. Two days after transient transfection of COS-7 *via* electroporation, cells transfected with recombinant plasmid coding for FLAG- or HA-tagged recombinant proteins, or non-transfected cells were harvested and resuspended in lysis buffer (50 mM Tris, pH 8.0, 150 mM NaCl, 1 % Triton X-100, 2 mM EDTA, 1 mM benzamidine, 2 mM phenylmethylsulfonylfluoride, 2 µg/ml leupeptin, and 2 µg/ml aprotinin) as described in section 2.3.22. Cells were gently agitated for 2 hours at 4 °C prior to centrifugation at 13,000 × g for 10 minutes at 4 °C. FLAG- and HA-tagged recombinant proteins were immunoprecipitated from the supernatant using 60 µl of a 50 % slurry of Protein A Sepharose, 8 µg of anti-FLAG and 10 µg of anti-HA monoclonal antibodies, respectively. Following overnight incubation at 4 °C, the immunoprecipitates were washed six times with 1 ml of ice-cold Tris-buffered saline, subjected to SDS-PAGE, and immunoblotted with either affinity-purified polyclonal SHIP-2 antibodies (neat, 5 µg/ml) or monoclonal filamin, Myc, or FLAG antibodies (all diluted 1:1000 in Tris-buffered saline). Signals were detected using HRP-conjugated sheep anti-mouse/rabbit IgG antibodies (diluted 1:10,000 in Tris-buffered saline).

2.3.24 Protein estimation

Protein concentration was determined by using the Bio-Rad protein assay reagent (Bio-Rad). The sample to be assayed was diluted in distilled water to a final volume of 800 µl to which 200 µl Bio-Rad protein assay dye reagent was added. The contents were mixed thoroughly and incubated at room temperature for 5 minutes before reading the absorbance at 595 nm in a spectrophotometer. The protein content was calculated by reference to a standard curve derived from known amounts of bovine serum albumin.

2.3.25 Sodium dodecylsulphate-polyacrylamide gel electrophoresis (SDS-PAGE)

The protein samples were mixed with an equal volume of SDS-PAGE reducing buffer (40 mM Tris pH 6.8 . 4 % SDS, 20 % glycerol, 0.002 % bromophenol blue, 10 % 2-mercaptoethanol) and incubated at 100 °C for 5 minutes. Samples were briefly centrifuged prior to loading onto the SDS-PAGE gel composed of an upper 4 % acrylamide 'stacking gel' and a lower 10 % acrylamide 'running gel'. The constituents of SDS-PAGE gels are listed below.

acrylamide concentration	**4 %**	**10 %**
0.75 M Tris pH 8.8	-	10 ml
0.25 M Tris pH 6.8	5 ml	-
distilled water	3.15 ml	2.39 ml
10 % SDS	0.05 ml	0.1 ml
30 % acrylamide	1.30 ml	6.50 ml
14 mg/ml ammonium persulfate	0.50 ml	1.0 ml
TEMED	0.005 ml	0.01 ml

Electrophoresis was carried out at 200 mA until the dye front reached the end of the gel. Following electrophoresis, the gels were Western transferred onto a polyvinylidene fluoride (PVDF) membrane.

2.3.26 Western blotting

Proteins separated by SDS-PAGE were transferred onto a PVDF membrane, which had been pre-wetted in methanol and equilibrated in transfer buffer, by re-electrophoresis for 1 hour at 250 mA. After transfer, the membrane was incubated in SDS-PAGE blocking buffer (5 % skim milk) for 1 hour at room temperature to minimise non-specific binding of antibodies to the membrane. The membrane was briefly washed with Tris-buffered saline and incubated with the appropriate primary antibody in a heat-sealed bag overnight at 4 °C with gentle agitation. The membrane was washed with Tris-buffered saline for 10 minutes three times and then incubated for 1 hour at room temperature with the horseradish peroxidase (HRP)-conjugated appropriate secondary antibody (diluted 1:10,000 in Tris-buffered saline). Immunoreactive proteins were detected using enhanced chemiluminescence (ECL) reagent according to the manufacturer's protocols.

2.3.27 Autoradiography

PVDF membranes treated with chemiluminescence reagents, or TLC plates were placed in cassettes containing intensifying screens and exposed to X-ray film. The duration of exposure was dependent on the strength of signal, ranging from 30 seconds to 10 minutes for Western blots, 2 to 24 hours for phosphoinositide 5-phosphatase assays, and 24 to 48 hours for Northern blots. Autoradiography was performed at room temperature or -70 °C depending on the sample. Films were developed using a Fuji medical film processor.

2.3.28 Isolation of human platelets

Human platelets were obtained from healthy volunteers, who had not taken anti-platelet medication in the preceding two weeks (Baenziger and Majerus, 1974). Whole blood was taken in the presence of anticoagulant, 6 volumes blood to 1 volume of anti-coagulant (90 mM trisodium citrate, 7 mM citric acid pH 4.6, 140 mM glucose, 70 mM theophylline). Platelet-rich plasma (PRP) was obtained by centrifugation of whole blood at 200 x g for 30 minutes without brake. PRP was transferred to a fresh tube and the platelets were sedimented by centrifugation at 2000 x g for 10 minutes. The resulting pellet was gently resuspended in 10 ml of platelet washing buffer (4.3 mM Na_2HPO_4, 24.3 mM $NaH_2PO_4.2H_2O$, 4.3 mM K_2HPO_4, 113 mM NaCl, 5.5 mM glucose, 0.5 % bovine serum albumin, 10 mM theophylline; pH 6.5) and contaminating erythrocytes were removed by centrifugation at 200 x g for 10 minutes without brake. The PRP was then transferred into a fresh tube and the platelets pelleted by centrifugation at 2000 x g for 10 minutes. The washes were performed and additional two times. Washed platelets were resuspended in platelet resuspension buffer (12 mM $NaHCO_3$, 10 mM HEPES, 137 mM NaCl, 2.7 mM KCl, 5.5 mM glucose; pH 7.5., 5 ml of buffer per 50 ml of blood taken). Platelets were aliquoted into 900 µl volumes. Some aliquots of platelets were stimulated with thrombin 1U/ml for 5 minutes at room temperature. Platelets were then lysed with 1/10 volume of 10 x platelet lysis buffer (200 mM Tris-HCl, pH 7.4, 10 % Triton X-100, 50 mM EGTA, 4 mM leupeptin, 4 mM aprotinin, 2.5 mg/ml PMSF) and extracted by gentle agitation at 4°C for 2 hours. Lysates were centrifuged at 15,400 x g for 10 minutes at 4 °C to separate the Triton X-100 soluble and insoluble (actin cytoskeletal) extracts. The resultant supernatant represents the Triton-soluble lysate. The cytoskeletal pellet was washed twice with 1 ml of ice-cold Tris-buffered saline and solubilized by incubation with 900 µl of RIPA buffer (10 mM NaH_2PO_4, pH 7.0, 150 mM NaCl, 2 mM EDTA, 250 µg/ml PMSF, 400 µM leupeptin,

400 μM aprotinin, 1 % Nonidet P-40, 1 % sodium deoxycholate, 0.1 % SDS) for 2 hours at 4 °C with gentle agitation. This platelet fraction was centrifuged at 15,400 x g for 10 minutes at 4 °C. The resultant supernatant represents the RIPA-extracted actin cytoskeleton. For immunoblotting 30 μl of the Triton-soluble fraction and the RIPA-extracted actin cytoskeletal fraction were subjected to SDS-PAGE and immunoblotted with affinity-purified SHIP-2 (neat, 5 μg/ml), GPIb (diluted 1:300 in Tris-buffered saline), p85 (diluted 1:1000 in Tris-buffered saline) polyclonal antibodies, or monoclonal filamin (diluted 1:1000 in Tris-buffered saline) antibodies. Polyclonal and monoclonal antibodies were detected using HRP-conjugated sheep anti-rabbit IgG or HRP-conjugated sheep anti-mouse IgG antibodies, respectively (all diluted 1:10,000 in Tris-buffered saline).

2.3.29 Platelet Immunoprecipitations

Platelet fractions were isolated as described in section 2.3.28. Immunoprecipitation of GPIb-IX, filamin and SHIP-2 was performed as follows; 5 μg of polyclonal GPIb antibodies, or 5 μg of affinity-purified polyclonal SHIP-2 antibodies, or 5 μg of monoclonal filamin antibodies, or 5 μl of pre-immune or non-immune sera were incubated overnight at 4 °C with 600 μl of Triton-soluble lysate or RIPA-extracted actin cytoskeletal platelet fractions and 60 μl of a 50 % slurry of protein-A-sepharose. The following day the protein-A-Sepharose pellets were washed six times with ice-cold Tris-buffered saline (20 mM Tris, pH 7.4, 10 mM NaCl) and subjected to SDS-PAGE. Immunoprecipitates subjected to SDS-PAGE were immunoblotted with polyclonal SHIP-2 (neat, 5 μg/ml) or GPIb (diluted 1:300 in Tris-buffered saline) antibodies or monoclonal filamin (diluted 1:1000 in Tris-buffered saline) or actin (diluted 1:1000 in Tris-buffered saline) antibodies. Polyclonal and monoclonal antibodies were detected using HRP-conjugated sheep anti-

rabbit IgG or HRP-conjugated sheep anti-mouse IgG antibodies, respectively (diluted 1:10,000 in Tris-buffered saline).

Immunoprecipitates that were subjected to PtdIns(3,4,5)P_3 5-phosphatase assays (section 2.3.31) were washed three times with 1 ml ice-cold Tris-buffered saline and three times with 1 ml of ice-cold kinase assay buffer (20 mM HEPES pH 7.4, 1 mM EGTA, 5 mM $MgCl_2$). All immunoprecipitates were assessed in duplicate for enzyme activity.

2.3.30 Intracellular localization of endogenous proteins in human platelets

Glass coverslips (12 mm x 12 mm) were coated with vWF (diluted to 10 μg/ml in platelet resuspension buffer) overnight at 4 °C. The following day, coverslips were washed three times with platelet resuspension buffer and blocked with platelet poor plasma containing 50 μg/ml PMSF for 1 hour at room temperature. Platelets obtained from healthy volunteers who had been medication free for at least ten days were washed and isolated as described in section 2.3.28 and applied to vWF-coated coverslips and allowed to spread at 37 °C for either 10, 20 or 45 minutes. Following this, coverslips were washed three times with platelet resuspension buffer (12 mM $NaHCO_3$, 10 mM HEPES, 137 mM NaCl, 2.7 mM KCl, 5.5 mM glucose), and platelets were fixed with 4 % formaldehyde and permeabilized with 0.5 % Triton X-100 (diluted in PBS). Platelets were stained with polyclonal GPIbα (diluted 1:300 in PBS), GPIbβ$_p$ (diluted 1:1000 in PBS) antibodies, affinity-purified polyclonal SHIP-2 antibodies (neat), monoclonal filamin antibodies (diluted 1:1000 in PBS) or Texas-Red-conjugated phalloidin (diluted 1:2000 in PBS) for 45 minutes at room temperature. Coverslips were then washed three times with PBS and the appropriate secondary antibodies(s) were applied, either FITC/TRITC-conjugated sheep anti-mouse (diluted 1:400 and 1:600 in PBS respectively) or FITC-conjugated anti-rabbit IgG antibodies (diluted 1:400 in PBS) and incubated for 45 minutes at room

temperature. Following this, coverslips were washed three times with PBS, mounted onto glass slides using SlowFade reagent and visualized by confocal microscopy.

2.3.31 PtdIns(3,4,5)P_3 5-phosphatase assay

Preparation of [^{32}P]-labelled PtdIns(3,4,5)P_3 substrate was undertaken as follows: 25 µg phosphatidylserine and 65 µg PtdIns(4,5)P_2 were mixed and dried under nitrogen gas, resuspended in 400 µl lipid resuspension buffer and sonicated for 5 minutes. 50 µl of the suspension was added to 5 nmol unlabelled ATP and 20 µl [γ-^{32}P]ATP (2 mCi, 3000 mCi/mmol), 5 µl 20 × kinase buffer (20 mM HEPES pH 7.5, 5 mM $MgCl_2$, 1 mM EGTA) and 1 µg affinity-purified recombinant PI3-kinase (Layton *et al.*, 1998). Following incubation overnight at room temperature, the reaction was terminated by addition of 100 µl 1 M HCl, and following the addition of 5 µg phosphatidylserine, the radiolabelled lipid was extracted with 200 µl chloroform:methanol (1:1) and 500 µl 2 M KCl saturated with chloroform. Extracted lipids were dried and resuspended in 300 µl lipid resuspension buffer (20 mM HEPES pH 7.5, 1 mM $MgCl_2$, 1 mM EGTA). 50 µl of the substrate and 5 µl of 20 × assay buffer (1 M Tris, pH 7.2 and 100 mM $MgCl_2$) were added to each of the immunoprecipitates and the total reaction volume was made up to 100 µl with lipid resuspension buffer. Reactions were incubated for 30 minutes at 37 °C before being terminated with 100 µl 1 M HCl. Lipids were extracted with 5 µg phosphatidylserine, 200 µl chloroform:methanol (1:1) and 500 µl 2 M KCl saturated with chloroform. Reaction products were resolved by TLC and detected by autoradiography. The migration of reaction products was compared with the migration of lipid standards, 40 µg PtdIns(4)P and PtdIns(4,5)P_2. These lipids were visualized by staining the TLC plate with iodine.

CHAPTER 3: The intracellular localization of SHIP-2 and its association with the actin-binding protein, filamin

3.1 Summary

SHIP-2 is a phosphatidylinositol 3,4,5-trisphosphate (PtdIns(3,4,5)P_3) 5-phosphatase that contains an N-terminal SH2 domain, a central 5-phosphatase domain and a C-terminal proline-rich domain. In this study the intracellular localization of SHIP-2 is investigated. In unstimulated cells SHIP-2 localized in a perinuclear cytosolic distribution and at the leading edge of the cell. Following epidermal growth factor stimulation endogenous and recombinant SHIP-2 localized to membrane ruffles, which was mediated by its C-terminal proline-rich domain. To identify proteins that bind to the SHIP-2 proline-rich domain, yeast two-hybrid screening was performed using the proline-rich domain as a "bait" which isolated the actin-binding protein, filamin C. In addition both filamin A and B specifically interacted with SHIP-2 in this assay. SHIP-2 co-immunoprecipitated with filamin from COS-7 cells and association between these species did not change following EGF stimulation.

3.2 Introduction

Phosphoinositides are ubiquitous membrane components which regulate proliferation, differentiation, inhibition of apoptosis, secretion, cell movement and the actin cytoskeleton. Receptor-regulated PI3-kinases phosphorylate phosphatidylinositol 4,5 bisphosphate (PtdIns(4,5)P_2) forming phosphatidylinositol 3,4,5 trisphosphate (PtdIns(3,4,5)P_3), that is dephosphorylated by the inositol polyphosphate 5-phosphatases (5-phosphatase) to phosphatidylinositol 3,4 bisphosphate (PtdIns(3,4)P_2) (Majerus, 1996; Martin, 1997). Both PtdIns(3,4,5)P_3 and PtdIns(3,4)P_2 localize signaling proteins to the inner wall of the plasma membrane and allosterically regulate these target proteins. PtdIns(3,4,5)P_3 and PtdIns(3,4)P_2-binding proteins include the serine/threonine kinase, Akt, which inhibits apoptosis, and proteins such as cytohesins and centaurins that regulate ADP ribosylation factor (ARF), and thereby vesicular trafficking and the peripheral actin cytoskeleton (Corvera *et al.*, 1999; Datta *et al.*, 1999). PtdIns(3,4,5)P_3 regulates growth factor-induced actin-dependent extension of lamellipodia, membrane ruffle formation and cell migration.

PtdIns(3,4,5)P_3 is metabolized by the removal of either the 5- or 3-position phosphate by specific 5- or 3-lipid phosphatases respectively. The product of the tumour suppressor gene PTEN (phosphatase and tensin homologue deleted on chromosome ten) is a PtdIns(3,4,5)P_3 3-phosphatase which hydrolyses PtdIns(3,4,5)P_3 forming PtdIns(4,5)P_2. The lipid 3-phosphatase activity of PTEN is critical for its tumour suppressor function, reviewed (Cantley and Neel, 1999).

The inositol polyphosphate 5-phosphatases hydrolyze the 5-position phosphate from both inositol phosphates and phosphoinositides and share the same catalytic mechanism to the apurinic/apyrimidinic (AP)-endonucleases (Majerus, 1996; Tsujishita *et al.*, 2001; Whisstock *et al.*, 2000). SHIP-2 is a widely expressed 5-phosphatase which

plays a significant role in negatively regulating insulin signaling (Clement *et al.*, 2001; Ishihara *et al.*, 1999). SHIP-2 contains an amino-terminal SH2 domain, a central 5-phosphatase domain, and a carboxyl-terminal proline-rich domain and bears significant sequence identity with the 5-phosphatase, SHIP-1, except in the proline-rich domain. SHIP-2 hydrolyzes the 5-position phosphate from PtdIns(3,4,5)P_3 and PtdIns(4,5)P_2 and in some, but not all studies has been shown to hydrolyze the soluble inositol phosphate Ins(1,3,4,5)P_4 (Pesesse *et al.*, 1997; Taylor *et al.*, 2000; Wisniewski *et al.*, 1999). In contrast to SHIP-1, which has a restricted hematopoetic expression, SHIP-2 is widely expressed. SHIP-2 undergoes cytokine-, growth factor- and insulin-stimulated phosphorylation in a number of cells lines (Habib *et al.*, 1998; Wisniewski *et al.*, 1999). In addition, SHIP-2 is constitutively tyrosine phosphorylated and associated with Shc in chronic myeloid leukemic progenitor cells, suggesting a role for SHIP-2 in $210^{bcr/abl}$-mediated myeloid expansion (Wisniewski *et al.*, 1999). SHIP-2 like PTEN regulates both PtdIns(3,4,5)P_3-mediated Akt activation and the induction of cell cycle arrest associated with increased stability of expression of the cell cycle inhibitor $p27^{KIP1}$ (Taylor *et al.*, 2000). Recent studies have demonstrated SHIP-2 negatively regulates insulin signaling. Homozygous mice lacking SHIP-2 develop severe neonatal hypoglycemia and prenatal death. Adult SHIP-2 heterozygous mutant mice demonstrate insulin sensitivity associated with increased translocation of GLUT4 to the plasma membrane in response to insulin treatment (Clement *et al.*, 2001).

This chapter examines the intracellular location of the 5-phosphatase SHIP-2 and demonstrates the enzyme localizes to membrane ruffles, which is mediated *via* its proline-rich domain. Furthermore it is demonstrated that SHIP-2 forms a constitutive association with the actin-binding protein, filamin in COS-7 cells.

3.3 Results

3.3.1 Domain structure of SHIP-2.

The SH2-containing inositol polyphosphate 5-phosphatase-2 (SHIP-2) is composed of an NH_2-terminal SH2 domain, a central catalytic 300 amino acid 5-phosphatase domain, followed by a COOH-terminal proline-rich domain (PRD). This domain structure is similar to that for the SH2-containing inositol polyphosphate 5-phosphatase-1 (SHIP-1). Sequence alignment of SHIP-1 and SHIP-2, at the protein level, demonstrates high sequence identity between the SH2 domains and the 5-phosphatase domains of SHIP-1 and SHIP-2, with no significant sequence homology observed between the proline-rich domains (Figure 3.1). Sequence analysis of the PRD of SHIP-2 has revealed this domain contains numerous protein-protein interaction motifs, scattered throughout the domain (Figure 3.2). Many sequences within the PRD of SHIP-2 conform to a number of consensus motifs for association with numerous proteins, including SH3 domain-containing proteins (PXXP), WW domain-containing proteins (PPLP), Ena-Vasp homology (EVH1) domain-containing proteins (E/DFPPPPXD/E), sterile alpha motif (SAM) domain-containing proteins and phosphorylation-dependent associations with proteins containing phosphotyrosine-binding (PTB) or SH2 domains (NPXY).

3.3.2 Intracellular localization of SHIP-2 in unstimulated and EGF stimulated cells.

The localization of endogenous SHIP-2 in both COS-7 cells and NIH3T3 cells (not shown), was investigated by indirect immunofluorescence using affinity-purified polyclonal antiserum raised to its unique C-terminal sequence (ITVPAPQLGHHRH-human sequence) (performed by Dr. Cindy O'Malley, Monash University). Similar results were found in both cell types. In unstimulated COS-7 cells, SHIP-2 was detected diffusely in the cytosol and concentrated at the plasma membrane at the leading edge of the cell

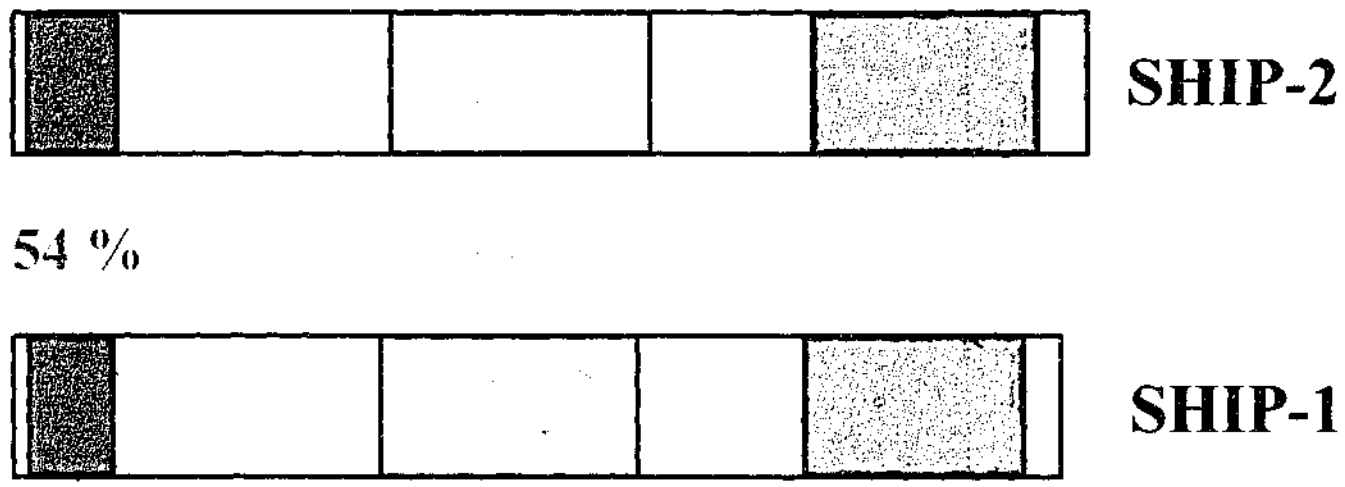

Figure 3.1 Structure of SHIP-2 and SHIP-1.

The structure of SHIP-2 and SHIP-1 is shown. The NH_2-terminal SH2 domain is shown in pink, the catalytic 5-phosphatase domain is indicated in blue, and the COOH-terminal proline-rich domain is shown in green. The amino acid identity between the SHIP-2 and SHIP-1 SH2 domains and 5-phosphatase domains is 54 % and 64 %, respectively.

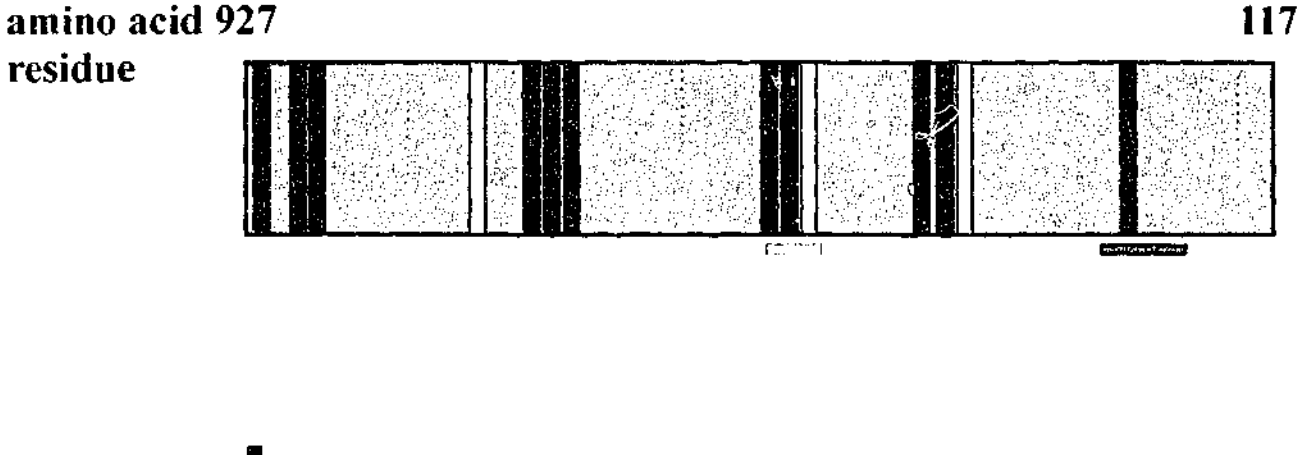

Figure 3.2 Putative protein interaction motifs present in the proline-rich domain of SHIP-2.

The proline-rich domain of SHIP-2 is illustrated in green. The putative protein interaction motifs include 11 SH3 domain binding motifs (PXXP), 1 phosphotyrosine-binding domain motif (NPXY), 2 WW binding domain motifs (PPLP), 1 EVH1 domain binding motif and 1 SAM domain.

(Figure 3.3). SHIP-2 co-localized with markers of submembraneous actin, including β-actin (not shown) and phalloidin-staining. Following epidermal growth factor (EGF) stimulation, conditions under which membrane ruffles and actin are actively formed and remodeled, SHIP-2 localized initially at membrane ruffles *ie.* areas at the edges of lamellipodia where the plasma membrane detaches from the support and rolls up (Cheresh *et al.*, 1999a; Scaife and Langdon, 2000a). After 5-10 minutes EGF stimulation, SHIP-2 was diffusely expressed at the membrane and was detected in areas of active cytoskeletal rearrangement. However, SHIP-2 did not at any time associate with stress fibers, although the enzyme was detected at focal adhesions (not shown) as recently reported (Prasad *et al.*, 2001). Pre-immune sera were non-reactive (not shown). Localization of recombinant human SHIP-2 tagged with either green fluorescent protein (GFP) (performed by Dr. Cindy O'Malley, Monash University) (Figure 3.4), or hemagglutinin (HA) (performed in conjunction with Jelena Becanovic, Monash University) (Figure 3.5), matched that of the endogenous protein. In non-stimulated cells GFP-SHIP-2, was expressed diffusely in the cytosol and in many cells concentrated in a perinuclear distribution. It was also present at the plasma membrane at the leading edge of the cell, co-localizing at this site with phalloidin staining. Following EGF stimulation at 1 minute, GFP-SHIP-2 concentrated at membrane ruffles, and by 5 minutes localized diffusely at the plasma membrane, co-localizing as shown in the merged images with phalloidin-staining of actin (Figure 3.4). It was noted that membrane ruffling was significantly reduced in many cells overexpressing SHIP-2 (see Chapter 4). Expression of HA-tagged SHIP-2 demonstrated a similar intracellular location to GFP-SHIP-2 (Figure 3.5). GFP or HA alone were detected diffusely through the cytosol and nucleus and localization did not change following EGF stimulation (not shown). Recombinant GFP-SHIP-2 was expressed as a 166-kDa protein on SDS-PAGE, with little proteolysis detected (Figure 3.6).

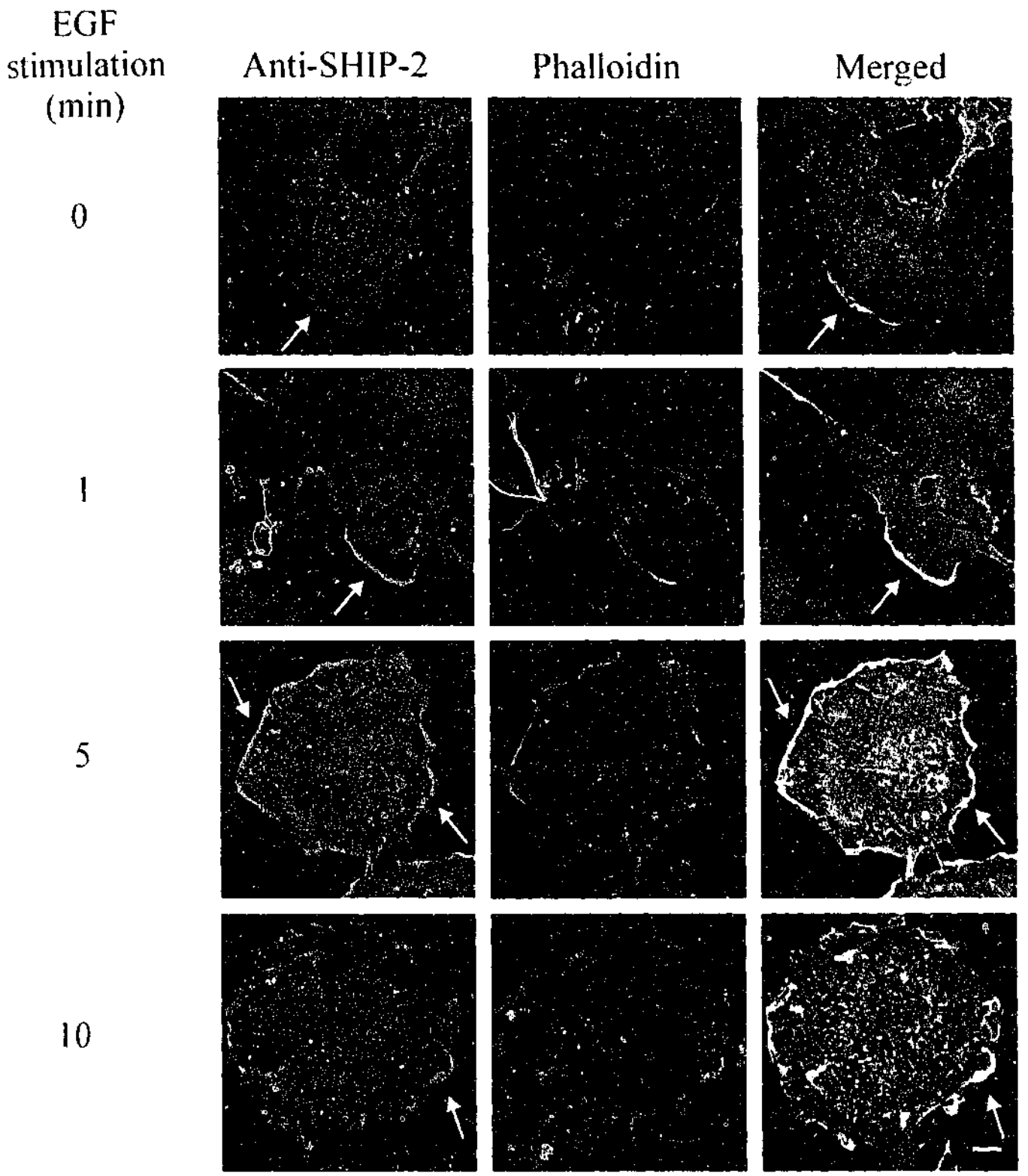

Figure 3.3 SHIP-2 localizes to actin-rich regions in COS-7 cells.

COS-7 cells were serum-starved and where indicated were stimulated with Epidermal Growth Factor (EGF) (100 ng/ml) for either 1, 5 or 10 minutes. Cells were fixed/permeabilized and co-stained with affinity-purified SHIP-2 antibodies and Texas Red-conjugated phalloidin. Cells were visualized by confocal microscopy. Arrows indicate membrane ruffle localization. Bar, 20 μm.

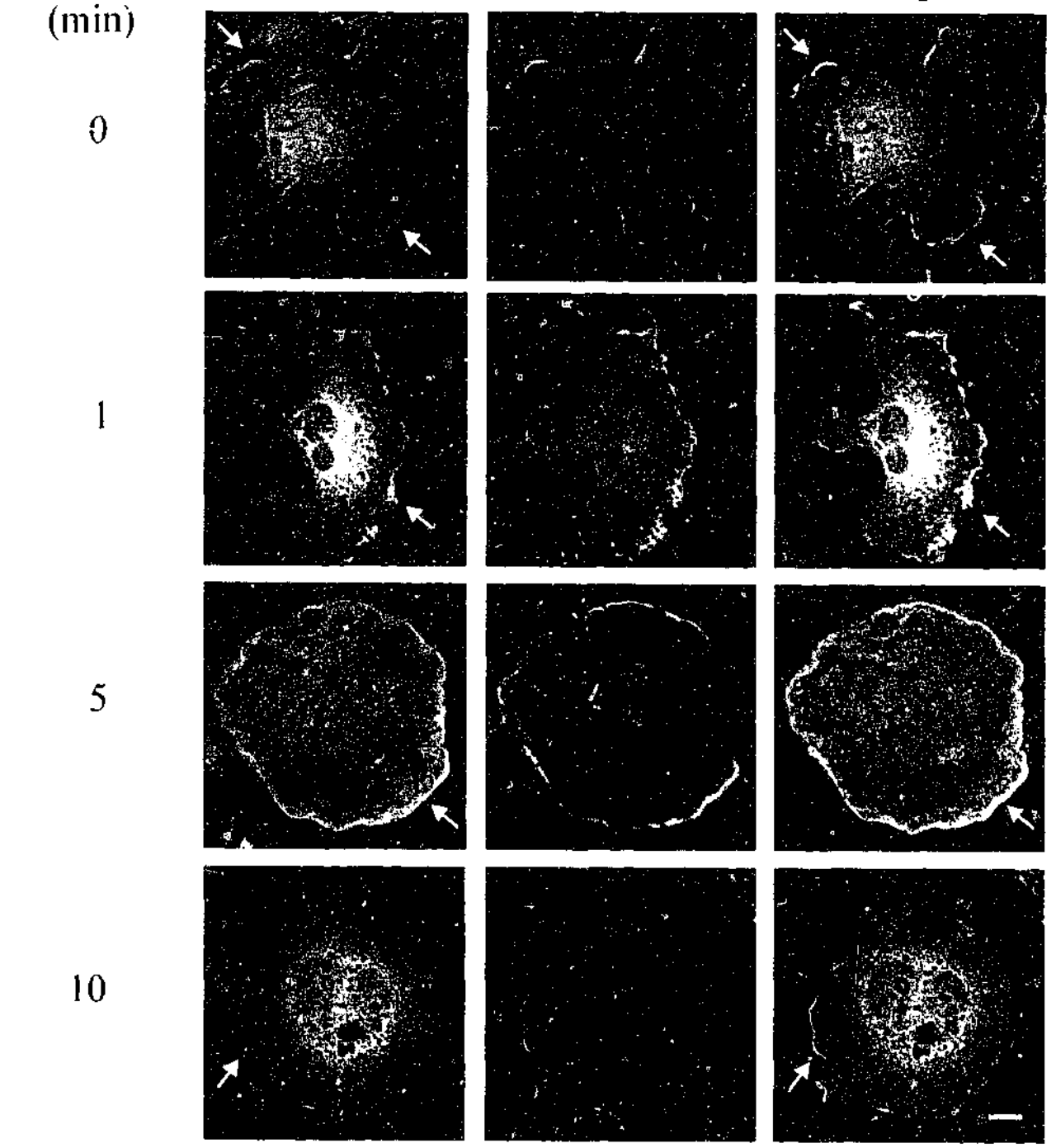

Figure 3.4 Recombinant SHIP-2 localizes to actin-rich regions in COS-7 cells. COS-7 cells were transiently transfected with GFP-SHIP-2, serum-starved and where indicated were stimulated with EGF (100 ng/ml) for either 1, 5 or 10 minutes. Cells were fixed/permeabilized and stained with Texas-Red conjugated phalloidin. Cells were visualized by confocal microscopy. Arrows indicate membrane ruffle localization. Bar, 20 μm.

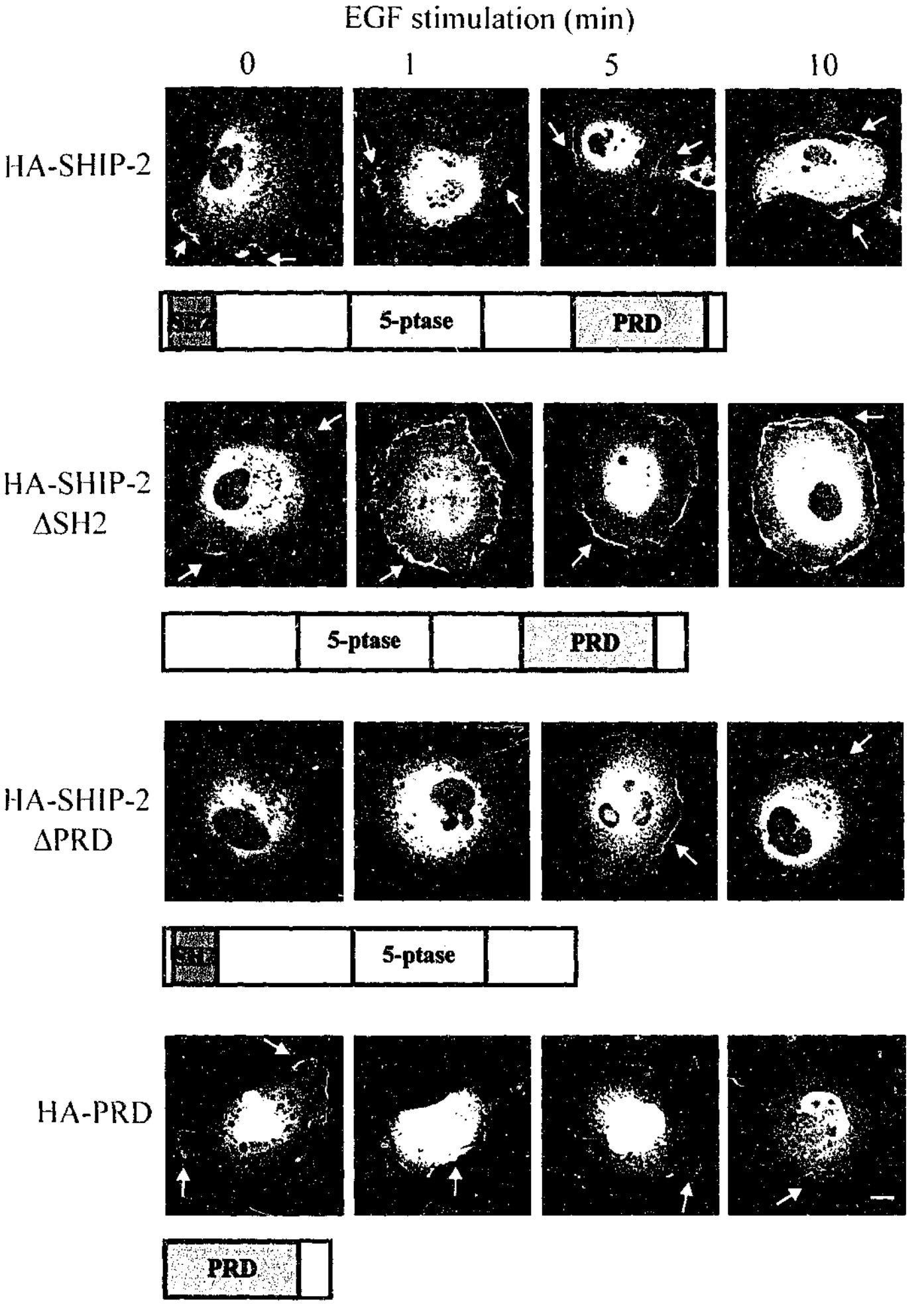

Figure 3.5 SHIP-2 localizes to membrane ruffles *via* its proline-rich domain. COS-7 cells were transiently transfected with either; HA-SHIP-2, HA-SHIP-2ΔSH2, HA-SHIP-2ΔPRD or HA-PRD, serum-starved and where indicated were stimulated with EGF (100 ng/ml) for either 1, 5 or 10 minutes. Cells were fixed/permeabilized and stained with HA antibodies. Cells were visualized by confocal microscopy. Arrows indicate membrane ruffle localization. Bar 20 μm.

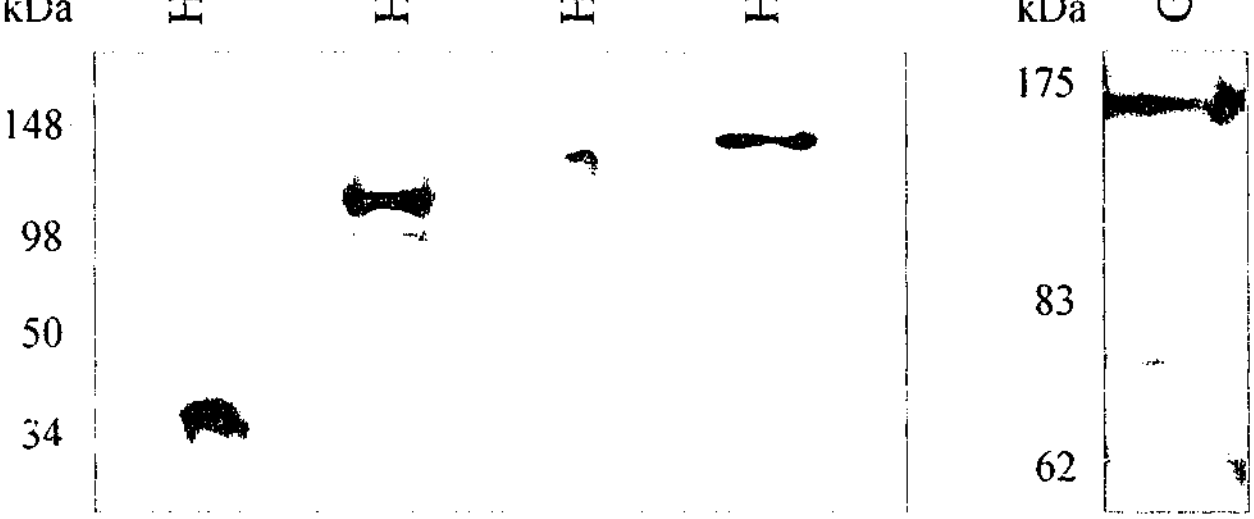

Figure 3.6 Immunoblot analysis of recombinant SHIP-2 proteins.

Immunoblot analysis of recombinant GFP-SHIP-2, HA-SHIP-2 wild type and HA-SHIP-2 mutant proteins. 100 μg of Triton X-100 soluble lysate from transiently transfected COS-7 cells (as indicated) was analyzed by immunoblot analysis using antibodies to GFP or HA. The migration of molecular weight protein markers is shown on the left.

3.3.3 Identification of peptide sequences mediating SHIP-2 localization to membrane ruffles.

SHIP-2 contains an N-terminal SH2 domain, a central catalytic 300 amino acid 5-phosphatase domain and an extensive C-terminal proline-rich domain. To investigate the structural domains mediating SHIP-2 intracellular location, specifically to membrane ruffles, a series of wild type and mutant SHIP-2 recombinants tagged with hemaglutinin (HA) were expressed in COS-7 cells (Figure 3.5) (performed in conjunction with Jelena Becanovic, Monash University). SHIP-2 that lacked the SH2 domain (HA-SHIP-2ΔSH2), localized to membrane ruffles similar to wild type SHIP-2 (Figure 3.5). SHIP-2 that lacked the proline-rich domain (HA-SHIP-2ΔPRD) showed no membrane association in the resting cell and failed to demonstrate membrane ruffle localization following 1 minute of EGF stimulation. However, following 5 minutes stimulation faint membraneous localization of HA-SHIP-2ΔPRD was detected, although this was much less intense than the wild type protein, suggesting that sequences independent of the proline-rich domain may contribute to plasma membrane localization following prolonged growth factor stimulation (Figure 3.5). This result is consistent with recent studies which have demonstrated SHIP-2 forms a complex with the adaptor protein $p130^{cas}$ *via* the SH2 domain and localizes to membrane ruffles and focal adhesions following cell adhesion (Prasad *et al.*, 2001). Studies in which only the proline-rich domain was expressed (HA-PRD) demonstrated this domain localized to the leading edge of the cell in resting cells, as shown for the wild type enzyme, and concentrated at membrane ruffles and submembraneous actin-rich structures immediately following EGF-stimulation. However, by 5 minutes stimulation expression at the membrane was less intense than the wild type enzyme (Figure 3.5). Wild type and mutant HA-SHIP-2 proteins were expressed intact with little proteolysis and migrated at their predicted molecular mass (Figure 3.6).

Collectively, these studies demonstrate the proline-rich domain mediates SHIP-2 membrane ruffle localization in the resting and in EGF-stimulated cells. In addition, sequences such as the SH2 domain may contribute to membrane localization following prolonged growth factor stimulation.

3.3.4 Identification of SHIP-2 binding partners using yeast-two hybrid analysis.

The SHIP-2 C-terminal proline-rich domain contains numerous "PXXP" motifs which conform to consensus sequences for SH3 binding domains, 1 WW binding domain motif (PPLP) which may bind to WW domain-containing proteins and one EVH1 binding domain motif (E/DFPPPPXD/E), which may link the cytoskeletal network to signal transduction pathways (Fedorov *et al.*, 1999). The SHIP-2 proline-rich domain sequence demonstrates no significant sequence homology over the extreme C-terminal 322 amino acids with SHIP-1. A search was performed for proteins that specifically interact with the proline-rich domain using yeast two-hybrid analysis. The entire SHIP-2 proline-rich domain (aa 936-1258) was expressed in yeast cells with a library of proteins expressed as fusions with the GAL4 transcription activation domain. Several rounds of screening a human skeletal muscle library ($4x10^6$ clones) identified a number of interacting clones in which growth on selective media suggested the presence of *bona fide* interactors for the proline-rich domain. Sequence analysis demonstrated that one clone, an 818 bp fragment, encoded amino acids 2,434 to 2,705 of the last C-terminal two and a half immunoglobulin repeats of the cytoskeletal actin-binding protein filamin C, which were in frame with the GAL4 activation domain (Figure 3.7). Filamin is located in the cortical cytoplasm subjacent to the plasma membrane, and binds actin, promoting orthogonal branching of actin filaments and thereby cell migration and membrane stability (reviewed by (Stossel *et al.*, 2001)). Filamin forms a complex with a variety of cell surface receptors including

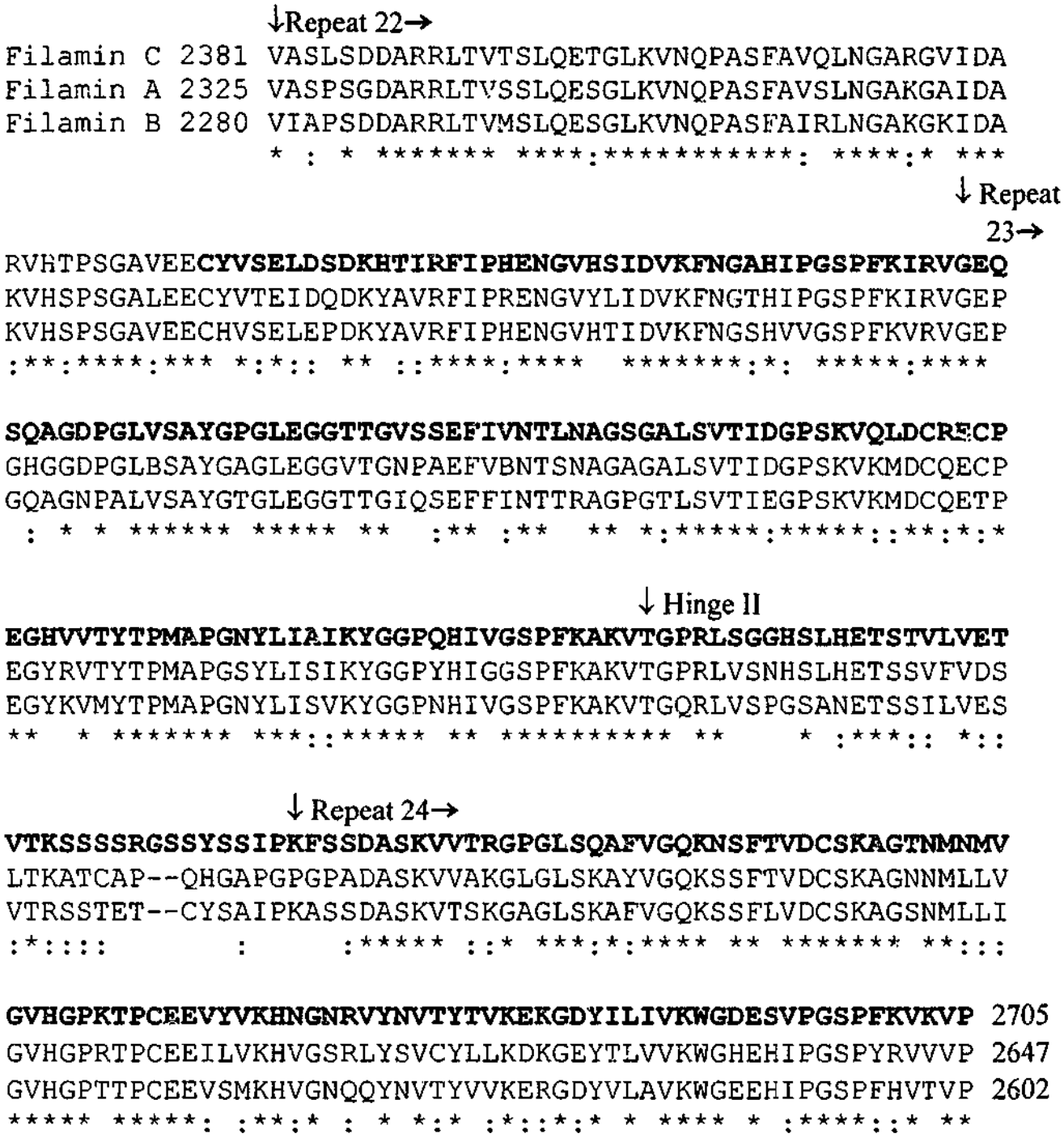

Figure 3.7 Optimized alignment of filamin A, B and C.

Optimized alignment of the predicted amino acid sequences of human filamin A, B and C. ↓ denotes the first amino acid of each repeat domain; astericks represents identical amino acids in all three sequences; a colon represents conservative substitutions. The filamin C sequence shown in bold, represents that encoded by the clone isolated in skeletal muscle library screening, using the SHIP-2 proline-rich domain as a bait in a yeast two-hybrid assay (modified from Xie *et al.*, 1998).

FcγRI, the platelet von Willebrand factor receptor, glycoprotein Ib-IX-V, β_1 and β_2 integrin receptors, and intracellular proteins involved in various signaling cascades including TRAF 2, granzyme B, caveolin-1, and the stress-activated protein kinase (reviewed by (Stossel *et al.*, 2001)).

Three human gene filamin paralogues have been identified. Filamin A encodes α-filamin (also called ABP-280) (Gorlin *et al.*, 1990), filamin B codes for β-filamin (also called ABP-278) (Takafuta *et al.*, 1998; Xu *et al.*, 1998), and filamin C encodes for γ-filamin (also called ABPL or FLN2), which is highly expressed in skeletal muscle (Xie *et al.*, 1998). In addition, differential splicing has been demonstrated for each gene (Maestrini *et al.*, 1993; Xie *et al.*, 1998; Xu *et al.*, 1998). All three filamin isoforms demonstrate a similar structure comprising an N-terminal actin-binding domain followed by 24 immunoglobulin-like repeat domains creating an extended rod like structure. The extreme C-terminal repeat 24 contains a homodimerization domain which is linked to other repeats by a calpain-sensitive "hinge II region" (reviewed by (Stossel *et al.*, 2001)). As each of the three filamin isoforms shows significant sequence identity in the C-terminal region (Figure 3.7), studies were performed to investigate if each isoform, interacted in co-transformation assays with the SHIP-2 proline-rich domain, expressed in frame with the DNA binding domain of GAL4 (DNA-BDPRD), or with recombinant mutant SHIP-2 which lacked the proline-rich domain (DNA-BDSHIP-2ΔPRD) *versus* control heterologous baits. The proline-rich domain "bait" (DNA-BDPRD), but not the SHIP-2 "bait" lacking the proline-rich domain (DNA-BDSHIP-2ΔPRD), interacted with the C-terminal four immunoglobulin repeats of filamin A and B, and the C-terminal two and a half immunoglobulin repeats of filamin C, indicated by expression of all three reporter genes *HIS3* and *ADE2* (Figure 3.8) and *LacZ* (not shown).

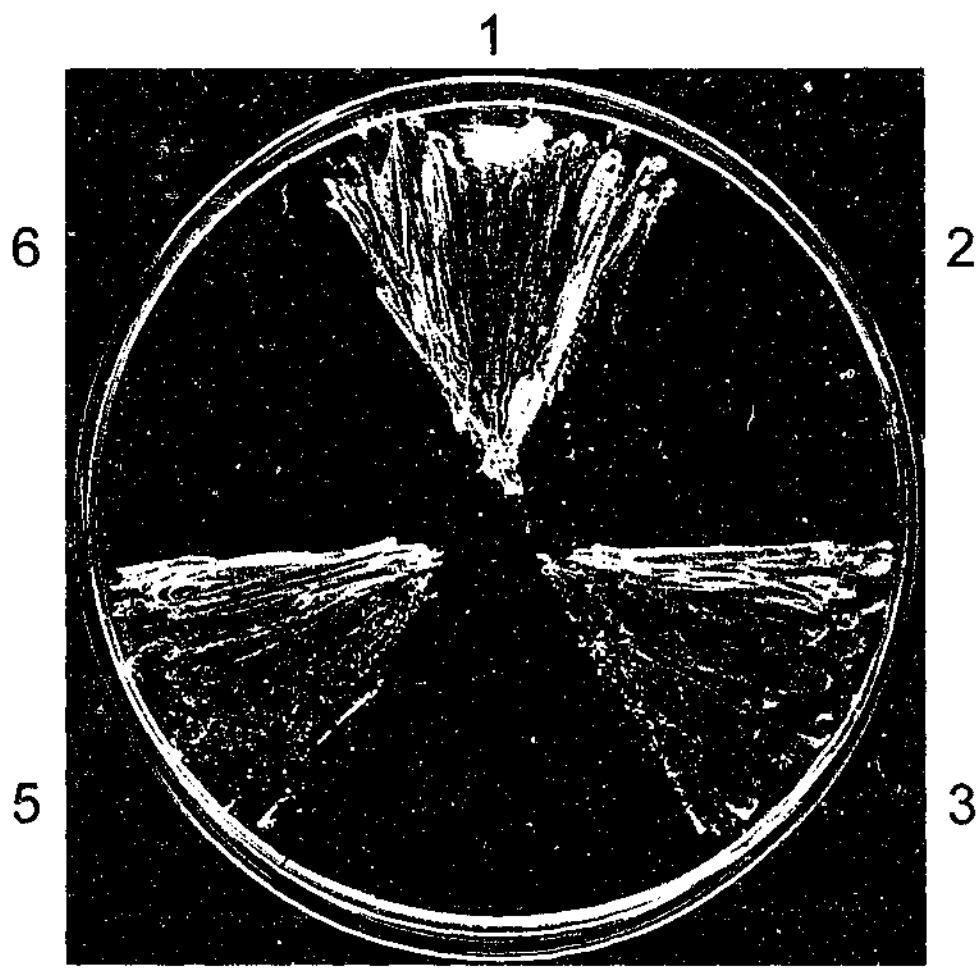

Figure 3.8 SHIP-2 interacts with filamin A, B and C in the yeast two-hybrid system.

Yeast expressing strain AH109 expressing the DNA-BDPRD "bait" were transformed with filamin A, B or C cDNA (1, 3, and 5, respectively), and yeast strain AH109 expressing the DNA-BDSHIP-2ΔPRD "bait" were transformed with filamin A, B, or C cDNA (2, 4, and 6, respectively) and plated onto medium lacking Tryptophan, Leucine, Hisitidine and Adenine.

3.3.5 Identification of filamin C sequences mediating interaction with SHIP-2.

To determine the region of filamin C specifically interacting with SHIP-2, a series of wild type and mutant filamin C constructs comprising the C-terminal immunoglobulin repeat regions R22-R24 (aa 2,434-2,705) which include a "hinge II region" (H2) between R23 and R24 were cloned into the activation domain and co-transformed with the DNA-BDPRD bait and interactions scored as strong (+++), or weak (+) (Figure 3.9). The fragment containing filamin C repeats 22 to 24 demonstrated the strongest binding to the proline-rich domain bait. Filamin C repeats 23 and 24, either alone or in combination, did not interact with SHIP-2. Repeats 22 and 23 in combination, with or without the hinge II region, interacted with SHIP-2 however, this was weaker than repeats 22-24 (Figure 3.9). All filamin C truncation mutants were expressed intact in the yeast strain AH109 (not shown).

Several approaches were undertaken to verify whether SHIP-2 interacted with filamin *in vivo* and thereby regulated the membrane localization of SHIP-2. First, it was investigated using co-transfection and co-immunopreciptation assays if filamin interacted with SHIP-2 in COS-7 cells. In addition, association of endogenous proteins using immunopreciptation and immunoblot analysis was also determined. In Chapter 4 the localization of SHIP-2 in filamin-deficient and filamin-replete cells is presented.

Association of SHIP-2 and filamin was demonstrated in COS-7 cells, which were co-transfected with FLAG-tagged SHIP-2 and HA-tagged filamin (encoding amino acids 2,434-2,705 of filamin C), followed by immunoprecipitation and immunoblot analysis using antibodies to each tag. FLAG-SHIP-2 was detected in HA immunoprecipitates of HA-filamin transfected cells, but not cells transfected with HA empty vector (Figure 3.10A). The effect of EGF stimulation on association between recombinant SHIP-2 and filamin was determined. COS-7 cells were co-transfected with Myc-filamin and FLAG-

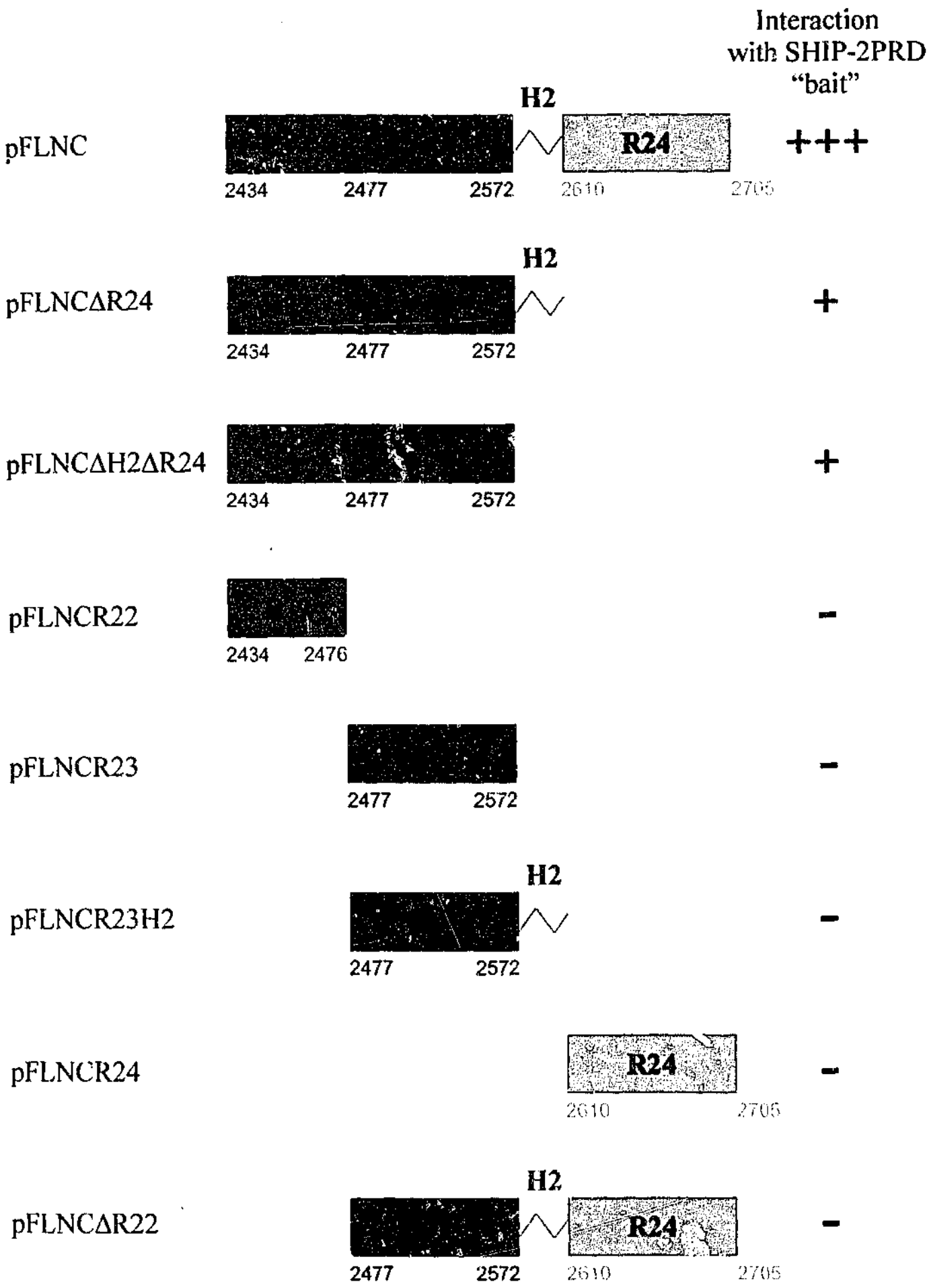

Figure 3.9 Repeats 22, 23, the Hinge II region and repeat 24 of filamin C are required for maximal association with SHIP-2 in the yeast two-hybrid system.
The filamin C wild-type (aa 2,434-2,705, pFLNC) or truncation mutants (see Table II) were prepared as described in Materials and methods. Yeast strain AH109 expressing the DNA-BDPRD "bait" were transformed with each FLNC mutant individually. The transformants were plated onto media lacking Tryptophan, Leucine, Histidine, and Adenine and assessed for LacZ expression. A strong or weak interaction is indicated by +++ or +, respectively. No interaction is indicated by -.

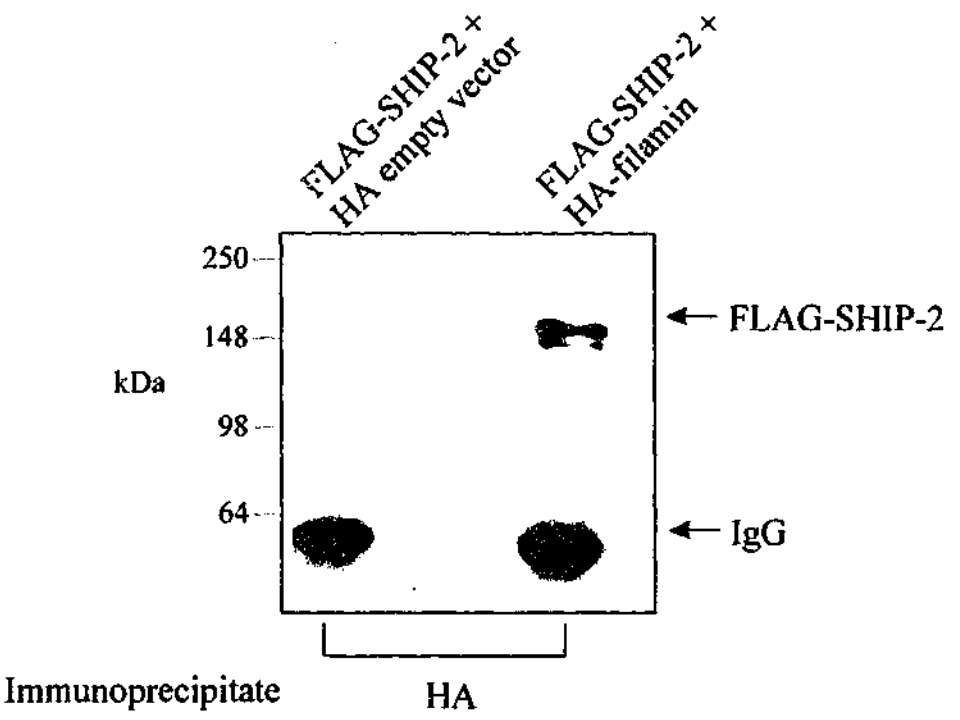

Figure 3.10 Recombinant SHIP-2 associates with recombinant filamin in resting and Epidermal Growth Factor (EGF)-stimulated COS-7 cells.

A. COS-7 cells were transiently co-transfected with FLAG-SHIP-2 and HA empty vector, or FLAG-SHIP-2 and HA-filamin (encoding aa 2,434 to 2,705). Cells were harvested and the Triton X-100-soluble lysate was immunoprecipitated with HA antibodies and immunoblotted with FLAG antibodies.

B. COS-7 cells were transiently co-transfected with FLAG empty vector and Myc-filamin (encoding aa 2,434 to 2,705), or FLAG-SHIP-2 and Myc-filamin. Where indicated COS-7 cells were serum-starved and treated with EGF (100 mg/ml) for 5 minutes. Cells were harvested and the Triton X-100-soluble fraction was immunoprecipitated with FLAG antibodies and immunoblotted with Myc antibodies.

SHIP-2 and following EGF stimulation for 5 minutes, Triton X-100-soluble lysates were immunoprecipitated using FLAG antibodies and immunoblotted with myc antibodies. The level of filamin in SHIP-2 immunoprecipitates was unchanged following 5 minutes EGF stimulation, compared to non-stimulated cells (Figure 3.10B). These studies were repeated expressing SHIP-2 and filamin as fusion proteins with different tags with similar results (not shown).

To confirm complex between endogenous SHIP-2 and filamin, recombinant Myc-tagged filamin (encoding amino acids 2,434-2,705 of filamin C) was transfected into COS-7 cells and following EGF stimulation immunoprecipitations using affinity-purified SHIP-2 antibodies, or affinity-purified pre-immune sera were performed, and immunoblotted with either affinity-purified SHIP-2 antibodies (upper panel), or myc antibodies to detect filamin (lower panel) (Figure 3.11A). This study demonstrated recombinant filamin formed a stable complex with endogenous SHIP-2 and association did not change following growth factor stimulation. In addition, COS-7 cell Triton X-100-soluble lysates immunoprecipitated using affinity-purified SHIP-2 antibodies and immunoblotted using filamin antibodies, demonstrated a 280 kDa polypeptide consistent with filamin in SHIP-2 immune, but not pre-immune immunoprecipitates (Figure 3.11B). In control studies immunoblot analysis of COS-7 Triton X-100-soluble cell lysates demonstrated the SHIP-2 and filamin antibodies recognized 148 kDa and 280 kDa proteins respectively, consistent with their predicted molecular weight (Figure 3.11C).

Collectively these studies demonstrate SHIP-2 localizes to membrane ruffles which is mediated *via* its proline-rich domain. Furthermore, SHIP-2 forms a complex with the actin-binding protein filamin in both resting and EGF-stimulated COS-7 which remains unchanged following growth factor stimulation.

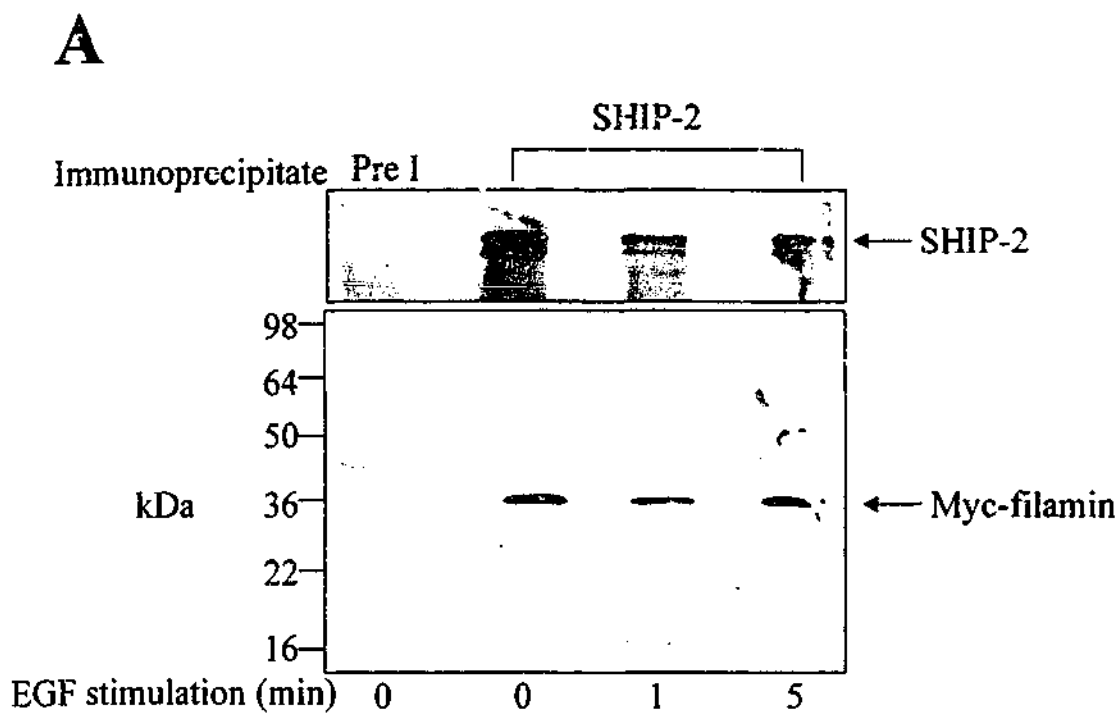

Figure 3.11 Endogenous SHIP-2 associates with filamin in COS-7 cells.

A. COS-7 cells were transiently transfected with Myc-filamin (encoding aa 2,434 to 2,705), serum-starved and where indicated treated with EGF for 1 or 5 minute(s). Cells were harvested and the Triton X-100-soluble lysate was immunoprecipitated with either affinity-purified preimmune sera (Pre I) or affinity-purified SHIP-2 antibodies, and immunoblotted with Myc antibodies.

B. COS-7 cells were harvested and the Triton X-100-soluble lysate was immunoprecipitated with either affinity-purified preimmune sera (Pre I) or affinity-purified SHIP-2 antibodies, and immunoblotted with filamin antibodies.

C. COS-7 cells were harvested and 100 μg of the Triton X-100-soluble lysate was immunoblotted with affinity-purified SHIP-2 antibodies or filamin antibodies.

CHAPTER 4: SHIP-2 regulates PtdIns(3,4,5)P_3 levels and submembraneous actin at membrane ruffles

4.1 Summary

To verify SHIP-2 and filamin form a complex *in vivo*, the localization of each species was investigated in various cell lines and tissues. Furthermore, the functional significance of this complex was investigated. SHIP-2 co-localized with filamin at Z-lines and the sarcolemma in striated muscle sections and at membrane ruffles in COS-7 cells, although the membrane ruffling response was reduced in cells overexpressing SHIP-2. SHIP-2 membrane ruffle localization was dependent on filamin binding, as SHIP-2 was expressed exclusively in the cytosol of filamin-deficient cells. Recombinant SHIP-2 regulated PtdIns(3,4,5)P_3 levels and submembraneous actin at membrane ruffles following growth factor stimulation, dependent on SHIP-2 catalytic activity. Collectively these studies demonstrate filamin-dependent SHIP-2 localization to membrane ruffles critically regulates PI3-kinase signaling to the actin cytoskeleton.

4.2 Introduction

Dynamic reorganization of the actin cytoskeleton alters cell shape and generates forces required for many cellular processes including cell locomotion, and phagocytosis (reviewed by (Stossel *et al.*, 2001)). Actin-filament structures range from parallel bundles to three-dimensional orthogonal networks. In response to signaling cascades, actin-binding proteins orchestrate the engineering of the actin cytoskeleton, that facilitates cell adhesion, membrane ruffling, and cell migration (reviewed by (Stossel *et al.*, 2001)).

Filamin is an actin-binding protein composed of an amino-terminal actin-binding domain, followed by 24 repeats of approximately 96 amino acids each (reviewed by (Stossel *et al.*, 2001)). Filamin is the most potent actin-filament cross-linking protein, however, the molecular mechanism by which it functions are incompletely understood (Bennett *et al.*, 1984; Brotschi *et al.*, 1978). The leading edge (lamellipodia) of motile cells contains a three-dimensional orthogonal array of actin filaments, at which, filamin has been detected (Hartwig *et al.*, 1989; Hartwig and Shevlin, 1986; Schliwa and van Blerkom, 1981).

In addition to binding actin, filamin has been shown to associate with over twenty different proteins, implicated in a variety of signaling cascades (reviewed by (Stossel *et al.*, 2001)). Moreover, the absence of filamin in mammalian fibroblasts, which have impaired motility, implicates filamin as a crucial actin-binding protein facilitating cell migration. Filamin-deficient melanoma cells (M2 cells) have an unstable surface and extend one or a few flattened ruffling lamellipodia and protrude and retract membrane "blebs". Reexpression of filamin in M2 cells reverses the phenotype of these cells (Cunningham *et al.*, 1992).

The PI3-kinase lipid product PtdIns(3,4,5)P_3, has been implicated in the regulation of the cytoskeleton. Studies using pharmacological inhibitors of PI3-kinase, mutant

receptors unable to activate PI3-kinase, and membrane-permeant esters of PtdIns(3,4,5)P_3, have in a variety of cell types, been demonstrated to interfere with stimulus-induced actin polymerization. Incubation of human neutrophils with a membrane-permeant ester of PtdIns(3,4,5)P_3 increases cell migration, whilst at the molecular level, there is an increase of F-actin at lamellipodia (Niggli, 2000). Moreover, the addition of a synthetic form of PtdIns(3,4,5)P_3 to porcine aortic endothelial cells stimulates membrane ruffling responses to the same extent as PDGF stimulation (Derman *et al.*, 1997). Conversely, expression of mutant PDGF receptors, in which the PI3-kinase binding site is destroyed, results in a failure of motility responses such as membrane ruffling (Wennstrom *et al.*, 1994a). Recent studies have demonstrated that filamin interacts with LL5β which associates with PtdIns(3,4,5)P_3 through its PH domain, suggesting filamin is involved in PI3-kinase signaling (Paranavitane *et al.*, 2002).

The actin cytoskeleton has been implicated in insulin-mediated events. Inhibition of actin polymerization prevents insulin-dependent association of the p85 subunit of PI3-kinase with the glucose transporter GLUT4 and recruitment of GLUT4-containing vesicles to the plasma membrane in skeletal muscle and adipocyte cell lines (Khayat *et al.*, 2000). Through the generation of SHIP-2-deficient mice, a significant role for SHIP-2 has emerged in signaling pathways downstream of the insulin receptor (Clement *et al.*, 2001). SHIP-2 -/- mice display hypoglycemia which results from insulin hypersensitivity and a decrease in expression of several gluceogenic enzymes. The loss of one SHIP-2 allele results in an increase in the translocation of GLUT4 to the cell surface in response to insulin

This chapter demonstrates that SHIP-2 co-localizes with filamin at membrane ruffles in COS-7 cells and to Z-lines in mature muscle. In addition, a filamin-dependent

enrichment of SHIP-2 at membrane ruffles where SHIP-2 regulates PtdIns(3,4,5)P_3 and submembraneous actin is detailed.

4.3 Results

4.3.1 Co-localization of fillamin and SHIP-2 in COS-7 cells.

Several approaches were undertaken to verify whether SHIP-2 interacted with filamin *in vivo* and thereby regulated the membrane localization of SHIP-2. Initially, the co-localization of SHIP-2 and filamin at membrane ruffles in resting and EGF-stimulated COS-7 cells was demonstrated. Secondly, the co-localization of filamin and SHIP-2 in mouse heart and skeletal muscle sections using immunolocalization of both species is shown. Finally, the membrane localization of SHIP-2 and its dependence on filamin, was determined by investigating the intracellular localization of SHIP-2 in cells which do not express filamin.

Endogenous filamin and recombinant SHIP-2 following EGF stimulation of COS-7 cells were co-localized (performed by Jelena Becanovic, Monash University). In non-stimulated cells filamin was located in the cytosol and at the leading edge of the cell (Figure 4.1). Although HA-SHIP-2 was expressed in the cytosol and membrane, co-localization with filamin was detected only at the membrane at the leading edge of the cell. Following EGF-stimulation filamin localized to a sub-plasma membrane distribution, initially at membrane ruffles and at the latter time points, evenly throughout a fine cortical rim at the periphery of the cell. Filamin co-localized intensely with HA-SHIP-2 at membrane ruffles and the cortical actin rim, but not in the cytosol.

It was then investigated whether the recombinant C-terminal filamin domain (aa 2434-2705) localized as endogenous filamin in COS-7 cells. In addition, it was also determined whether this recombinant filamin C-terminal domain, which represents the SHIP-2 binding site, when expressed at high levels, could displace endogenous SHIP-2 localized at membrane ruffles. The Myc-filamin recombinant protein may actually inhibit the localization of SHIP-2 to membrane ruffles by blocking binding to endogenous filamin.

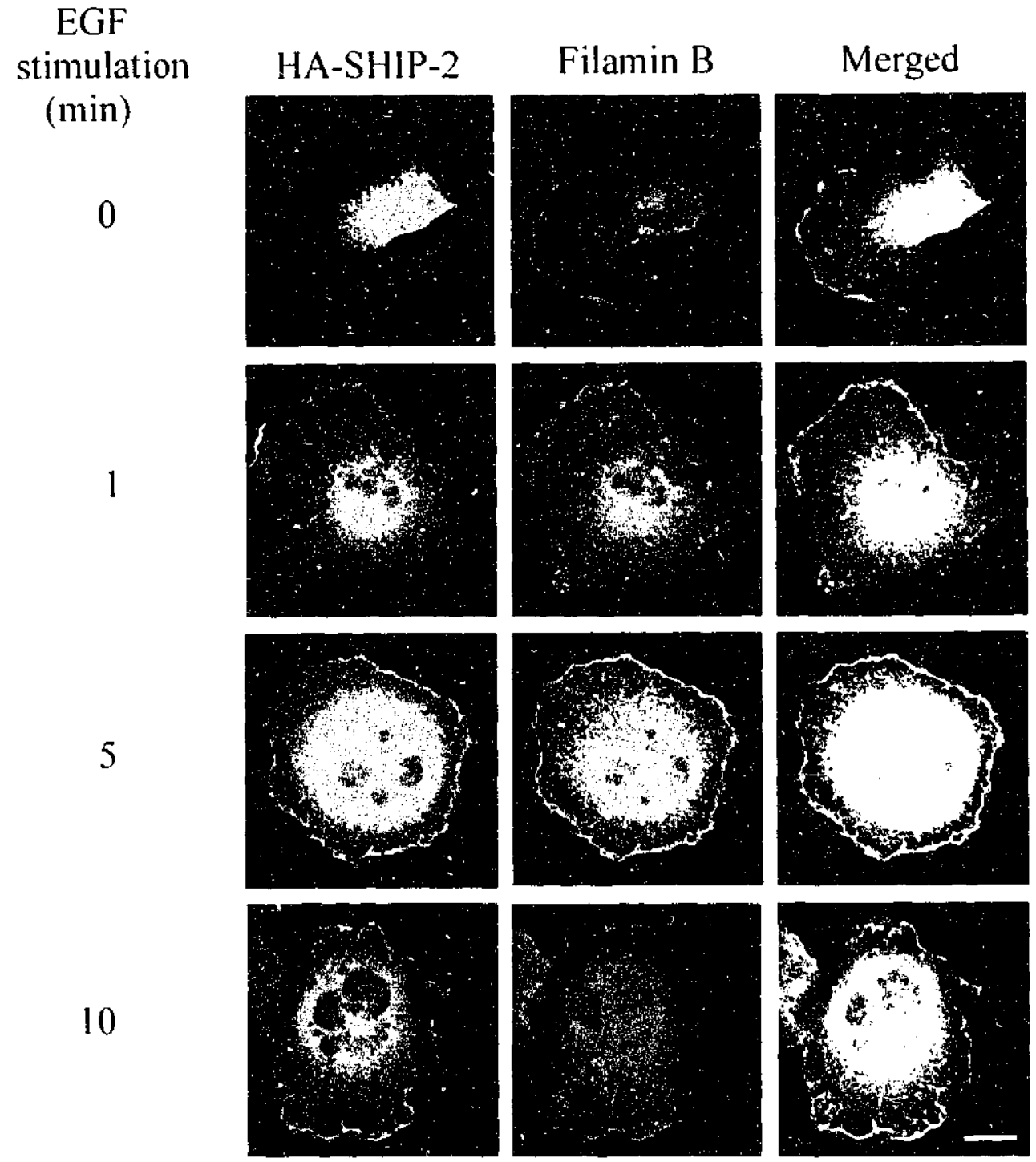

Figure 4.1 SHIP-2 colocalizes with filamin in resting and EGF-stimulated cells. COS-7 cells were transiently transfected with HA-SHIP-2. Cells were serum-starved and where indicated were treated with EGF (100 ng/ml) for 1, 5 or 10 minute(s), fixed/permeabilized and co-stained with HA and filamin B antibodies. Cells were visualized by confocal microscopy. Bar, 20 μm.

In both low and high Myc-filamin expressing cells the localization of the recombinant protein matched that of endogenous filamin at membrane ruffles in unstimulated (not shown) and more prominently in EGF-stimulated cells (Figure 4.2). However, in cells expressing Myc-filamin at very high levels in addition to membrane staining, an increased expression of filamin in the cytosol was also noted. Localization of endogenous SHIP-2 in Myc-filamin expressing cells was determined by indirect immunofluorescence. In cells expressing low levels of Myc-filamin, endogenous SHIP-2 localized to membrane ruffles in both resting (not shown) and more prominently in EGF-stimulated cells (Figure 4.2). In contrast, in cells expressing high levels of Myc-filamin SHIP-2 localized in a perinuclear distribution in the cytosol and staining was less intense at the plasma membrane (Figure 4.2).

4.3.2 Co-localization of filamin and SHIP-2 in heart and skeletal muscle.

Filamin C is highly expressed in striated muscle where it is predominantly localized in myofibrillar Z-discs, with a minor fraction of the protein showing sub-sarcolemma localization (van der Ven *et al.*, 2000). SHIP-2 is also expressed in skeletal muscle, although its intracellular location in this tissue has not been reported. SHIP-2 homozygous null mice demonstrate increased sensitivity to insulin (Clement *et al.*, 2001). One of the major sites of insulin action is skeletal muscle, where insulin stimulates the translocation of the glucose transporter GLUT4 in a PI3-kinase dependent manner to the sarcolemma (Khan *et al.*, 2000). It was investigated whether SHIP-2 and filamin co-localized in striated muscle. Mouse heart striated muscle sections were isolated, fixed and probed with specific affinity-purified SHIP-2 antibodies (Figure 4.3a)(cryosectioning performed by Imogen Coghill, Monash University). Soleus muscle showed similar localization (not shown). In longitudinal sections SHIP-2 antibodies stained intensively in an alternate banding pattern

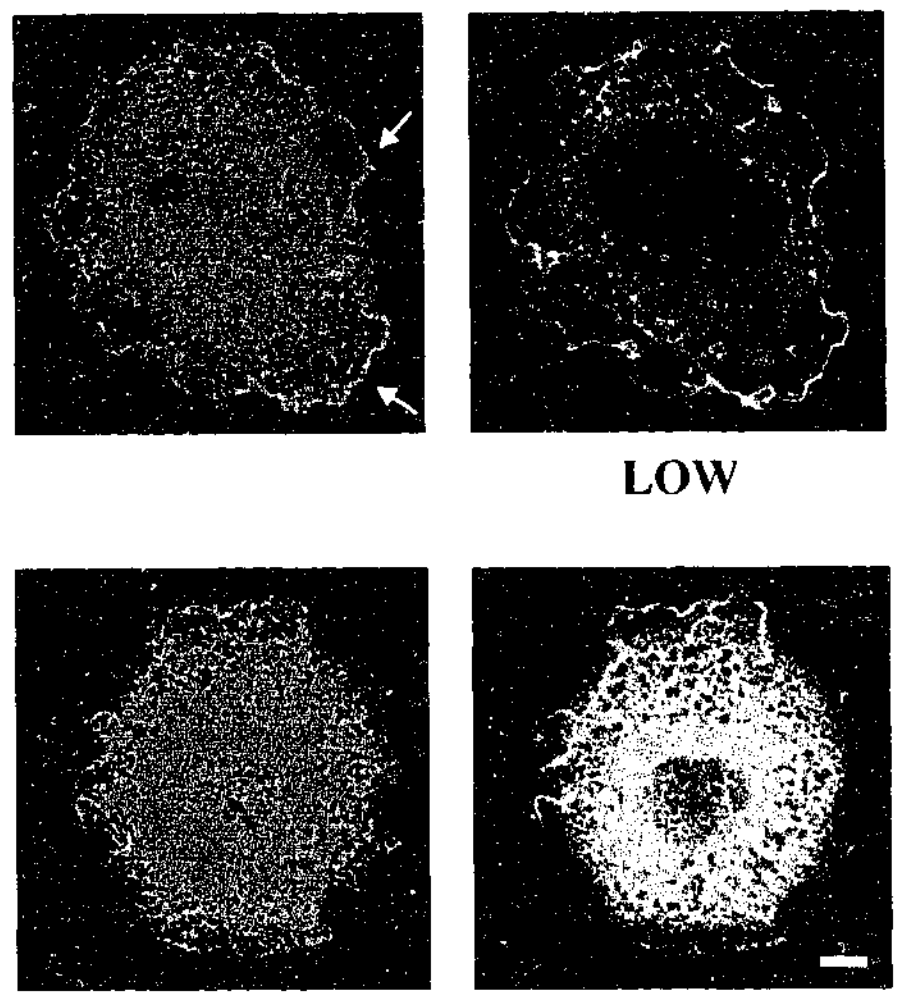

Figure 4.2 High overexpression of Myc-filamin displaces SHIP-2 from membrane ruffles in EGF-stimulated COS-7 cells.

COS-7 cells were transiently transfected with Myc-filamin (encoding amino acids 2,434-2,705), serum-starved, and treated with EGF (100 ng/ml) for 5 minutes. Cells were scored as expressing high or low levels of this recombinant protein, as determined by intensity of staining using antibodies to the Myc tag by indirect immunofluorescence. The localization of endogenous SHIP-2 was determined using affinity-purified SHIP-2 antibodies in cells expressing either low or high levels of Myc-filamin. Arrows indicate the localization of SHIP-2 to membrane ruffles. Cells were visualized by confocal microscopy. Bar, 20 μm.

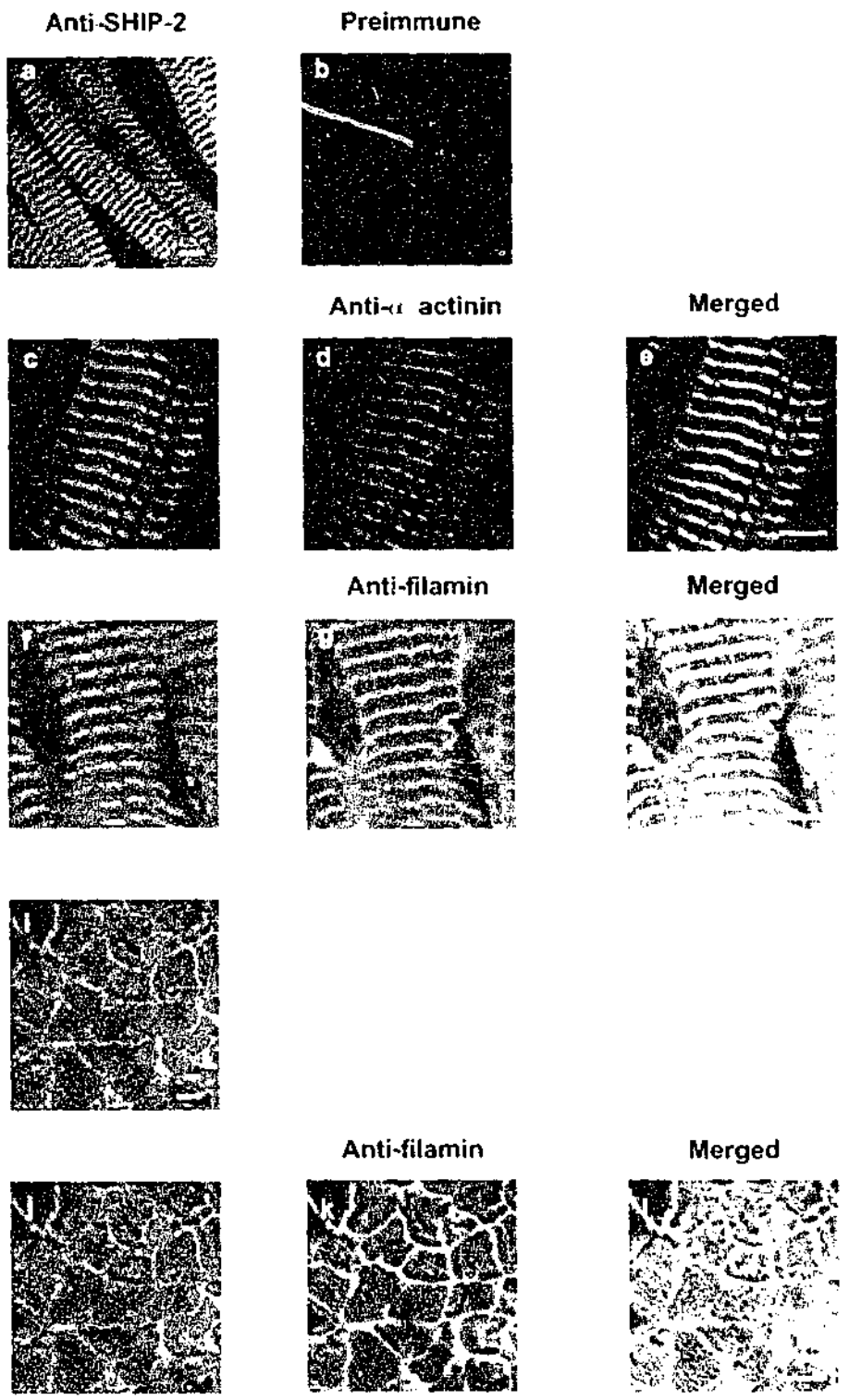

Figure 4.3 SHIP-2 co-localizes with filamin at Z-lines in mouse heart and skeletal muscle sections.

Mouse adult heart longitudinal cryosections were cut 7 μm thick and stained with affinity-purifed SHIP-2 antibodies (a,e and f) or affinity-purifed pre-immune sera (b). SHIP-2 was co-localized with α-actinin (d) and filamin (g) at the Z-line. Merged images between SHIP-2 and α-actinin, and SHIP-2 and filamin, are indicated in panels e and h, respectively. Cross-sectional sections of skeletal muscle were stained affinity-purifed SHIP-2 antibodies (i and j) and counterstained with filamin antibodies (k). Merged image is shown in panel l. Sections were visualized by confocal microscopy. Bars, 20 μm.

at areas that resembled Z-lines. No staining of any structure was observed using pre-immune serum (Figure 4.3b). Counter-staining sections using antibodies to filamin and the Z-line specific protein α-actinin demonstrated both co-localized with SHIP-2 (Figure 4.3c-h). Cross-sectional analysis of skeletal muscle demonstrated both filamin and SHIP-2 localized to the sarcolemma, the site of insulin stimulated GLUT4 translocation (Figure 4.3i -l).

4.3.3 Intracellular localization of SHIP-2 in filamin-deficient cells.

To investigate if SHIP-2 membrane ruffle localization was dependent on an interaction with filamin, the intracellular localization of SHIP-2 in a cell line (M2), derived from a human malignant melanoma, that does not express detectable filamin messenger RNA or protein (Cunningham *et al.*, 1992) was examined. M2 cells demonstrate a distinct phenotype characterized by extensive membrane blebbing and defective locomotion, which is reversed by the stable transfection of filamin A cDNA (A7 subline). Equivalent SHIP-2 expression was demonstrated in A7 and M2 cells as shown by immunoblot analysis using SHIP-2 anti-peptide antibodies of 100 μg of cell lysate (Figure 4.4A and B). The intracellular localization of SHIP-2 was determined by indirect immunofluorescence of the endogenous enzyme using SHIP-2 anti-peptide antibodies, or cells transfected with HA-tagged SHIP-2 with detection by staining with antibodies to the tag (not shown) with the same result. In non-stimulated M2 cells SHIP-2 was expressed diffusely in the cytosol and did not co-localize with markers of submembraneous actin such as phalloidin (Figure 4.4A). Upon EGF stimulation M2 cells transiently form membrane ruffles, or membrane "blebs", which can be detected by phalloidin staining (reviewed by (Stossel *et al.*, 2001)). SHIP-2 remained in the cytosol in stimulated cells and did not co-localize with filamin at membrane ruffles. In contrast in A7 cells, which have been stably transfected with filamin,

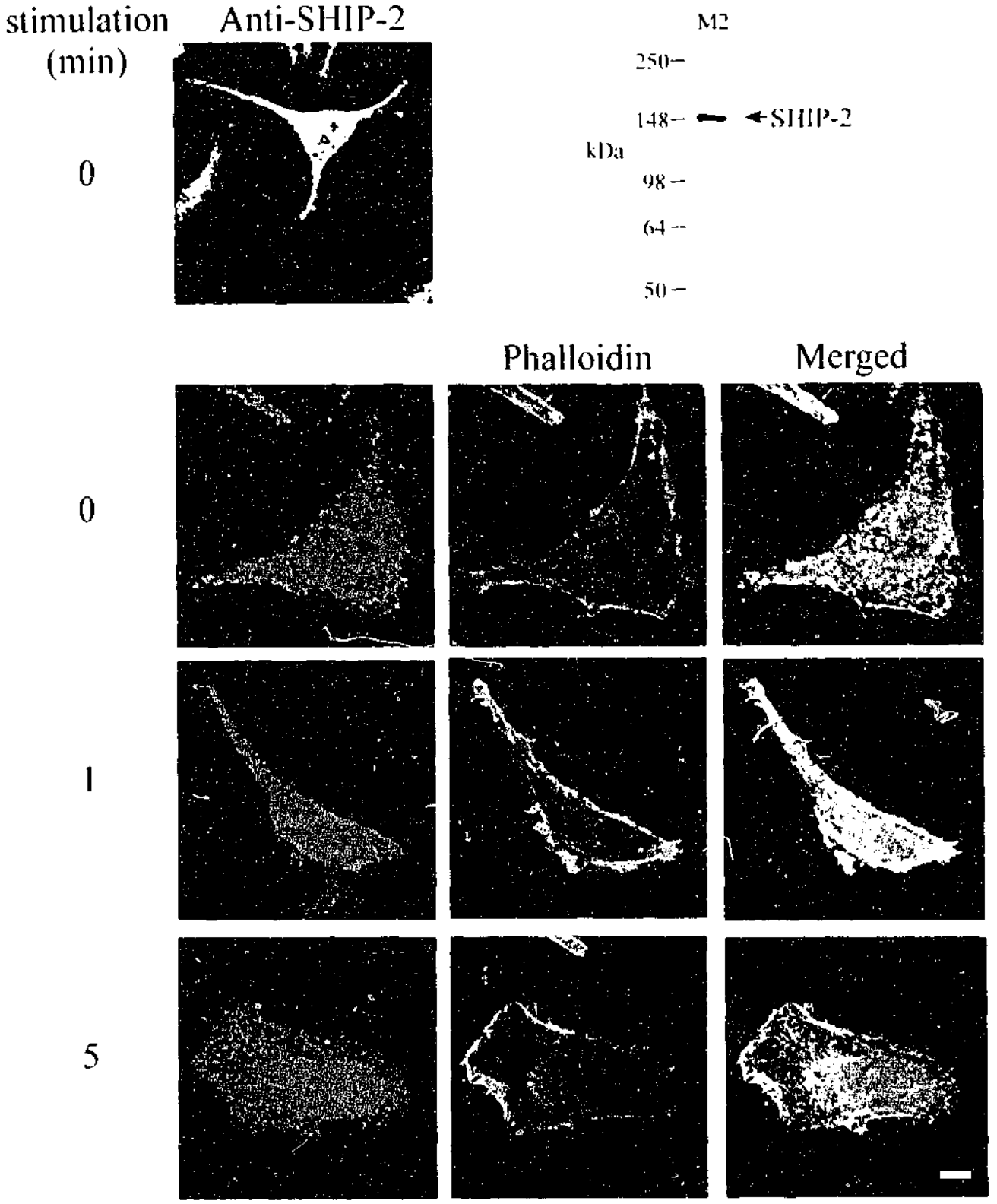

Figure 4.4 Filamin is required for membrane ruffle localization of SHIP-2.

A. M2 (filamin-deficient) cells were serum-starved and where indicted treated with EGF (100 ng/ml) for either 1 or 5 minute(s), fixed/permeabilized and co-stained with Texas Red-conjugated phalloidin and affinity-purifed SHIP-2 antibodies. Cells were visualized by confocal microscopy. Bar, 20 μm. M2 cells were harvested and 100 μg of the Triton X-100-soluble lysate was immunoblotted with affinity-purified SHIP-2 antibodies.

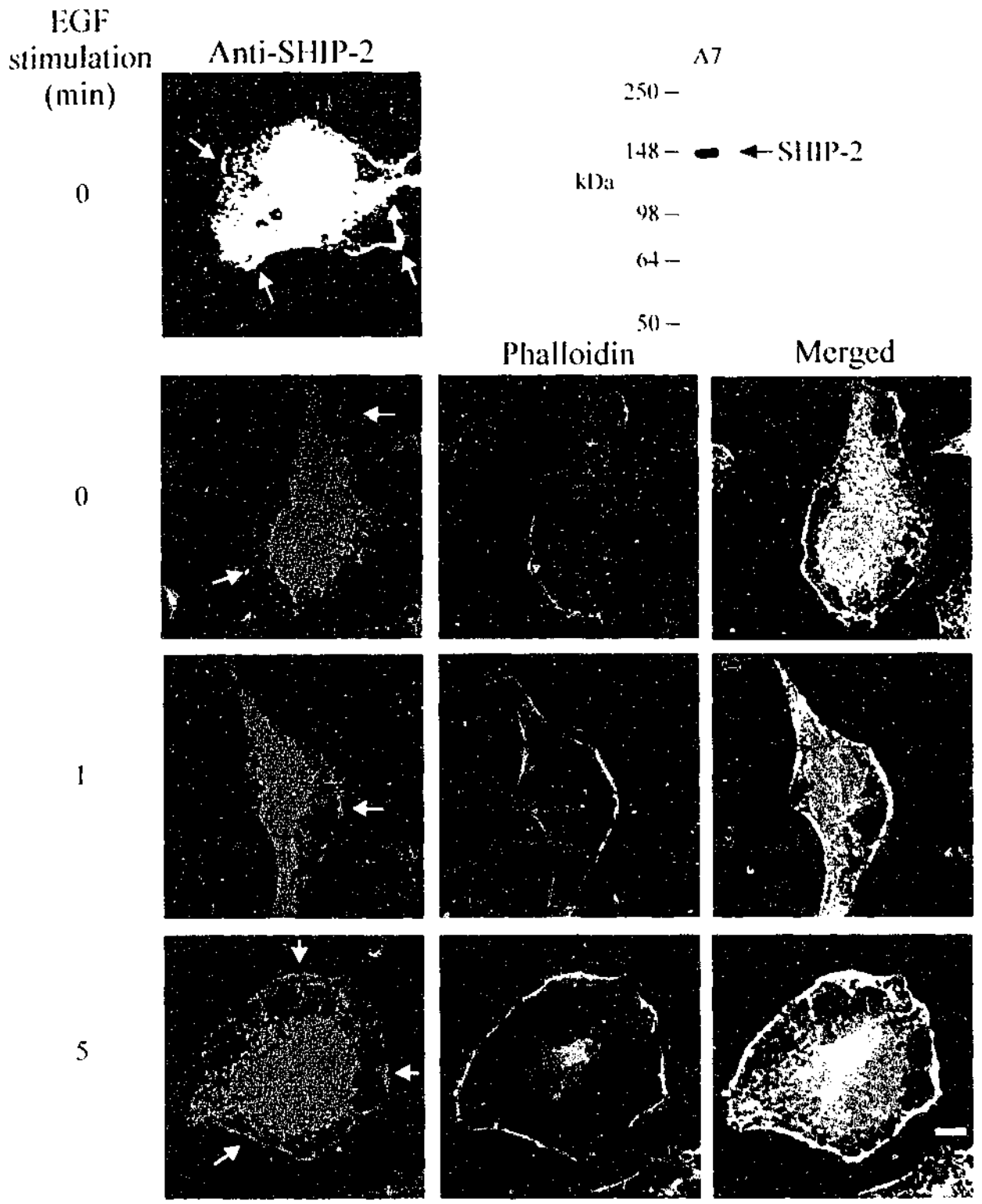

Figure 4.4 Filamin is required for membrane ruffle localization of SHIP-2.

B. A7 (filamin-replete) cells were serum-starved and where indicated treated with EGF (100 ng/ml) for either 1 or 5 minute(s), fixed/permeabilized and co-stained with Texas Red-conjugated phalloidin and affinity-purifed SHIP-2 antibodies. Cells were visualized by confocal microscopy. Arrows indicate SHIP-2 membrane ruffle localization. Bar, 20 μm. A7 cells were harvested and 100 μg of the Triton X-100-soluble lysate was immunoblotted with affinity-purified SHIP-2 antibodies.

SHIP-2 localized to membrane ruffles upon EGF stimulation (Figure 4.4B) and co-localized with phalloidin staining. Collectively these studies demonstrate SHIP-2 localization at membrane ruffles is dependent on filamin expression.

4.3.4 SHIP-2 regulates PtdIns(3,4,5)P_3 and β-actin at membrane ruffles.

To establish that recombinant SHIP-2 localized at membrane ruffles was active and to determine the functional consequences on PtdIns(3,4,5)P_3 levels, the PH domain of ARNO was employed, which has high affinity for PtdIns(3,4,5)P_3 to assess local plasma membrane concentrations of this phosphoinositide (Balla *et al.*, 2000). Several studies have demonstrated that GFP-tagged PH domains with specificity for PtdIns(3,4,5)P_3 can be used to accurately detect PtdIns(3,4,5)P_3 at the leading edge of the cell, reviewed (Rickert *et al.*, 2000). Although it has been established that SHIP-2 regulates total cellular PtdIns(3,4,5)P_3 levels, the membrane ruffle localized regulation of PtdIns(3,4,5)P_3 has not been reported (Blero *et al.*, 2001; Pesesse *et al.*, 2001). In addition, the functional role of SHIP-2 membrane location in regulating PtdIns(3,4,5)P_3 degradation has not been determined. GFP-fused with the PH domain of ARNO (GFP-PH/ARNO) was co-expressed with either empty vector (HA), or HA-SHIP-2, or the proline-rich domain (HA-PRD), or mutant SHIP-2 which lacked the proline-rich domain (HA-SHIP-2ΔPRD) (Figure 4.5) (performed in conjunction with Jelena Becanovic, Monash University). In addition, the effect of overexpressing the C-terminal filamin fragment (aa 2434-2705), which binds SHIP-2 in COS-7 cells on PtdIns(3,4,5)P_3 levels was determined, as overexpression of recombinant Myc-filamin was shown to displace endogenous SHIP-2 from membrane ruffles (see Figure 4.2). In non-stimulated cells transfected with HA empty vector and GFP-PH/ARNO, plasma membrane staining of GFP-PH/ARNO was not detected. Upon EGF activation GFP-PH/ARNO translocated rapidly to membrane ruffles following one minute

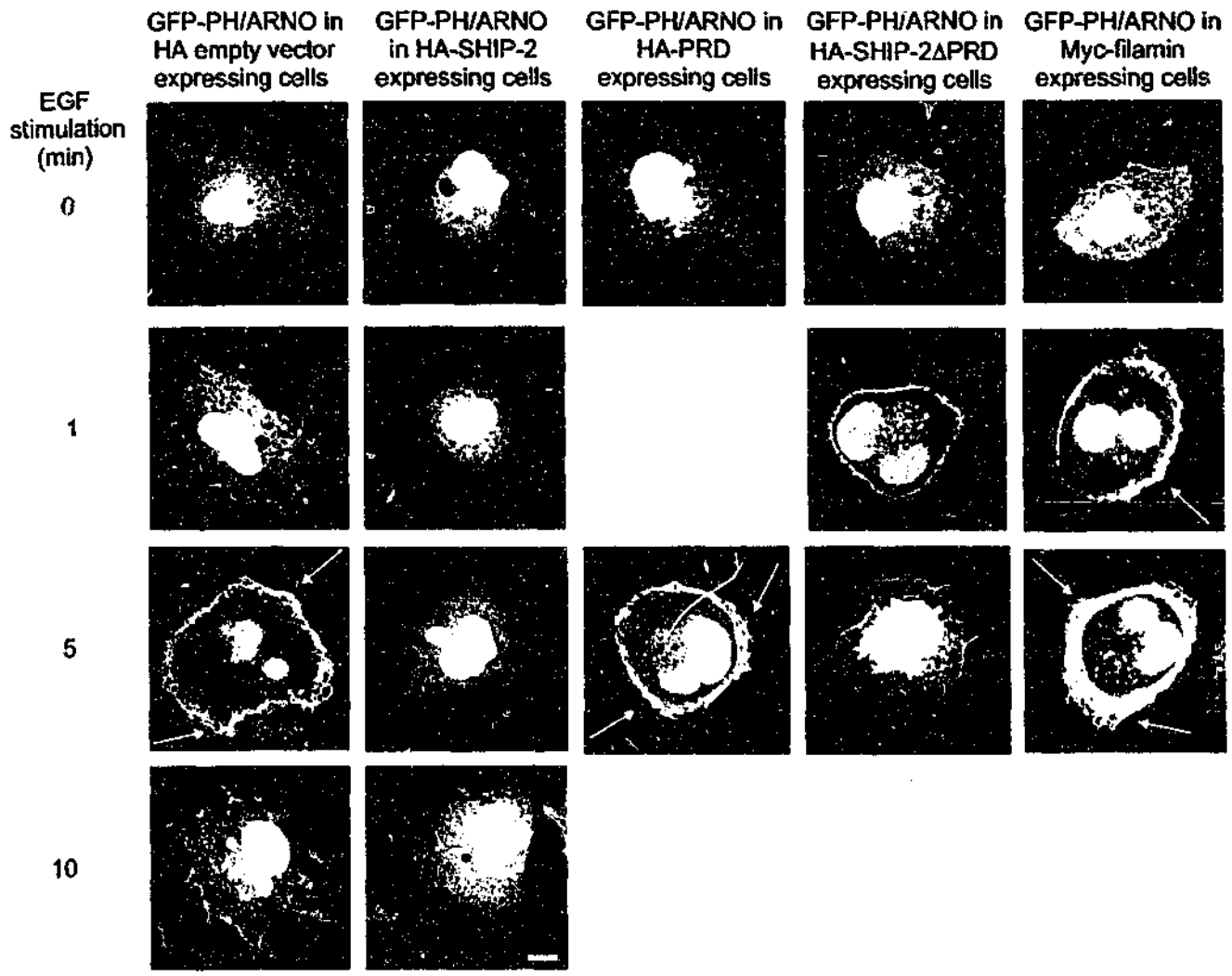

Figure 4.5 SHIP-2 regulates PtdIns(3,4,5)P_3 at membrane ruffles in COS-7 cells. COS-7 cells were transiently co-transfected with GFP-PH/ARNO and with either; HA empty vector, HA-SHIP-2, HA-PRD (the proline-rich domain of SHIP-2), HA-SHIP-2ΔPRD (SHIP-2 lacking the proline-rich domain), or Myc-filamin (encoding amino acids 2,434-2,705). Cells were serum-starved and treated with EGF (100 ng/ml) for the indicated times, fixed/permeabilized and stained with either HA or Myc antibodies to identifiy co-transfected cells (not shown). Cells were visualized by confocal microscopy for GFP-PH/ARNO expression which is shown. Arrows indicate areas of high GFP-PH/ARNO expression. Bar, 20 μm.

stimulation and by 5 minutes intense plasma membrane staining was detected (Figure 4.5). In contrast, cells overexpressing SHIP-2 demonstrated no or low expression of GFP-PH/ARNO at the plasma membrane of EGF-stimulated cells. However, cells expressing the SHIP-2 proline-rich domain (HA-PRD), which lacks the SH2 domain and catalytic domain, demonstrated strong plasma membrane expression of GFP-PH/ARNO, comparable to HA empty vector expressing cells following EGF stimulation. In cells expressing SHIP-2 which lacks the proline-rich domain (HA-SHIP-2ΔPRD), but contains the SH2 and 5-phosphatase catalytic domain, GFP-PH/ARNO demonstrated growth factor-dependent relocalization to the plasma membrane. However, staining was less intense at 5 minutes compared to HA empty vector expressing cells, but was greater than intact SHIP-2 expressing cells. To confirm these observations transfected cells were scored as showing high or low GFP-PH/ARNO plasma membrane expression following 5 minutes EGF stimulation. Over 40 cells were scored per transfection for three independent experiments by an independent observor. The expression of GFP-PH/ARNO at the plasma membrane was low or not detected in greater than 90 % of cells overexpressing SHIP-2, with less than 10 % of cells showing high plasma membrane expression of GFP-PH/ARNO. In contrast, 35 % of cells in which mutant SHIP-2 which lacks the proline-rich domain was overexpressed demonstrated high plasma membrane expression of GFP/ARNO, with 60 % of cells demonstrating low expression. In control studies the majority of cells (greater than 85 %) expressing the proline-rich domain demonstrated high expression of GFP/ARNO at the plasma membrane. Finally, the effect of overexpression of Myc-filamin on PtdIns(3,4,5)P_3 levels was determined. Cells expressing Myc-filamin at high levels demonstrated a dramatic increase in GFP-PH/ARNO staining at the plasma membrane of EGF-treated cells, most apparent after 5 minutes stimulation. This result is consistent with the contention that expression of this C-terminal filamin domain displaces endogenous

SHIP-2 from membrane ruffles and therefore leads to enhanced PI3-kinase signals. Collectively these studies indicate the SHIP-2-filamin interaction regulates plasma membrane PtdIns(3,4,5)P_3.

PI3-kinase plays a key role in signalling to the actin cytoskeleton and inducing membrane ruffling *via* regulation of Rac and Cdc42, (reviewed by (Rickert *et al.*, 2000)). As SHIP-2 hydrolyzes PtdIns(3,4,5)P_3 and localizes to membrane ruffles *via* association with filamin, we investigated the regulation of actin at membrane ruffles by this 5-phosphatase. Cells overexpressing SHIP-2 (HA-SHIP-2), or the proline-rich domain of SHIP-2 (HA-PRD), which lacks the catalytic 5-phosphatase domain but localizes to membrane ruffles and complexes with filamin, were stained for submembraneous actin by β-actin immunoreactivity. β-actin is ubiquitously expressed and localizes specifically at the leading edge of the cell at sub-plasma membrane cortical sites, rather than stress fibers. HA-SHIP-2 co-localized with β-actin in both resting and EGF-stimulated cells (Figure 4.6A)(performed in conjunction with Jelena Becanovic, Monash University). In addition the intensity of β-actin staining was significantly reduced in cells overexpressing SHIP-2, compared to the SHIP-2 proline-rich domain (Figure 4.6A), or empty vector (not shown). To quantitate these differences, cells overexpressing HA-SHIP-2 or the proline-rich domain were scored for the intensity of β-actin staining following EGF stimulation (5 minutes), 40 cells per transfection for three experiments by an independent observor. Greater than 80 % of cells expressing HA-SHIP-2, compared to less than 20 % of cells overexpressing the proline-rich domain which has no 5-phosphatase activity, demonstrated low level β-actin staining. The minority of HA-SHIP-2 expressing cells (less than 20 %) demonstrated intense β-actin staining compared to 75 % of cells expressing the proline-rich domain. To further establish whether SHIP-2 regulates submembraneous actin, cells overexpressing HA-SHIP-2, or empty vector were stained with phalloidin which stains

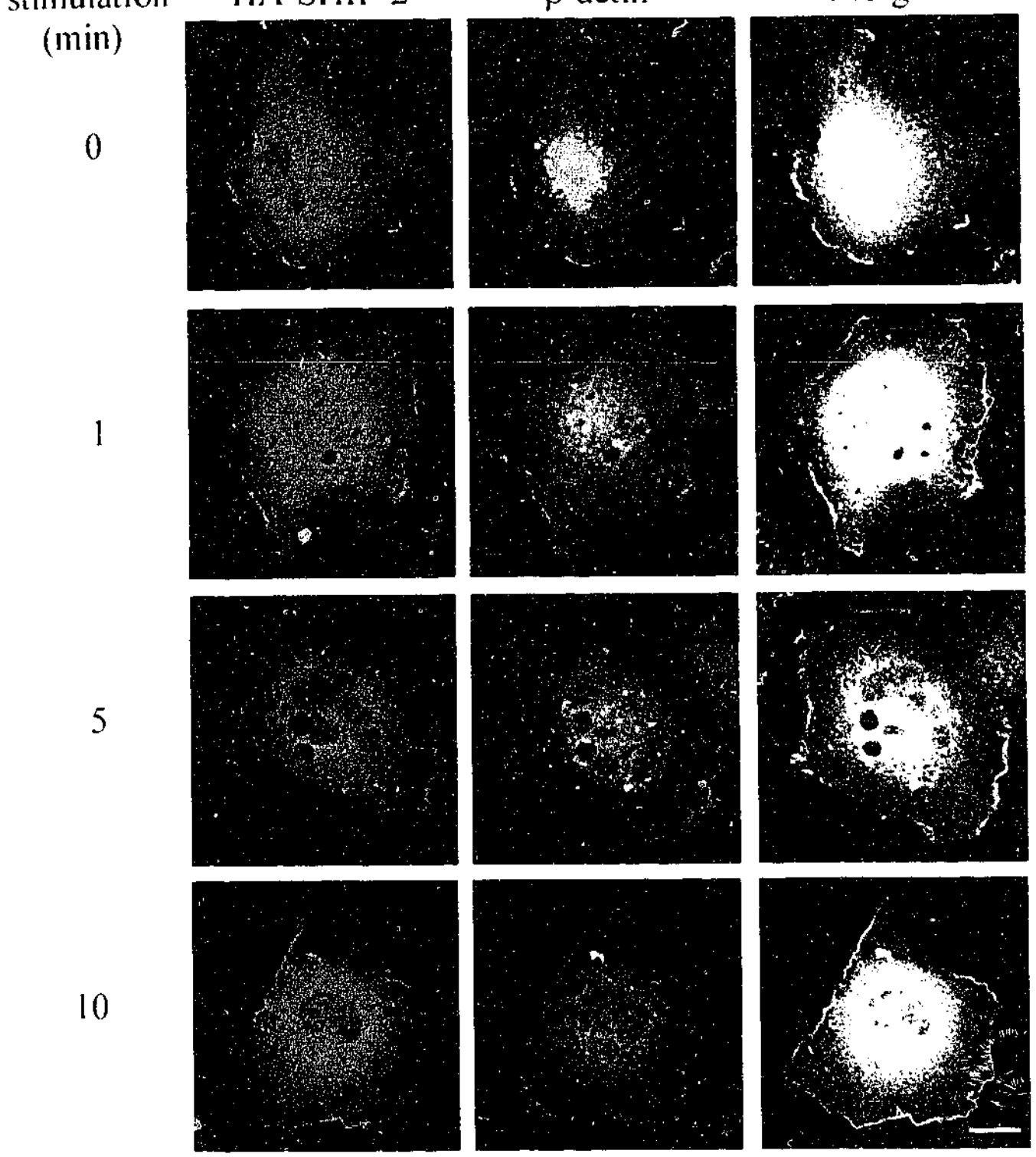

Figure 4.6 SHIP-2 regulates β-actin expression at membrane ruffles.

A. COS-7 cells were transiently transfected with either HA-SHIP-2 (this page) or HA-PRD (following page). Cells were serum-starved and where indicated treated with EGF (100 ng/ml) for 1, 5 or 10 minute(s). Cells were fixed/permeabilized and co-stained with HA and β-actin antibodies. Cells were visualized by confocal microscopy. Arrows indicate areas of high β-actin expression. Bars, 20 μm.

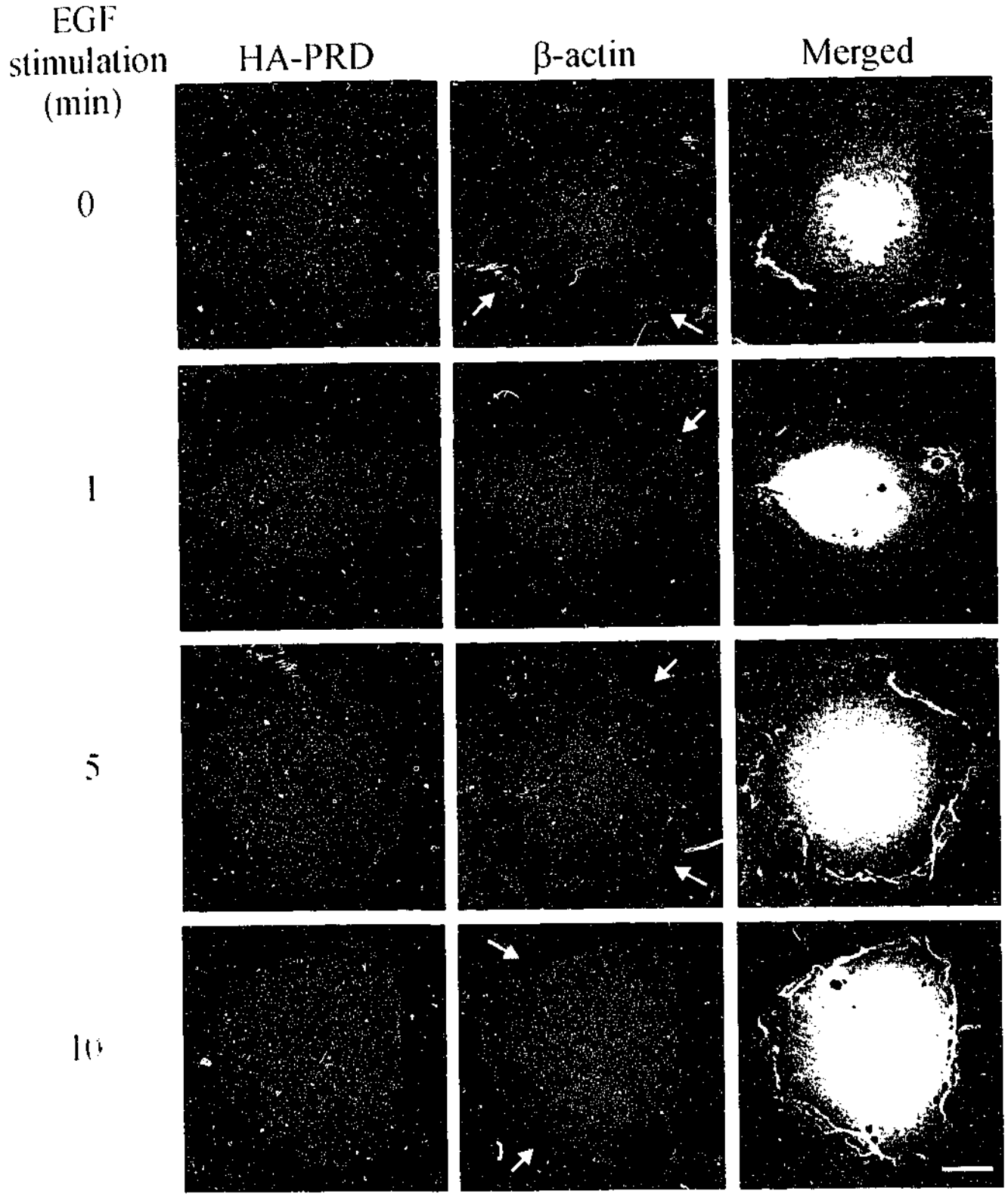
EGF stimulation (min)
HA-PRD
β-actin
Merged
0
1
5
10

polymerized actin (Figure 4.6B). Cells overexpressing high levels of HA-SHIP-2 demonstrated significantly decreased staining of actin at membrane ruffles, and decreased membrane ruffling. Following 5 minutes EGF stimulation in many HA-SHIP-2 overexpressing cells only a fine cortical rim of actin was stained by phalloidin. The intensity of phalloidin staining of actin at the membrane was scored as high or low following 5 minutes EGF stimulation in HA-SHIP-2 *versus* HA empty vector expressing cells for 40 cells per transfection for three independent experiments by and independent observor. Greater than 70 % of HA-SHIP-2 expressing cells, compared to 30 % of cells expressing the HA empty vector, demonstrated low intensity phalloidin staining at membrane ruffles. In addition only 25 % of SHIP-2 *versus* 75 % of HA empty vector expressing cells demonstrated high intensity phalloidin staining at membrane ruffles.

Collectively these studies demonstrate SHIP-2 localizes to membrane ruffles *via* association with filamin and regulates PtdIns(3,4,5)P_3, β-actin and membrane ruffling.

B

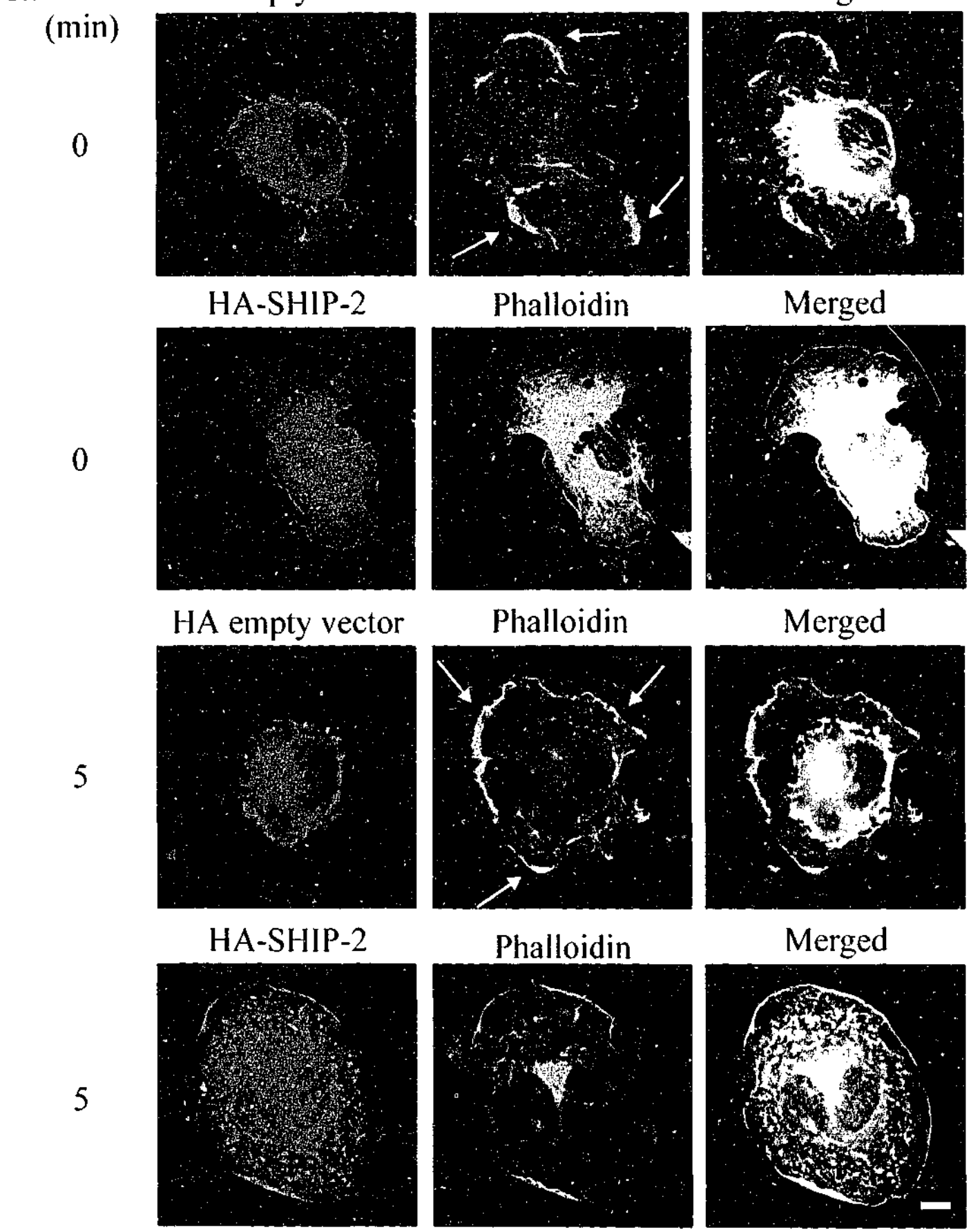

Figure 4.6 SHIP-2 regulates β-actin expression at membrane ruffles.

B. COS-7 cells were transiently transfected with either HA-SHIP-2 or HA empty vector, serum-starved and where indicated treated with EGF (100 ng/ml) for 5 minutes. Cells were fixed/permeabilized and co-stained with HA antibodies and Texas Red-conjugated phalloidin. Cells were visualized by confocal microscopy. Arrows indicate areas of high phalloidin staining. Bar, 20 μm.

CHAPTER 5: SHIP-2 forms a dynamic tetrameric complex with actin and GPIb-IX-V : Localization of SHIP-2 to the activated platelet cytoskeleton

5.1 Summary

The platelet receptor for von Willebrand factor (vWF), the glycoprotein (GP)Ib-IX-V complex, mediates platelet adhesion at sites of vascular injury. The cytoplasmic tail of the GPIbα subunit interacts with the actin-binding protein, filamin, anchoring the receptor in the cytoskeleton. In motile cells, the second messenger PtdIns(3,4,5)P_3 induces localized submembraneous actin remodeling. The inositol polyphosphate 5-phosphatase, SHIP-2, hydrolyzes phosphoinositide 3,4,5 trisphosphate (PtdIns(3,4,5)P_3) forming PtdIns(3,4)P_2, and regulates membrane ruffling *via* complex formation with filamin. In this study we investigated the intracellular location and association of SHIP-2 with filamin, actin, and the GPIb-IX-V complex in unstimulated and spreading platelets. Immunoprecipitation of SHIP-2 from the Triton-soluble fraction of unstimulated platelets demonstrated association between SHIP-2, filamin, actin and GPIb-IX-V. SHIP-2 associated with filamin, or GPIb-IX-V, was functionally active, as demonstrated by the presence of PtdIns(3,4,5)P_3 5-phosphatase activity. Following thrombin or vWF-induced platelet activation, association between SHIP-2, filamin and the receptor complex decreased in the Triton-soluble fraction. In platelets spreading on a vWF matrix, SHIP-2 localized intensely with actin at the central actin ring and co-localized with actin and filamin at filopodia and lamellipodia. In spread platelets, GPIb-IX-V localized to the centre of the platelet and showed little co-localization with filamin at the plasma membrane. These studies demonstrate a functionally active tetrameric complex between SHIP-2, filamin, actin and GPIb-IX-V which may orchestrate the localized hydrolysis of PtdIns(3,4,5)P_3 and thereby regulate cortical and submembraneous actin.

5.2 Introduction

Following vascular injury, platelet adhesion and aggregation mediate the immediate arrest of bleeding; however, in pathological states this response may contribute to arterial blockage leading to cerebrovascular and coronary arterial occlusion. The interaction of the platelet membrane glycoprotein (GP)Ib-IX-V complex with its adhesive ligand, von Willebrand factor (vWF), in the subendothelial matrix initiates platelet adhesion under conditions of rapid blood flow in the arterial circulation. The GPIb-IX-V complex can also bind plasma vWF under conditions of pathological shear stress, leading to platelet aggregation and thrombosis (Ruggeri, 1997; Savage *et al.*, 1998; Savage *et al.*, 1996). Following binding of vWF, the GPIb-IX-V complex initiates intracellular signals inducing platelet activation, spreading and activation of the integrin $\alpha_{IIb}\beta_3$ receptor from a low to high affinity state (inside out signalling). The molecular mechanisms regulating vWF-GPIb-IX-V-induced signaling, however, remain to be fully delineated (Berndt *et al.*, 2001). The GPIb-IX-V complex is composed of four subunits; GPIbα disulphide-linked to GPIbβ, GPV and GPIX. The extracellular N-terminal globular domain of GPIbα contains the binding site for vWF. The 96 amino acid cytoplasmic tail of GPIbα contains no overt signaling domains, but directly binds the actin binding–protein, filamin 1a, and the signaling adaptor protein, 14-3-3ζ (Munday *et al.*, 2000; Takafuta *et al.*, 1998). Filamins are large actin-binding proteins that stabilize submembraneous actin webs and link them to cellular membranes. Filamins promote high angle actin filament branching and thereby actin gelation, although the molecular mechanisms mediating this effect are incompletely understood. The interaction of filamin with GPIb-IX-V is essential for regulating the shape of resting platelets, the spreading of activated platelets and the anchoring of the receptor complex to the membrane skeleton (Fox, 1985; Takafuta *et al.*, 1998; Williamson *et al.*, 2002; Xu *et al.*, 1998). The stabilization of the platelet membrane resulting from the

interaction of filamin with GPIb-IX-V may not only prevent platelet membrane deformation under conditions of high fluid shear stress, but also regulate the adhesive function of the receptor complex itself and the ability of the receptor complex to maintain adhesion to vWF under conditions of high shear stress (Englund *et al.*, 2001; Williamson *et al.*, 2002). Following platelet adhesion, vWF binding to GPIb-IX-V induces the cytoskeletal translocation and activation of the p85/p110 form of PI3-kinase (Jackson *et al.*, 1994). Under shear conditions, PI3-kinase is essential for vWF-induced calcium release (Yap *et al.*, 2002). A potential mechanism for activation of PI3-kinase *via* GPIb-IX-V has been demonstrated in studies from our laboratory, which have shown that the p85 subunit of PI3-kinase forms a complex with both 14-3-3ζ and the receptor complex (Munday *et al.*, 2000).

The inositol lipids phosphatidylinositol 4,5 bisphosphate ($PtdIns(4,5)P_2$) and phosphatidylinositol 3,4,5 trisphosphate ($PtdIns(3,4,5)P_3$), play a central role in the regulation of actin polymerization and thereby cell motility (Rickert *et al.*, 2000; Stephens *et al.*, 2002). Many recent studies have demonstrated in motile cells that $PtdIns(3,4,5)P_3$ spatially localizes to the leading edge of the cell, at membrane ruffles (lamellipodia). Production of this lipid determines where and when submembraneous actin polymerization takes place. $PtdIns(3,4,5)P_3$ localizes many signaling and actin-regulatory proteins to the inner wall of the plasma membrane and allosterically regulates their function (reviewed by (Vanhaesebroeck *et al.*, 2001)). In this manner, $PtdIns(3,4,5)P_3$ mediates agonist-induced actin-dependent extension of lamellipodia and cell migration. The agonist-induced transient accumulation of $PtdIns(3,4,5)P_3$ at the leading edge of motile cells results from a balance between its synthesis by the PI3-kinase and hydrolysis by specific lipid phosphatases (Comer and Parent, 2002). Recent studies have demonstrated the SH2-inositol polyphosphate 5-phosphatase, SHIP-2, hydrolyzes the 5-position phosphate from

PtdIns(3,4,5)P_3 forming PtdIns(3,4)P_2 and is localized to the leading edge of the cell, whereby the 5-phosphatase regulates submembraneous actin and membrane ruffling (see Chapter 4). This 5-phosphatase is a widely expressed enzyme that contains an amino-terminal SH2 domain, a central 5-phosphatase domain, and a carboxyl-terminal proline-rich domain (Ishihara *et al.*, 1999). It bears significant sequence identity with the hematopoietic specific 5-phosphatase, SHIP-1, except in the proline-rich domain where the two 5-phosphatases demonstrate significant sequence diversity (Pesesse *et al.*, 1997).

Recent studies have demonstrated SHIP-2 is localized to membrane ruffles and regulates PtdIns(3,4,5)P_3-induced actin remodeling at this site. Cells overexpressing SHIP-2 demonstrate decreased submembraneous actin and membrane ruffling. SHIP-2 localization to membrane ruffles is mediated *via* complex formation through its C-terminal proline-rich domain with the actin-binding protein, filamin (see Chapters 3 and 4). Further evidence for the role SHIP-2 plays in regulating submembraneous actin has been demonstrated by studies which have shown SHIP-2 forms a complex with $p130^{Cas}$ at focal adhesions and regulates cell adhesion (Prasad *et al.*, 2001). Collectively these studies suggest that SHIP-2 regulates the localized changes in PtdIns(3,4,5)P_3 that instruct submembraneous actin remodeling, membrane ruffling and promote cell adhesion.

As SHIP-2 appears to significantly influence cytoskeletal remodeling, the localization and expression of SHIP-2 in platelets was investigated. Platelets are highly motile cells with a complex cytoskeleton. At early time points in platelets spreading on a vWF matrix, SHIP-2 localized initially to filopodia and the central actin ring, and with filamin and submembraneous actin at lamellipodia. The association of SHIP-2 with actin, filamin and the GPIb-IX-V complex in resting and vWF-activated platelets was investigated. These studies show in human platelets that actin, GPIb-IX-V, SHIP-2 and filamin form a dynamic tetrameric complex and that association between these species

decreases in the Triton-soluble fraction following platelet activation. Collectively these studies provide evidence that SHIP-2 localizes in spreading platelets to sites of active actin remodeling and thereby may regulate localized concentrations of PtdIns(3,4,5)P_3.

5.3 Results

5.3.1 SHIP-2 is expressed in platelets.

Although SHIP-2 has been strongly implicated in regulating actin dynamics at the leading edge of the cell, this signal-terminating enzyme has not been characterised in highly motile cells, such as platelets. Analysis of the expression profile of SHIP-2, has revealed widespread expression in skeletal muscle, heart, brain, lung and some hematopoietic cells including T and B cells (Muraille *et al.*, 1999; Pesesse *et al.*, 1997). However, expression of SHIP-2 in platelets has yet to be fully characterized. Northern analysis was therefore performed using a probe encoding sequences unique to SHIP-2 (nucleotides 3017 to 3989) that have no homology to SHIP-1. Analysis of various cancer cell lines including adenocarcinoma (Hela), a human megakaryocytic cell line (MEG-01), T cell leukemia (Jurkat), lung cancer (A 549), neuroteratocarcinoma (NT) and glioma (C6) demonstrated expression of a 4.75 kb message, consistent with the predicted size of the SHIP-2 transcript (Figure 5.1A)(Northern blot prepared by Dr. Harshal Nandurkar, Monash University). The expression level of SHIP-2 in the megakaryocyte cell line, MEG-01, when standardised by reprobing the Northern blot with an actin probe, was comparable to that observed in the other cell lines .

To further characterize SHIP-2 in platelets, immunoblot analysis of platelet subcellular fractions from both resting and thrombin-activated platelets using a previously characterized affinity-purified SHIP-2-specific anti-peptide antibody was performed (see Chapters 4 and 5). The subcellular compartmentalization of SHIP-2, filamin and GPIb in resting *versus* thrombin-stimulated platelets was compared to that of the p85 subunit of PI3-kinase. In unstimulated platelets, SHIP-2 was detected in the Triton-soluble fraction, but not in the actin cytoskeleton (Figure 5.1B). Minor proteolysis of SHIP-2 was demonstrated by the presence of a slightly faster migrating polypeptide, which others have

Figure 5.1 SHIP-2 is expressed in a megakaryocyte cell line and human platelets.

Membranes containing approximately 20 μg of mRNA from the indicated cell lines, adenocarcinoma of the cervix (HeLa), megakaryoblast (MEG-01), T cell leukemia (Jurkat), lung carcinoma (A549), neuroteratocarcinoma (NT) and glioma (C6), were hybridized with human SHIP-2 cDNA (nucleotides 3017-3989) and washed as described under "Materials and Methods". After exposure, the membrane was allowed to decay and subsequently hybridized to an actin probe.

B. Platelets were either left untreated or treated with thrombin (1 U/ml, final concentration) for 5 minutes at room temperature, and then lysed. The Triton X-100-soluble and actin cytoskeletal (Actin CSK) fractions were isolated and immunoblotted with antibodies to SHIP-2, filamin, glycocalicin (GPIb), or p85 as indicated. Results shown are typical of three separate experiments.

C. The Triton X-100-soluble fraction of platelets was isolated and immunoprecipitated (IP:) with either Pre-immune (Pre I) sera, which had been previously passaged over a SHIP-2 peptide coupled column, or affinity-purified SHIP-2 anti-peptide antibodies and immunoblotted with antibodies to SHIP-2.

A

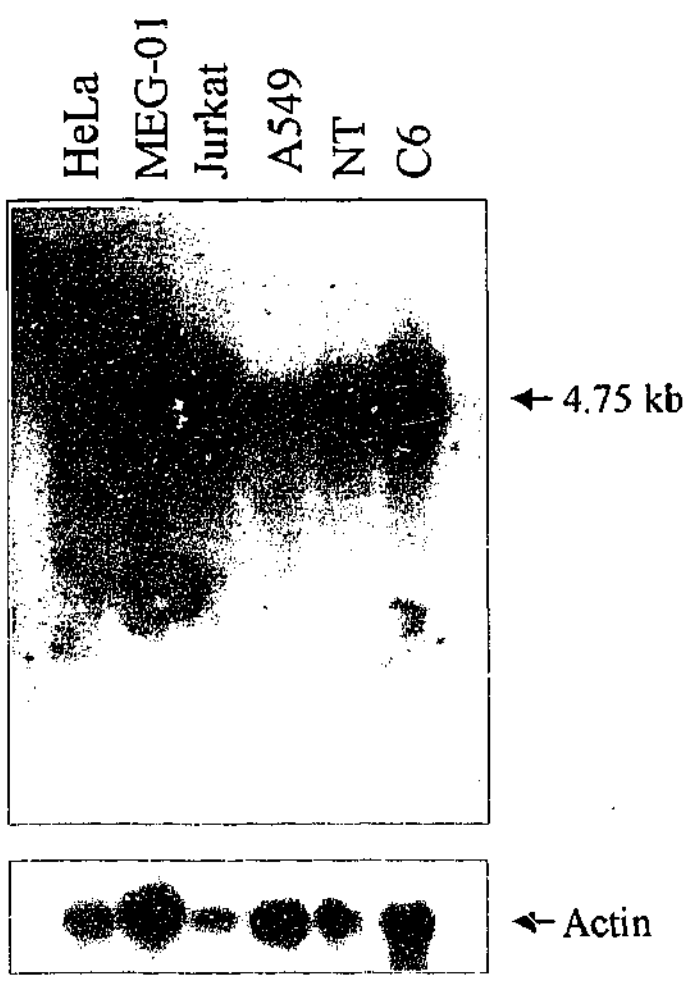
HeLa
MEG-01
Jurkat
A549
NT
C6
4.75 kb
Actin

B

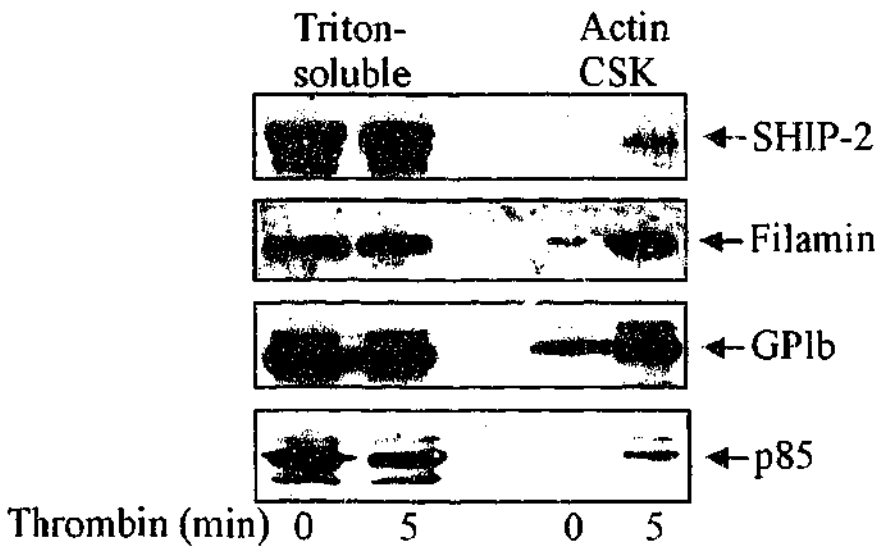
Triton-soluble
Actin CSK
SHIP-2
Filamin
GPIb
p85
Thrombin (min) 0 5 0 5

C

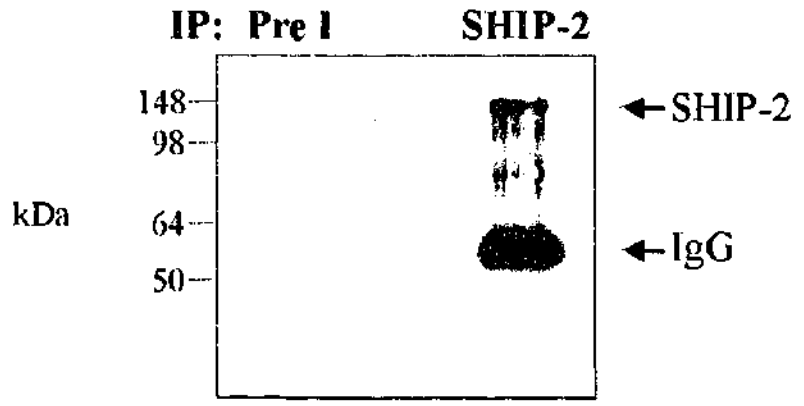
IP: Pre I
SHIP-2
148
98
64
50
kDa
SHIP-2
IgG

previously detected in various cell lysates (Habib *et al.*, 1998). In resting platelets, both filamin and GPIb were present in the unstimulated platelet actin cytoskeleton. Following thrombin activation, the level of SHIP-2 expression in the Triton-soluble fraction remained relatively unchanged. However, a small amount of SHIP-2 translocated to the actin cytoskeleton following thrombin stimulation (Figure 5.1B). Increased amounts of GPIb and filamin in the actin cytoskeleton following 5 minutes thrombin stimulation was also noted. The temporal correlation of the translocation of SHIP-2 to the actin cytoskeleton matched that of the p85 subunit of PI3-kinase. SHIP-2 expression in the Triton–soluble fraction of human platelets was also shown by immunoprecipitation and immunoblot analysis, using SHIP-2 specific anti-peptide antibodies (Figure 5.1C). This analysis demonstrated the presence of a 150-kDa polypeptide in SHIP-2 immune, but not pre-immune immunoprecipitates.

5.3.2 Intracellular localization of SHIP-2 in vWF stimulated platelets.

Many motile cells respond to agonists and chemokines by localized actin remodeling or membrane ruffling (lamellipodia) in the direction of the stimulus (Small *et al.*, 2002). Platelets are terminally differentiated anucleate cells, with a highly specialized cytoskeleton, and the formation of filopodia and lamellipodia in response to platelet activation is well described. The intracellular localization of SHIP-2 in platelets spreading on a vWF matrix using confocal microscopy was investigated. In addition, in order to improve the size of the platelet images and the resolution, high powered confocal microscopy was performed using 400 x magnification.

The intracellular localization of SHIP-2 in platelets spreading on a vWF matrix was dynamic with respect to specific phases of platelet activation and was different to that we previously reported in resting and EGF-stimulated COS-7 cells. At early phases of platelet

adhesion, SHIP-2 staining was intense in small unspread platelets and did not specifically localize to any discernable structure however, staining was absent from the centre of the platelet (Figure 5.2Aa). As platelets spread, SHIP-2 localized to filopodia (Figure 5.2Ab see arrow), and also SHIP-2 antibodies stained a central ring structure, with no staining within the ring (Figure 5.2Bc see arrow). SHIP-2 also localized to lamellipodia (Figure 5.2A see arrow in d). In spread platelets SHIP-2 staining was diffuse at the plasma membrane and staining at the central ring was maintained, but was less clearly demarcated (Figure 5.2Ae). Pre-immune staining was non-reactive. The outline of the platelets used for pre-immune staining was demonstrated by phalloidin staining.

To compare the localization of SHIP-2 with respect to actin in platelets spreading on a vWF matrix, we co-stained for SHIP-2 and polymerized actin, the latter was detected using phalloidoin. In partially spread platelets, the staining of SHIP-2 at filopodia co-localized intensely with actin, (see arrow Figure 5.2Ba and b) and at the central actin ring (also called the granulomere) (Obergfell *et al.*, 2002) (Figure 5.2Ba and b). With increased platelet spreading, SHIP-2 co-localization with the central actin ring was predominantly on the inner aspect of the actin ring (Figure 5.2Bc see arrow in merged images). In some platelets as the actin ring enlarged, SHIP-2 staining was predominantly internal to the actin ring, and was diffuse rather than "ring–like" at this site (Figure 5.2Bd arrow in SHIP-2 staining). Localization of SHIP-2 to lamellipodia was demonstrated in the merged images by the eccentric co-localization of SHIP-2 with actin staining at one side of the platelet (Figure 5.2Bd, see arrow in merged image). These studies demonstrate a novel localization of SHIP-2 in spreading platelets, to filopodia and the central actin ring, in addition to lamellipodia. The localization of SHIP-2 to these sites, may serve to regulate PtdIns(3,4,5)P_3 hydrolysis and thereby actin remodeling.

A

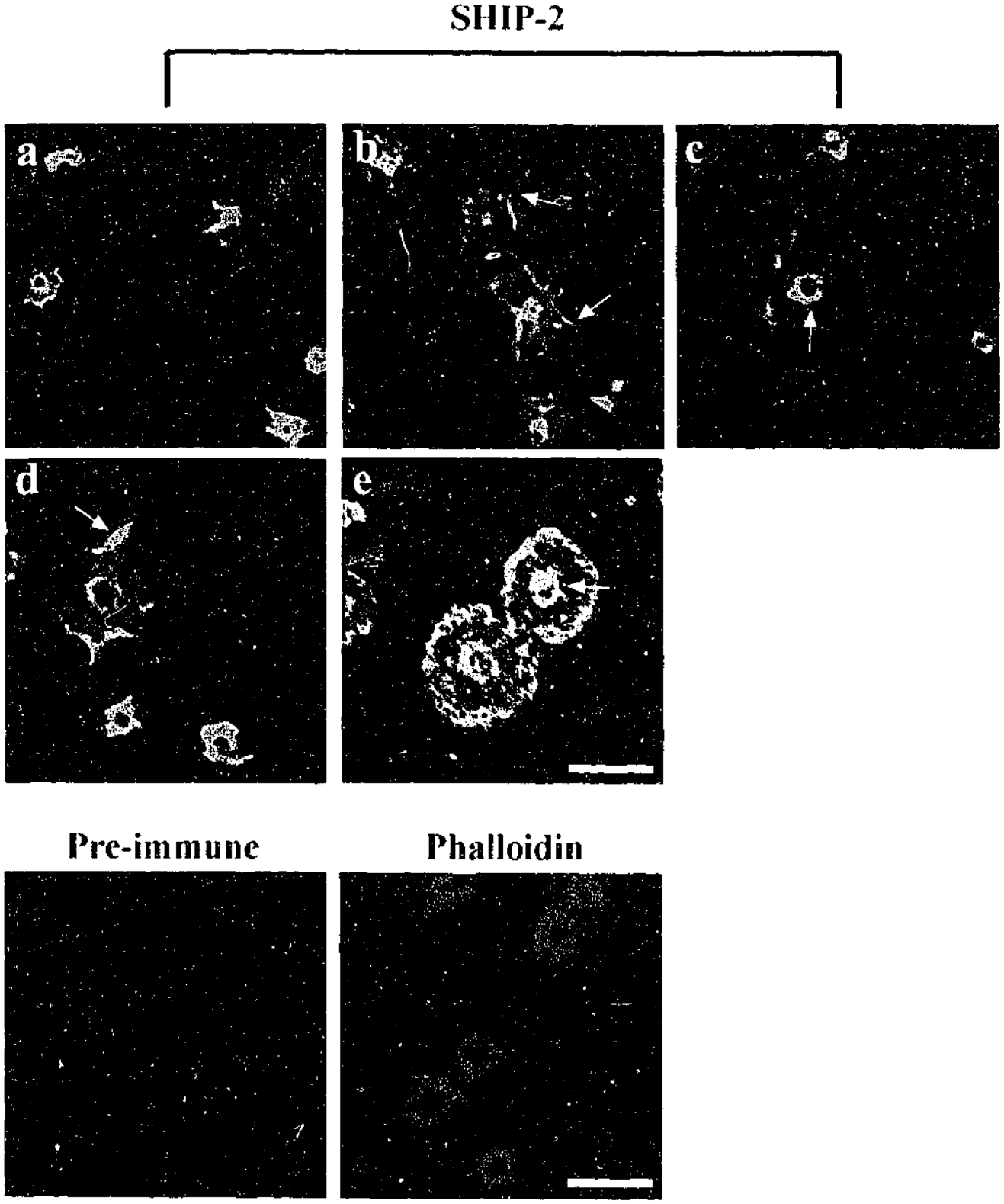

Figure 5.2 SHIP-2 localizes to actin-rich regions in spreading platelets.

A. Platelets spread on a vWF matrix were fixed/permeabilized and co-stained with affinity-purified SHIP-2 antibodies, or co-stained with affinity-purified pre-immune sera and Texas Red-conjugated phalloidin, and visualized by confocal microscopy. Arrows indicate SHIP-2 localization at filopodia (b), at the central actin ring (c), and at lamellipodia (d). The arrow showing SHIP-2 localization in (e) indicates diffuse central staining detected in some spread platelets. Bar, 10 μm.

As shown in Chapter 3 the SHIP-2 proline-rich domain binds the actin-binding protein, filamin, at the C-terminal immunoglobulin repeats 22-24. In COS-7 cells, co-immunoprecipitation of SHIP-2 and filamin demonstrates the two species form a constitutive complex *in vivo*, which is unaltered by EGF stimulation. The investigation of this association in human platelets was further pursued to investigate other potential components in this complex ie. actin and GPIbα. The complexes SHIP-2 forms with filamin, actin and GPIbα in both unstimulated and thrombin- or vWF-stimulated platelets was investigated. Filamin binds polymerized actin *via* its N-terminal actin-binding domain (Figure 5.3A). The SHIP-2 binding site on filamin is present at the filamin C-terminus, involving repeats 22-24 (Figure 5.3A) (see Chapter 3). Consistent with these findings, SHIP-2 immunoprecipitates, but not pre-immune immunoprecipitates, demonstrated a 250 kDa polypeptide recognised by filamin antibodies (Figure 5.3B, upper panel), consistent with association between SHIP-2 and filamin in unstimulated platelet Triton-soluble lysates. Under these conditions, SHIP-2 immunoprecipitates also contained actin (Figure 5.3B, lower panel). These studies thus confirm a trimeric complex between SHIP-2, filamin and actin in the Triton-soluble lysate from resting platelets.

5.3.3 SHIP-2, filamin and GPIb form a complex in the Triton-soluble compartment of resting platelets, but not stimulated platelets.

The intracellular domain of GPIbα associates with filamin, which in turn directly binds actin (Fox, 1985; Takafuta *et al.*, 1998). In resting platelets, this interaction stabilizes the platelet membrane. In addition, under conditions of high shear the interaction between GPIbα and filamin is essential for receptor anchorage to vWF matrix (Berndt *et al.*, 2001; Fox, 1985). As it was shown SHIP-2 associates with filamin and actin, it was determined whether GPIbα was also present in this complex (platelet immunoprecipitation performed

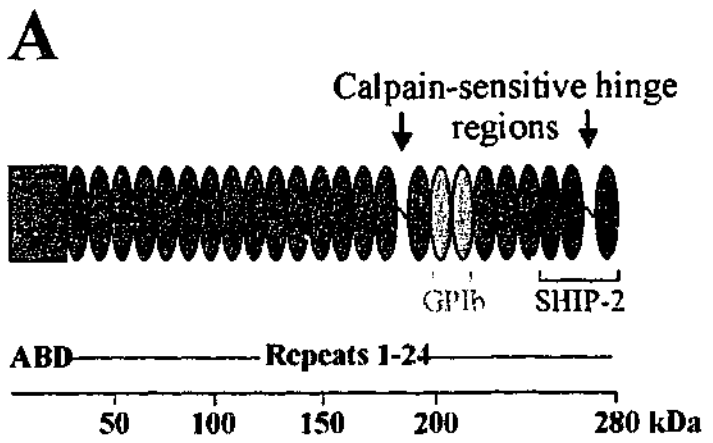

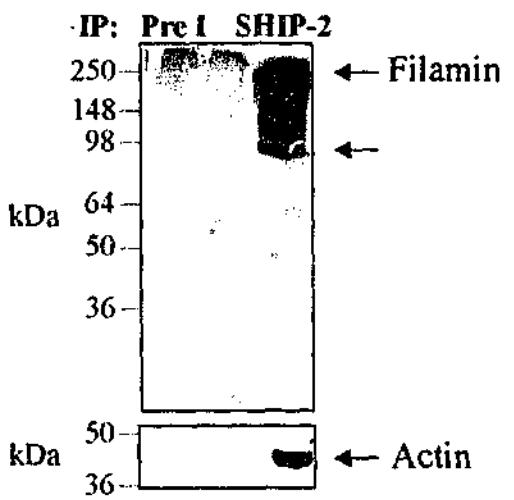

Figure 5.3 SHIP-2 associates with filamin and actin.

A. Schematic of the calpain-mediated cleavage profile of filamin A. The orange box represents the actin-binding domain (ABD) and repeats 1-24 of filamin are shown as elipses. Blue and pink filled elipses represent GPIb and SHIP-2 binding sites, respectively. The calpain cleavage sites on intact filamin are shown.

B. The Triton X-100-soluble fraction of platelets was immunoprecipitated (IP:) with either affinity-purified Preimmune (Pre I) sera, or affinity-purified SHIP-2 antibodies and immunoblotted with filamin antibodies (upper panel), or actin antibodies (lower panel). Arrows indicate the migration of intact filamin and calpain-cleaved filamin fragments. Results are typical of three separate experiments.

in conjunction with Dr. Adam Munday, Monash University). This was also of interest, as it has previously been shown that PI3-kinase binds to GPIbα *via* an interaction with 14-3-3, and therefore may generate PtdIns(3,4,5)P_3, the substrate for SHIP-2, in close association with the receptor (Munday *et al.*, 2000). Triton-soluble platelet lysates were isolated in the presence of EGTA (to minimize calpain cleavage of filamin) from resting or thrombin-activated platelets and immunoprecipitated with SHIP-2 specific antibodies and immunoblotted with antibodies to filamin, or anti-glycocalicin (Figure 5.4A). The latter antibody recognizes the extracellular domain of GPIbα (Munday *et al.*, 2000). Both intact filamin and cleaved-filamin were detected in SHIP-2 immunoprecipitates from the Triton-soluble fraction of unstimulated platelets. Following platelet activation, there was a dramatic reduction in the level of filamin detected in the Triton-soluble fraction, although the total level of SHIP-2 and filamin in this fraction prior to immunoprecipitation was unchanged by thrombin activation (see Figure 5.1B). SHIP-2 immunoprecipitates were probed with GPIb antibodies and detected a 125 kDa polypeptide, consistent with association of GPIb and SHIP-2 in the Triton-soluble fraction of unstimulated platelets. The association between GPIb and SHIP-2 was reduced significantly in this fraction following thrombin activation. These results are in contrast to the constitutive association of SHIP-2 and filamin previously reported in EGF-stimulated COS-7 cells (see Chapter 3).

To confirm an interaction between SHIP-2, filamin and GPIb, reciprocal immunoprecipitation experiments were performed in which filamin was immunoprecipitated from the Triton-soluble fraction derived from resting or thrombin-stimulated platelets, and probed using affinity-purified polyclonal antibodies to SHIP-2 or GPIb (Figure 5.4B). SHIP-2 was present in anti-filamin immunoprecipitates of the Triton-soluble fraction of resting or thrombin-stimulated platelets (Figure 5.4B), but association decreased significantly following thrombin stimulation. Some proteolysis of SHIP-2 in

Figure 5.4 Filamin and GPIb co-immunoprecipitate with SHIP-2.

A. The Triton X-100-soluble fraction of platelets was isolated from resting, or thrombin-stimulated platelets (1 U/ml, final concentration for 5 minutes). The Triton X-100-soluble fraction was immunoprecipitated (IP:) with either affinity-purified Pre-immune (Pre I) sera, or affinity-purified SHIP-2 antibodies and immunoblotted with filamin or GPIb antibodies.

B. Platelet Triton X-100-soluble fractions of platelets were isolated as in (A), immunoprecipitated (IP:) with either non-immune (Non I) sera or filamin antibodies and immunoblotted with either affinity-purified SHIP-2 antibodies or GPIb antibodies.

C. Platelet Triton X-100-soluble fractions of platelets were isolated as in (A), immunoprecipitated (IP:) with either non-immune (Non I) sera or GPIb antibodies and immunoblotted with affinity-purified SHIP-2 antibodies or filamin antibodies. Results are typical of three separate experiments.

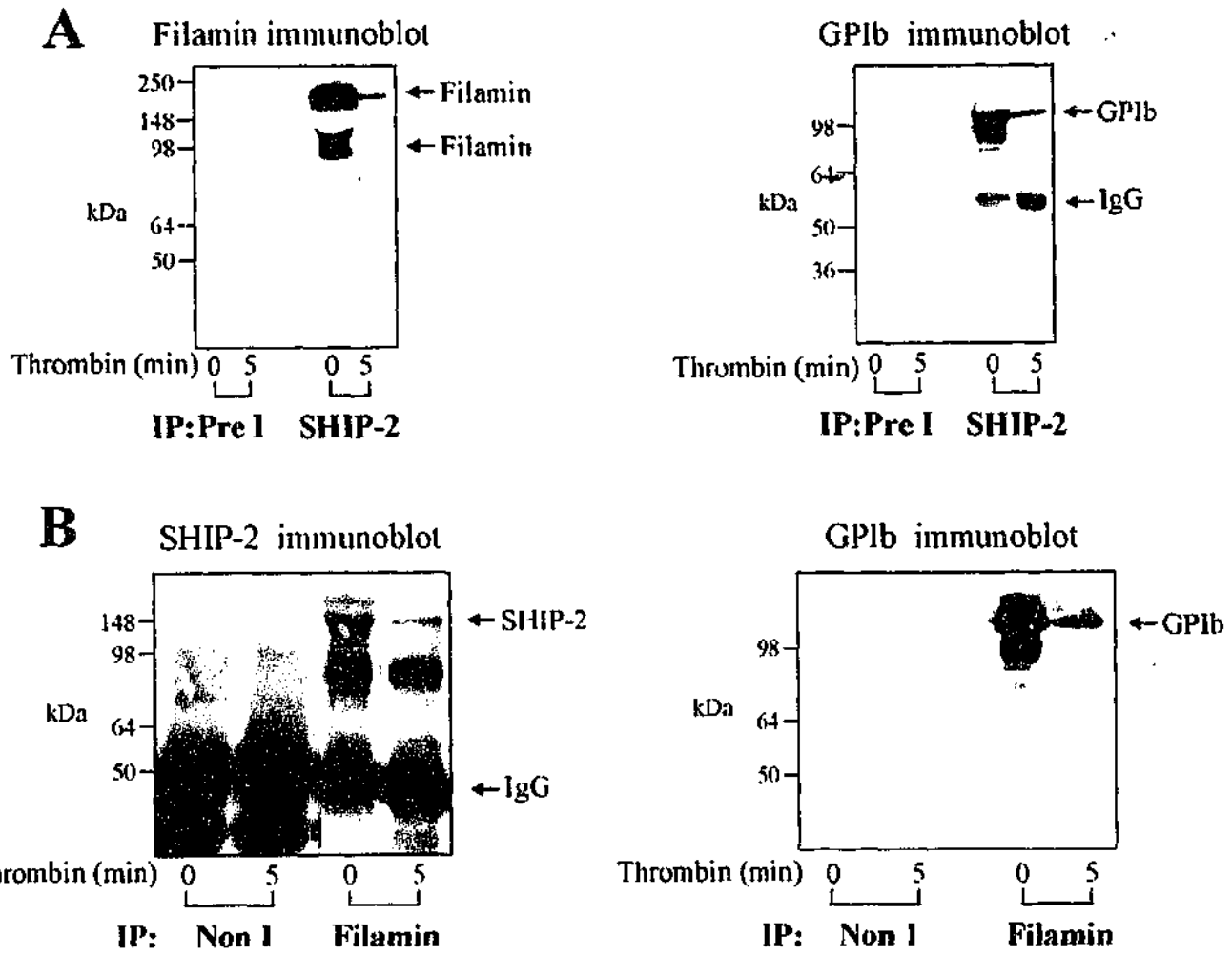
A
Filamin immunoblot
250
148
98
kDa
64
50
Filamin
Filamin
Thrombin (min) 0 5 0 5
IP:Pre I SHIP-2
GPIb immunoblot
98
64
kDa
50
36
GPIb
IgG
Thrombin (min) 0 5 0 5
IP:Pre I SHIP-2
B
SHIP-2 immunoblot
148
98
kDa
64
50
SHIP-2
IgG
Thrombin (min) 0 5 0 5
IP: Non I Filamin
GPIb immunoblot
98
kDa
64
50
GPIb
Thrombin (min) 0 5 0 5
IP: Non I Filamin
C
SHIP-2 immunoblot
250
148
kDa
98
64
SHIP-2
IgG
Thrombin (min) 0 5 0 5
IP: Non I GPIb
Filamin immunoblot
250
148
98
kDa
64
50
Filamin
Thrombin (min) 0 5 0 5
IP: Non I GPIb

filamin immunoprecipitates was also noted. Filamin immunoprecipitates demonstrated GPIb in complex in the Triton-soluble fraction of unstimulated platelets. However, GPIb detected in the immunoprecipitate decreased following thrombin activation.

Anti-GPIb immunoprecipitations of the Triton-soluble fraction of resting or thrombin-stimulated platelets were performed and probed with polyclonal antibodies to SHIP-2 or monoclonal antibodies to filamin (Figure 5.4C). SHIP-2 was present in anti-GPIb immunoprecipitates of the Triton-soluble platelet fraction of unstimulated platelets, with loss of association in this fraction following thrombin stimulation. Association between GPIb and filamin was detected in the Triton-soluble fraction of unstimulated platelets. However, this association decreased upon thrombin activation.

5.3.4 SHIP-2/filamin/GPIb complex in vWF stimulated platelets.

vWF mediates platelet adhesion through the binding of matrix-bound vWF to GPIb-IX-V, which then transmits signals leading to platelet activation. We investigated whether the association of SHIP-2 and filamin was also influenced by signaling, specifically mediated through the GPIb-IX-V complex. Anti-SHIP-2 immunoprecipitates from the Triton-soluble fraction of untreated or vWF-stimulated platelets were immunoblotted with filamin or GPIb antibodies (Figure 5.5A and B, respectively). These studies demonstrated that SHIP-2 immunoprecipitates contained both filamin and GPIb. However, following vWF treatment, SHIP-2 association with filamin and GPIb in the Triton-soluble fraction decreased.

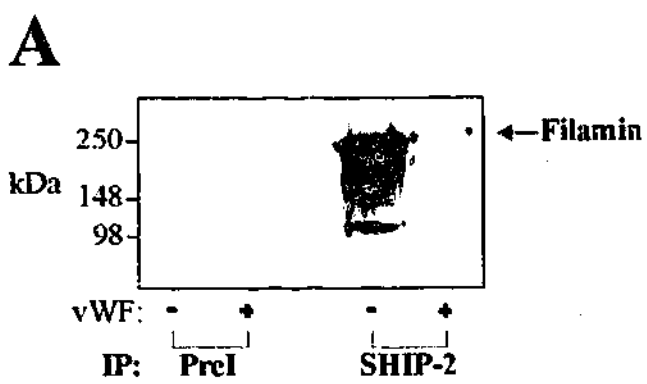

Figure 5.5 Decreased filamin and SHIP-2 complex in the Triton-soluble fractions of vWF-stimulated platelets.

Triton X-100-soluble fractions were isolated from platelets either untreated or treated with vWF (10μg/ml) and botrocetin (3 μg/ml) for 5 minutes. The Triton X-100-soluble fraction was immunoprecipitated with either affinity-purified Preimmune (Pre I) sera, or affinity-purified SHIP-2 antibodies and immunoblotted with either filamin (A), or GPIb (B) antibodies. Results are typical of three separate experiments.

5.3.5 SHIP-2 in the SHIP-2/filamin/GPIb complex in resting platelets is catalytically active.

SHIP-2 hydrolyzes the 5-position phosphate from PtdIns(3,4,5)P_3 generating PtdIns(3,4)P_2 and thereby regulates PtdIns(3,4,5)P_3-induced actin remodeling. We investigated in unstimulated platelets whether SHIP-2 bound to filamin/actin and GPIb was enzymatically active. Anti-SHIP-2, anti-filamin and anti-GPIb immunoprecipitates from the Triton-soluble fraction of unstimulated platelets were bound to protein-A-Sepharose, and washed extensively. The protein-A-Sepharose pellets were incubated with PtdIns(^{32}P-3,4,5)P_3 and standard 5-phosphatase enzyme assays were performed. PtdIns(3,4,5)P_3 and the lipid products of the 5-phosphatase assays were extracted and analyzed by thin layer chromatography (Figure 5.6). Incubation of pre-immune immunoprecipitates with PtdIns(3,4,5)P_3 resulted in little formation of PtdIns(3,4)P_2. In contrast, the anti-SHIP-2, anti-filamin and anti-GPIb immunoprecipitates all demonstrated evidence of significant PtdIns(3,4,5)P_3 5-phosphatase activity. In these immunoprecipitates, but not pre-immune immunoprecipitates, the addition of PtdIns(3,4,5)P_3 resulted in the formation of PtdIns(3,4)P_2, consistent with expression of functionally active SHIP-2 enzyme in complex with both filamin/actin and GPIb in unstimulated platelets.

5.3.6 Localization of SHIP-2, filamin and GPIb with actin in spreading platelets.

The results of the immunoprecipitation analysis demonstrate SHIP-2 in a complex with filamin, actin and GPIbα. Following thrombin-stimulation the association between SHIP-2 and filamin, and filamin and GPIb decreases in the Triton-soluble fraction. The association between SHIP-2, filamin, actin and GPIb-IX-V in the RIPA-extracted cytoskeletal fraction was investigated using immunoprecipitation of each species and immunoblot analysis. No complex was detected between SHIP-2 and filamin and or GPIb-

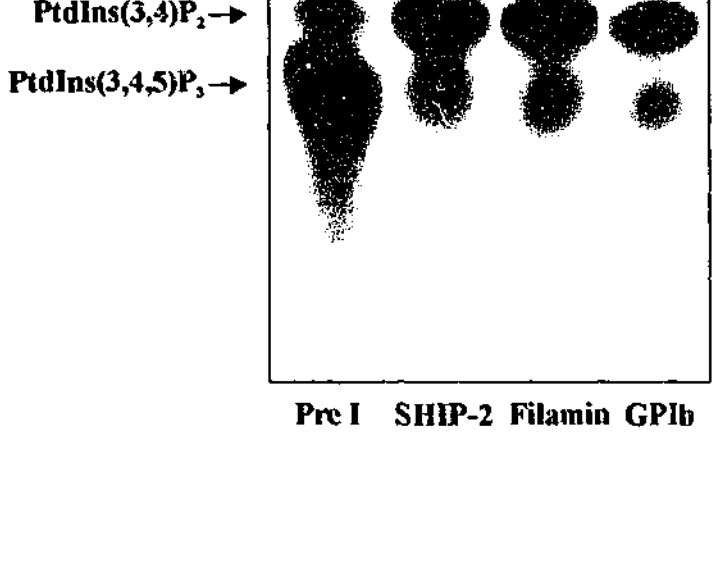

Figure 5.6 SHIP-2, filamin and GPIb immunoprecipitates from platelets have associated PtdIns(3,4,5)P_3 5-phosphatase activity.

Triton X-100-soluble fractions were isolated from untreated platelets and immunoprecipitated with either affinity-purified Preimmune (Pre I) sera, affinity-purified SHIP-2 antibodies, filamin antibodies, or GPIb antibodies. Immunoprecipitates captured on protein-A-Sepharose were subjected to PtdIns(3,4,5)P_3 5-phosphatase assays and the lipid products of the enzyme assay examined by thin layer chromatography. The migration of the phospholipids was compared to known standards PtdIns(3,4,5)P_3 and PtdIns(3,4)P_2. Results are typical of three separate experiments.

IX-V in the RIPA-extracted cytoskeletal fraction from either the unstimulated or activated platelets (data not shown). As protein complexes may disassociate in the presence of the RIPA-extraction buffer which contains 1 % NP40 and 0.1 % SDS, and in order to investigate the relationship between these proteins in the cytoskeleton in a functional model of activated platelets, the intracellular localization of SHIP-2, filamin, and GPIb (detected using specific antibodies) with actin (detected by phalloidin staining, which stains polymerized actin) was performed in platelets spreading on a vWF matrix (Figure 5.7). The co-localization of filamin and GPIb with actin in spreading platelets has not been previously reported.

In partially spread platelets, filamin localized in the cytosol and plasma membrane staining was prominent (Figure 5.7Aa). Patchy co-localization with actin was demonstrated in between filamin and actin at the central actin ring (Figure 5.7Aa merged image). With increased platelet spreading, intense filamin staining was demonstrated at the plasma membrane, with little cytosolic staining (Figure 5.7Ab). Filamin staining co-localized with submembraneous actin at the plasma membrane lamellipodia (Figure 5.7Ab, see arrows in merged images). In spread platelets there was little co-localization between filamin and actin at the central actin ring.

To determine the intracellular localization of GPIb, two distinct antibodies, polyclonal antibodies to GPIbβp, which recognizes cytoplasmic sequence within the GPIbβ chain (Figure 5.7B), and polyclonal antibodies to the extracellular domain of GPIbα were utilized (Figure 5.7C). Results with both antibodies were comparable. GPIbβp antibodies stained intensely a central region of the platelet, which was localized predominantly internal to the central actin ring (Figure 5.7B). Only very faint plasma membrane staining was detected using this antibody. Antibodies to the extracellular region of GPIbα demonstrated intense staining at the centre of the spreading platelet, which

Figure 5.7 Localization of filamin, GPIb and actin in spreading platelets.

Platelets spread on a vWF matrix were fixed, permeabilized and co-stained with filamin antibodies and phalloidin (Aa and b), GPIbβ_p antibodies and phalloidin (B), GPIbα antibodies and phalloidin (C), GPIbβ_p and filamin antibodies (D), and GPIbα and filamin antibodies (E). Arrows in merged images in (7Ab) indicate co-localization of filamin and submembraneous actin at lamellipodia. Cells were visualized by confocal microscopy. Bars, 10 μm.

A

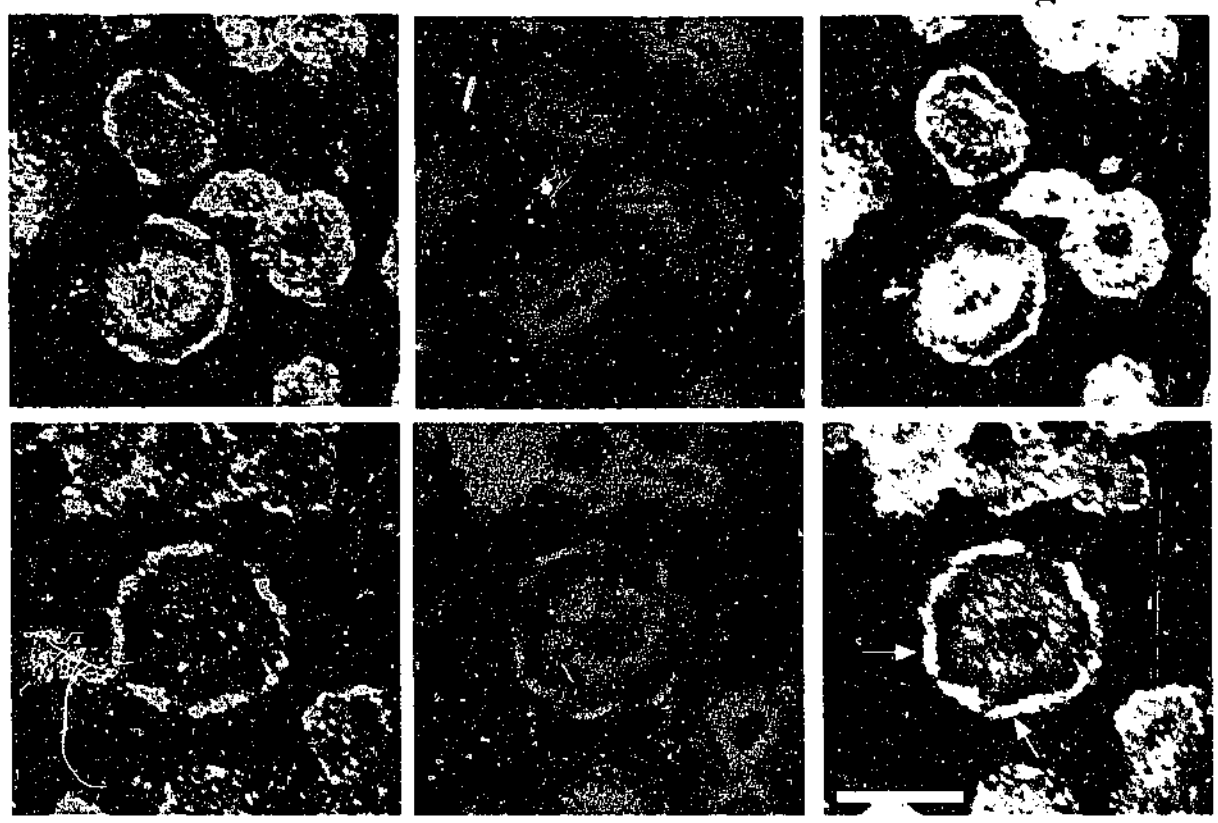
Filamin
Phalloidin
Merged
a
b

B

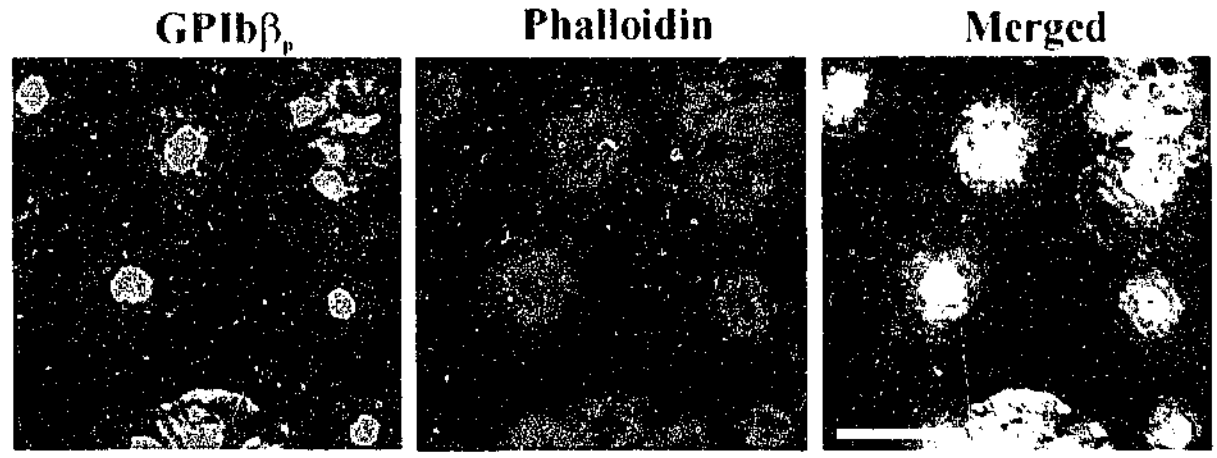
GPIbβp
Phalloidin
Merged

C

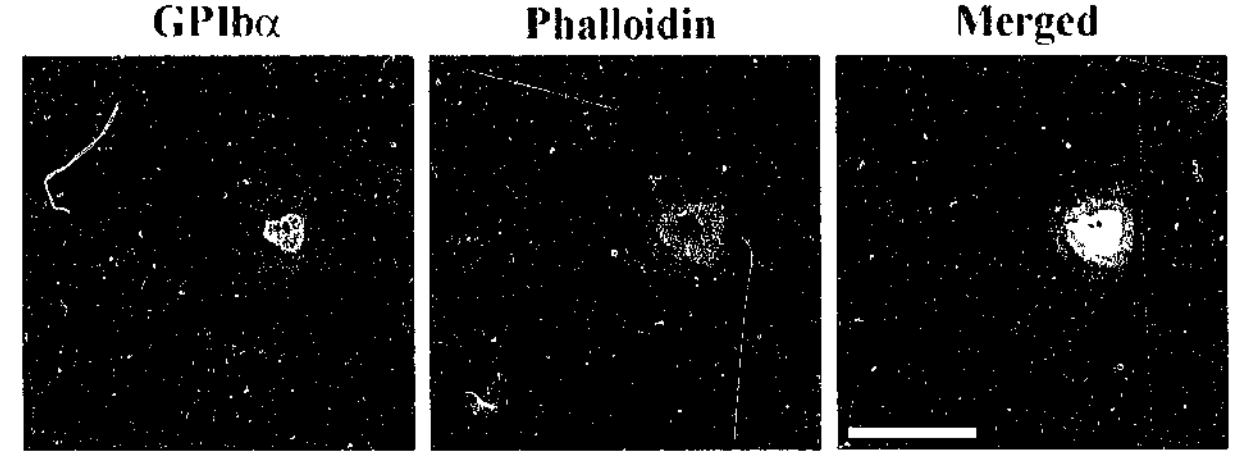
GPIbα
Phalloidin
Merged

D

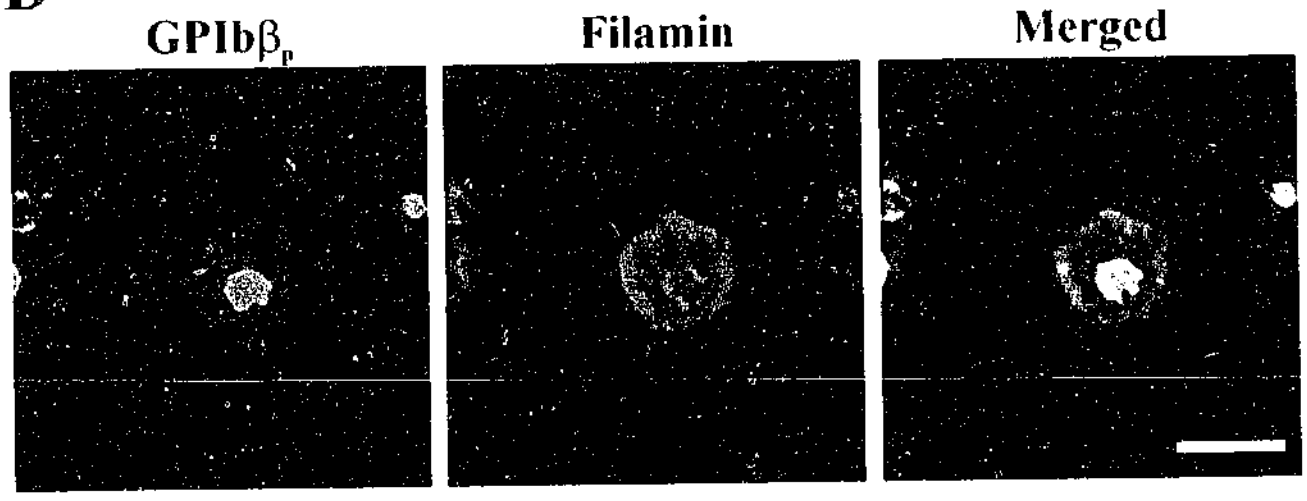

E

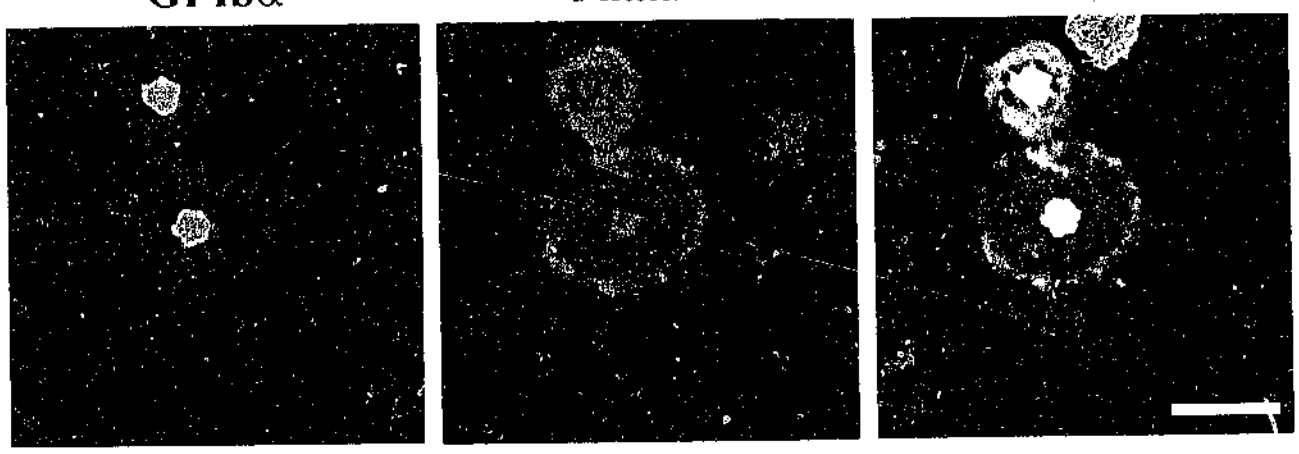

localized internal to the central actin ring and demonstrated patchy co-localization with actin at this site. No plasma membrane staining was demonstrated using this antibody (Figure 5.7C). Co-localization of GPIb with filamin was examined (Figure 5.7D and E). Consistent with the immunoprecipitation data demonstrating decreased association between filamin and GPIb with platelet activation, only patchy co-localization between these species was observed. In spread platelets, filamin localized predominantly at the plasma membrane, whilst the receptor localized to the centre of the platelet. Patchy co-localization was detected at the centre of the spread platelet, with no co-localization detected at the plasma membrane (Figure 5.7D and E).

The co-localization of SHIP-2 with filamin in spreading platelets was determined (Figure 5.8). SHIP-2 and filamin co-localized intensely at filopodia and also demonstrated co-localization at the central actin ring (Figure 5.8a and b). In spread platelets filamin localized most intensely at the plasma membrane (Figure 5.8c). Patchy co-localization between filamin and SHIP-2 was demonstrated at plasma membrane lamellipodia (Figure 5.8c merged image). In the cytosol SHIP-2 staining was detected, but filamin staining was less intense and the two species demonstrated only patchy co-localization at this site.

In summary, these studies demonstrate SHIP-2 is part of a dynamic tetrameric complex with filamin, actin and GPIb-IX-V. In spreading platelets SHIP-2 localizes intensely with actin at the central ring and co-localizes with actin and filamin at filopodia and lamellipodia.

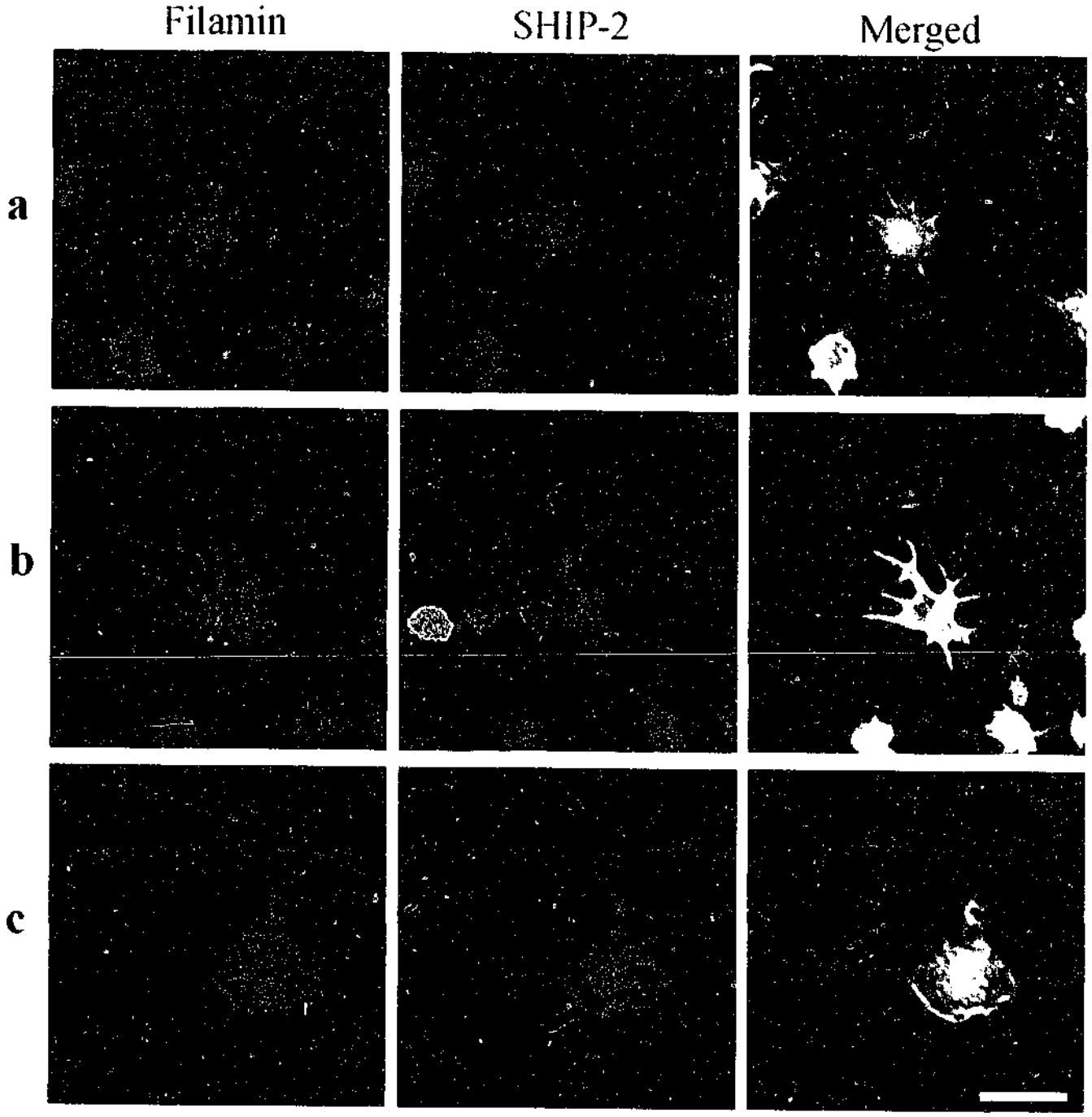

Figure 5.8 SHIP-2 co-localizes with filamin in spreading platelets at lamellipodia.

Platelets spread on a vWF matrix were fixed/permeabilized and co-stained with filamin antibodies and affinity-purified SHIP-2 antibodies, and visualized by confocal microscopy. Bar, 10 μm.

CHAPTER 6: General Discussion

6.1 Discussion

This study characterizes the localization of the SH2-containing inositol polyphosphate 5-phosphatase-2, SHIP-2, identifies and characterizes its association with the actin-binding protein, filamin, in adherent and non-adherent cells, and investigates the functional significance of this association. Specifically, these studies have demonstrated SHIP-2 localizes to actin-rich regions. In COS-7 cells, SHIP-2 localizes to membrane ruffles which is mediated *via* its C-terminal proline-rich domain. In contrast, SHIP-2 localizes to filopodia, lamellipodia and the central actin-ring in spreading platelets. SHIP-2 associates *via* its proline-rich domain, specifically with filamin A, B and C through the C-terminal region of filamin, with repeats 22, 23 and 24 of filamin required for maximal association of the two species. In contrast to adherent COS-7 cells where association of filamin and SHIP-2 was demonstrated to be constitutive, in platelets, the association of the two species is dynamic and sensitive to platelet activation. Furthermore, in platelets, SHIP-2 and filamin are part of tetrameric complex with actin and GPIb-IX-V. Filamin and SHIP-2 co-localized to Z-lines and the sarcloemma of skeletal muscle, and in mammalian cell lines to membrane ruffles. The association of SHIP-2 and filamin may serve to localize the 5-phosphatase to membrane ruffles, where it regulates PtdIns(3,4,5)P_3 and thereby submembraneous actin at this site.

6.1.1 Inositol polyphosphate 5-phosphatases and the cytoskeleton.

Increasing evidence indicates that both mammalian and yeast 5-phosphatase isoforms, *via* hydrolysis of PtdIns(4,5)P_2 and or PtdIns(3,4,5)P_3, play a significant role in regulating cytoskeletal reorganization. The 5-phosphatases comprise ten mammalian and four yeast isoforms with many spliced variants described. Null mutation of any two yeast Sac-1 domain containing 5-phosphatases results in a phenotype which includes

disorganization of polymerized actin and delocalization of actin patches from the growing yeast bud to the daughter cell, (reviewed by (Hughes *et al.*, 2000a)). The yeast 5-phosphatases, Inp52p and Inp53p, translocate to actin patches upon osmotic stress, the site of plasma membrane invaginations. In addition, overexpression of Inp52p and Inp53p, but not catalytically inactive Inp52p, results in a significant reduction in the repolarization time of actin patches following osmotic stress (Ooms *et al.*, 2000). The mammalian 5-phosphatase, synaptojanin-1, hydrolyzes PtdIns(4,5)P_2 bound to the actin regulatory proteins, α-actinin, vinculin, gelsolin and profilin, and decreases the number of stress fibers in the cell (Sakisaka *et al.*, 1997). Synaptojanin-2 directly interacts with Rac1 in a GTP-dependent manner, resulting in translocation of the 5-phosphatase to membrane ruffles and inhibition of endocytosis (Malecz *et al.*, 2000). Overexpression of SKIP (Skeletal muscle and Kidney enriched inositol phosphatase) results in loss of actin stress fibers in areas of SKIP expression (Ijuin *et al.*, 2000). The recently identified proline-rich inositol polyphosphate 5-phosphatase (PIPP) localizes to membrane ruffles, but unlike SHIP-2 does not appear to regulate the actin cytoskeleton (Mochizuki and Takenawa, 1999). SHIP-2 regulation of submembraneous actin levels is most probably mediated *via* localized regulation of PtdIns(3,4,5)P_3. However, both SHIP-1 and SHIP-2 also hydrolyze PtdIns(4,5)P_2 forming PtdIns(4)P (Kisseleva *et al.*, 2000; Taylor *et al.*, 2000).

6.1.2 Role of SHIP-2 association with filamin in insulin signaling.

The recent characterization of SHIP-2 homozygous null mice has demonstrated that this 5-phosphatase plays a significant role in regulating insulin sensitivity (Clement *et al.*, 2001). Although the signaling pathways mediating the phenotype of insulin-hypersensitivity have yet to be fully determined, insulin-stimulated GLUT4 translocation to the plasma membrane appears to be enhanced in mice lacking SHIP-2. In addition

overexpression of SHIP-2, but not catalytically inactive SHIP-2, in 3T3-L1 adipocytes results in negative regulation of insulin-induced signaling (Wada *et al.*, 2001). The submembraneous actin microfilament network links various signaling proteins including IRS-1 and PI3-kinase that regulate GLUT4 translocation to the plasma membrane. Insulin-induced reorganization of the sub-plasma membrane actin filaments may allow exocytic GLUT4 vesicles to fuse with the plasma membrane during stimulation by insulin (Khayat *et al.*, 2000). GLUT4 expression is restricted to muscle and adipose tissue. Insulin-stimulated glucose disposal in skeletal muscle accounts for 80 % of glucose uptake post-prandial (Khayat *et al.*, 2000), localizing GLUT4 to the sarcolemma. Filamin may provide a scaffold for the juxtaposition of SHIP-2 to the sarcolemma localizing the enzyme to PtdIns(3,4,5)P_3 following insulin treatment and thereby regulating GLUT4 translocation.

6.1.3 Role of SHIP-2 association with filamin in the actin cytoskeleton.

Filamin forms a scaffold for the binding of Rho GTPases including Rac1, Cdc42, Rho A and RalA and their activators such as Trio, a Rho GEF (Ohta *et al.*, 1999). The localization of both Rho GTPases and their activators on filamin may allow spatial co-ordination of actin nucleation at sites where newly assembled actin filaments are crosslinked. It is noteworthy that many filamin-binding proteins, including Trio and SHIP-2, bind to the extreme C-terminal repeats 21-24 of filamin, by a variety of interacting modules including proline-rich domains as is the case for SHIP-2 and pleckstrin homology domains as shown for Trio. This would therefore provide close proximity between all these signaling proteins, including SHIP-2, that regulate actin polymerization on a filamin scaffold.

Several recent studies in fibroblasts and the neutrophil cell line HL60 have demonstrated using the PH domain of PtdIns(3,4,5)P_3-binding proteins fused to GFP, that

PI3-kinase signals are generated at the leading edge of the cell (Balla *et al.*, 2000; Blomberg *et al.*, 1999; Servant *et al.*, 2000; Watton and Downward, 1999). These PH domains function as an accurate probe for the localized agonist-dependent accumulation of PtdIns(3,4,5)P_3. It has been proposed, but not previously shown, that this asymmetric distribution of PtdIns(3,4,5)P_3 may result from its localized synthesis or degradation (Rickert *et al.*, 2000). The results of these studies reported in this thesis are consistent with this contention. These studies provide strong evidence for the spatially controlled synthesis of PtdIns(3,4,5)P_3 at membrane ruffles is regulated by the PtdIns(3,4,5)P_3 5-phosphatase SHIP-2, which also localizes to membrane ruffles.

SHIP-2 localization to membrane ruffles is mediated by its C-terminal proline-rich domain binding to the actin-binding protein filamin. The expression of SHIP-2 in filamin-deficient cells is exclusively cytosolic. In addition SHIP-2 membrane localization appears to contribute to localized PtdIns(3,4,5)P_3 hydrolysis. SHIP-2 C-terminal truncation mutants were not as efficient at regulating PtdIns(3,4,5)P_3 at membrane ruffles as intact SHIP-2. Furthermore, displacement of endogenous SHIP-2 by overexpression of the SHIP-2 filamin-binding domain (Myc-filamin aa 2434-2705) leads to the marked enhancement of the PI3-kinase signal PtdIns(3,4,5)P_3. Several recent reports have shown the membrane localization of the highly related SHIP-2 homologue SHIP-1 is also important for PtdIns(3,4,5)P_3 hydrolysis (Phee *et al.*, 2000). Enforced plasma membrane localization of SHIP-1, mediated by overexpression of a human CD8-SHIP-1 chimera, decreased the total cellular levels of PtdIns(3,4,5)P_3. Membrane targeting of SHIP-1 mediated by the C-terminal proline-rich domain appears to be important in B cell inhibitory function (Aman *et al.*, 2000). In addition the SHIP-1 C-terminus is essential for PtdIns(3,4,5)P_3 hydrolysis and inhibition of mast cell degranulation (Damen *et al.*, 2001). Collectively these studies show

membrane targeting of these two 5-phosphatases mediated by their respective C-terminal proline-rich domain plays an important functional role in regulating PI3-kinase signals.

SHIP-2 associates with the $p130^{Cas}$ adaptor protein at focal adhesions and regulates cell spreading, which is dependent on the SHIP-2 SH2 domain and is enhanced by tyrosine phosphorylation and cell adhesion (Prasad *et al.*, 2001). These studies reported here have shown SHIP-2 and filamin also form a functionally significant complex both in the resting cells and following cellular activation at membrane ruffles. Therefore the binding of SHIP-2 to filamin may provide a mechanism for exquisite localized hydrolysis of PtdIns(3,4,5)P_3 in resting, growth-factor and insulin-stimulated cells at the leading edge of cell.

6.1.4 Role of SHIP-2 in platelet signaling.

Recent reports have suggested a role for SHIP-2 in integrin-dependent cell adhesion. These studies demonstrated SHIP-2 is tyrosine-phosphorylated by the Src family of kinases in cells plated on an integrin-activating surface, moreover, increased adhesion was observed in adherent HeLa cells transiently expressing exogenous SHIP-2. The function of this signal-terminating enzyme, however, has not been characterized in highly motile cells. Therefore, the localization of SHIP-2 and its association with the actin-binding protein, filamin, in highly motile cells, namely platelets was investigated and reported in Chapter 5. Furthermore, an association between the platelet-specific receptor GPIb-V-IX, filamin, SHIP-2 and actin was demonstrated which may serve to link extracellular signals with phosphoinositide metabolism and cytoskeletal reorganization.

The results of this study demonstrate a number of significant novel findings. First, in human platelets, SHIP-2 forms an indirect complex with actin *via* interaction with the actin-binding protein, filamin. In spreading platelets, SHIP-2 co-localizes with actin at filopodia, lamellipodia and the central actin ring. The enzyme also dynamically relocates in

spread platelets internal to the central actin ring. Second, SHIP-2 forms a functionally active, dynamic complex with filamin, and this complex decreases in the Triton-soluble fraction following platelet adhesion and activation. This is in contrast to adherent cells in which the complex between these proteins is constitutive. Third, SHIP-2 also complexes with GPIb-IX-V and dissociates from this receptor following platelet activation. Fourth, the relationship between SHIP-2/filamin/actin and GPIb-IX-V demonstrated by imaging the co-localization of these species in platelets spreading on a vWF matrix. These studies indicate GPIb-IX-V is primarily localized to the centre of the platelet, whilst filamin localizes with SHIP-2 at lamellipodia.

PtdIns(3,4,5)P_3 is a critical regulator of many intracellular signaling pathways. Recent studies have highlighted the role this lipid signaling cascade, in particular PtdIns(3,4,5)P_3, plays in instructing actin remodeling (Comer and Parent, 2002; Rickert *et al.*, 2000; Stephens *et al.*, 2002). PtdIns(3,4,5)P_3 localizes to lamellipodia and regulates Rac and Rho activation. The metabolism of PtdIns(3,4,5)P_3 has emerged as molecular mechanism regulating cell migration (Fox *et al.*, 2002; Funamoto *et al.*, 2002; Marino *et al.*, 2002). SHIP-2 localizes to lamellipodia and inhibits membrane ruffling, *via* regulation of PtdIns(3,4,5)P_3. In platelets SHIP-2 indirectly binds actin *via* an association with filamin. The signaling adaptor protein, 14-3-3ζ, directly binds the cytoplasmic domain of GPIbα and also PI3-kinase indicating PtdIns(3,4,5)P_3 is generated in close proximity to the receptor (Munday *et al.*, 2000). The demonstration of functionally active SHIP-2, a specific PtdIns(3,4,5)P_3-5-phosphatase associated with GPIb-IX-V, provides evidence for the localized regulation of this signaling molecule in unstimulated platelets.

The results from the studies reported here showing decreased association of SHIP-2 with filamin, in thrombin or vWF stimulated platelets is different to the constitutive association of SHIP-2 and filamin in adherent EGF-stimulated COS-7 cells. In human

platelets which express high levels of calpain, the decreased association of SHIP-2 with filamin in activated platelets may result from calpain-mediated cleavage of filamin at the hinge region, thereby disrupting the SHIP-2 binding site. As shown using yeast two-hybrid analysis, the association between SHIP-2 and filamin is maximal when mediated by filamin repeats 22-24, which includes the calpain-cleaved hinge II region, located between repeats 23 and 24 (see Figure 3A). Repeats 22 and 23 in combination, with or without the hinge region II interacted with SHIP-2, however, this was weaker than with intact repeats 22-24. Alternatively the disassociation of SHIP-2 from filamin may result from SHIP-2 phosphorylation and recruitment into other signaling complexes. In addition the possibility cannot be excluded that the decreased complex between SHIP-2 and filamin/GPIb-IX-V reflects the incorporation of this complex from the Triton-soluble fraction into the cytoskeletal fraction. In this regard studies reported in Chapter 5 have shown using immunoconfocal microscopy that SHIP-2 and filamin, but not GPIb-IX-V, co-localize in platelets spreading on a vWF matrix at plasma membrane lamellipodia.

Filamin plays a complex role in regulating platelet activation. In addition to binding GPIb-IX-V, filamin binds various other macromolecules, including engaging the β-chain of β-3 integrin, as well as in other cells the small GTPases, Cdc42, Rac, and their guanine nucleotide exchange factor, Trio (reviewed by (Stossel *et al.*, 2001)). To date, over 20 binding partners have been identified and many of these binding partners facilitate the activation of localized signaling pathways involving actin polymerization. The GPIbα chain binds repeats 17-19 of filamin (Meyer *et al.*, 1997). The sequences of the GPIbα receptor that mediate this interaction have recently been shown to encompass residues 570-90, which are also essential for membrane anchorage of the receptor complex under conditions of high shear stress (Williamson *et al.*, 2002).

The results of the study reported here demonstrate filamin may also provide a scaffold for the assembly of signaling proteins, such as SHIP-2, to facilitate signaling *via* the GPIb-IX-V receptor. These associations markedly decreased in the Triton-soluble platelet compartment on platelet activation with either thrombin or vWF. In this regard, also demonstrated in spreading platelets, filamin and the GPIb-IX-V complex are predominantly localized in distinct cytoskeletal compartments; filamin at the submembraneous cytoskeleton and the GPIb-IX-V receptor centralized to the inner central actin ring. This receptor localization is consistent with previous studies using electron microscopy that GPIb-IX-V is located centrally, and although receptor localization with respect to polymerized actin or co-localization with filamin was not demonstrated, receptor centralization was shown to be dependent on an intact actin cytoskeleton (Kovacsovics and Hartwig, 1996). However, in contrast to findings reported in this thesis which show a decrease in filamin and GPIb-IX-V association in activated platelets, Kovacsovics and Hartwig showed constitutive association between these species by co-immunoprecipitation analysis (Kovacsovics and Hartwig, 1996). The reason for these differences may relate to technical differences in that we did not include DNase-I, which potently inhibits actin polymerization, or phallacidin, which stabilizes existing actin filaments in either the lysis or the immunoprecipitation buffer. The results of immunoprecipitation data and co-localization of these species are consistent with the contention that as platelets spread and actin polymerizes, GPIb remains internal to the central actin ring and filamin localizes with SHIP-2 to submembraneous actin, rather than incorporating with a centralized/internalized receptor complex.

Phosphoinositides are well established regulators of the actin cytoskeleton. Through its lipid product PtdIns(3,4,5)P_3, PI3-kinase has been established as an essential modulator for chemotaxis and associated cytoskeletal regulation. The downstream targets

of PI3-kinase and its lipid product involved in cytoskeletal regulation are being identified. To date the PAK-1 signaling pathway is one of most well defined in the regulation of actin filaments required for cell motility responses such as membrane ruffling. Based on the studies presented here it can be speculated that SHIP-2 may be involved in this signaling pathway at two points.

The catalytic activity of many PAK proteins is regulated by their association with PtdIns(3,4,5)P_3-activated Rho family of GTPases, $Rac1^{GTP}$ and $Cdc42^{GTP}$. Recently, it has been demonstrated that filamin associates with, and is a substrate for, PAK-1, which is required for PAK-1-mediated actin assembly, including lamellipodia formation. PAK-1 specifically influences actin assembly through its actions on LIM kinase and subsequent inactivation of cofilin, thus promoting F-actin organization and lamellipodia formation (reviewed by (Chung *et al.*, 2001)). Furthermore, the gelating activity of filamin is influenced by its association with phosphoinositides. Within this pathway SHIP-2 may serve to negatively regulate actin assembly either by inhibiting the Rho family of GTPases, Rac1 and Cdc42 through hydrolysis of PtdIns(3,4,5)P_3, or by directly influencing the gelating activity of filamin through hydrolysis of bound phosphoinositides.

Recent studies in our laboratory have suggested an association between SHIP-2 and the Ena/VASP (Enabled/vasodilator-stimulated phosphoprotein) family of proteins (Megan Astle, personal communication). Biochemical mechanisms have emerged depicting Ena/VASP proteins as enhancers of actin filament formation, however, increasing evidence suggests these proteins may also possess inhibitory activities in processes such as cell migration. SHIP-2 may influence actin polymerization through its association with this family of proteins. Interestingly, like the Ena/VASP proteins, studies from our laboratory have implicated SHIP-2 in the negative regulation of cell migration (Megan Astle, personal communication).

In summary, this study characterizes the localization of the SHIP-2 5-phosphatase to membrane ruffles, its association with filamin in adherent and non-adherent cells, and suggests through this association, SHIP-2 may regulate PtdIns(3,4,5)P_3 levels and submembraneous actin at actin-rich sites.

References

Adey, N.B., L. Huang, P.A. Ormonde, M.L. Baumgard, R. Pero, D.V. Byreddy, S.V. Tavtigian, and P.L. Bartel. 2000. Threonine phosphorylation of the MMAC1/PTEN PDZ binding domain both inhibits and stimulates PDZ binding. *Cancer Res.* **60**:35-7.

Akasaki, T., H. Koga, and H. Sumimoto. 1999. Phosphoinositide 3-kinase-dependent and -independent activation of the small GTPase Rac2 in human neutrophils. *Journal of Biciogical Chemistry.* **274**:18055-9.

Alessi, D.R., M. Andjelkovic, B. Caudwell, P. Cron, N. Morrice, P. Cohen, and B.A. Hemmings. 1996. Mechanism of activation of protein kinase B by insulin and IGF-1. *Embo J.* **15**:6541-51.

Alessi, D.R., S.R. James, C.P. Downes, A.B. Holmes, P.R. Gaffney, C.B. Reese, and P. Cohen. 1997. Characterization of a 3-phosphoinositide-dependent protein kinase which phosphorylates and activates protein kinase Balpha. *Curr Biol.* **7**:261-9.

Aman, M.J., S.F. Walk, M.E. March, H.P. Su, D.J. Carver, and K.S. Ravichandran. 2000. Essential role for the C-terminal noncatalytic region of SHIP in FcgammaRIIB1-mediated inhibitory signaling. *Mol Cell Biol.* **20**:3576-89.

Ambruso, D.R., C. Knall, A.N. Abell, J. Panepinto, A. Kurkchubasche, G. Thurman, C. Gonzalez-Aller, A. Hiester, M. deBoer, R.J. Harbeck, R. Oyer, G.L. Johnson, and D. Roos. 2000. Human neutrophil immunodeficiency syndrome is associated with an inhibitory Rac2 mutation. *Proc Natl Acad Sci U S A.* **97**:4654-9.

Andjelkovic, M., D.R. Alessi, R. Meier, A. Fernandez, N.J. Lamb, M. Frech, P. Cron, P. Cohen, J.M. Lucocq, and B.A. Hemmings. 1997. Role of translocation in the activation and function of protein kinase B. *J Biol Chem.* **272**:31515-24.

Andrews, R.K., and J.E. Fox. 1992. Identification of a region in the cytoplasmic domain of the platelet membrane glycoprotein Ib-IX complex that binds to purified actin-binding protein.PG - 18605-11. *J Biol Chem*. **267**:18605-11.

Arcaro, A. 1998. The small GTP-binding protein Rac promotes the dissociation of gelsolin from actin filaments in neutrophils. *Journal of Biological Chemistry*. **273**:805-13.

Arcaro, A., S. Volinia, M.J. Zvelebil, R. Stein, S.J. Watton, M.J. Layton, I. Gout, K. Ahmadi, J. Downward, and M.D. Waterfield. 1998. Human phosphoinositide 3-kinase C2beta, the role of calcium and the C2 domain in enzyme activity. *Journal of Biological Chemistry*. **273**:33082-90.

Asano, T., Y. Mochizuki, K. Matsumoto, T. Takenawa, and T. Endo. 1999. Pharbin, a novel inositol polyphosphate 5-phosphatase, induces dendritic appearances in fibroblasts. *Biochem Biophys Res Commun*. **261**:188-95.

Auethavekiat, V., C.S. Abrams, and P.W. Majerus. 1997. Phosphorylation of platelet pleckstrin activates inositol polyphosphate 5-phosphatase I. *J Biol Chem*. **272**:1786-90.

Baenziger, N.L., and P.W. Majerus. 1974. Isolation of human platelets and platelet surface membranes. *Methods Enzymol*. **31**:149-55.

Balla, T., T. Bondeva, and P. Varnai. 2000. How accurately can we image inositol lipids in living cells? *Trends Pharmacol Sci*. **21**:238-41.

Banfic, H., C.P. Downes, and S.E. Rittenhouse. 1998. Biphasic activation of PKBalpha/Akt in platelets. Evidence for stimulation both by phosphatidylinositol 3,4-bisphosphate, produced via a novel pathway, and by phosphatidylinositol 3,4,5-trisphosphate. *J Biol Chem*. **273**:11630-7.

Baukrowitz, T., U. Schulte, D. Oliver, S. Herlitze, T. Krauter, S.J. Tucker, J.P. Ruppersberg, and B. Fakler. 1998. PIP2 and PIP as determinants for ATP inhibition of KATP channels. *Science*. **282**:1141-4.

Bear, J.E., M. Krause, and F.B. Gertler. 2001. Regulating cellular actin assembly. *Curr Opin Cell Biol*. **13**:158-66.

Belisle, B., and A. Abo. 2000. N-Formyl peptide receptor ligation induces rac-dependent actin reorganization through Gbeta gamma subunits and class Ia phosphoinositide 3-kinases. *J Biol Chem*. **275**:26225-32.

Bellanger, J.M., C. Astier, C. Sardet, Y. Ohta, T.P. Stossel, and A. Debant. 2000. The Rac1- and RhoG-specific GEF domain of Trio targets filamin to remodel cytoskeletal actin. *Nat Cell Biol*. **2**:888-92.

Benard, V., B.P. Bohl, and G.M. Bokoch. 1999a. Characterization of rac and cdc42 activation in chemoattractant-stimulated human neutrophils using a novel assay for active GTPases. *J Biol Chem*. **274**:13198-204.

Benard, V., G.M. Bokoch, and B.A. Diebold. 1999b. Potential drug targets: small GTPases that regulate leukocyte function. *Trends Pharmacol Sci*. **20**:365-70.

Bennett, J.P., K.S. Zaner, and T.P. Stossel. 1984. Isolation and some properties of macrophage alpha-actinin: evidence that it is not an actin gelling protein. *Biochemistry*. **23**:5081-6.

Bensen, E.S., G. Costaguta, and G.S. Payne. 2000. Synthetic genetic interactions with temperature-sensitive clathrin in Saccharomyces cerevisiae. Roles for synaptojanin-like Inp53p and dynamin-related Vps1p in clathrin-dependent protein sorting at the trans-Golgi network. *Genetics*. **154**:83-97.

Berndt, M.C., C. Gregory, A. Kabral, H. Zola, D. Fournier, and P.A. Castaldi. 1985. Purification and preliminary characterization of the glycoprotein Ib complex in the human platelet membrane. *Eur J Biochem.* **151**:637-49.

Berndt, M.C., Y. Shen, S.M. Dopheide, E.E. Gardiner, and R.K. Andrews. 2001. The vascular biology of the glycoprotein Ib-IX-V complex. *Thromb Haemost.* **86**:178-88.

Berridge, M.J. 1993a. Cell signalling. A tale of two messengers. *Nature.* **365**:388-9.

Berridge, M.J. 1993b. Inositol trisphosphate and calcium signalling. *Nature.* **361**:315-25.

Bishop, A.L., and A. Hall. 2000. Rho GTPases and their effector proteins. *Biochem J.* **348**:241-55.

Blero, D., F. De Smedt, X. Pesesse, N. Paternotte, C. Moreau, B. Payrastre, and C. Erneux. 2001. The sh2 domain containing inositol 5-phosphatase ship2 controls phosphatidylinositol 3,4,5-trisphosphate levels in cho-ir cells stimulated by insulin. *Biochem Biophys Res Commun.* **282**:839-43.

Blomberg, N., E. Baraldi, M. Nilges, and M. Saraste. 1999. The PH superfold: a structural scaffold for multiple functions. *Trends Biochem Sci.* **24**:441-5.

Bootman, M.D., T.J. Collins, C.M. Peppiatt, L.S. Prothero, L. MacKenzie, P. De Smet, M. Travers, S.C. Tovey, J.T. Seo, M.J. Berridge, F. Ciccolini, and P. Lipp. 2001. Calcium signalling--an overview. *Semin Cell Dev Biol.* **12**:3-10.

Bourne, H.R., D.A. Sanders, and F. McCormick. 1990. The GTPase superfamily: a conserved switch for diverse cell functions. *Nature.* **348**:125-32.

Brauweiler, A., I. Tamir, S. Marschner, C.D. Helgason, and J.C. Cambier. 2001. Partially distinct molecular mechanisms mediate inhibitory FcgammaRIIB signaling in resting and activated B cells. *J Immunol.* **167**:204-11.

Bretscher, A. 1999. Regulation of cortical structure by the ezrin-radixin-moesin protein family. *Curr Opin Cell Biol.* **11**:109-16.

Brotschi, E.A., J.H. Hartwig, and T.P. Stossel. 1978. The gelation of actin by actin-binding protein. *J Biol Chem.* **253**:8988-93.

Brown, R.A., J. Domin, A. Arcaro, M.D. Waterfield, and P.R. Shepherd. 1999. Insulin activates the alpha isoform of class II phosphoinositide 3-kinase. *Journal of Biological Chemistry.* **274**:14529-32.

Calderwood, D.A., A. Huttenlocher, W.B. Kiosses, D.M. Rose, D.G. Woodside, M.A. Schwartz, and M.H. Ginsberg. 2001. Increased filamin binding to beta-integrin cytoplasmic domains inhibits cell migration.PG - 1060-8. *Nat Cell Biol.* **3**:1060-8.

Campbell, J.K., R. Gurung, S. Romero, C.J. Speed, R.K. Andrews, M.C. Berndt, and C.A. Mitchell. 1997. Activation of the 43 kDa inositol polyphosphate 5-phosphatase by 14-3-3zeta. *Biochemistry.* **36**:15363-70.

Cantley, L.C., and B.G. Neel. 1999. New insights into tumor suppression: PTEN suppresses tumor formation by restraining the phosphoinositide 3-kinase/AKT pathway. *Proc Natl Acad Sci U S A.* **96**:4240-5.

Cantrell, D.A. 2001. Phosphoinositide 3-kinase signalling pathways. *J Cell Sci.* **114**:1439-45.

Carlier, M.F., F. Ressad, and D. Pantaloni. 1999. Control of actin dynamics in cell motility. Role of ADF/cofilin. *J Biol Chem.* **274**:33827-30.

Chan, T.O., S.E. Rittenhouse, and P.N. Tsichlis. 1999. AKT/PKB and other D3 phosphoinositide-regulated kinases: kinase activation by phosphoinositide-dependent phosphorylation. *Annu Rev Biochem.* **68**:965-1014.

Cheatham, B., C.J. Vlahos, L. Cheatham, L. Wang, J. Blenis, and C.R. Kahn. 1994. Phosphatidylinositol 3-kinase activation is required for insulin stimulation of pp70

S6 kinase, DNA synthesis, and glucose transporter translocation. *Mol Cell Biol.* **14**:4902-11.

Cheng, S., J. Mao, and V. Rehder. 2000. Filopodial behavior is dependent on the phosphorylation state of neuronal growth cones.PG - 337-50. *Cell Motil Cytoskeleton.* **47**:337-50.

Cheresh, D.A., J. Leng, and R.L. Klemke. 1999a. Regulation of cell contraction and membrane ruffling by distinct signals in migratory cells. *J Cell Biol.* **146**:1107-16.

Cheresh, D.A., J. Leng, and R.L. Klemke. 1999b. Regulation of cell contraction and membrane ruffling by distinct signals in migratory cells.PG - 1107-16. *J Cell Biol.* **146**:1107-16.

Chong, L.D., A. Traynor-Kaplan, G.M. Bokoch, and M.A. Schwartz. 1994. The small GTP-binding protein Rho regulates a phosphatidylinositol 4-phosphate 5-kinase in mammalian cells. *Cell.* **79**:507-13.

Chung, C.Y., and R.A. Firtel. 1999. PAKa, a putative PAK family member, is required for cytokinesis and the regulation of the cytoskeleton in Dictyostelium discoideum cells during chemotaxis. *J Cell Biol.* **147**:559-76.

Chung, C.Y., S. Funamoto, and R.A. Firtel. 2001. Signaling pathways controlling cell polarity and chemotaxis. *Trends Biochem Sci.* **26**:557-66.

Clement, S., U. Krause, F. Desmedt, J.-F. Tanti, J. Behrends, X. Pesesse, T. Sasaki, J. Penninger, M. Doherty, W. Malaisse, J.E. Dumont, Y. Le Marchand-Brustel, C. Erneux, L. Hue, and S. Schurmans. 2001. The lipid phosphatase SHIP2 controls insulin sensitivity. *Nature.* **409**:92-97.

Comer, F.I., and C.A. Parent. 2002. PI 3-kinases and PTEN: how opposites chemoattract. *Cell.* **109**:541-4.

Connolly, T.M., W.J. Lawing, Jr., and P.W. Majerus. 1986. Protein kinase C phosphorylates human platelet inositol trisphosphate 5'-phosphomonoesterase, increasing the phosphatase activity. *Cell.* **46**:951-8.

Cooke, F.T., S.K. Dove, R.K. McEwen, G. Painter, A.B. Holmes, M.N. Hall, R.H. Michell, and P.J. Parker. 1998. The stress-activated phosphatidylinositol 3-phosphate 5-kinase Fab1p is essential for vacuole function in S. cerevisiae. *Curr Biol.* **8**:1219-22.

Corvera, S., A. D'Arrigo, and H. Stenmark. 1999. Phosphoinositides in membrane traffic. *Curr Opin Cell Biol.* 11:460-5.

Cremona, O., G. Di Paolo, M.R. Wenk, A. Luthi, W.T. Kim, K. Takei, L. Daniell, Y. Nemoto, S.B. Shears, R.A. Flavell, D.A. McCormick, and P. De Camilli. 1999. Essential role of phosphoinositide metabolism in synaptic vesicle recycling. *Cell.* **99**:179-88.

Critchley, D.R. 2000. Focal adhesions - the cytoskeletal connection. *Curr Opin Cell Biol.* **12**:133-9.

Cunningham, C.C., J.B. Gorlin, D.J. Kwiatkowski, J.H. Hartwig, P.A. Janmey, H.R. Byers, and T.P. Stossel. 1992. Actin-binding protein requirement for cortical stability and efficient locomotion. *Science.* **255**:325-7.

Cunningham, J.G., S.C. Meyer, and J.E. Fox. 1996. The cytoplasmic domain of the alpha-subunit of glycoprotein (GP) Ib mediates attachment of the entire GP Ib-IX complex to the cytoskeleton and regulates von Willebrand factor-induced changes in cell morphology.PG - 11581-7. *J Biol Chem.* **271**:11581-7.

Damen, J.E., L. Liu, P. Rosten, R.K. Humphries, A.B. Jefferson, P.W. Majerus, and G. Krystal. 1996. The 145-kDa protein induced to associate with Shc by multiple

cytokines is an inositol tetraphosphate and phosphatidylinositol 3,4,5-triphosphate 5-phosphatase. *Proc Natl Acad Sci U S A*. **93**:1689-93.

Damen, J.E., L. Liu, M.D. Ware, M. Ermolaeva, P.W. Majerus, and G. Krystal. 1998. Multiple forms of the SH2-containing inositol phosphatase, SHIP, are generated by C-terminal truncation. *Blood*. **92**:1199-205.

Damen, J.E., M.D. Ware, J. Kalesnikoff, M.R. Hughes, and G. Krystal. 2001. SHIP's C-terminus is essential for its hydrolysis of PIP(3) and inhibition of mast cell degranulation. *Blood*. **97**:1343-1351.

Datta, S.R., A. Brunet, and M.E. Greenberg. 1999. Cellular survival: a play in three Akts. *Genes Dev*. **13**:2905-27.

Davies, P.J., D. Wallach, M.C. Willingham, I. Pastan, M. Yamaguchi, and R.M. Robson. 1978. Filamin-actin interaction. Dissociation of binding from gelation by Ca2+-activated proteolysis.PG - 4036-42. *J Biol Chem*. **253**:4036-42.

De Camilli, P., S.D. Emr, P.S. McPherson, and P. Novick. 1996. Phosphoinositides as regulators in membrane traffic. *Science*. **271**:1533-9.

De Smedt, F., A. Boom, X. Pesesse, S.N. Schiffmann, and C. Erneux. 1996. Post-translational modification of human brain type I inositol-1,4,5-trisphosphate 5-phosphatase by farnesylation. *J Biol Chem*. **271**:10419-24.

Dekker, L.V., and A.W. Segal. 2000. Perspectives: signal transduction. Signals to move cells. *Science*. **287**:982-3, 985.

Derman, M.P., A. Toker, J.H. Hartwig, K. Spokes, J.R. Falck, C.S. Chen, L.C. Cantley, and L.G. Cantley. 1997. The lipid products of phosphoinositide 3-kinase increase cell motility through protein kinase C. *Journal of Biological Chemistry*. **272**:6465-70.

Domin, J., I. Gaidarov, M.E. Smith, J.H. Keen, and M.D. Waterfield. 2000. The class II phosphoinositide 3-kinase PI3K-C2alpha is concentrated in the trans-Golgi network and present in clathrin-coated vesicles. *J Biol Chem.* **275**:11943-50.

Dove, S.K., F.T. Cooke, M.R. Douglas, L.G. Sayers, P.J. Parker, and R.H. Michell. 1997. Osmotic stress activates phosphatidylinositol-3,5-bisphosphate synthesis. *Nature.* **390**:187-92.

Dowler, S., A.C. R, G.C. D, M. Deak, G. Kular, C.P. Downes, and R.A. D. 2000. Identification of pleckstrin-homology-domain-containing proteins with novel phosphoinositide-binding specificities. *Biochem J.* **351**:19-31.

Dressman, M.A., I.M. Olivos-Glander, R.L. Nussbaum, and S.F. Suchy. 2000. Ocrl1, a PtdIns(4,5)P(2) 5-phosphatase, is localized to the trans-Golgi network of fibroblasts and epithelial cells. *J Histochem Cytochem.* **48**:179-90.

Englund, G.D., R.J. Bodnar, Z. Li, Z.M. Ruggeri, and X. Du. 2001. Regulation of von Willebrand factor binding to the platelet glycoprotein Ib-IX by a membrane skeleton-dependent inside-out signal. *J Biol Chem.* **276**:16952-9.

Erneux, C., F. De Smedt, C. Moreau, M. Rider, and D. Communi. 1995. Production of recombinant human brain type I inositol-1,4,5-trisphosphate 5-phosphatase in Escherichia coli. Lack of phosphorylation by protein kinase C. *Eur J Biochem.* **234**:598-602.

Erneux, C., C. Govaerts, D. Communi, and X. Pesesse. 1998. The diversity and possible functions of the inositol polyphosphate 5-phosphatases. *Biochim Biophys Acta.* **1436**:185-99.

Fawcett, J., and T. Pawson. 2000. Signal transduction. N-WASP regulation--the sting in the tail. *Science.* **290**:725-6.

Fedorov, A.A., E. Fedorov, F. Gertler, and S.C. Almo. 1999. Structure of EVH1, a novel proline-rich ligand-binding module involved in cytoskeletal dynamics and neural function. *Nat Struct Biol.* 6:661-5.

Flanagan, L.A., J. Chou, H. Falet, R. Neujahr, J.H. Hartwig, and T.P. Stossel. 2001. Filamin A, the Arp2/3 complex, and the morphology and function of cortical actin filaments in human melanoma cells. *J Cell Biol.* **155**:511-7.

Fleming, I.N., A. Gray, and C.P. Downes. 2000. Regulation of the Rac1-specific exchange factor Tiam1 involves both phosphoinositide 3-kinase-dependent and -independent components. *Biochem J.* **351**:173-82.

Fox, J.A., K. Ung, S.G. Tanlimco, and F.R. Jirik. 2002. Disruption of a single Pten allele augments the chemotactic response of B lymphocytes to stromal cell-derived factor-1. *J Immunol.* **169**:49-54.

Fox, J.E. 1985. Identification of actin-binding protein as the protein linking the membrane skeleton to glycoproteins on platelet plasma membranes. *J Biol Chem.* **260**:11970-7.

Franke, T.F., D.R. Kaplan, L.C. Cantley, and A. Toker. 1997. Direct regulation of the Akt proto-oncogene product by phosphatidylinositol-3,4-bisphosphate. *Science.* **275**:665-8.

Fruman, D.A., R.E. Meyers, and L.C. Cantley. 1998. Phosphoinositide kinases. *Annu Rev Biochem.* **67**:481-507.

Fry, M.J. 1994. Structure, regulation and function of phosphoinositide 3-kinases. *Biochim Biophys Acta.* **1226**:237-68.

Funamoto, S., R. Meili, S. Lee, L. Parry, and R.A. Firtel. 2002. Spatial and temporal regulation of 3-phosphoinositides by PI 3-kinase and PTEN mediates chemotaxis. *Cell.* **109**:611-23.

Funamoto, S., K. Milan, R. Meili, and R.A. Firtel. 2001. Role of phosphatidylinositol 3' kinase and a downstream pleckstrin homology domain-containing protein in controlling chemotaxis in dictyostelium. *J Cell Biol.* **153**:795-810.

Furuhashi, K., M. Inagaki, S. Hatano, K. Fukami, and T. Takenawa. 1992. Inositol phospholipid-induced suppression of F-actin-gelating activity of smooth muscle filamin.PG - 1261-5. *Biochem Biophys Res Commun.* **184**:1261-5.

Gaidarov, I., M.E. Smith, J. Domin, and J.H. Keen. 2001. The class II phosphoinositide 3-kinase C2alpha is activated by clathrin and regulates clathrin-mediated membrane trafficking. *Mol Cell.* 7:443-9.

Geier, S.J., P.A. Algate, K. Carlberg, D. Flowers, C. Friedman, B. Trask, and L.R. Rohrschneider. 1997. The human SHIP gene is differentially expressed in cell lineages of the bone marrow and blood. *Blood.* **89**:1876-85.

Gillooly, D.J., and H. Stenmark. 2001. Cell biology. A lipid oils the endocytosis machine. *Science.* **291**:993-4.

Giuriato, S., B. Payrastre, A.L. Drayer, M. Plantavid, R. Woscholski, P. Parker, C. Erneux, and H. Chap. 1997. Tyrosine phosphorylation and relocation of SHIP are integrin-mediated in thrombin-stimulated human blood platelets. *J Biol Chem.* **272**:26857-63.

Gorlin, J.B., R. Yamin, S. Egan, M. Stewart, T.P. Stossel, D.J. Kwiatkowski, and J.H. Hartwig. 1990. Human endothelial actin-binding protein (ABP-280, nonmuscle filamin): a molecular leaf spring. *J Cell Biol.* **111**:1089-105.

Gu, J., M. Tamura, R. Pankov, E.H. Danen, T. Takino, K. Matsumoto, and K.M. Yamada. 1999. Shc and FAK differentially regulate cell motility and directionality modulated by PTEN. *J Cell Biol.* **146**:389-403.

Guo, S., L.E. Stolz, S.M. Lemrow, and J.D. York. 1999. SAC1-like domains of yeast SAC1, INP52, and INP53 and of human synaptojanin encode polyphosphoinositide phosphatases. *J Biol Chem*. **274**:12990-5.

Gupta, N., A.M. Scharenberg, D.A. Fruman, L.C. Cantley, J.P. Kinet, and E.O. Long. 1999. The SH2 domain-containing inositol 5'-phosphatase (SHIP) recruits the p85 subunit of phosphoinositide 3-kinase during FcgammaRIIb1-mediated inhibition of B cell receptor signaling. *J Biol Chem*. **274**:7489-94.

Habib, T., J.A. Hejna, R.E. Moses, and S.J. Decker. 1998. Growth factors and insulin stimulate tyrosine phosphorylation of the 51C/SHIP2 protein. *J Biol Chem*. **273**:18605-9.

Haffner, C., G.D. Paolo, J.A. Rosenthal, and P. de Camilli. 2000. Direct interaction of the 170 kDa isoform of synaptojanin 1 with clathrin and with the clathrin adaptor AP-2. *Curr Biol*. **10**:471-4.

Haffner, C., K. Takei, H. Chen, N. Ringstad, A. Hudson, M.H. Butler, A.E. Salcini, P.P. Di Fiore, and P. De Camilli. 1997. Synaptojanin 1: localization on coated endocytic intermediates in nerve terminals and interaction of its 170 kDa isoform with Eps15. *FEBS Lett*. **419**:175-80.

Han, J., K. Luby-Phelps, B. Das, X. Shu, Y. Xia, R.D. Mosteller, U.M. Krishna, J.R. Falck, M.A. White, and D. Broek. 1998. Role of substrates and products of PI 3-kinase in regulating activation of Rac-related guanosine triphosphatases by Vav. *Science*. **279**:558-60.

Harmer, S.L., and A.L. DeFranco. 1999. The src homology domain 2-containing inositol phosphatase SHIP forms a ternary complex with Shc and Grb2 in antigen receptor-stimulated B lymphocytes. *J Biol Chem*. **274**:12183-91.

Harris, T.W., E. Hartwieg, H.R. Horvitz, and E.M. Jorgensen. 2000. Mutations in synaptojanin disrupt synaptic vesicle recycling. *J Cell Biol.* **150**:589-600.

Harrison, P.T., W. Davis, J.C. Norman, A.R. Hockaday, and J.M. Allen. 1994. Binding of monomeric immunoglobulin G triggers Fc gamma RI-mediated endocytosis. *J Biol Chem.* **269**:24396-402.

Hartwig, J.H. 1992. Mechanisms of actin rearrangements mediating platelet activation. *J Cell Biol.* **118**:1421-42.

Hartwig, J.H., K.A. Chambers, and T.P. Stossel. 1989. Association of gelsolin with actin filaments and cell membranes of macrophages and platelets. *J Cell Biol.* **108**:467-79.

Hartwig, J.H., and P. Shevlin. 1986. The architecture of actin filaments and the ultrastructural location of actin-binding protein in the periphery of lung macrophages. *J Cell Biol.* **103**:1007-20.

Hawkins, P.T., A. Eguinoa, R.G. Qiu, D. Stokoe, F.T. Cooke, R. Walters, S. Wennstrom, L. Claesson-Welsh, T. Evans, M. Symons, and et al. 1995. PDGF stimulates an increase in GTP-Rac via activation of phosphoinositide 3-kinase. *Curr Biol.* **5**:393-403.

He, X., Y. Li, J. Schembri-King, S. Jakes, and J. Hayashi. 2000. Identification of actin binding protein, ABP-280, as a binding partner of human Lnk adaptor protein. *Mol Immunol.* **37**:603-12.

Hejna, J.A., H. Saito, L.S. Merkens, T.V. Tittle, P.M. Jakobs, M.A. Whitney, M. Grompe, A.S. Friedberg, and R.E. Moses. 1995. Cloning and characterization of a human cDNA (INPPL1) sharing homology with inositol polyphosphate phosphatases. *Genomics.* **29**:285-7.

Helgason, C.D., J.E. Damen, P. Rosten, R. Grewal, P. Sorensen, S.M. Chappel, A. Borowski, F. Jirik, G. Krystal, and R.K. Humphries. 1998. Targeted disruption of SHIP leads to hemopoietic perturbations, lung pathology, and a shortened life span. *Genes Dev.* **12**:1610-20.

Heller-Harrison, R.A., M. Morin, A. Guilherme, and M.P. Czech. 1996. Insulin-mediated targeting of phosphatidylinositol 3-kinase to GLUT4-containing vesicles. *J Biol Chem.* **271**:10200-4.

Herman, P.K., and S.D. Emr. 1990. Characterization of VPS34, a gene required for vacuolar protein sorting and vacuole segregation in Saccharomyces cerevisiae. *Mol Cell Biol.* **10**:6742-54.

Hermosura, M.C., H. Takeuchi, A. Fleig, A.M. Riley, B.V. Potter, M. Hirata, and R. Penner. 2000. InsP4 facilitates store-operated calcium influx by inhibition of InsP3 5-phosphatase. *Nature.* **408**:735-40.

Hilgemann, D.W., and R. Ball. 1996. Regulation of cardiac Na+,Ca2+ exchange and KATP potassium channels by PIP2. *Science.* **273**:956-9.

Hinchliffe, K.A. 2001. Cellular signalling: stressing the importance of PIP3. *Curr Biol.* **11**:R371-2.

Hirsch, E., V.L. Katanaev, C. Garlanda, O. Azzolino, L. Pirola, L. Silengo, S. Sozzani, A. Mantovani, F. Altruda, and M.P. Wymann. 2000a. Central role for G protein-coupled phosphoinositide 3-kinase gamma in inflammation. *Science.* **287**:1049-53.

Hirsch, E., M.P. Wymann, E. Patrucco, E. Tolosano, G. Bulgarelli-Leva, S. Marengo, M. Rocchi, and F. Altruda. 2000b. Analysis of the murine phosphoinositide 3-kinase gamma gene. *Gene.* **256**:69-81.

Hock, R.S., G. Davis, and D.W. Speicher. 1990. Purification of human smooth muscle filamin and characterization of structural domains and functional sites.PG - 9441-51. *Biochemistry*. **29**:9441-51.

Honda, A., M. Nogami, T. Yokozeki, M. Yamazaki, H. Nakamura, H. Watanabe, K. Kawamoto, K. Nakayama, A.J. Morris, M.A. Frohman, and Y. Kanaho. 1999. Phosphatidylinositol 4-phosphate 5-kinase alpha is a downstream effector of the small G protein ARF6 in membrane ruffle formation. *Cell*. **99**:521-32.

Howell, B.W., L.M. Lanier, R. Frank, F.B. Gertler, and J.A. Cooper. 1999. The disabled 1 phosphotyrosine-binding domain binds to the internalization signals of transmembrane glycoproteins and to phospholipids. *Mol Cell Biol*. **19**:5179-88.

Huber, M., C.D. Helgason, J.E. Damen, L. Liu, R.K. Humphries, and G. Krystal. 1998a. The src homology 2-containing inositol phosphatase (SHIP) is the gatekeeper of mast cell degranulation. *Proc Natl Acad Sci U S A*. **95**:11330-5.

Huber, M., C.D. Helgason, J.E. Damen, M.P. Scheid, V. Duronio, V. Lam, R.K. Humphries, and G. Krystal. 1999. The role of the SRC homology 2-containing inositol 5'-phosphatase in Fc epsilon R1-induced signaling. *Curr Top Microbiol Immunol*. **244**:29-41.

Huber, M., C.D. Helgason, M.P. Scheid, V. Duronio, R.K. Humphries, and G. Krystal. 1998b. Targeted disruption of SHIP leads to Steel factor-induced degranulation of mast cells. *Embo J*. **17**:7311-9.

Hughes, W.E., F.T. Cooke, and P.J. Parker. 2000a. Sac phosphatase domain proteins. *Biochem J*. **350**:337-352.

Hughes, W.E., R. Woscholski, F.T. Cooke, R.S. Patrick, S.K. Dove, N.Q. McDonald, and P.J. Parker. 2000b. SAC1 encodes a regulated lipid phosphoinositide phosphatase,

defects in which can be suppressed by the homologous Inp52p and Inp53p phosphatases. *J Biol Chem*. **275**:801-8.

Hynes, R.O. 1992. Integrins: versatility, modulation, and signaling in cell adhesion. *Cell*. **69**:11-25.

Iijima, M., and P. Devreotes. 2002. Tumor suppressor PTEN mediates sensing of chemoattractant gradients. *Cell*. **109**:599-610.

Iijima, M., Y.E. Huang, and P. Devreotes. 2002. Temporal and spatial regulation of chemotaxis Tumor suppressor PTEN mediates sensing of chemoattractant gradients. *Dev Cell*. **3**:469-78.

Ijuin, T., Y. Mochizuki, K. Fukami, M. Funaki, T. Asano, and T. Takenawa. 2000. Identification and characterization of a novel inositol polyphosphate 5-phosphatase. *J Biol Chem*. **275**:10870-5.

Ingham, R.J., H. Okada, M. Dang-Lawson, J. Dinglasan, P. van Der Geer, T. Kurosaki, and M.R. Gold. 1999. Tyrosine phosphorylation of shc in response to B cell antigen receptor engagement depends on the SHIP inositol phosphatase. *J Immunol*. **163**:5891-5.

Insall, R.H., and O.D. Weiner. 2001. PIP3, PIP2, and cell movement--similar messages, different meanings? *Dev Cell*. **1**:743-7.

Ishihara, H., T. Sasaoka, H. Hori, T. Wada, H. Hirai, T. Haruta, W.J. Langlois, and M. Kobayashi. 1999. Molecular cloning of rat SH2-containing inositol phosphatase 2 (SHIP2) and its role in the regulation of insulin signaling. *Biochem Biophys Res Commun*. **260**:265-72.

Ishihara, H., T. Sasaoka, M. Ishiki, T. Wada, H. Hori, S. Kagawa, M. Kobayashi, Y. Choi, J. Zhang, C. Murga, H. Yu, E. Koller, B.P. Monia, J.S. Gutkind, W. Li, M. Funaki, S. Murakami, T. Haruta, T. Asano, W. Ogawa, H. Hirai, W.J. Langlois, T. Habib,

J.A. Hejna, R.E. Moses, and S.J. Decker. 2002. Membrane localization of Src homology 2-containing inositol 5'-phosphatase 2 via Shc association is required for the negative regulation of insulin signaling in Rat1 fibroblasts overexpressing insulin receptors

Itoh, T., and T. Takenawa. 2002. Phosphoinositide-binding domains. Functional units for temporal and spatial regulation of intracellular signalling. *Cell Signal.* **14**:733-43.

Jackson, S.P., N. Mistry, and Y. Yuan. 2000. Platelets and the injured vessel wall--"rolling into action": focus on glycoprotein Ib/V/IX and the platelet cytoskeleton.PG - 192-7. *Trends Cardiovasc Med.* **10**:192-7.

Jackson, S.P., S.M. Schoenwaelder, M. Matzaris, S. Brown, and C.A. Mitchell. 1995. Phosphatidylinositol 3,4,5-trisphosphate is a substrate for the 75 kDa inositol polyphosphate 5-phosphatase and a novel 5-phosphatase which forms a complex with the p85/p110 form of phosphoinositide 3-kinase. *Embo J.* **14**:4490-500.

Jackson, S.P., S.M. Schoenwaelder, Y. Yuan, I. Rabinowitz, H.H. Salem, and C.A. Mitchell. 1994. Adhesion receptor activation of phosphatidylinositol 3-kinase. von Willebrand factor stimulates the cytoskeletal association and activation of phosphatidylinositol 3-kinase and pp60c-src in human platelets. *J Biol Chem.* **269**:27093-9.

Janmey, P.A. 1994. Phosphoinositides and calcium as regulators of cellular actin assembly and disassembly. *Annu Rev Physiol.* **56**:169-91.

Janmey, P.A., W. Xian, and L.A. Flanagan. 1999. Controlling cytoskeleton structure by phosphoinositide-protein interactions: phosphoinositide binding protein domains and effects of lipid packing. *Chem Phys Lipids.* **101**:93-107.

Janne, P.A., S.F. Suchy, D. Bernard, M. MacDonald, J. Crawley, A. Grinberg, A. Wynshaw-Boris, H. Westphal, and R.L. Nussbaum. 1998. Functional overlap

between murine Inpp5b and Ocrl1 may explain why deficiency of the murine orthiolog for OCRL1 does not cause Lowe syndrome in mice. *J Clin Invest.* **101**:2042-53.

Jefferson, A.B., V. Auethavekiat, D.A. Pot, L.T. Williams, and P.W. Majerus. 1997. Signaling inositol polyphosphate-5-phosphatase. Characterization of activity and effect of GRB2 association. *J Biol Chem.* **272**:5983-8.

Jefferson, A.B., and P.W. Majerus. 1995. Properties of type II inositol polyphosphate 5-phosphatase. *J Biol Chem.* **270**:9370-7.

Jess, T.J., C.M. Belham, F.J. Thomson, P.H. Scott, R.J. Plevin, and G.W. Gould. 1996. Phosphatidylinositol 3'-kinase, but not p70 ribosomal S6 kinase, is involved in membrane protein recycling: wortmannin inhibits glucose transport and downregulates cell-surface transferrin receptor numbers independently of any effect on fluid-phase endocytosis in fibroblasts. *Cell Signal.* **8**:297-304.

Jones, D.R., A. Gonzalez-Garcia, E. Diez, A.C. Martinez, A.C. Carrera, and I. Merida. 1999. The identification of phosphatidylinositol 3,5-bisphosphate in T-lymphocytes and its regulation by interleukin-2. *J Biol Chem.* **274**:18407-13.

Kalesnikoff, J., V. Lam, and G. Krystal. 2002. SHIP represses mast cell activation and reveals that IgE alone triggers signaling pathways which enhance normal mast cell survival. *Mol Immunol.* **38**:1201.

Kavanaugh, W.M., D.A. Pot, S.M. Chin, M. Deuter-Reinhard, A.B. Jefferson, F.A. Norris, F.R. Masiarz, L.S. Cousens, P.W. Majerus, and L.T. Williams. 1996. Multiple forms of an inositol polyphosphate 5-phosphatase form signaling complexes with Shc and Grb2. *Curr Biol.* **6**:438-45.

Khan, A.H., D.C. Thurmond, C. Yang, B.P. Ceresa, and J.E. Pessin. 2000. Munc18c regulates insulin-stimulated GLUT4 translocation to the transverse tubules in skeletal muscle. *J Biol Chem*. **38**:12.

Khayat, Z.A., P. Tong, K. Yaworsky, R.J. Bloch, and A. Klip. 2000. Insulin-induced actin filament remodeling colocalizes actin with phosphatidylinositol 3-kinase and GLUT4 in L6 myotubes. *J Cell Sci*. **113**:279-90.

Khvotchev, M., and T.C. Sudhof. 1998. Developmentally regulated alternative splicing in a novel synaptojanin. *J Biol Chem*. **273**:2306-11.

Kiener, P.A., M.N. Lioubin, L.R. Rohrschneider, J.A. Ledbetter, S.G. Nadler, and M.L. Diegel. 1997. Co-ligation of the antigen and Fc receptors gives rise to the selective modulation of intracellular signaling in B cells. Regulation of the association of phosphatidylinositol 3-kinase and inositol 5'-phosphatase with the antigen receptor complex. *J Biol Chem*. **272**:3838-44.

Kimura, T., H. Sakamoto, E. Appella, and R.P. Siraganian. 1997. The negative signaling molecule SH2 domai"-containing inositol-polyphosphate 5-phosphatase (SHIP) binds to the tyrosine-phosphorylated beta subunit of the high affinity IgE receptor. *J Biol Chem*. **272**:13991-6.

Kisseleva, M.V., L. Cao, and P.W. Majerus. 2002. Phosphoinositide-specific inositol polyphosphate 5-phosphatase IV inhibits Akt/protein kinase B phosphorylation and leads to apoptotic cell death. *J Biol Chem*. **277**:6266-72.

Kisseleva, M.V., M.P. Wilson, and P.W. Majerus. 2000. The isolation and characterization of a cDNA encoding phospholipid-specific inositol polyphosphate 5-phosphatase. *J Biol Chem*. **275**:20110-6.

Klarlund, J.K., A. Guilherme, J.J. Holik, J.V. Virbasius, A. Chawla, and M.P. Czech. 1997. Signaling by phosphoinositide-3,4,5-trisphosphate through proteins containing pleckstrin and Sec7 homology domains [see comments]. *Science.* **275**:1927-30.

Klippel, A., W.M. Kavanaugh, D. Pot, and L.T. Williams. 1997. A specific product of phosphatidylinositol 3-kinase directly activates the protein kinase Akt through its pleckstrin homology domain. *Mol Cell Biol.* **17**:338-44.

Kong, A.M., C.J. Speed, C.J. O'Malley, M.J. Layton, T. Meehan, K.L. Loveland, S. Cheema, L.M. Ooms, and C.A. Mitchell. 2000. Cloning and characterization of a 72-kDa inositol-polyphosphate 5-phosphatase localized to the Golgi network. *J Biol Chem.* **275**:24052-64.

Kotani, K., A.J. Carozzi, H. Sakaue, K. Hara, L.J. Robinson, S.F. Clark, K. Yonezawa, D.E. James, and M. Kasuga. 1995. Requirement for phosphoinositide 3-kinase in insulin-stimulated GLUT4 translocation in 3T3-L1 adipocytes. *Biochem Biophys Res Commun.* **209**:343-8.

Kovacsovics, T.J., and J.H. Hartwig. 1996. Thrombin-induced GPIb-IX centralization on the platelet surface requires actin assembly and myosin II activation. *Blood.* **87**:618-29.

Kuroiwa, A., Y. Yamashita, M. Inui, T. Yuasa, M. Ono, A. Nagabukuro, Y. Matsuda, and T. Takai. 1998. Association of tyrosine phosphatases SHP-1 and SHP-2, inositol 5-phosphatase SHIP with gp49B1, and chromosomal assignment of the gene. *J Biol Chem.* **273**:1070-4.

Layton, M.J., A.G. Harpur, G. Panayotou, P.I. Bastiaens, and M.D. Waterfield. 1998. Binding of a diphosphotyrosine-containing peptide that mimics activated platelet-derived growth factor receptor beta induces oligomerization of phosphatidylinositol 3-kinase. *J Biol Chem.* **273**:33379-85.

Lecoq-Lafon, C., F. Verdier, S. Fichelson, S. Chretien, S. Gisselbrecht, C. Lacombe, and P. Mayeux. 1999. Erythropoietin induces the tyrosine phosphorylation of GAB1 and its association with SHC, SHP2, SHIP, and phosphatidylinositol 3-kinase. *Blood*. **93**:2578-85.

Lee, J.O., H. Yang, M.M. Georgescu, A. Di Cristofano, T. Maehama, Y. Shi, J.E. Dixon, P. Pandolfi, and N.P. Pavletich. 1999. Crystal structure of the PTEN tumor suppressor: implications for its phosphoinositide phosphatase activity and membrane association. *Cell*. **99**:323-34.

Lemmon, M.A., K.M. Ferguson, and C.S. Abrams. 2002. Pleckstrin homology domains and the cytoskeleton. *FEBS Lett*. **513**:71-6.

Leonardi, A., H. Ellinger-Ziegelbauer, G. Franzoso, K. Brown, and U. Siebenlist. 2000. Physical and functional interaction of filamin (actin-binding protein-280) and tumor necrosis factor receptor-associated factor 2. *J Biol Chem*. **275**:271-8.

Lewis, T.S., P.S. Shapiro, and N.G. Ahn. 1998. Signal transduction through MAP kinase cascades. *Adv Cancer Res*. **74**:49-139.

Li, D.M., and H. Sun. 1997. TEP1, encoded by a candidate tumor suppressor locus, is a novel protein tyrosine phosphatase regulated by transforming growth factor beta. *Cancer Res*. **57**:2124-9.

Li, J., C. Yen, D. Liaw, K. Podsypanina, S. Bose, S.I. Wang, J. Puc, C. Miliaresis, L. Rodgers, R. McCombie, S.H. Bigner, B.C. Giovanella, M. Ittmann, B. Tycko, H. Hibshoosh, M.H. Wigler, and R. Parsons. 1997. PTEN, a putative protein tyrosine phosphatase gene mutated in human brain, breast, and prostate cancer [see comments]. *Science*. **275**:1943-7.

Liliental, J., S.Y. Moon, R. Lesche, R. Mamillapalli, D. Li, Y. Zheng, H. Sun, and H. Wu. 2000. Genetic deletion of the Pten tumor suppressor gene promotes cell motility by activation of Rac1 and Cdc42 GTPases. *Curr Biol.* **10**:401-4.

Lin, R., V. Canfield, and R. Levenson. 2002. Dominant negative mutants of filamin a block cell surface expression of the d2 dopamine receptor. *Pharmacology.* **66**:173-81.

Lioubin, M.N., P.A. Algate, S. Tsai, K. Carlberg, A. Aebersold, and L.R. Rohrschneider. 1996. p150Ship, a signal transduction molecule with inositol polyphosphate-5-phosphatase activity. *Genes Dev.* **10**:1084-95.

Liu, Q., A.J. Oliveira-Dos-Santos, S. Mariathasan, D. Bouchard, J. Jones, R. Sarao, I. Kozieradzki, P.S. Ohashi, J.M. Penninger, and D.J. Dumont. 1998a. The inositol polyphosphate 5-phosphatase ship is a crucial negative regulator of B cell antigen receptor signaling. *J Exp Med.* **188**:1333-42.

Liu, Q., T. Sasaki, I. Kozieradzki, A. Wakeham, A. Itie, D.J. Dumont, and J.M. Penninger. 1999. SHIP is a negative regulator of growth factor receptor-mediated PKB/Akt activation and myeloid cell survival. *Genes Dev.* **13**:786-91.

Liu, Q., F. Shalaby, J. Jones, D. Bouchard, and D.J. Dumont. 1998b. The SH2-containing inositol polyphosphate 5-phosphatase, ship, is expressed during hematopoiesis and spermatogenesis. *Blood.* **91**:2753-9.

Liu, Y., B. Jenkins, J.L. Shin, and L.R. Rohrschneider. 2001. Scaffolding protein gab2 mediates differentiation signaling downstream of fms receptor tyrosine kinase. *Mol Cell Biol.* **21**:3047-56.

Loijens, J.C., and R.A. Anderson. 1996. Type I phosphatidylinositol-4-phosphate 5-kinases are distinct members of this novel lipid kinase family. *J Biol Chem.* **271**:32937-43.

Loo, D.T., S.B. Kanner, and A. Aruffo. 1998. Filamin binds to the cytoplasmic domain of the beta1-integrin. Identification of amino acids responsible for this interaction. *J Biol Chem.* **273**:23304-12.

Lucas, D.M., and L.R. Rohrschneider. 1999. A novel spliced form of SH2-containing inositol phosphatase is expressed during myeloid development. *Blood.* **93**:1922-33.

Luckhoff, A., and D.E. Clapham. 1992. Inositol 1,3,4,5-tetrakisphosphate activates an endothelial Ca(2+)-permeable channel. *Nature.* **355**:356-8.

Luttrell, L.M., Y. Daaka, and R.J. Lefkowitz. 1999. Regulation of tyrosine kinase cascades by G-protein-coupled receptors. *Curr Opin Cell Biol.* **11**:177-83.

Ma, A.D., A. Metjian, S. Bagrodia, S. Taylor, and C.S. Abrams. 1998. Cytoskeletal reorganization by G protein-coupled receptors is dependent on phosphoinositide 3-kinase gamma, a Rac guanosine exchange factor, and Rac. *Mol Cell Biol.* **18**:4744-51.

MacDougall, L.K., J. Domin, and M.D. Waterfield. 1995. A family of phosphoinositide 3-kinases in Drosophila identifies a new mediator of signal transduction. *Curr Biol.* **5**:1404-15.

Maehama, T., and J.E. Dixon. 1998. The tumor suppressor, PTEN/MMAC1, dephosphorylates the lipid second messenger, phosphatidylinositol 3,4,5-trisphosphate. *J Biol Chem.* **273**:13375-8.

Maestrini, E., C. Patrosso, M. Mancini, S. Rivella, M. Rocchi, M. Repetto, A. Villa, A. Frattini, M. Zoppe, P. Vezzoni, and et al. 1993. Mapping of two genes encoding isoforms of the actin binding protein ABP-280, a dystrophin like protein, to Xq28 and to chromosome 7. *Hum Mol Genet.* **2**:761-6.

Maghazachi, A.A. 2000. Intracellular signaling events at the leading edge of migrating cells. *Int J Biochem Cell Biol.* **32**:931-43.

Majerus, P.W. 1996. Inositols do it all. *Genes Dev.* **10**:1051-3.

Majerus, P.W., M.V. Kisseleva, and F.A. Norris. 1999. The role of phosphatases in inositol signaling reactions. *J Biol Chem.* **274**:10669-72.

Malecz, N., P.C. McCabe, C. Spaargaren, R. Qiu, Y. Chuang, and M. Symons. 2000. Synaptojanin 2, a novel rac1 effector that regulates clathrin-mediated endocytosis. *Curr Biol.* **10**:1383-6.

Marino, S., P. Krimpenfort, C. Leung, H.A. van der Korput, J. Trapman, I. Camenisch, A. Berns, and S. Brandner. 2002. PTEN is essential for cell migration but not for fate determination and tumourigenesis in the cerebellum. *Development.* **129**:3513-22.

Marti, A., Z. Luo, C. Cunningham, Y. Ohta, J. Hartwig, T.P. Stossel, J.M. Kyriakis, and J. Avruch. 1997. Actin-binding protein-280 binds the stress-activated protein kinase (SAPK) activator SEK-1 and is required for tumor necrosis factor-alpha activation of SAPK in melanoma cells. *J Biol Chem.* **272**:2620-8.

Martin, T.F. 1997. Phosphoinositides as spatial regulators of membrane traffic. *Curr Opin Neurobiol.* **7**:331-8.

Martin, T.F. 1998. Phosphoinositide lipids as signaling molecules: common themes for signal transduction, cytoskeletal regulation, and membrane trafficking. *Annu Rev Cell Dev Biol.* **14**:231-64.

Matzaris, M., S.P. Jackson, K.M. Laxminarayan, C.J. Speed, and C.A. Mitchell. 1994. Identification and characterization of the phosphatidylinositol-(4, 5)-bisphosphate 5-phosphatase in human platelets. *J Biol Chem.* **269**:3397-402.

Matzaris, M., C.J. O'Malley, A. Badger, C.J. Speed, P.I. Bird, and C.A. Mitchell. 1998. Distinct membrane and cytosolic forms of inositol polyphosphate 5-phosphatase II. Efficient membrane localization requires two discrete domains. *J Biol Chem.* **273**:8256-67.

McPherson, P.S., E.P. Garcia, V.I. Slepnev, C. David, X. Zhang, D. Grabs, W.S. Sossin, R. Bauerfeind, Y. Nemoto, and P. De Camilli. 1996. A presynaptic inositol-5-phosphatase. *Nature*. **379**:353-7.

Meier, R., D.R. Alessi, P. Cron, M. Andjelkovic, and B.A. Hemmings. 1997. Mitogenic activation, phosphorylation, and nuclear translocation of protein kinase Bbeta. *J Biol Chem*. **272**:30491-7.

Meili, R., C. Ellsworth, S. Lee, T.B. Reddy, H. Ma, and R.A. Firtel. 1999. Chemoattractant-mediated transient activation and membrane localization of Akt/PKB is required for efficient chemotaxis to cAMP in Dictyostelium. *Embo J.* **18**:2092-105.

Mejean, C., M.C. Lebart, M. Boyer, C. Roustan, and Y. Benyamin. 1992. Localization and identification of actin structures involved in the filamin-actin interaction.PG - 555-62. *Eur J Biochem*. **209**:555-62.

Meyer, S.C., S. Zuerbig, C.C. Cunningham, J.H. Hartwig, T. Bissell, K. Gardner, and J.E. Fox. 1997. Identification of the region in actin-binding protein that binds to the cytoplasmic domain of glycoprotein IBalpha. *J Biol Chem*. **272**:2914-9.

Minagawa, T., T. Ijuin, Y. Mochizuki, and T. Takenawa. 2001. Identification and characterization of a sac domain-containing phosphoinositide 5-phosphatase. *J Biol Chem*. **276**:22011-5.

Mitchell, C.A., S. Brown, J.K. Campbell, A.D. Munday, and C.J. Speed. 1996. Regulation of second messengers by the inositol polyphosphate 5-phosphatases. *Biochem Soc Trans*. **24**:994-1000.

Miura, K., K.M. Jacques, S. Stauffer, A. Kubosaki, K. Zhu, D.S. Hirsch, J. Resau, Y. Zheng, and P.A. Randazzo. 2002. ARAP1: a point of convergence for Arf and Rho signaling. *Mol Cell*. **9**:109-19.

Mochizuki, Y., and T. Takenawa. 1999. Novel inositol polyphosphate 5-phosphatase localizes at membrane ruffles. *J Biol Chem.* **274**:36790-5.

Munday, A.D., M.C. Berndt, and C.A. Mitchell. 2000. Phosphoinositide 3-kinase forms a complex with platelet membrane glycoprotein Ib-IX-V complex and 14-3-3zeta. *Blood.* **96**:577-84.

Muraille, E., D. Dassesse, J.M. Vanderwinden, H. Cremer, B. Rogister, C. Erneux, and S.N. Schiffmann. 2001. The SH2 domain-containing 5-phosphatase SHIP2 is expressed in the germinal layers of embryo and adult mouse brain: increased expression in N-CAM-deficient mice. *Neuroscience.* **105**:1019-30.

Muraille, E., X. Pesesse, C. Kuntz, and C. Erneux. 1999. Distribution of the src-homology-2-domain-containing inositol 5-phosphatase SHIP-2 in both non-haemopoietic and haemopoietic cells and possible involvement of SHIP-2 in negative signalling of B-cells. *Biochem J.* **342**:697-705.

Myers, M.P., I. Pass, I.H. Batty, J. Van der Kaay, J.P. Stolarov, B.A. Hemmings, M.H. Wigler, C.P. Downes, and N.K. Tonks. 1998. The lipid phosphatase activity of PTEN is critical for its tumor supressor function. *Proc Natl Acad Sci U S A.* **95**:13513-8.

Nemoto, Y., and P. De Camilli. 1999. Recruitment of an alternatively spliced form of synaptojanin 2 to mitochondria by the interaction with the PDZ domain of a mitochondrial outer membrane protein. *Embo J.* **18**:2991-3006.

Nemoto, Y., B.G. Kearns, M.R. Wenk, H. Chen, K. Mori, J.G. Alb, Jr., P. De Camilli, and V.A. Bankaitis. 2000. Functional characterization of a mammalian Sac1 and mutant exhibiting substrate-specific defects in phosphoinositide phosphatase activity. *J Biol Chem.* **275**:34293-305.

Niggli, V. 2000. A membrane-permeant ester of phosphatidylinositol 3,4, 5-trisphosphate (PIP(3)) is an activator of human neutrophil migration. *FEBS Lett.* **473**:217-21.

Niggli, V., and H. Keller. 1997. The phosphatidylinositol 3-kinase inhibitor wortmannin markedly reduces chemotactic peptide-induced locomotion and increases in cytoskeletal actin in human neutrophils. *Eur J Pharmacol.* **335**:43-52.

Nikki, M., J. Merilainen, and V.P. Lehto. 2002. FAP52 regulates actin organization via binding to filamin. *J Biol Chem.* **277**:11432-40.

Nimnual, A.S., B.A. Yatsula, and D. Bar-Sagi. 1998. Coupling of Ras and Rac guanosine triphosphatases through the Ras exchanger Sos. *Science.* **279**:560-3.

Obergfell, A., K. Eto, A. Mocsai, C. Buensuceso, S.L. Moores, J.S. Brugge, C.A. Lowell, and S.J. Shattil. 2002. Coordinate interactions of Csk, Src, and Syk kinases with [alpha]IIb[beta]3 initiate integrin signaling to the cytoskeleton.PG - 265-75. *J Cell Biol.* **157**:265-75.

Odorizzi, G., M. Babst, and S.D. Emr. 2000. Phosphoinositide signaling and the regulation of membrane trafficking in yeast. *Trends Biochem Sci.* **25**:229-35.

Ohta, Y., N. Suzuki, S. Nakamura, J.H. Hartwig, and T.P. Stossel. 1999. The small GTPase RalA targets filamin to induce filopodia. *Proc Natl Acad Sci U S A.* **96**:2122-8.

Ono, M., S. Bolland, P. Tempst, and J.V. Ravetch. 1996. Role of the inositol phosphatase SHIP in negative regulation of the immune system by the receptor Fc(gamma)RIIB. *Nature.* **383**:263-6.

Ooms, L.M., B.K. McColl, F. Wiradjaja, A.P. Wijayaratnam, P. Gleeson, M.J. Gething, J. Sambrook, and C.A. Mitchell. 2000. The yeast inositol polyphosphate 5-phosphatases inp52p and inp53p translocate to actin patches following hyperosmotic stress: mechanism for regulating phosphatidylinositol 4,5-bisphosphate at plasma membrane invaginations. *Mol Cell Biol.* **20**:9376-90.

Osborne, M.A., G. Zenner, M. Lubinus, X. Zhang, Z. Songyang, L.C. Cantley, P. Majerus, P. Burn, and J.P. Kochan. 1996. The inositol 5'-phosphatase SHIP binds to immunoreceptor signaling motifs and responds to high affinity IgE receptor aggregation. *J Biol Chem.* **271**:29271-8.

Panaretou, C., J. Domin, S. Cockcroft, and M.D. Waterfield. 1997. Characterization of p150, an adaptor protein for the human phosphatidylinositol (PtdIns) 3-kinase. Substrate presentation by phosphatidylinositol transfer protein to the p150.Ptdins 3-kinase complex. *J Biol Chem.* **272**:2477-85.

Paranavitane, V., W.J. Coadwell, A. Eguinoa, P.T. Hawkins, and L. Stephens. 2002. LL5beta is a PtdIns(3,4,5)P3-sensor that can bind the cytoskeletal adaptor,gamma filamin. *J Biol Chem.* **9**:9.

Pesesse, X., S. Deleu, F. De Smedt, L. Drayer, and C. Erneux. 1997. Identification of a second SH2-domain-containing protein closely related to the phosphatidylinositol polyphosphate 5-phosphatase SHIP. *Biochem Biophys Res Commun.* **239**:697-700.

Pesesse, X., V. Dewaste, F. De Smedt, M. Laffargue, S. Giuriato, C. Moreau, B. Payrastre, and C. Erneux. 2001. The src homology 2 domain containing inositol 5-phosphatase ship2 is recruited to the epidermal growth factor (egf) receptor and dephosphorylates phosphatidylinositol 3,4,5-trisphosphate in egf-stimulated cos-7 cells. *J Biol Chem.* **276**:28348-55.

Pesesse, X., C. Moreau, A.L. Drayer, R. Woscholski, P. Parker, and C. Erneux. 1998. The SH2 domain containing inositol 5-phosphatase SHIP2 displays phosphatidylinositol 3,4,5-trisphosphate and inositol 1,3,4,5-tetrakisphosphate 5-phosphatase activity. *FEBS Lett.* **437**:301-3.

Pfaff, M., S. Liu, D.J. Erle, and M.H. Ginsberg. 1998. Integrin beta cytoplasmic domains differentially bind to cytoskeletal proteins.PG - 6104-9. *J Biol Chem.* **273**:6104-9.

Phee, H., A. Jacob, and K.M. Coggeshall. 2000. Enzymatic activity of the src homology 2 domain-containing inositol phosphatase is regulated by a plasma membrane location [In Process Citation]. *J Biol Chem*. **275**:19090-7.

Pike, L.J., and L. Casey. 1996. Localization and turnover of phosphatidylinositol 4,5-bisphosphate in caveolin-enriched membrane domains. *J Biol Chem*. **271**:26453-6.

Pollard, T.D., and J.A. Cooper. 1986. Actin and actin-binding proteins. A critical evaluation of mechanisms and functions.PG - 987-1035. *Annu Rev Biochem*. **55**:987-1035.

Prasad, N., R.S. Topping, and S.J. Decker. 2001. SH2-Containing Inositol 5'-Phosphatase SHIP2 Associates with the p130(Cas) Adapter Protein and Regulates Cellular Adhesion and Spreading. *Mol Cell Biol*. **21**:1416-1428.

Prior, I.A., and M.J. Clague. 1999. Localization of a class II phosphatidylinositol 3-kinase, PI3KC2alpha, to clathrin-coated vesicles. *Mol Cell Biol Res Commun*. **1**:162-6.

Pruyne, D., and A. Bretscher. 2000. Polarization of cell growth in yeast. *J Cell Sci*. **113**:571-85.

Pumphrey, N.J., V. Taylor, S. Freeman, M.R. Douglas, P.F. Bradfield, S.P. Young, J.M. Lord, M.J. Wakelam, I.N. Bird, M. Salmon, and C.D. Buckley. 1999. Differential association of cytoplasmic signalling molecules SHP-1, SHP-2, SHIP and phospholipase C-gamma1 with PECAM-1/CD31. *FEBS Lett*. **450**:77-83.

Qualmann, B., J. Roos, P.J. DiGregorio, and R.B. Kelly. 1999. Syndapin I, a synaptic dynamin-binding protein that associates with the neural Wiskott-Aldrich syndrome protein. *Mol Biol Cell*. **10**:501-13.

Rameh, L.E., and L.C. Cantley. 1999. The role of phosphoinositide 3-kinase lipid products in cell function. *J Biol Chem*. **274**:8347-50.

Rameh, L.E., K.F. Tolias, B.C. Duckworth, and L.C. Cantley. 1997. A new pathway for synthesis of phosphatidylinositol-4,5-bisphosphate. *Nature*. **390**:192-6.

Ramjaun, A.R., and P.S. McPherson. 1996. Tissue-specific alternative splicing generates two synaptojanin isoforms with differential membrane binding properties. *J Biol Chem*. **271**:24856-61.

Raucher, D., T. Stauffer, W. Chen, K. Shen, S. Guo, J.D. York, M.P. Sheetz, and T. Meyer. 2000. Phosphatidylinositol 4,5-bisphosphate functions as a second messenger that regulates cytoskeleton-plasma membrane adhesion. *Cell*. **100**:221-8.

Ravetch, J.V., and L.L. Lanier. 2000. Immune inhibitory receptors. *Science*. **290**:84-9.

Rickert, P., O.D. Weiner, F. Wang, H.R. Bourne, and G. Servant. 2000. Leukocytes navigate by compass: roles of PI3Kgamma and its lipid products. *Trends Cell Biol*. **10**:466-73.

Roberts, A.W., C. Kim, L. Zhen, J.B. Lowe, R. Kapur, B. Petryniak, A. Spaetti, J.D. Pollock, J.B. Borneo, G.B. Bradford, S.J. Atkinson, M.C. Dinauer, and D.A. Williams. 1999. Deficiency of the hematopoietic cell-specific Rho family GTPase Rac2 is characterized by abnormalities in neutrophil function and host defense. *Immunity*. **10**:183-96.

Rohrschneider, L.R., J.F. Fuller, I. Wolf, Y. Liu, and D.M. Lucas. 2000. Structure, function, and biology of SHIP proteins. *Genes Dev*. **14**:505-20.

Ruggeri, Z.M. 1997. Mechanisms initiating platelet thrombus formation. *Thromb Haemost*. **78**:611-6.

Sakisaka, T., T. Itoh, K. Miura, and T. Takenawa. 1997. Phosphatidylinositol 4,5-bisphosphate phosphatase regulates the rearrangement of actin filaments. *Mol Cell Biol*. **17**:3841-9.

Sambrook, J., E.F. Fritsch, and T. Maniatis. 1989. Molecular Cloning: A Laboratory Manual. Cold Spring Harbor Laboratory, Cold Spring Harbour.

Sasaoka, T., H. Hori, T. Wada, M. Ishiki, T. Haruta, H. Ishihara, and M. Kobayashi. 2001. SH2-containing inositol phosphatase 2 negatively regulates insulin-induced glycogen synthesis in L6 myotubes. *Diabetologia*. **44**:1258-67.

Sattler, M., R. Salgia, G. Shrikhande, S. Verma, J.L. Choi, L.R. Rohrschneider, and J.D. Griffin. 1997. The phosphatidylinositol polyphosphate 5-phosphatase SHIP and the protein tyrosine phosphatase SHP-2 form a complex in hematopoietic cells which can be regulated by BCR/ABL and growth factors. *Oncogene*. **15**:2379-84.

Savage, B., F. Almus-Jacobs, Z.M. Ruggeri, and E. Saldivar. 1998. Specific synergy of multiple substrate-receptor interactions in platelet thrombus formation under flow Initiation of platelet adhesion by arrest onto fibrinogen or translocation on von Willebrand factor. *Cell*. **94**:657-66.

Savage, B., E. Saldivar, and Z.M. Ruggeri. 1996. Initiation of platelet adhesion by arrest onto fibrinogen or translocation on von Willebrand factor. *Cell*. **84**:289-97.

Sbrissa, D., O.C. Ikonomov, and A. Shisheva. 1999. PIKfyve, a mammalian ortholog of yeast Fab1p lipid kinase, synthesizes 5-phosphoinositides. Effect of insulin. *J Biol Chem*. **274**:21589-97.

Scaife, R.M., and W.Y. Langdon. 2000a. c-Cbl localizes to actin lamellae and regulates lamellipodia formation and cell morphology. *J Cell Sci*. **113**:215-26.

Scaife, R.M., and W.Y. Langdon. 2000b. c-Cbl localizes to actin lamellae and regulates lamellipodia formation and cell morphology.PG - 215-26. *J Cell Sci*. **113**:215-26.

Schafer, D.A., and J.A. Cooper. 1995. Control of actin assembly at filament ends. *Annu Rev Cell Dev Biol*. **11**:497-518.

Schliwa, M., and J. van Blerkom. 1981. Structural interaction of cytoskeletal components. *J Cell Biol.* **90**:222-35.

Schmidt, A., and M.N. Hall. 1998. Signaling to the actin cytoskeleton. *Annu Rev Cell Dev Biol.* **14**:305-38.

Schoenwaelder, S.M., and K. Burridge. 1999. Evidence for a calpeptin-sensitive protein-tyrosine phosphatase upstream of the small GTPase Rho. A novel role for the calpain inhibitor calpeptin in the inhibition of protein-tyrosine phosphatases.PG - 14359-67. *J Biol Chem.* **274**:14359-67.

Schurmans, S., R. Carrio, J. Behrends, V. Pouillon, J. Merino, and S. Clement. 1999. The mouse SHIP2 (Inppl1) gene: complementary DNA, genomic structure, promoter analysis, and gene expression in the embryo and adult mouse. *Genomics.* **62**:260-71.

Sechi, A.S., and J. Wehland. 2000. The actin cytoskeleton and plasma membrane connection: PtdIns(4,5)P(2) influences cytoskeletal protein activity at the plasma membrane. *J Cell Sci.* **113**:3685-95.

Seet, L.F., S. Cho, A. Hessel, and D.J. Dumont. 1998. Molecular cloning of multiple isoforms of synaptojanin 2 and assignment of the gene to mouse chromosome 17A2-3.1. *Biochem Biophys Res Commun.* **247**:116-22.

Servant, G., O.D. Weiner, P. Herzmark, T. Balla, J.W. Sedat, and H.R. Bourne. 2000. Polarization of chemoattractant receptor signaling during neutrophil chemotaxis. *Science.* **287**:1037-40.

Shepherd, P.R., D.J. Withers, and K. Siddle. 1998. Phosphoinositide 3-kinase: the key switch mechanism in insulin signalling. *Biochem J.* **333**:471-90.

Shisheva, A., B. Rusin, O.C. Ikonomov, C. DeMarco, and D. Sbrissa. 2000. Localization and insulin-regulated relocation of 5'-phosphoinositide kinase PIKfyve in 3T3-L1 adipocytes. *J Biol Chem.* **39**:51.

Singer-Kruger, B., Y. Nemoto, L. Daniell, S. Ferro-Novick, and P. De Camilli. 1998. Synaptojanin family members are implicated in endocytic membrane traffic in yeast. *J Cell Sci.* **111**:3347-56.

Small, J.V., T. Stradal, E. Vignal, and K. Rottner. 2002. The lamellipodium: where motility begins. *Trends Cell Biol.* **12**:112-20.

Speed, C.J., P.J. Little, J.A. Hayman, and C.A. Mitchell. 1996. Underexpression of the 43 kDa inositol polyphosphate 5-phosphatase is associated with cellular transformation. *Embo J.* **15**:4852-61.

Speed, C.J., M. Matzaris, P.I. Bird, and C.A. Mitchell. 1995. Tissue distribution and intracellular localisation of the 75-kDa inositol polyphosphate 5-phosphatase. *Eur J Biochem.* **234**:216-24.

Srinivasan, S., M. Seaman, Y. Nemoto, L. Daniell, S.F. Suchy, S. Emr, P. De Camilli, and R. Nussbaum. 1997. Disruption of three phosphatidylinositol-polyphosphate 5-phosphatase genes from Saccharomyces cerevisiae results in pleiotropic abnormalities of vacuole morphology, cell shape, and osmohomeostasis [published erratum appears in Eur J Cell Biol 1998 Mar;75(3):246]. *Eur J Cell Biol.* **74**:350-60.

Stauffer, T.P., S. Ahn, and T. Meyer. 1998. Receptor-induced transient reduction in plasma membrane PtdIns(4,5)P2 concentration monitored in living cells. *Curr Biol.* **8**:343-6.

Steck, P.A., M.A. Pershouse, S.A. Jasser, W.K. Yung, H. Lin, A.H. Ligon, L.A. Langford, M.L. Baumgard, T. Hattier, T. Davis, C. Frye, R. Hu, B. Swedlund, D.H. Teng, and

S.V. Tavtigian. 1997. Identification of a candidate tumour suppressor gene, MMAC1, at chromosome 10q23.3 that is mutated in multiple advanced cancers. *Nat Genet.* **15**:356-62.

Stenmark, H., and R. Aasland. 1999. FYVE-finger proteins--effectors of an inositol lipid. *J Cell Sci.* **112**:4175-83.

Stephens, L., C. Ellson, and P. Hawkins. 2002. Roles of PI3Ks in leukocyte chemotaxis and phagocytosis. *Curr Opin Cell Biol.* **14**:203-13.

Stephens, L.R., K.T. Hughes, and R.F. Irvine. 1991. Pathway of phosphatidylinositol(3,4,5)-trisphosphate synthesis in activated neutrophils. *Nature.* **351**:33-9.

Stephens, L.R., T.R. Jackson, and P.T. Hawkins. 1993. Agonist-stimulated synthesis of phosphatidylinositol(3,4,5)-trisphosphate: a new intracellular signalling system? *Biochim Biophys Acta.* **1179**:27-75.

Stolz, L.E., C.V. Huynh, J. Thorner, and J.D. York. 1998a. Identification and characterization of an essential family of inositol polyphosphate 5-phosphatases (INP51, INP52 and INP53 gene products) in the yeast Saccharomyces cerevisiae. *Genetics.* **148**:1715-29.

Stolz, L.E., W.J. Kuo, J. Longchamps, M.K. Sekhon, and J.D. York. 1998b. INP51, a yeast inositol polyphosphate 5-phosphatase required for phosphatidylinositol 4,5-bisphosphate homeostasis and whose absence confers a cold-resistant phenotype. *J Biol Chem.* **273**:11852-61.

Stossel, T.P. 1993. On the crawling of animal cells. *Science.* **260**:1086-94.

Stossel, T.P., J. Condeelis, L. Cooley, J.H. Hartwig, A. Noegel, M. Schleicher, and S.S. Shapiro. 2001. Filamins as integrators of cell mechanics and signalling. *Nat Rev Mol Cell Biol.* **2**:138-45.

Stossel, T.P., J.H. Hartwig, P.A. Janmey, and D.J. Kwiatkowski. 1999. Cell crawling two decades after Abercrombie. *Biochem Soc Symp*. **65**:267-80.

Takada, F., D.L. Vander Woude, H.Q. Tong, T.G. Thompson, S.C. Watkins, L.M. Kunkel, and A.H. Beggs. 2001. Myozenin: an alpha-actinin- and gamma-filamin-binding protein of skeletal muscle Z lines. *Proc Natl Acad Sci U S A*. **98**:1595-600.

Takafuta, T., G. Wu, G.F. Murphy, and S.S. Shapiro. 1998. Human beta-filamin is a new protein that interacts with the cytoplasmic tail of glycoprotein Ibalpha. *J Biol Chem*. **273**:17531-8.

Takeshita, S., N. Namba, J.J. Zhao, Y. Jiang, H.K. Genant, M.J. Silva, M.D. Brodt, C.D. Helgason, J. Kalesnikoff, M.J. Rauh, R.K. Humphries, G. Krystal, S.L. Teitelbaum, and F.P. Ross. 2002. SHIP-deficient mice are severely osteoporotic due to increased numbers of hyper-resorptive osteoclasts. *Nat Med*. **8**:943-9.

Tamura, M., J. Gu, K. Matsumoto, S. Aota, R. Parsons, and K.M. Yamada. 1998. Inhibition of cell migration, spreading, and focal adhesions by tumor suppressor PTEN. *Science*. **280**:1614-7.

Tamura, M., J. Gu, T. Takino, and K.M. Yamada. 1999. Tumor suppressor PTEN inhibition of cell invasion, migration, and growth: differential involvement of focal adhesion kinase and p130Cas. *Cancer Res*. **59**:442-9.

Taylor, V., M. Wong, C. Brandts, L. Reilly, N.M. Dean, L.M. Cowsert, S. Moodie, and D. Stokoe. 2000. 5' phospholipid phosphatase SHIP-2 causes protein kinase B inactivation and cell cycle arrest in glioblastoma cells. *Mol Cell Biol*. **20**:6860-71.

Terauchi, Y., Y. Tsuji, S. Satoh, H. Minoura, K. Murakami, A. Okuno, K. Inukai, T. Asano, Y. Kaburagi, K. Ueki, H. Nakajima, T. Hanafusa, Y. Matsuzawa, H. Sekihara, Y. Yin, J.C. Barrett, H. Oda, T. Ishikawa, Y. Akanuma, I. Komuro, M. Suzuki, K. Yamamura, T. Kodama, H. Suzuki, T. Kadowaki, and et al. 1999.

Increased insulin sensitivity and hypoglycaemia in mice lacking the p85 alpha subunit of phosphoinositide 3-kinase. *Nat Genet.* **21**:230-5.

Thompson, T.G., Y.M. Chan, A.A. Hack, M. Brosius, M. Rajala, H.G. Lidov, E.M. McNally, S. Watkins, and L.M. Kunkel. 2000. Filamin 2 (FLN2): A muscle-specific sarcoglycan interacting protein. *J Cell Biol.* **148**:115-26.

Toker, A. 1998. The synthesis and cellular roles of phosphatidylinositol 4,5-bisphosphate. *Curr Opin Cell Biol.* **10**:254-61.

Toker, A., and L.C. Cantley. 1997. Signalling through the lipid products of phosphoinositide-3-OH kinase. *Nature.* **387**:673-6.

Tridandapani, S., T. Kelley, M. Pradhan, D. Cooney, L.B. Justement, and K.M. Coggeshall. 1997. Recruitment and phosphorylation of SH2-containing inositol phosphatase and Shc to the B-cell Fc gamma immunoreceptor tyrosine-based inhibition motif peptide motif. *Mol Cell Biol.* **17**:4305-11.

Tridandapani, S., M. Pradhan, J.R. LaDine, S. Garber, C.L. Anderson, and K.M. Coggeshall. 1999. Protein interactions of Src homology 2 (SH2) domain-containing inositol phosphatase (SHIP): association with Shc displaces SHIP from FcgammaRIIb in B cells. *J Immunol.* **162**:1408-14.

Tsakiridis, T., H.E. McDowell, T. Walker, C.P. Downes, H.S. Hundal, M. Vranic, and A. Klip. 1995. Multiple roles of phosphatidylinositol 3-kinase in regulation of glucose transport, amino acid transport, and glucose transporters in L6 skeletal muscle cells. *Endocrinology.* **136**:4315-22.

Tsubokawa, H., K. Oguro, H.P. Robinson, T. Masuzawa, and N. Kawai. 1996. Intracellular inositol 1,3,4,5-tetrakisphosphate enhances the calcium current in hippocampal CA1 neurones of the gerbil after ischaemia. *J Physiol.* **497**:67-78.

Tsujishita, Y., S. Guo, L.E. Stolz, J.D. York, and J.H. Hurley. 2001. Specificity determinants in phosphoinositide dephosphorylation: crystal structure of an archetypal inositol polyphosphate 5-phosphatase. *Cell*. **105**:379-89.

Tu, Z., J.M. Ninos, Z. Ma, J.W. Wang, M.P. Lemos, C. Desponts, T. Ghansah, J.M. Howson, and W.G. Kerr. 2001. Embryonic and hematopoietic stem cells express a novel SH2-containing inositol 5'-phosphatase isoform that partners with the Grb2 adapter protein. *Blood*. **98**:2028-38.

Turner, S.J., J. Domin, M.D. Waterfield, S.G. Ward, and J. Westwick. 1998. The CC chemokine monocyte chemotactic peptide-1 activates both the class I p85/p110 phosphatidylinositol 3-kinase and the class II PI3K-C2alpha. *J Biol Chem*. **273**:25987-95.

Tyler, J.M., J.M. Anderson, and D. Branton. 1980. Structural comparison of several actin-binding macromolecules. *J Cell Biol*. **85**:489-95.

Vadlamudi, R.K., F. Li, L. Adam, D. Nguyen, Y. Ohta, T.P. Stossel, and R. Kumar. 2002. Filamin is essential in actin cytoskeletal assembly mediated by p21-activated kinase 1. *Nat Cell Biol*. **4**:681-90.

van der Flier, A., I. Kuikman, D. Kramer, D. Geerts, M. Kreft, T. Takafuta, S.S. Shapiro, and A. Sonnenberg. 2002. Different splice variants of filamin-B affect myogenesis, subcellular distribution, and determine binding to integrin [beta] subunits.PG - 361-76. *J Cell Biol*. **156**:361-76.

van der Flier, A., and A. Sonnenberg. 2001. Structural and functional aspects of filamins. *Biochim Biophys Acta*. **1538**:99-117.

van der Ven, P.F., W.M. Obermann, B. Lemke, M. Gautel, K. Weber, and D.O. Furst. 2000. Characterization of muscle filamin isoforms suggests a possible role of

gamma-filamin/ABP-L in sarcomeric Z-disc formation. *Cell Motil Cytoskeleton.* **45**:149-62.

van Der Ven, P.F., S. Wiesner, P. Salmikangas, D. Auerbach, M. Himmel, S. Kempa, K. Hayess, D. Pacholsky, A. Taivainen, R. Schroder, O. Carpen, and D.O. Furst. 2000. Indications for a novel muscular dystrophy pathway. gamma-filamin, the muscle-specific filamin isoform, interacts with myotilin. *J Cell Biol.* **151**:235-48.

Vanhaesebroeck, B., S.J. Leevers, K. Ahmadi, J. Timms, R. Katso, P.C. Driscoll, R. Woscholski, P.J. Parker, and M.D. Waterfield. 2001. Synthesis and function of 3-phosphorylated inositol lipids. *Annu Rev Biochem.* **70**:535-602.

Vanhaesebroeck, B., S.J. Leevers, G. Panayotou, and M.D. Waterfield. 1997. Phosphoinositide 3-kinases: a conserved family of signal transducers. *Trends Biochem Sci.* **22**:267-72.

Vanhaesebroeck, B., and M.D. Waterfield. 1999. Signaling by distinct classes of phosphoinositide 3-kinases. *Exp Cell Res.* **253**:239-54.

Varnai, P., and T. Balla. 1998. Visualization of phosphoinositides that bind pleckstrin homology domains: calcium- and agonist-induced dynamic changes and relationship to myo-[3H]inositol-labeled phosphoinositide pools. *J Cell Biol.* **143**:501-10.

Vely, F., S. Olivero, L. Olcese, A. Moretta, J.E. Damen, L. Liu, G. Krystal, J.C. Cambier, M. Daeron, and E. Vivier. 1997. Differential association of phosphatases with hematopoietic co-receptors bearing immunoreceptor tyrosine-based inhibition motifs. *Eur J Immunol.* **27**:1994-2000.

Venkateswarlu, K., P.B. Oatey, J.M. Tavare, and P.J. Cullen. 1998. Insulin-dependent translocation of ARNO to the plasma membrane of adipocytes requires phosphatidylinositol 3-kinase. *Curr Biol.* **8**:463-6.

Wada, T., T. Sasaoka, M. Funaki, H. Hori, S. Murakami, M. Ishiki, T. Haruta, T. Asano, W. Ogawa, H. Ishihara, and M. Kobayashi. 2001. Overexpression of SH2-Containing Inositol Phosphatase 2 Results in Negative Regulation of Insulin-Induced Metabolic Actions in 3T3-L1 Adipocytes via Its 5'-Phosphatase Catalytic Activity. *Mol Cell Biol.* **21**:1633-1646.

Wang, F., P. Herzmark, O.D. Weiner, S. Srinivasan, G. Servant, and H.R. Bourne. 2002. Lipid products of PI(3)Ks maintain persistent cell polarity and directed motility in neutrophils. *Nat Cell Biol.* **4**:513-8.

Wang, K., and S.J. Singer. 1977. Interaction of filamin with f-actin in solution. *Proc Natl Acad Sci U S A.* **74**:2021-5.

Ware, M.D., P. Rosten, J.E. Damen, L. Liu, R.K. Humphries, and G. Krystal. 1996. Cloning and characterization of human SHIP, the 145-kD inositol 5-phosphatase that associates with SHC after cytokine stimulation. *Blood.* **88**:2833-40.

Watton, S.J., and J. Downward. 1999. Akt/PKB localisation and 3' phosphoinositide generation at sites of epithelial cell-matrix and cell-cell interaction. *Curr Biol.* **9**:433-6.

Weiner, O.D., P.O. Neilsen, G.D. Prestwich, M.W. Kirschner, L.C. Cantley, and H.R. Bourne. 2002. A PtdInsP(3)- and Rho GTPase-mediated positive feedback loop regulates neutrophil polarity. *Nat Cell Biol.* **4**:509-13.

Welch, M.D., D.A. Holtzman, and D.G. Drubin. 1994. The yeast actin cytoskeleton. *Curr Opin Cell Biol.* **6**:110-9.

Wennstrom, S., P. Hawkins, F. Cooke, K. Hara, K. Yonezawa, M. Kasuga, T. Jackson, L. Claesson-Welsh, and L. Stephens. 1994a. Activation of phosphoinositide 3-kinase is required for PDGF-stimulated membrane ruffling. *Curr Biol.* **4**:385-93.

Wennstrom, S., A. Siegbahn, K. Yokote, A.K. Arvidsson, C.H. Heldin, S. Mori, and L. Claesson-Welsh. 1994b. Membrane ruffling and chemotaxis transduced by the PDGF beta-receptor require the binding site for phosphatidylinositol 3' kinase. *Oncogene*. **9**:651-60.

Whisstock, J.C., S. Romero, R. Gurung, H. Nandurkar, L.M. Ooms, S.P. Bottomley, and C.A. Mitchell. 2000. The inositol polyphosphate 5-phosphatases and the Apurinic/Apyrimidinic base excision repair endonucleases share a common mechanism for catalysis. *J Biol Chem*. **275**:37055-61.

Whiteford, C.C., C.A. Brearley, and E.T. Ulug. 1997. Phosphatidylinositol 3,5-bisphosphate defines a novel PI 3-kinase pathway in resting mouse fibroblasts. *Biochem J*. **323**:597-601.

Williamson, D., I. Pikovski, S.L. Cranmer, P. Mangin, N. Mistry, T. Domagala, S. Chehab, F. Lanza, H.H. Salem, and S.P. Jackson. 2002. Interaction between platelet glycoprotein Ibalpha and filamin-1 is essential for glycoprotein Ib/IX receptor anchorage at high shear. *J Biol Chem*. **277**:2151-9.

Winsor, B., and E. Schiebel. 1997. Review: an overview of the Saccharomyces cerevisiae microtubule and microfilament cytoskeleton.PG - 399-434. *Yeast*. **13**:399-434.

Wiradjaja, F., L.M. Ooms, J.C. Whisstock, B.K. McColl, L. Helfenbaum, J.F. Sambrook, M.J. Gething, and C.A. Mitchell. 2000. The yeast inositol polyphosphate 5-phosphatase Inp54p localizes to the endoplasmic reticulum via a C-terminal hydrophobic anchoring-tail. Regulation of secretion from the endoplasmic reticulum. *J Biol Chem*. **14**:7643-7653.

Wisniewski, D., A. Strife, S. Swendeman, H. Erdjument-Bromage, S. Geromanos, W.M. Kavanaugh, P. Tempst, and B. Clarkson. 1999. A novel SH2-containing phosphatidylinositol 3,4,5-trisphosphate 5-phosphatase (SHIP2) is constitutively

tyrosine phosphorylated and associated with src homologous and collagen gene (SHC) in chronic myelogenous leukemia progenitor cells. *Blood*. **93**:2707-20.

Woscholski, R., P.M. Finan, E. Radley, and P.J. Parker. 1998. Identification and characterisation of a novel splice variant of synaptojanin1. *FEBS Lett*. **432**:5-8.

Woscholski, R., P.M. Finan, E. Radley, N.F. Totty, A.E. Sterling, J.J. Hsuan, M.D. Waterfield, and P.J. Parker. 1997. Synaptojanin is the major constitutively active phosphatidylinositol-3,4,5-trisphosphate 5-phosphatase in rodent brain. *J Biol Chem*. **272**:9625-8.

Wu, X., K. Hepner, S. Castelino-Prabhu, D. Do, M.B. Kaye, X.J. Yuan, J. Wood, C. Ross, C.L. Sawyers, and Y.E. Whang. 2000a. Evidence for regulation of the PTEN tumor suppressor by a membrane-localized multi-PDZ domain containing scaffold protein MAGI-2. *Proc Natl Acad Sci U S A*. **97**:4233-8.

Wu, X., K. Senechal, M.S. Neshat, Y.E. Whang, and C.L. Sawyers. 1998. The PTEN/MMAC1 tumor suppressor phosphatase functions as a negative regulator of the phosphoinositide 3-kinase/Akt pathway. *Proceedings of the National Academy of Sciences of the United States of America*. **95**:15587-91.

Wu, Y., D. Dowbenko, M.T. Pisabarro, L. Dillard-Telm, H. Koeppen, and L.A. Lasky. 2001. Pten 2, a golgi-associated testis-specific homologue of the pten tumor suppressor lipid phosphatase. *J Biol Chem*. **276**:21745-53.

Wu, Y., D. Dowbenko, S. Spencer, R. Laura, J. Lee, Q. Gu, and L.A. Lasky. 2000b. Interaction of the tumor suppressor PTEN/MMAC with a PDZ domain of MAGI3, a novel membrane-associated guanylate kinase. *J Biol Chem*. **275**:21477-85.

Wymann, M.P., and L. Pirola. 1998. Structure and function of phosphoinositide 3-kinases. *Biochim Biophys Acta*. **1436**:127-50.

Xie, Z., W. Xu, E.W. Davie, and D.W. Chung. 1998. Molecular cloning of human ABPL, an actin-binding protein homologue. *Biochem Biophys Res Commun.* **251**:914-9.

Xu, W., Z. Xie, D.W. Chung, and E.W. Davie. 1998. A novel human actin-binding protein homologue that binds to platelet glycoprotein Ibalpha. *Blood.* **92**:1268-76.

Yap, C.L., K.E. Anderson, S.C. Hughan, S.M. Dopheide, H.H. Salem, and S.P. Jackson. 2002. Essential role for phosphoinositide 3-kinase in shear-dependent signaling between platelet glycoprotein Ib/V/IX and integrin alpha(IIb)beta(3). *Blood.* **99**:151-8.

Zhang, J., H. Banfic, F. Straforini, L. Tosi, S. Volinia, and S.E. Rittenhouse. 1998a. A type II phosphoinositide 3-kinase is stimulated via activated integrin in platelets. A source of phosphatidylinositol 3-phosphate. *Journal of Biological Chemistry.* **273**:14081-4.

Zhang, X., P.A. Hartz, E. Philip, L.C. Racusen, and P.W. Majerus. 1998b. Cell lines from kidney proximal tubules of a patient with Lowe syndrome lack OCRL inositol polyphosphate 5-phosphatase and accumulate phosphatidylinositol 4,5-bisphosphate. *J Biol Chem.* **273**:1574-82.

Zhang, X., A.B. Jefferson, V. Auethavekiat, and P.W. Majerus. 1995. The protein deficient in Lowe syndrome is a phosphatidylinositol-4,5-bisphosphate 5-phosphatase. *Proc Natl Acad Sci U S A.* **92**:4853-6.

Zhang, X., J.C. Loijens, I.V. Boronenkov, G.J. Parker, F.A. Norris, J. Chen, O. Thum, G.D. Prestwich, P.W. Majerus, and R.A. Anderson. 1997. Phosphatidylinositol-4-phosphate 5-kinase isozymes catalyze the synthesis of 3-phosphate-containing phosphatidylinositol signaling molecules. *J Biol Chem.* **272**:17756-61.

Zhang, X., and P.W. Majerus. 1998. Phosphatidylinositol signalling reactions. *Semin Cell Dev Biol.* **9**:153-60.

Zheng, Y. 2001. Dbl family guanine nucleotide exchange factors. *Trends Biochem Sci.* **26**:724-32.

Article

The SH2-containing inositol polyphosphate 5-phosphatase, SHIP-2, binds filamin and regulates submembraneous actin

Jennifer M. Dyson,[1] Cindy J. O'Malley,[1] Jelena Becanovic,[1] Adam D. Munday,[1] Michael C. Berndt,[2] Imogen D. Coghill,[1] Harshal H. Nandurkar,[1] Lisa M. Ooms,[1] and Christina A. Mitchell[1]

[1]Department of Biochemistry and Molecular Biology, Monash University, Clayton, Victoria, 3800 Australia
[2]Baker Medical Research Institute, Prahran, Victoria, 3181 Australia

SHIP-2 is a phosphoinositidylinositol 3,4,5 trisphosphate (PtdIns[3,4,5]P_3) 5-phosphatase that contains an NH_2-terminal SH2 domain, a central 5-phosphatase domain, and a COOH-terminal proline-rich domain. SHIP-2 negatively regulates insulin signaling. In unstimulated cells, SHIP-2 localized in a perinuclear cytosolic distribution and at the leading edge of the cell. Endogenous and recombinant SHIP-2 localized to membrane ruffles, which were mediated by the COOH-terminal proline–rich domain. To identify proteins that bind to the SHIP-2 proline–rich domain, yeast two-hybrid screening was performed, which isolated actin-binding protein filamin C. In addition, both filamin A and B specifically interacted with SHIP-2 in this assay. SHIP-2 coimmunoprecipitated with filamin from COS-7 cells, and association between these species did not change after epidermal growth factor stimulation. SHIP-2 colocalized with filamin at Z-lines and the sarcolemma in striated muscle sections and at membrane ruffles in COS-7 cells, although the membrane ruffling response was reduced in cells overexpressing SHIP-2. SHIP-2 membrane ruffle localization was dependent on filamin binding, as SHIP-2 was expressed exclusively in the cytosol of filamin-deficient cells. Recombinant SHIP-2 regulated PtdIns(3,4,5)P_3 levels and submembraneous actin at membrane ruffles after growth factor stimulation, dependent on SHIP-2 catalytic activity. Collectively these studies demonstrate that filamin-dependent SHIP-2 localization critically regulates phosphatidylinositol 3 kinase signaling to the actin cytoskeleton.

Introduction

Phosphoinositides are ubiquitous membrane components which regulate proliferation, differentiation, inhibition of apoptosis, secretion, cell movement, and the actin cytoskeleton. Receptor-regulated phosphoinositide 3 (PI-3)* kinases phosphorylate phosphatidylinositol 4,5 bisphosphate (PtdIns[4,5]P_2) forming phosphatidylinositol 3,4,5 trisphosphate (PtdIns[3,4,5]P_3) that is dephosphorylated by the inositol polyphosphate 5-phosphatases (5-phosphatase) to PtdIns(3,4)P_2 (Majerus, 1996; Martin, 1997). Both PtdIns(3,4,5)P_3 and PtdIns(3,4)P_2 localize signaling proteins to the inner wall of the plasma membrane and allosterically regulate these target proteins. PtdIns(3,4,5)P_3 and PtdIns(3,4)P_2 binding proteins include the serine/threonine kinase, Akt, which inhibits apoptosis, and proteins such as cytohesins and centaurins that regulate ADP ribosylation factor (ARF), and thereby vesicular trafficking and the peripheral actin cytoskeleton (Corvera et al., 1999; Datta et al., 1999). PtdIns(3,4,5)P_3 regulates growth factor–induced actin-dependent extension of lamellipodia, membrane ruffle formation, and cell migration.

PtdIns(3,4,5)P_3 is metabolized by the removal of either the 5- or 3-position phosphate by specific 5- or 3-lipid phosphatases, respectively. The product of the tumor suppressor gene phosphatase and tensin homologue deleted on chromosome 10 (PTEN) is a PtdIns(3,4,5)P_3 3-phosphatase which hydrolyses PtdIns(3,4,5)P_3, forming PtdIns(4,5)P_2. The lipid 3-phosphatase activity of PTEN is critical for its tumor suppressor function (for review see Cantley and Neel, 1999).

The 5-phosphatases hydrolyze the 5-position phosphate from both inositol phosphates and phosphoinositides and share the

Address correspondence to Christina A. Mitchell, Dept. of Biochemistry and Molecular Biology, Monash University, Clayton, Victoria, 3800 Australia. Tel.: (61) 3990-53790. Fax: (61) 3990-54699. E-mail: christina.mitchell@med.monash.edu.au

*Abbreviations used in this paper: aa, amino acid; 5-phosphatase, inositol polyphosphate 5-phosphatase; FLNC, filamin C; GFP, green fluorescent protein; HA, hemagglutinin; PH, pleckstrin homology; PI-3, phosphatidylinositol 3; PtdIns, phosphatidylinositol; PTEN, phosphatase and tensin homologue deleted on chromosome 10; SHIP, SH2 domain–containing inositol polyphosphate 5-phosphatase.

Key words: SHIP-2; inositol polyphosphate 5-phosphatase; filamin; cytoskeleton; phosphatidylinositol 3,4,5-trisphosphate

The Journal of Cell Biology, Volume 155, Number 6, December 10, 2001 1065–1079
http://www.jcb.org/cgi/doi/10.1083/jcb.200104005

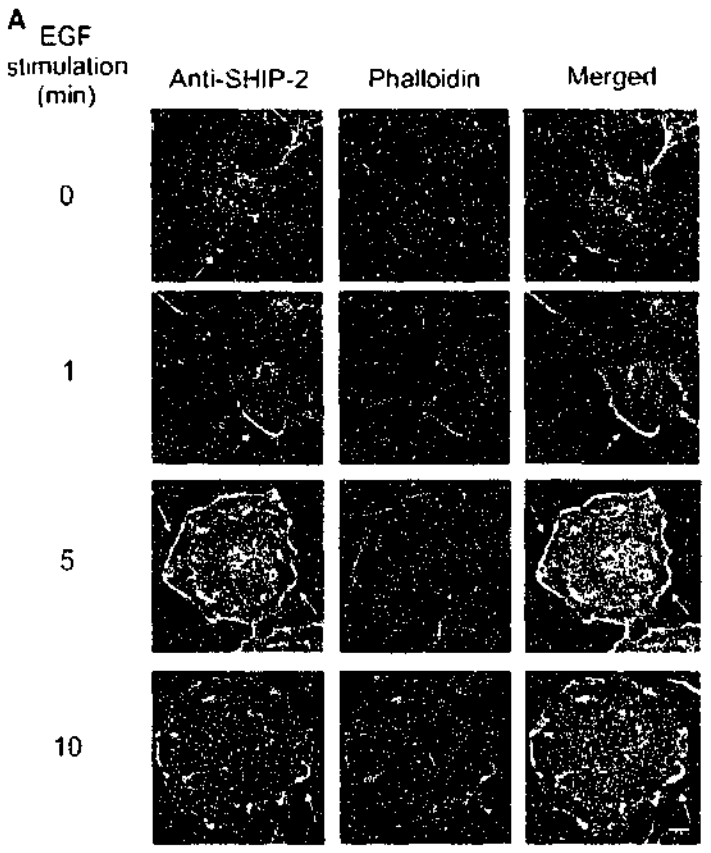

Figure 1. **SHIP-2 localizes to actin-rich regions in COS-7 cells.** (A) COS-7 cells were either left resting or serum-starved and then stimulated with EGF (100 ng/ml) for the indicated times, costained with the SHIP-2 antibody and phalloidin, and then visualized by confocal microscopy. Arrows indicate membrane ruffle localization. (B) COS-7 cells were transiently transfected with GFP-SHIP-2 and either left unstimulated or serum-starved, then stimulated with EGF (100 ng/ml) for the indicated times, and fixed and phalloidin stained. Arrows indicate SHIP-2 membrane localization. (C) COS-7 cells were transiently transfected with the indicated HA-SHIP-2 constructs (see Table I) and where indicated, stimulated with EGF (100 ng/ml), fixed and stained with anti-HA antibodies, and visualized by confocal microscopy. Arrows indicate SHIP-2 membrane localization. (D) Immunoblot analysis of recombinant GFP-SHIP-2 or HA-SHIP-2 wild-type and mutant proteins. 100 μg of Triton X-100–soluble lysate from transfected cells (as indicated) was analyzed by immunoblot analysis using antibodies to GFP, or HA. The migration of molecular weight markers is shown on the left. Bars, 20 μm.

same catalytic mechanism to the apurinic/apyrimidinic endonucleases (Majerus, 1996; Whisstock et al., 2000; Tsujishita et al., 2001). SHIP-2 is a widely expressed 5-phosphatase which plays a significant role in negatively regulating insulin signaling (Ishihara et al., 1999; Clement et al., 2001). SHIP-2 contains an NH_2-terminal SH2 domain, a central 5-phosphatase domain, and a COOH-terminal proline–rich domain and bears significant sequence identity with the 5-phosphatase, SHIP-1, except in the proline-rich domain. SHIP-2 hydrolyses the 5-position phosphate from PtdIns(3,4,5)P_3 and PtdIns(4,5)P_2, and in some, but not all, studies has been shown to hydrolyze the soluble inositol

phosphate Ins(1,3,4,5)P_4 (Pesesse et al., 1997; Wisniewski et al., 1999; Taylor et al., 2000). In contrast to SHIP-1, which has a restricted hematopoietic expression, SHIP-2 is widely expressed. SHIP-2 undergoes cytokine-, growth factor–, and insulin-stimulated phosphorylation in a number of cell lines (Habib et al., 1998; Wisniewski et al., 1999). In addition, SHIP-2 is constitutively tyrosine phosphorylated and associated with Shc in chronic myeloid leukemic progenitor cells, suggesting a role for SHIP-2 in $210^{bcr/abl}$-mediated myeloid expansion (Wisniewski et al., 1999). SHIP-2, like PTEN, regulates both PtdIns(3,4,5)P_3-mediated Akt activation and the induction of cell cycle arrest associated with increased stability of expression of the cell cycle inhibitor $p27^{KIP1}$ (Taylor et al., 2000). Recent studies have demonstrated SHIP-2 negatively regulates insulin signaling. Homozygous mice lacking SHIP-2 develop severe neonatal hypoglycemia and prenatal death. Adult SHIP-2 heterozygous mutant mice demonstrate insulin sensitivity associated with increased translocation of GLUT4 to the plasma membrane in response to insulin treatment (Clement et al., 2001).

In this study we examine the intracellular location of the 5-phosphatase SHIP-2 and demonstrate the enzyme is located at membrane ruffles mediated via its proline-rich domain. SHIP-2 forms a complex with the actin binding protein, filamin, and thereby regulates PtdIns(3,4,5)P_3 and actin at the leading edge of the cell. This may represent a mechanism for the tight spatial regulation of PtdIns(3,4,5)P_3 at specific sites after growth factor or insulin stimulation.

Results

Intracellular localization of SHIP-2 in unstimulated and EGF-stimulated cells

We localized endogenous SHIP-2 in both COS-7 cells and NIH3T3 cells (unpublished data) by indirect immunofluorescence using affinity-purified antiserum raised to its unique COOH-terminal sequence. Similar results were found in both cell types. In unstimulated COS-7 cells, SHIP-2 was detected diffusely in the cytosol and concentrated at the plasma membrane at the leading edge of the cell (Fig. 1 A). SHIP-2 colocalized with markers of submembraneous actin, including β-actin (unpublished data) and phalloidin staining. After EGF stimulation, conditions under which membrane ruffles and actin are actively formed and remodeled, SHIP-2 localized initially at membrane ruffles i.e., areas at the edges of lamellipodia where the plasma membrane detaches from the support and rolls up. After 5–10 min EGF stimulation, SHIP-2 was diffusely expressed at the membrane and was detected in areas of active cytoskeletal rearrangement. However, SHIP-2 did not at any time associate with stress fibers, although the enzyme was detected at focal adhesions (unpublished data) as recently reported (Prasad et al., 2001). Preimmune sera were nonreactive (unpublished data). Localization of recombinant SHIP-2 tagged with either green fluorescent protein (GFP) (Fig. 1 B) or hemagglutinin (HA) (Fig. 1 C), matched that of the endogenous protein. In nonstimulated cells, GFP–SHIP-2 was expressed diffusely in the cytosol and in many cells concentrated in a perinuclear distribution. It was also present at the plasma membrane at the leading edge of the cell, colocalizing at this site with phalloidin staining. After EGF stimulation at 1 min, GFP–SHIP-2 concentrated at membrane ruffles, and by 5 min localized diffusely at the plasma membrane, colocalizing as shown in the merged images with phalloidin-staining of actin (Fig. 1 B). We noted membrane ruffling was significantly reduced in many cells overexpressing SHIP-2 (see Fig. 9). Expression of HA-tagged SHIP-2 demonstrated a similar intracellular location to GFP–SHIP-2 (Fig. 1 C). GFP or HA alone were detected diffusely through the cytosol and nucleus and localization did not change after EGF stimulation (unpublished data). Recombinant GFP–SHIP-2 was expressed as a 166-kD protein on SDS-PAGE, with little proteolysis detected (Fig. 1 D).

Identification of peptide sequences mediating SHIP-2 localization to membrane ruffles

SHIP-2 contains an NH_2-terminal SH2 domain, a central catalytic 300 amino acid 5-phosphatase domain, and an extensive COOH-terminal proline–rich domain. To investigate the structural domains mediating SHIP-2 intracellular location, specifically to membrane ruffles, a series of wild-type and mutant SHIP-2 recombinants tagged with HA were expressed in COS-7 cells (Fig. 1 C and Table I). SHIP-2 that lacked the SH2 domain (HA–SHIP-2ΔSH2) localized to membrane ruffles similarly to wild-type SHIP-2 (Fig. 1 C). SHIP-2 that lacked the proline-rich domain (HA–SHIP-2ΔPRD) showed no membrane association in the resting cell and failed to demonstrate membrane ruffle localization after 1 min of EGF stimulation. However, after 5 min of stimulation, faint membraneous localization of HA–SHIP-2ΔPRD was detected, although this was much less intense than the wild-type protein, suggesting that sequences independent of the proline-rich domain may contribute to plasma membrane localization after prolonged growth factor stimulation (Fig. 1 C). This result is consistent with recent studies which have demonstrated SHIP-2 forms a complex with the adaptor protein $p130^{cas}$ via the SH2 domain and localizes to membrane ruffles and focal adhesions after cell adhesion (Prasad et al., 2001). Studies in which only the pro-

Table I. **Oligonucleotides used for the generation of SHIP-2 truncation mutants**

Name of construct	5′ oligonucleotide	3′ oligonucleotide	Polypeptide expressed
HA–SHIP-2 ΔSH2	5′tatctagagagggtgagcgagagccg-3′	5′-atatctagatcaatgatgatgatgatgatgctgctgagctgcagggt-3′	5-phosphatase and proline-rich domain (aa 118–1,258 with COOH-terminal hexa HisTag)
HA–SHIP-2 ΔPRD	5′-gtctagaagccaggcccccctcctgg-3′	5′-tctagatcatggttcttcaaataacctgg-3′	SH2 domain and 5-phosphatase domain (aa 16–936)
HA-PRD	5′-gtctagagagaaaccgccaccaacgggg-3′	5′-tctagatcatggttcttcaaataacctgg-3′	proline-rich domain (aa 936–1,258)

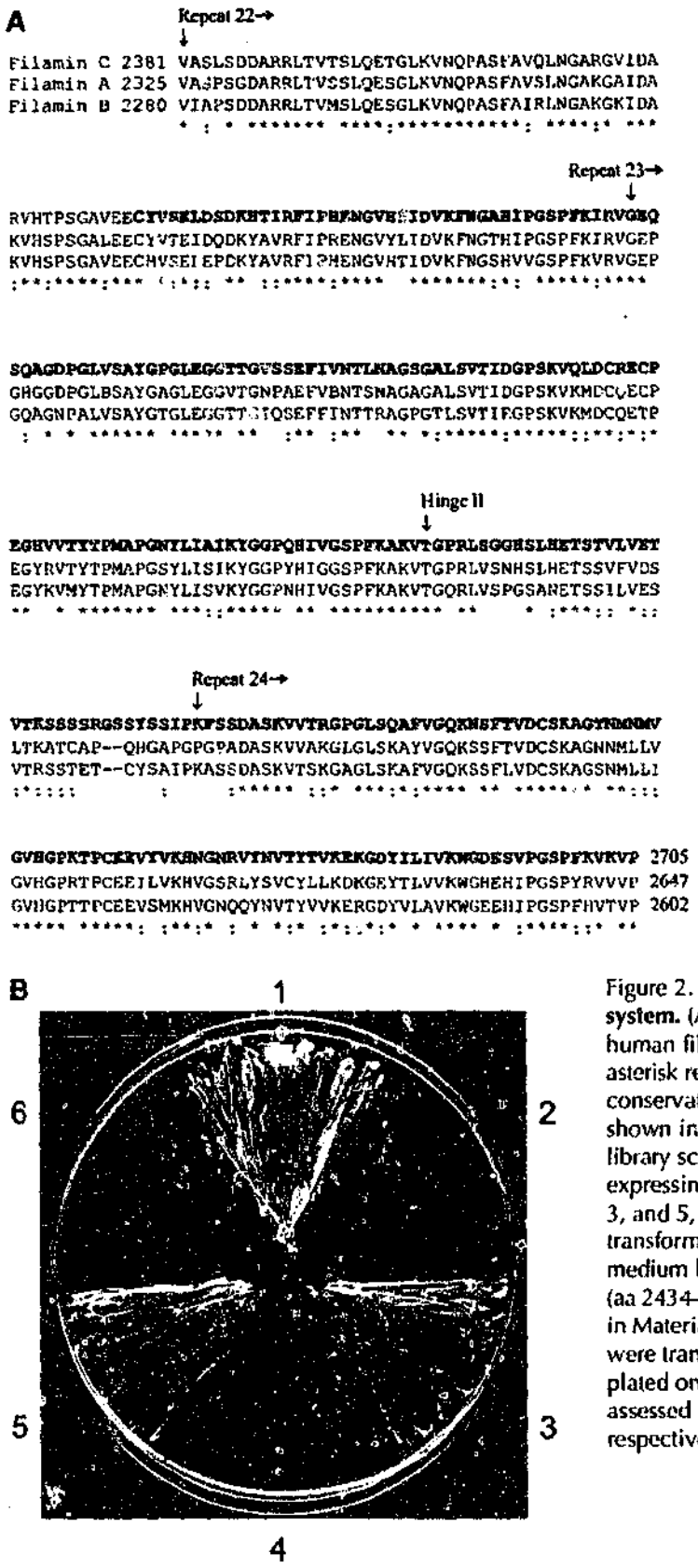

Figure 2. **SHIP-2 interacts with filamin A, B, and C in the yeast two-hybrid system.** (A) Optimized alignment of the predicted amino acid sequences of human filamin A, B, and C. ↓ denotes the first amino acid of each domain; an asterisk represents identical amino acids in all three sequences; a colon represents conservative substitutions. Modified from Xie et al. (1998). The FLNC sequence shown in bold represents that encoded by the clone isolated in skeletal muscle library screening, using the SHIP-2 proline-rich domain as a bait. (B) Yeast expressing DNA-BDPRD bait were transformed with filamin A, B, or C cDNA (1, 3, and 5, respectively), and yeast expressing DNA-BDSHIP2ΔPRD were transformed with filamin A, B, or C (2, 4, and 6, respectively) and plated on medium lacking Tryptophan, Leucine, Histidine, and Adenine. (C) FLNC wild-type (aa 2434–2705 pFLNC) or truncation mutants (Table II) were prepared as described in Materials and methods. Yeast strain AH109 expressing the DNA-BDPRD "bait" were transformed with each FLNC mutant individually. The transformants were plated onto media lacking Tryptophan, Leucine, Adenine, and Histidine and assessed for LacZ. A strong or weak interaction is indicated by + + + or +, respectively. No interaction is indicated by (−).

line-rich domain was expressed (HA-PRD) demonstrated this domain localized to the leading edge of the cell in resting cells, as shown for the wild-type enzyme, and concentrated at membrane ruffles and submembraneous actin–rich structures immediately after EGF stimulation. After 5-min stimulation, however, expression at the membrane was less intense than the wild-type enzyme (Fig. 1 C). Wild-type and mutant HA–SHIP-2 proteins were expressed intact with little proteolysis and migrated at their predicted molecular mass (Fig. 1 D). Collectively, these studies demonstrate that the proline-rich domain mediates SHIP-2 membrane ruffle localization in the resting and in EGF-stimulated cells. In addition, sequences such as the SH2 domain may contribute to membrane localization after prolonged growth factor stimulation.

Identification of SHIP-2 binding partners using yeast two-hybrid analysis

The SHIP-2 COOH-terminal proline–rich domain contains numerous "PXXP" motifs which conform to consensus sequences for SH3 binding domains, 1 WW binding domain motif (PPLP) which may bind to WW domain-containing proteins, and one EVH1 binding domain motif (E/DFPPPPXD/E) which may link the cytoskeletal network to signal transduction pathways (Fedorov et al., 1999). The SHIP-2

proline–rich domain sequence demonstrates no significant sequence homology over the extreme COOH-terminal 322 amino acids with SHIP-1. We searched for proteins that specifically interact with the proline-rich domain using yeast two-hybrid analysis. The entire SHIP-2 proline-rich domain (amino acids [aa] 936–1258) was expressed in yeast cells with a library of proteins expressed as fusions with the GAL4 transcription activation domain. Several rounds of screening a human skeletal muscle library (4×10^6 clones) identified a number of interacting clones in which growth on selective media suggested the presence of bona fide interactors for the proline-rich domain. Sequence analysis demonstrated that one clone, an 818 bp fragment, encoded aa 2434–2705 of the last COOH-terminal two and a half immunoglobulin repeats of the cytoskeletal actin-binding protein filamin C (FLNC), which were in frame with the GAL4 activation domain (Fig. 2 A). Filamin is located in the cortical cytoplasm subjacent to the plasma membrane, and binds actin, promoting orthogonal branching of actin filaments and thereby cell migration and membrane stability (reviewed by Stossel et al., 2001). Filamin forms a complex with a variety of cell surface receptors including FcγRI, the platelet von Willebrand factor receptor, glycoprotein Ib-IX-V, β_1 and β_2 integrin receptors, and intracellular proteins involved in various signaling cascades including Traf 2, granzyme B, caveolin-1, and the stress-activated protein kinase (reviewed by Stossel et al., 2001).

Three human gene filamin paralogues have been identified. Filamin A encodes α-filamin (also called ABP-280) (Gorlin et al., 1990), filamin B codes for β-filamin (also called ABP-278) (Takafuta et al., 1998; Xu et al., 1998), and FLNC encodes for γ-filamin (also called ABPL or FLN2), which is highly expressed in skeletal muscle (Xie et al., 1998). In addition, differential splicing has been demonstrated for each gene (Maestrini et al., 1993; Xie et al., 1998; Xu et al., 1998). All three filamin isoforms demonstrate a similar structure comprising an NH_2-terminal actin binding domain followed by 24 immunoglobulin-like repeat domains creating an extended rod like structure. The extreme COOH-terminal repeat 24 contains a homodimerization domain which is linked to other repeats by a calpain-sensitive "hinge II region" (reviewed by Stossel et al., 2001). As each of the three filamin isoforms shows significant sequence identity in the COOH-terminal region (Fig. 2 A), we investigated if each isoform interacted in cotransformation assays with the proline-rich domain expressed in frame with the DNA binding domain of GAL4 (DNA-BDPRD), or with recombinant mutant SHIP-2 which lacked the proline-rich domain (DNA-BDSHIP-2ΔPRD), versus control heterologous baits. The proline-rich domain "bait" (DNA-BDPRD), but not the SHIP-2 "bait" lacking the proline-rich domain (DNA-BD-SHIP-2ΔPRD), interacted with the COOH-terminal four immunoglobulin repeats of filamin A and B, and the COOH-terminal two and a half immunoglobulin repeats of FLNC, indicated by expression of all three reporter genes *HIS3* and *ADE2* (Fig. 2 B) and *LacZ* (unpublished data).

Identification of FLNC sequences mediating interaction with SHIP-2

To determine the region of FLNC specifically interacting with SHIP-2, a series of wild-type and mutant FLNC constructs comprising the COOH-terminal immunoglobulin repeat regions R22–R24 (aa 2434–2705), which include a "hinge II region" between R23 and R24, were cloned into the activation domain and cotransformed with the DNA-BD-PRD bait and interactions scored as strong (+++), or weak (+) (Fig. 2 C). The fragment containing FLNC repeats 22–24 demonstrated the strongest binding to the proline-rich domain bait. FLNC repeats 23 and 24, either alone or in combination, did not interact with SHIP-2. Repeats 22 and 23 in combination, with or without the hinge II region, interacted with SHIP-2; however, this was weaker than repeats 22–24 (Fig. 2 C). All FLNC truncation mutants were expressed in the yeast strain AH109 and were soluble (unpublished data).

We took several approaches to verify whether SHIP-2 interacted with filamin in vivo and thereby regulated the

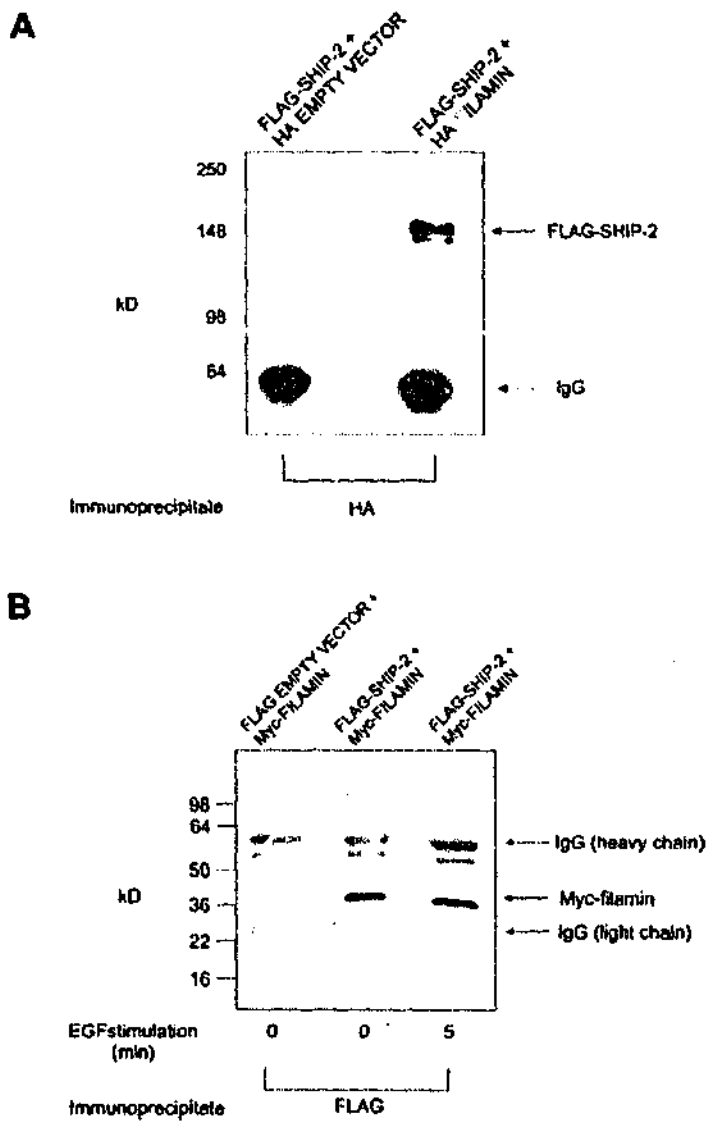

Figure 3. **SHIP-2 associates with filamin in resting and EGF-stimulated COS-7 cells.** (A) COS-7 cells were transiently cotransfected with FLAG–SHIP-2 and HA empty vector, or FLAG–SHIP-2 and HA-filamin (encoding aa 2,434 to 2,705). Cells were harvested and the Triton X-100–soluble lysate was immunoprecipitated with HA antibodies and immunoblotted with FLAG antibodies. (B) COS-7 cells were transiently cotransfected with FLAG empty vector and Myc-filamin (encoding aa 2,434–2,705), or FLAG–SHIP-2 and Myc-filamin. Where indicated, COS-7 cells were EGF treated (100 ng/ml) for 5 min. Cells were harvested and the Triton X-100–soluble lysate was immunoprecipitated with FLAG antibodies and immunoblotted with Myc antibodies.

membrane localization of SHIP-2. First, we investigated using cotransfection and coimmunopreciptation assays if filamin interacted with SHIP-2 in COS-7 cells. We also determined association of endogenous proteins using immunoprecipitation and immunoblot analysis. Second, we demonstrated colocalization of SHIP-2 and filamin at membrane ruffles in resting and EGF-stimulated COS-7 cells. Third, we showed colocalization of filamin and SHIP-2 in mouse heart and skeletal muscle sections using immunolocalization of both species. Finally, we showed the membrane localization of SHIP-2 is dependent on filamin by determining the intracellular localization of SHIP-2 in cells which do not express filamin.

Association of SHIP-2 and filamin was demonstrated in COS-7 cells, which were cotransfected with FLAG-tagged SHIP-2 and HA-tagged filamin (encoding aa 2434–2705 of FLNC), followed by immunoprecipitation and immunoblot analysis using antibodies to each tag. FLAG–SHIP-2 was detected in HA immunoprecipitates of HA-filamin–transfected cells, but not cells transfected with HA empty vector (Fig. 3 A). We determined the effect of EGF stimulation on association between recombinant SHIP-2 and filamin. COS-7 cells were cotransfected with myc-filamin and FLAG–SHIP-2, and after EGF stimulation for 5 min, Triton X-100–soluble lysates were immunoprecipitated using FLAG antibody and immunoblotted with myc antibody. The level of filamin in SHIP-2 immunoprecipitates was unchanged after 5 min EGF stimulation, compared with nonstimulated cells (Fig. 3 B). These studies were repeated expressing SHIP-2 and filamin as fusion proteins with different tags with similar results (unpublished data).

To confirm a complex between endogenous SHIP-2 and filamin, we transfected recombinant myc-tagged filamin (encoding aa 2434–2705 of FLNC) into COS-7 cells and after EGF stimulation performed immunoprecipitations using SHIP-2 antibodies, or preimmune sera, and immunoblotted with either SHIP-2 antibodies (top), or myc tag antibodies to detect filamin (bottom) (Fig. 4 A). This study demonstrated recombinant filamin formed a stable complex with endogenous SHIP-2 and association did not change after growth factor stimulation. In addition, COS-7 cell Triton X-100–soluble lysates immunoprecipitated using SHIP-2 antibodies and immunoblotted using filamin antibodies demonstrated a 280-kD polypeptide consistent with filamin in SHIP-2 immune, but not preimmune immunoprecipitates (Fig. 4 B). In control studies, immunoblot analysis of COS-7 Triton X-100–soluble cell lysates demonstrated the SHIP-2 and filamin antibodies recognized 148- and 280-kD proteins, respectively, consistent with their predicted molecular weight (Fig. 4 C). Collectively, these studies demonstrate SHIP-2 and filamin form a complex in both resting and EGF-stimulated COS-7 cells and the SHIP-2–filamin complex remains unchanged after growth factor stimulation.

We colocalized endogenous filamin and recombinant SHIP-2 after EGF stimulation of COS-7 cells. In nonstimulated cells filamin was located in the cytosol and at the leading edge of the cell (Fig. 5 A). Although HA–SHIP-2 was expressed in the cytosol and membrane, colocalization with filamin was detected only at the membrane at the leading edge of the cell. After EGF stimulation, filamin localized to

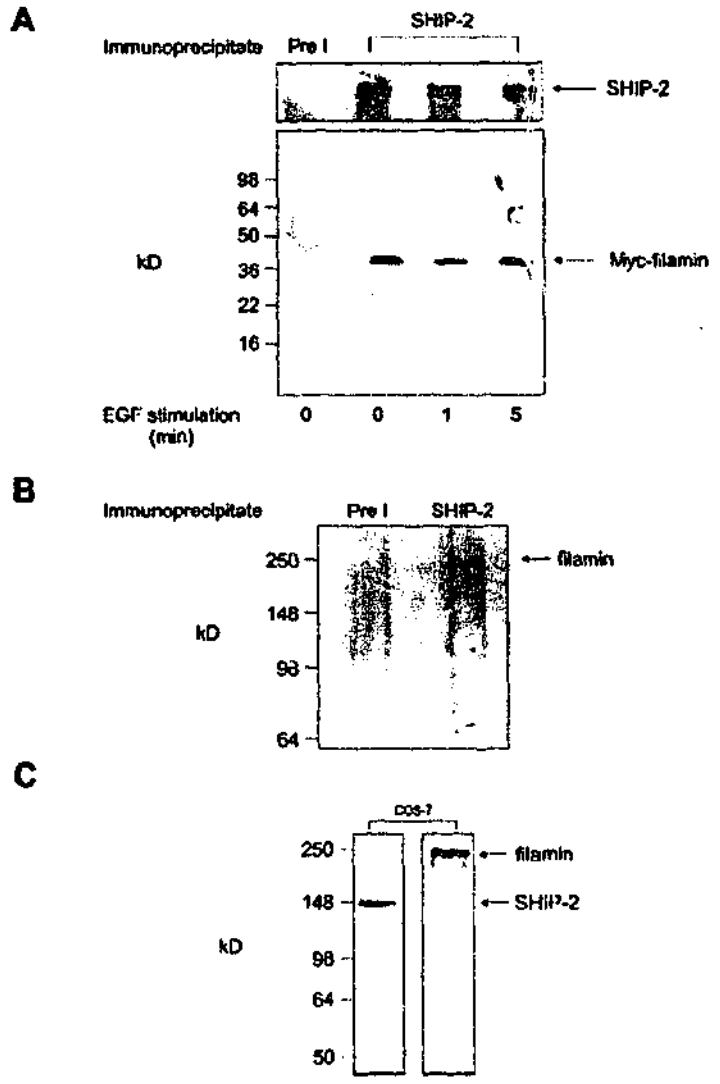

Figure 4. **Endogenous SHIP-2 associates with filamin in COS-7 cells.** (A) COS-7 cells were transiently transfected with Myc-filamin and treated with EGF (100 ng/ml) as indicated. Cells were harvested and the Triton X-100–soluble lysate was immunoprecipitated with either preimmune sera (Pre I) or anti–SHIP-2 sera and immunoblotted with myc antibodies (bottom), then reprobed with anti–SHIP-2 sera to confirm SHIP-2 immunoprecipitation (top). (B) COS-7 cells were harvested and the Triton X-100–soluble lysate was immunoprecipitated with either preimmune sera (Pre I) or anti–SHIP-2 sera and immunoblotted with antibodies to endogenous filamin. (C) COS-7 cells were harvested and 100 μg of the Triton X-100–soluble lysate was immunoblotted with SHIP-2 or filamin antibodies.

a subplasma membrane distribution, initially at membrane ruffles and at the latter time points evenly throughout a fine cortical rim at the periphery of the cell. Filamin colocalized intensely with HA–SHIP-2 at membrane ruffles and the cortical actin rim, but not in the cytosol.

We investigated whether the recombinant COOH-terminal filamin domain (aa 2434–2705) localized as endogenous filamin in COS-7 cells. We also determined whether this recombinant filamin COOH-terminal domain, which represents the SHIP-2 binding site, when expressed at high levels, could displace endogenous SHIP-2 localized at membrane ruffles. The myc-filamin recombinant protein may actually inhibit the localization of SHIP-2 to membrane ruffles by blocking binding to endogenous filamin. In both low and high myc-filamin–expressing cells, the localization of the recombinant protein

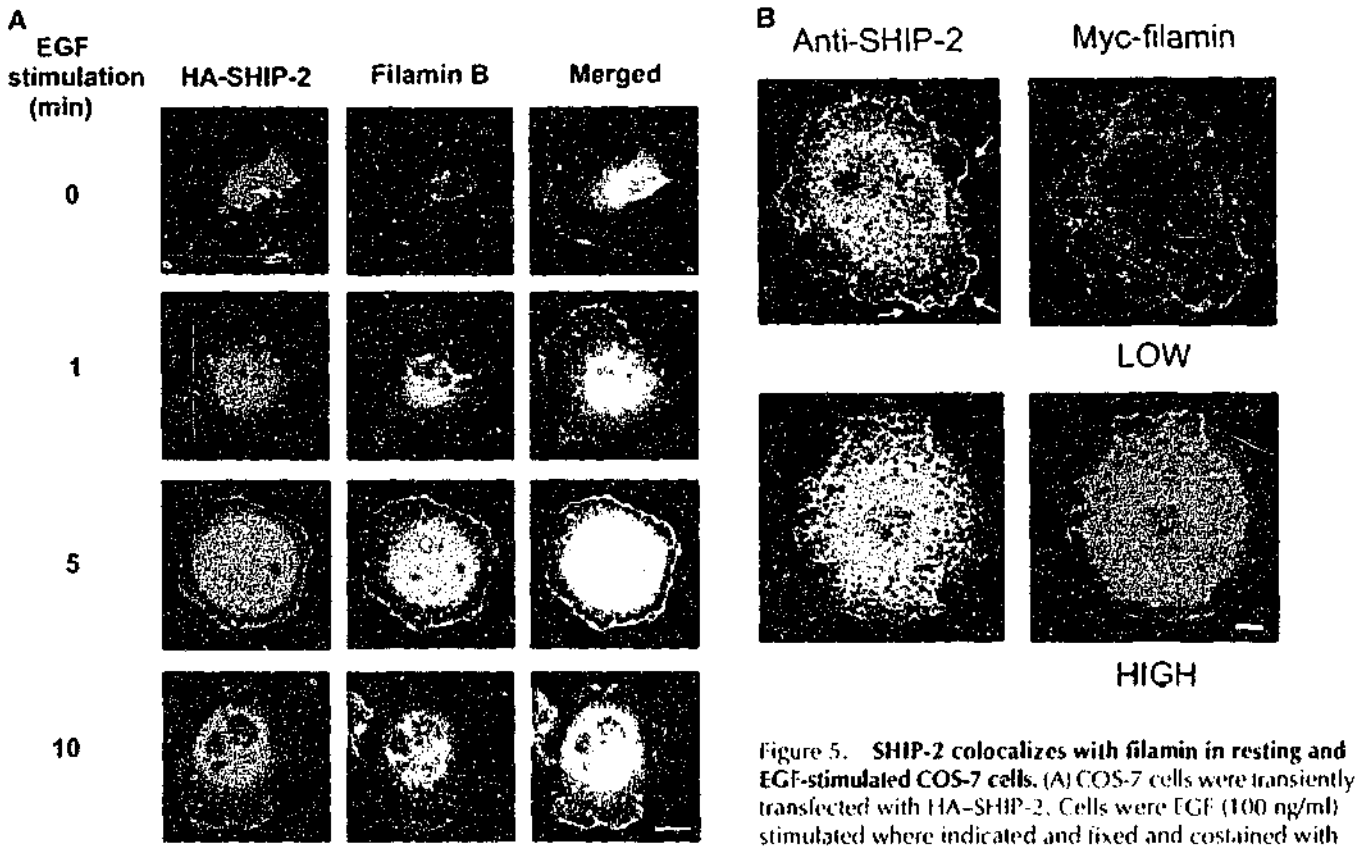

Figure 5. **SHIP-2 colocalizes with filamin in resting and EGF-stimulated COS-7 cells.** (A) COS-7 cells were transiently transfected with HA–SHIP-2. Cells were EGF (100 ng/ml) stimulated where indicated and fixed and costained with HA and filamin B antibodies. Cells were visualized by confocal microscopy. (B) COS-7 cells were transiently transfected with myc-filamin (encoding aa 2,434–2,705) and EGF stimulated for 5 min. Cells were scored as expressing high or low levels of this recombinant protein, as determined by intensity of staining using antibodies to the myc tag by indirect immunofluorescence. The localization of endogenous SHIP-2 was determined using specific SHIP-2 antibodies in cells expressing either low or high levels of myc-filamin. Arrows indicate the localization of SHIP-2 to membrane ruffles. Bars, 20 μM.

matched that of endogenous filamin at membrane ruffles in unstimulated (unpublished data) and more prominently in EGF-stimulated cells (Fig. 5 B). However, in cells expressing myc-filamin at very high levels we noted increased expression of filamin in the cytosol in addition to membrane staining. Localization of endogenous SHIP-2 in myc-filamin–expressing cells was determined by indirect immunofluorescence. In cells expressing low levels of myc-filamin, endogenous SHIP-2 localized to membrane ruffles in both resting (unpublished data) and more prominently in EGF-stimulated cells (Fig. 5 B). In contrast, in cells expressing high levels of myc-filamin, SHIP-2 localized in a perinuclear distribution in the cytosol and staining was less intense at the plasma membrane (Fig. 5 B).

Colocalization of filamin and SHIP-2 in heart and skeletal muscle

FLNC is highly expressed in striated muscle, where it is predominantly localized in myofibrillar Z-discs, with a minor fraction of the protein showing subsarcolemma localization (van der Ven et al., 2000). SHIP-2 is also expressed in skeletal muscle, although its intracellular location in this tissue has not been reported. SHIP-2 homozygous null mice demonstrate increased sensitivity to insulin (Clement et al., 2001). One of the major sites of insulin action is skeletal muscle, where insulin stimulates the translocation of the glucose transporter GLUT4 in a PI-3 kinase–dependent manner to the sarcolemma (Khan et al., 2000). We investigated whether SHIP-2 and filamin colocalized in striated muscle. Mouse heart striated muscle sections were isolated, fixed, and probed with specific affinity purified SHIP-2 antibodies (Fig. 6 A). Soleus muscle showed similar localization (unpublished data). In longitudinal sections SHIP-2 antibodies stained intensively in an alternate banding pattern at areas that resembled Z-lines. No staining of any structure was observed using preimmune serum (Fig. 6 B). Counter-staining sections using antibodies to filamin and the Z-line–specific protein α-actinin demonstrated both colocalized with SHIP-2 (Fig. 6, C–H). Cross-sectional analysis of skeletal muscle demonstrated both filamin and SHIP-2 localized to the sarcolemma, the site of insulin-stimulated GLUT4 translocation (Fig. 6, I–L).

Intracellular localization of SHIP-2 in filamin-deficient cells

To investigate if SHIP-2 membrane ruffle localization was dependent on an interaction with filamin, we examined the intracellular localization of SHIP-2 in a cell line (M2) derived from a human malignant melanoma that does not express detectable filamin messenger RNA or protein (Cunningham et al., 1992). M2 cells demonstrate a distinct phenotype characterized by extensive membrane blebbing and defective locomotion, which is reversed by the stable transfection of filamin A cDNA (A7 subline). Equivalent SHIP-2 expression was demonstrated in A7 and M2 cells as shown by immunoblot analysis using SHIP-2 antipeptide

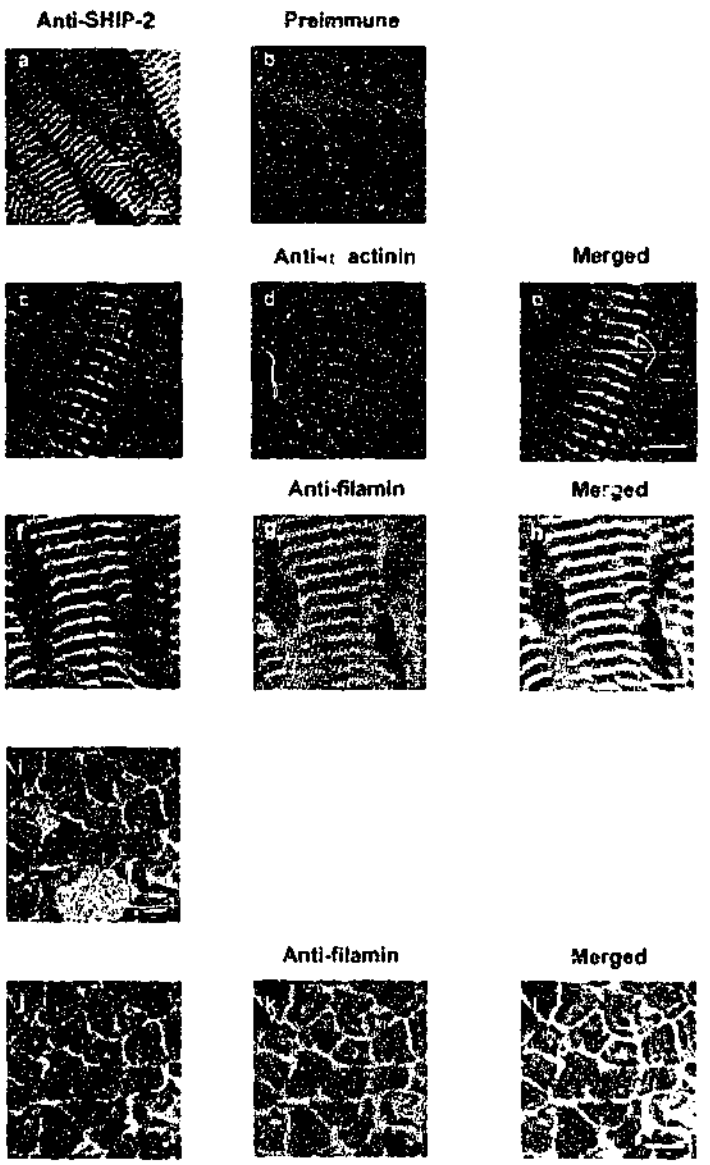

Figure 6. **SHIP-2 colocalizes with filamin at Z-lines in mouse heart and skeletal muscle sections.** Mouse adult heart longitudinal cryosections were cut 7 μm thick and stained with SHIP-2 antibodies (a, c, and f) or preimmune sera (b). SHIP-2 was colocalized with α-actinin (d) at the Z-line and also with antifilamin (g) at the Z-line. Merged images are indicated between SHIP-2 and filamin in panels e and h, respectively. Cross-sectional sections of skeletal muscle were stained with SHIP-2 antibodies (i and j) and counterstained with filamin antibodies (k). Merged images are shown in panel l. Sections were visualized by confocal microscopy. Bars, 20 μm.

antibodies of 100 μg of cell lysate (Fig. 7, A and B). The intracellular localization of SHIP-2 was determined by indirect immunofluorescence of endogenous enzyme using SHIP-2 antipeptide antibodies, or cells transfected with HA-tagged SHIP-2 with detection by staining with antibodies to the tag (unpublished data) with the same result. In nonstimulated M2 cells, SHIP-2 was expressed diffusely in the cytosol and did not colocalize with markers of submembraneous actin such as phalloidin (Fig. 7 A). Upon EGF stimulation, M2 cells transiently form membrane ruffles, or membrane "blebs," which can be detected by phalloidin staining (for review see Stossel et al., 2001). SHIP-2 remained in the cytosol in stimulated cells and did not colocalize with filamin at membrane ruffles. In contrast, in A7 cells, which have been stably transfected with filamin, SHIP-2 localized to membrane ruffles upon EGF stimulation (Fig. 7 B) and colocalized with phalloidin staining. Collectively, these studies demonstrate SHIP-2 localization at membrane ruffles is dependent on filamin expression.

SHIP-2 regulates PtdIns(3,4,5)P_3 and β-actin at membrane ruffles

To establish that recombinant SHIP-2 localized at membrane ruffles was active and to determine the functional consequences on PtdIns(3,4,5)P_3 levels, we employed the pleckstrin homology (PH) domain of ARNO, which has high affinity for PtdIns(3,4,5)P_3 to assess local plasma membrane concentrations of this phosphoinositide (Balla et al., 2000). Several studies have demonstrated that GFP-tagged PH domains with specificity for PtdIns(3,4,5)P_3 can be used to accurately detect PtdIns(3,4,5)P_3 at the leading edge of the cell (for review see Rickert et al., 2000). Although it has been established that SHIP-2 regulates total cellular PtdIns(3,4,5)P_3 levels, the membrane ruffle localized regulation of PtdIns(3,4,5)P_3 has not been reported (Blero et al., 2001; Pesesse et al., 2001). In addition, the functional role of SHIP-2 membrane location in regulating PtdIns(3,4,5)P_3 degradation has not been determined. GFP-fused with the PH domain of ARNO (GFP-PH/ARNO) was coexpressed with either empty vector (HA), or HA–SHIP-2, or the proline-rich domain (HA-PRD), or mutant SHIP-2 which lacked the proline-rich domain (HA–SHIP-2ΔPRD) (Fig. 8). In addition, we determined the effect of overexpressing the COOH-terminal myc-tagged fragment (aa 2434–2705) which binds SHIP-2 in COS-7 cells on PtdIns(3,4,5)P_3 levels, as we have shown overexpression of recombinant myc-filamin displaces endogenous SHIP-2 from membrane ruffles (Fig. 5 B). In nonstimulated cells transfected with HA empty vector and GFP-PH/ARNO, plasma membrane staining of GFP-PH/ARNO was not detected. Upon EGF activation GFP-PH/ARNO translocated rapidly to membrane ruffles after 1 min of stimulation and by 5 min intense plasma membrane staining was detected (Fig. 8). In contrast, cells overexpressing SHIP-2 demonstrated no or low expression of GFP-PH/ARNO at the plasma membrane of EGF-stimulated cells. However, cells expressing the SHIP-2 proline-rich domain (HA-PRD), which lacks the SH2 and catalytic domain, demonstrated strong plasma membrane expression of GFP-PH/ARNO, comparable to HA empty vector expressing cells after EGF stimulation. In cells expressing SHIP-2, which lacks the proline-rich domain (HA-SHIP-2ΔPRD) but contains the SH2 and 5-phosphatase catalytic domain, GFP-PH/ARNO demonstrated growth factor–dependent relocalization to the plasma membrane. However, staining was less intense at 5 min compared with empty vector–expressing cells, but was greater than intact SHIP-2 expressing cells. To confirm these observations, transfected cells were scored as showing high or low GFP-PH/ARNO plasma membrane expression after 5 min of EGF stimulation. Over 40 cells were scored per transfection for three independent experiments by an independent observer. The expression of GFP-PH/ARNO at the plasma membrane was low or not detected in >90% of cells overexpressing SHIP-2, with <10% of cells showing high plasma mem-

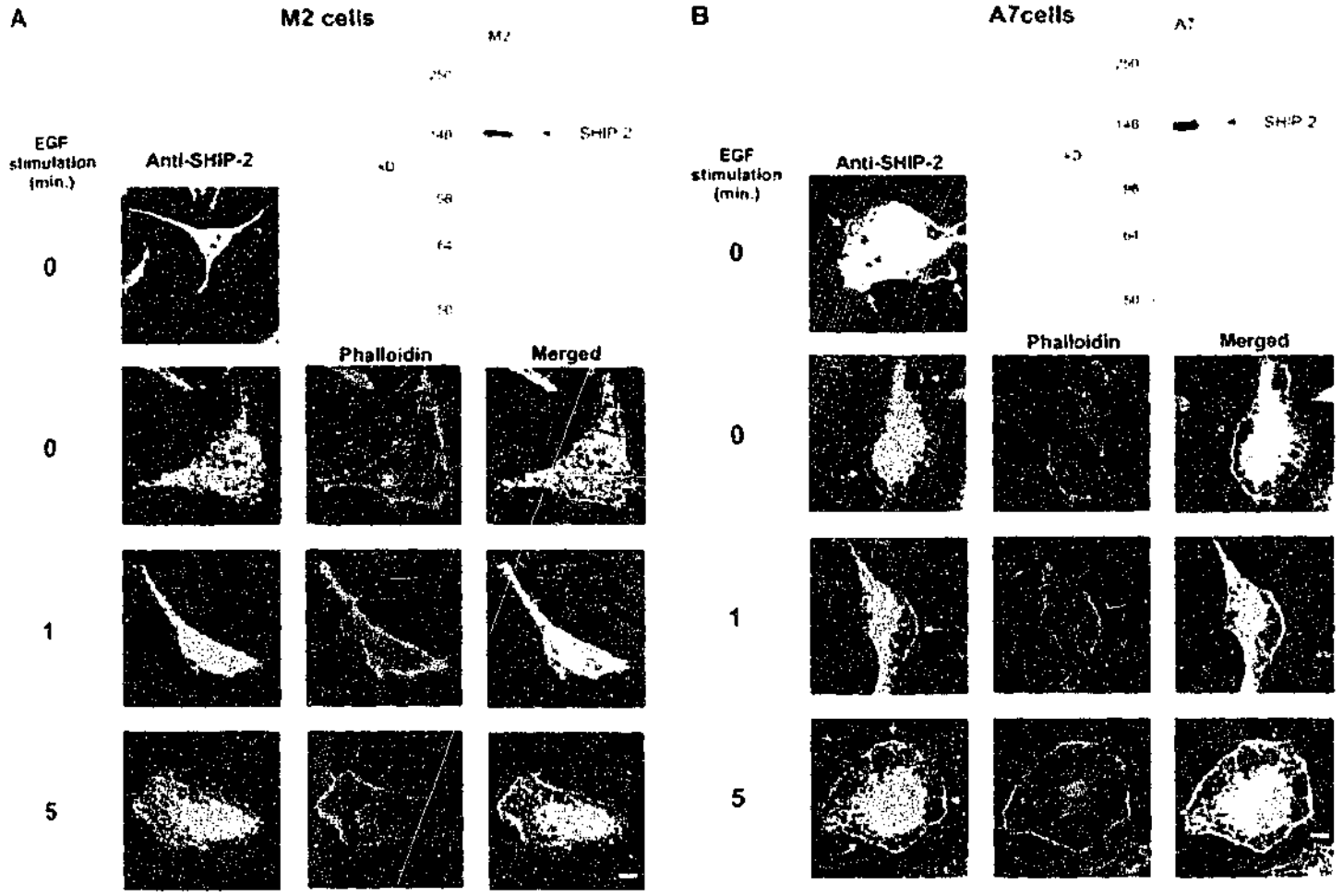

Figure 7. **Filamin is required for membrane localization of SHIP-2.** (A) M2 (filamin-deficient) cells were fixed and costained with phalloidin and anti SHIP-2 sera. Cells were visualized by confocal microscopy. M2 cells were harvested and 100 μg of the Triton X-100–soluble lysate was immunoblotted with anti-SHIP-2 sera. (B) A7 (filamin-replete) cells were fixed, costained, and immunoblotted as for M2 cells. Arrows indicate SHIP-2 membrane ruffle localization. Cells were visualized by confocal microscopy. A7 cells were harvested and 100 μg of the Triton X-100–soluble lysate was immunoblotted with anti-SHIP-2 sera. Bars, 20 μm.

brane expression of GFP-PH/ARNO. In contrast, 35% of cells in which mutant SHIP-2 lacking the proline-rich domain was overexpressed demonstrated high plasma membrane expression of GFP/ARNO, with 60% of cells demonstrating low expression. In control studies, the majority of cells (>85%) expressing the proline-rich domain demonstrated high expression of GFP/ARNO at the plasma membrane. Finally, the effect of overexpression of myc-filamin on PtdIns(3,4,5)P_3 levels was determined. Cells expressing myc-filamin at high levels demonstrated a dramatic increase in GFP-PH/ARNO staining at the plasma membrane of EGF-treated cells, most apparent after 5 min stimulation. This result is consistent with the contention that expression of this COOH-terminal filamin domain displaces endogenous SHIP-2 from membrane ruffles and therefore leads to enhanced PI-3 kinase signals. Collectively, these studies indicate the SHIP-2–filamin interaction regulates plasma membrane PtdIns(3,4,5)P_3.

PI-3 kinase plays a key role in signaling to the actin cytoskeleton and inducing membrane ruffling via regulation of Rac and Cdc42 (for review see Rickert et al., 2000). As SHIP-2 hydrolyses PtdIns(3,4,5)P_3 and localizes to membrane ruffles via association with filamin, we investigated the regulation of actin at membrane ruffles by this 5-phosphatase. Cells overexpressing SHIP-2 (HA–SHIP-2) or the proline-rich domain of SHIP-2 (HA-PRD), which lacks the catalytic 5-phosphatase domain but localizes to membrane ruffles and complexes with filamin, were stained for submembraneous actin by β-actin immunoreactivity. β-actin is ubiquitously expressed and localizes specifically at the leading edge of the cell at subplasma membrane cortical sites, rather than stress fibers. HA–SHIP-2 colocalized with β-actin in both resting and EGF-stimulated cells (Fig. 9 A). In addition, the intensity of β-actin staining was significantly reduced in cells overexpressing SHIP-2, compared with the SHIP-2 proline-rich domain (Fig. 9 A) or vector alone (unpublished data). To quantitate these differences, cells overexpressing HA–SHIP-2 or the proline-rich domain were scored for the intensity of β-actin staining after EGF stimulation (5 min): 40 cells per transfection for three experiments by an independent observer. Greater than 80% of cells expressing HA–SHIP-2, compared with <20% of cells overexpressing the proline-rich domain which has no 5-phosphatase activity, demonstrated low level β-actin staining. The minority of HA-SHIP-2–expressing cells (<20%) demonstrated intense β-actin staining compared with 75% of cells expressing the proline-rich domain. To further establish whether SHIP-2 regulates submembraneous actin, cells overexpressing HA–SHIP-2 or empty vector were stained with phalloidin which stains polymerized actin (Fig. 9 B). Cells overexpressing high

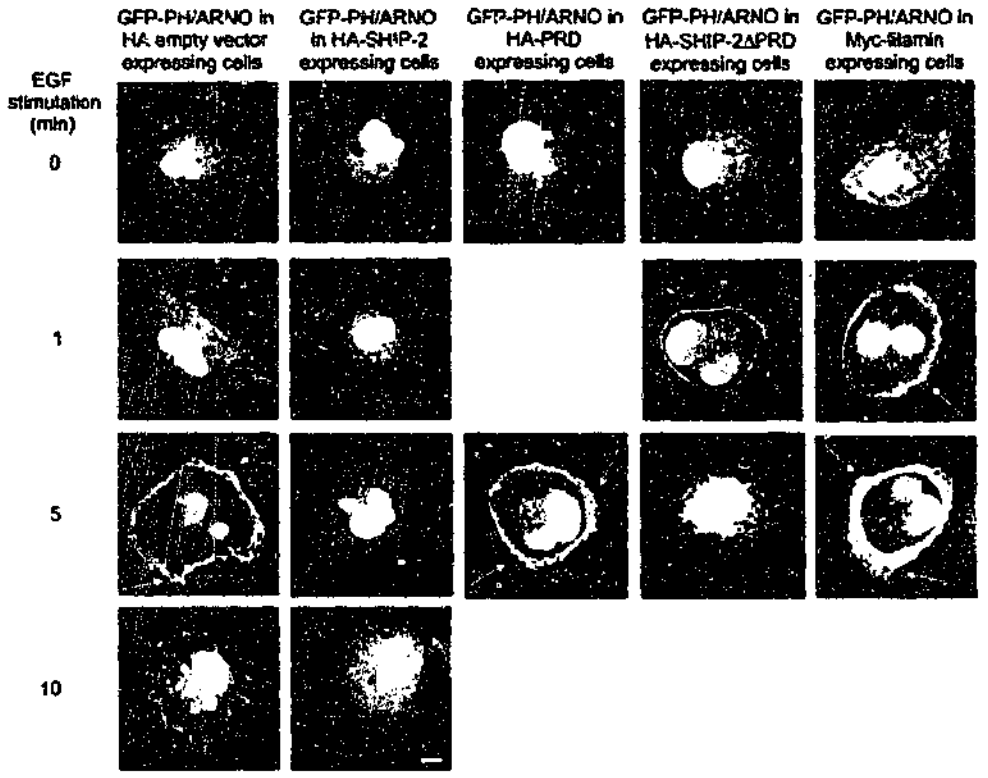

Figure 8. **SHIP-2 regulates PtdIns(3,4,5)P_3 at membrane ruffles.** COS-7 cells were transiently cotransfected with the GFP-PH/ARNO and with either empty vector (HA), HA–SHIP-2, the proline-rich domain (HA-PRD), mutant SHIP-2 which lacked the proline-rich domain (HA–SHIP-2ΔPRD), or Myc-filamin. Cells were EGF treated (100 ng/ml) for the indicated times and stained with HA or Myc antibodies to identify cotransfected cells (unpublished data). Cells were visualized by confocal microscopy for GFP-PH/ARNO expression which is shown. Arrows indicate areas of high GFP-PH/ARNO expression. Bar equals 20 μm.

levels of HA–SHIP-2 demonstrated significantly decreased staining of actin at membrane ruffles and decreased membrane ruffling. In many HA–SHIP-2 overexpressing cells, only a fine cortical rim of actin was stained by phalloidin after 5 min EGF stimulation. The intensity of phalloidin staining of actin at the membrane was scored as high or low after 5 min EGF stimulation in HA–SHIP-2 versus HA empty vector expressing cells for 40 cells per transfection for three independent experiments by an independent observer. Greater than 70% of HA-SHIP-2–expressing cells, compared with 30% of cells expressing the HA empty vector, demonstrated low intensity phalloidin staining at membrane ruffles. In addition, only 25% of SHIP-2 versus 75% of HA empty vector–expressing cells demonstrated high intensity phalloidin staining at membrane ruffles. Collectively, these studies demonstrate SHIP-2 localizes to membrane ruffles via association with filamin and regulates PtdIns(3,4,5)P_3, β-actin, and membrane ruffling.

Discussion

The results of this study demonstrate the 5-phosphatase SHIP-2 forms a functionally significant complex with the actin-binding protein, filamin. SHIP-2 interacts via its proline-rich domain, specifically with filamin A, B, and C isoforms in yeast two hybrid assays. Filamin and SHIP-2 colocalized to Z-lines and the sarcolemma of skeletal muscle, and in mammalian cell lines to membrane ruffles. We demonstrated by reciprocal coimmunoprecipitation studies that SHIP-2 and filamin form a stable complex in COS-7 cells and the level of association between these species does not change after EGF stimulation. SHIP-2 membrane localization is dependent on filamin expression, as membrane association was not detected in a well-characterized melanoma cell line, which does not express filamin. The association of SHIP-2 with filamin serves to regulate PtdIns(3,4,5)P_3 and β-actin at membrane ruffles.

Inositol polyphosphate 5-phosphatases and the cytoskeleton

Increasing evidence indicates that both mammalian and yeast 5-phosphatase isoforms, via hydrolysis of PtdIns(4,5)P_2 and or PtdIns(3,4,5)P_3, play a significant role in regulating cytoskeletal reorganization. The 5-phosphatases comprise 10 mammalian and 4 yeast isoforms with many spliced variants described. Null mutation of any two yeast Sac-1 domain containing 5-phosphatases results in a phenotype which includes disorganization of polymerized actin and delocalization of actin patches from the growing yeast bud to the mother cell (for review see Hughes et al., 2000). The yeast 5-phosphatases, Inp52p and Inp53p, translocate to actin patches upon osmotic stress, the site of plasma membrane invaginations. In addition, overexpression of Inp52p and Inp53p, but not catalytically inactive Inp52p, results in a significant reduction in the repolarization time of actin patches after osmotic stress (Ooms et al., 2000). The mammalian 5-phosphatase, synaptojanin-1, hydrolyses PtdIns(4,5)P_2 bound to the actin regulatory proteins, α-actinin, vinculin, gelsolin, and profilin, and decreases the number of stress fibers in the cell (Sakisaka et al., 1997). Synaptojanin-2 directly interacts with Rac1 in a GTP-dependent manner, resulting in translocation of the 5-phosphatase to membrane ruffles and inhibition of endocytosis (Malecz et al., 2000). Overexpression of SKIP (skeletal muscle and kidney-enriched inositol phosphatase) results in loss of actin stress fibers in areas of SKIP expression (Ijuin et al., 2000). The recently identified proline-rich inositol polyphosphate 5-phosphatase (PIPP) localizes to membrane ruffles, but unlike SHIP-2 does not appear to regulate the actin cytoskeleton (Mochizuki and Takenawa, 1999). SHIP-2 regulation of submembraneous actin levels is most probably mediated via localized regulation of PtdIns(3,4,5)P_3. However, both SHIP-1 and SHIP-2 also hydrolyze PtdIns(4,5)P_2, forming PtdIns(4)P (Kisseleva et al., 2000; Taylor et al., 2000).

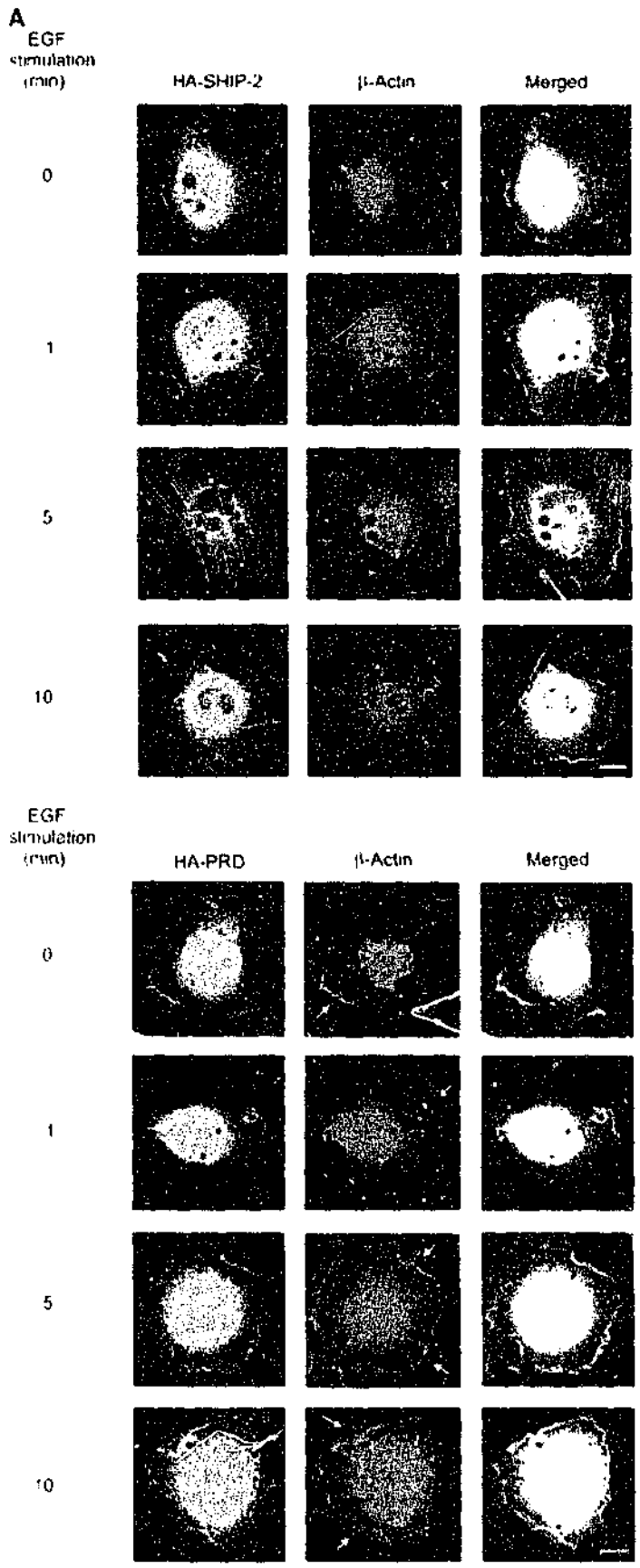

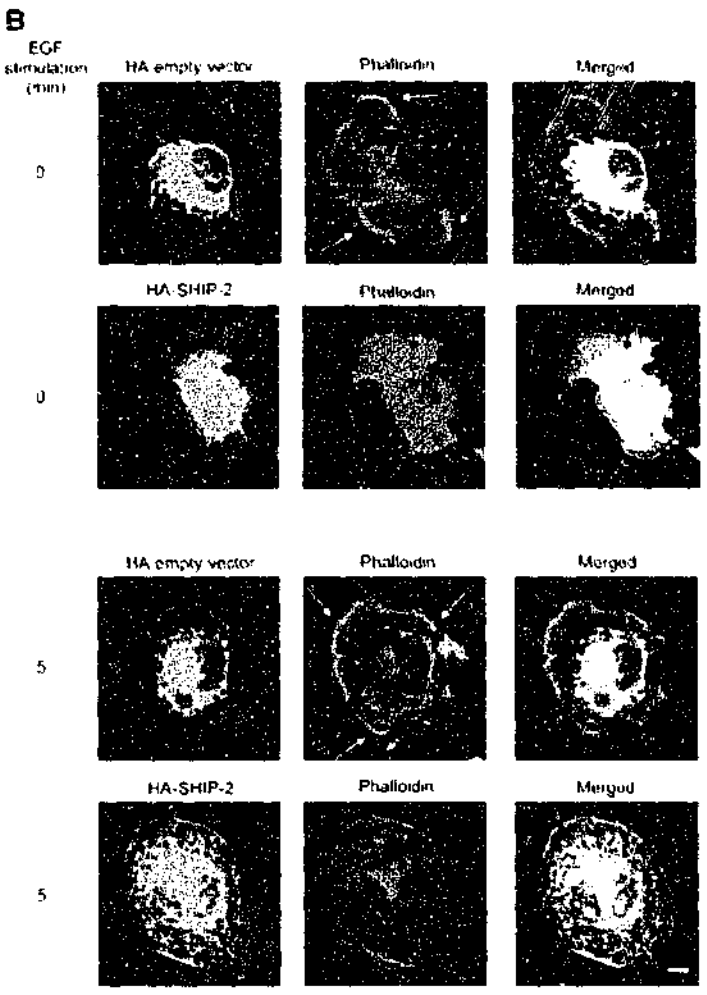

Figure 9. **SHIP-2 regulates β-actin expression at membrane ruffles.** (A) COS-7 cells were transiently transfected with either HA–SHIP-2 or HA-PRD. Where indicated, cells were treated with EGF (100 ng/ml) for 1, 5, or 10 min. Cells were fixed and costained with HA and β-actin antibodies and visualized by confocal microscopy. Arrows indicate areas of high β-actin expression. (B) COS-7 cells were transiently transfected with either HA–SHIP-2 or HA empty vector. Where indicated, cells were treated with EGF (100 ng/ml) for 5 min. Cells were fixed and stained with HA antibodies and actin stained with phalloidin. Cells were visualized by confocal microscopy. Arrows indicate areas of high phalloidin staining. Bars, 20 μm.

Role of SHIP-2 association with FLNC in insulin signaling

The recent characterization of SHIP-2 homozygous null mice has demonstrated that this 5-phosphatase plays a significant role in regulating insulin sensitivity (Clement et al., 2001). Although the signaling pathways mediating the phenotype of insulin hypersensitivity have yet to be fully determined, insulin-stimulated GLUT4 translocation to the plasma membrane appears to be enhanced in mice lacking SHIP-2. In addition, overexpression of SHIP-2, but not catalytically inactive SHIP-2, in 3T3-L1 adipocytes results in negative regulation of insulin-induced signaling (Wada et al., 2001). The submembraneous actin microfilament network links various signaling proteins, including IRS-1 and PI-3 kinase, that regulate GLUT4 translocation to the plasma membrane. Insulin-induced reorganization of the subplasma membrane actin filaments may allow exocytic GLUT4 vesicles to fuse with the plasma mem-

brane during stimulation by insulin (Khayat et al., 2000). GLUT4 expression is restricted to muscle and adipose tissue. Insulin-stimulated glucose disposal in skeletal muscle accounts for 80% of glucose uptake postprandial (Khayat et al., 2000), localizing GLUT4 to the sarcolemma. Filamin may provide a scaffold for the juxtaposition of SHIP-2 to the sarcolemma, localizing the enzyme to PtdIns(3,4,5)P_3 after insulin treatment and thereby regulating GLUT4 translocation.

Filamin forms a scaffold for the binding of Rho GTPases, including Rac1, Cdc42, Rho A, and RalA, and their activators such as Trio, a Rho guanine nucleotide exchange factor (GEF) (Ohta et al., 1999). The localization of both Rho GTPases and their activators on filamin may allow spatial coordination of actin nucleation at sites where newly assembled actin filaments are cross-linked. It is noteworthy that many filamin-binding proteins, including Trio and SHIP-2, bind to the extreme COOH-terminal repeats 21–24 of filamin, by a variety of interacting modules, including proline-rich domains, as is the case for SHIP-2 and PH domains as shown for Trio. This would therefore provide close proximity between all these signaling proteins, including SHIP-2, that regulate actin polymerization on a filamin scaffold.

Several recent studies in fibroblasts and the neutrophil cell line HL60 have demonstrated using the PH domain of PtdIns(3,4,5)P_3-binding proteins fused to GFP, that PI-3 kinase signals are generated at the leading edge of the cell (Blomberg et al., 1999; Watton and Downward, 1999; Balla et al., 2000; Servant et al., 2000). These PH domains function as an accurate probe for the localized agonist-dependent accumulation of PtdIns(3,4,5)P_3. It has been proposed, but not previously shown, that this asymmetric distribution of PtdIns(3,4,5)P_3 may result from its localized synthesis or degradation (Rickert et al., 2000). The results of the study reported here are consistent with this contention. We have shown the spatially controlled synthesis of PtdIns(3,4,5)P_3 at membrane ruffles is regulated by the PtdIns(3,4,5)P_3 5-phosphatase SHIP-2, which also localizes to membrane ruffles.

We have demonstrated SHIP-2 localization to membrane ruffles is mediated by its COOH-terminal proline-rich domain binding to the actin binding protein filamin. The expression of SHIP-2 in filamin deficient cells is exclusively cytosolic. In addition, SHIP-2 membrane localization appears to contribute to localized PtdIns(3,4,5)P_3 hydrolysis. SHIP-2 COOH-terminal truncation mutants were not as efficient at regulating PtdIns(3,4,5)P_3 at membrane ruffles as intact SHIP-2. Furthermore, displacement of endogenous SHIP-2 by overexpression of the SHIP-2 filamin binding domain (myc filamin aa 2434–2705) lead to the marked enhancement of the PI-3 kinase signal PtdIns(3,4,5)P_3. Several recent reports have shown the membrane localization of the highly related SHIP-2 homologue SHIP-1 is also important for PtdIns(3,4,5)P_3 hydrolysis (Phee et al., 2000). Enforced plasma membrane localization of SHIP-1, mediated by overexpression of a human CD8–SHIP-1 chimera, decreased the total cellular levels of PtdIns(3,4,5)P_3. Membrane targeting of SHIP-1 mediated by the COOH-terminal proline-rich domain appears to be important in B cell inhibitory function (Aman et al., 2000). In addition, the SHIP-1 COOH terminus is essential for PtdIns(3,4,5)P_3 hydrolysis and inhibition of mast cell degranulation (Damen et al., 2001). Collectively, these studies show membrane targeting of these two 5-phosphatases mediated by their respective COOH-terminal proline-rich domains plays an important functional role in regulating PI-3 kinase signals.

SHIP-2 associates with the $p130^{Cas}$ adaptor protein at focal adhesions and regulates cell spreading, which is dependent on the SHIP-2 SH2 domain and is enhanced by tyrosine phosphorylation and cell adhesion (Prasad et al., 2001). We have shown SHIP-2 and filamin also form a functionally significant complex both in the resting cells and after cellular activation at membrane ruffles. We therefore propose the binding of SHIP-2 to filamin provides a mechanism for exquisite localized hydrolysis of PtdIns(3,4,5)P_3 in resting, growth factor– and insulin–stimulated cells at the leading edge of cell.

Materials and methods

Restriction and DNA-modifying enzymes were obtained from New England Biolabs, Inc., Fermentas, or Promega. Big dye terminator cycle sequencing was from PE Applied Systems. Synthetic peptides were from Chiron Mimotopes. COS-7 cells were purchased from the American Type Culture Collection. M2 and A7 cell lines were a gift from Dr. T. Stossel (Brigham and Women's Hospital, Boston, MA). Oligonucleotides were obtained from Bresatec and the Department of Microbiology, Monash University, Melbourne, Australia. Partially purified rabbit polyclonal antibodies to human filamin B were a gift from Dr. Dominic Chung (Department of Biochemistry, University of Washington School of Medicine, WA). Goat polyclonal antibodies to chicken gizzard filamin and monoclonal antibodies to α-actinin (α-actinin) and FLAG were obtained from Sigma-Aldrich. Monoclonal antibodies to HA were obtained from Silenus, GFP antibodies were from Buehringer, β-actin antibodies were from Sigma-Aldrich, and antifilamin antibodies (raised to platelet filamin) were from Chemicon. Phalloidin stain was obtained from Molecular Probes. The GFP-PH/ARNO construct was a gift from Dr. Tamas Balla (National Institutes of Health, Bethesda, MD). The yeast two-hybrid system Matchmaker 3 and the pEGFP-C2 vector were obtained from CLONTECH Laboratories, Inc. and the pCGN vector was a gift from Dr. Tony Tiganis (Monash University, Melbourne, Australia). pEFBOS-Myc and pEFBOS-FLAG vectors were a gift from Dr. Tracey Willson (Walter and Eliza Hall Institute of Medical Research, Melbourne, Australia). Filamin A and B cDNAs were a gift from Dr. Joe Trapani and Kylie Browne (Peter MacCallum Cancer Institute, Melbourne, Australia). All other reagents were from Sigma-Aldrich unless otherwise stated.

Production of antipeptide antibodies

SHIP-2 antipeptide antibodies were generated to a fusion peptide comprising the NH_2-terminal seven amino acids of SHIP-2 fused to the COOH-terminal seven amino acids of SHIP-2 (MASACGADTLQLSK) (SHIP-2NC), or to the amino acid sequence, 1019–1030 (ITVPAPQLGHHRH) (SHIP-2P). SHIP-2NC antibodies were used for all experiments except indirect immunofluorescence of COS-7, M2, and A7 cells in which the SHIP-2P antibody was used. Peptide conjugated to diphtheria toxoid was injected subcutaneously into female New Zealand white rabbits. Affinity-purified antipeptide antibodies were obtained by chromatography of immune sera on the specific peptide coupled to thiopropyl-Sepharose 6B resin. After extensive washing, specific antibodies were eluted from the column with 0.1 M glycine-HCl, pH 2.5.

Generation of full-length SHIP-2 and SHIP-2 truncation mutants

Human SHIP-2 cDNA was generated by ligation of EST aa 279072 to the cDNA encoding INPPL-1, obtained from Dr. James Hejna (Oregon Health Sciences University, Portland, OR) (Hejna et al., 1995). Several rounds of PCR amplification enabled prolongation of the 5′-end of the clone to encompass SHIP-2 nucleotides 257–3988, which correspond to aa 16–1258 plus a COOH-terminal hexa-His-tag. SHIP-2 cDNA was cloned in-frame into pCGN (XbaI site), pEGFP-C2 (EcoRI site) and pEFBOS (MluI site) vectors, that encode for HA, GFP, and FLAG-tagged SHIP-2 fusion proteins, respectively, using PCR amplification with the introduction of specific restriction sites. Truncation mutants of SHIP-2 were also generated and were subsequently cloned into the XbaI site of pCGN. The oligonucleotide sequences and a description of the constructs generated are listed in Table I. Fidelity of all PCR products and the final constructs was confirmed by dideoxy sequencing.

Table II. **Oligonucleotides used for the generation of FLNC truncation mutants in pGADT7**

Name of construct	5′ oligonucleotide	3′ oligonucleotide	FLNC polypeptide expressed
pFLNCΔR24	5′-cgaattctgctacgtctctgagctg-3′	5′-cgaattctcaggcatctgaggagaactt-3′	Nucleotides 2,434–2,476 of repeat 22 and 23 and Hinge II region; aa 2,654–2,705
pFLNCΔH2ΔR24	5′-cgaattctgctacgtctctgagctg-3′	5′-cgaattctcacagcctcggaccagtgac-3′	Nucleotides 2,434–2,476 of repeat 22 and 23; aa 2,434–2,578
pFLNCΔR22	5′-cgaattcatgcccttcaagatccgcgttg-3′	5′-ggaattctcaagggaccttgacttg-3′	Repeat 23 and 24 and Hinge II region; aa 2,471–2,705
pFLNCR23H2	5′-cgaattcatgcccttcaagatccgcgttg-3′	5′-cgaattctcaggcatctgaggagaactt-3′′	Repeat 23 and Hinge II region; aa 2,471–2614
pFLNCR22 alone	5′-cgaattctgctacgtctctgagctg-3′	5′-gaattctcaagcctggctctgctcccc-3′	Nucleotides 2,434–2,476 of repeat 22; aa 2,434–2,481
pFLNCR23 alone	5′-cgaattcatgcccttcaagatccgcgttg-3′	5′-cgaattctcacagcctcggaccagtgac-3′	Repeat 23; aa 2,471– to 2,577
pFLNC24 alone	5′-cgaattcatgagctacagctccatcccc-3′	5′-cgaattctcaagggaccttgacttg-3′	Repeat 24; aa 2,602–to 2,705

Yeast two-hybrid analysis

The yeast two-hybrid Matchmaker III GAL4-based system was used for all yeast two-hybrid studies. The proline-rich domain of human SHIP-2 comprising nucleotides 3017–3989 (aa 936–1258), was cloned into the EcoRI site of pGBKT7, creating a GAL4 fusion protein, the "bait." "Bait" protein-expressing yeast (AH109) were transformed with human skeletal muscle cDNA library (CLONTECH Laboratories, Inc.) according to the manufacturer's guidelines. Yeast plasmid was extracted from positive clones as described (Ausubel et al., 1991).

SHIP-2 proline-rich domain–expressing yeast were transformed with filamin A and B isoforms cDNA (aa 2171–2647 and 2130–2602, respectively) to investigate an interaction. Specificity of the interactions with the SHIP-2 proline-rich domain was confirmed using a p53 "bait." In addition, a "bait" lacking the proline-rich domain of SHIP-2, but containing the SH2 domain and 5-phosphatase domain (comprising nucleotides 210–3016) was constructed using a PCR based strategy and was also used as a negative control "bait."

Immunoblot of endogenous SHIP-2, HA, and GFP-tagged SHIP-2 constructs

M2 and A7 cells were maintained as described (Cunningham et al., 1992; Ohta et al., 1999). COS-7 cells were maintained in DME, 10% (vol/vol) fetal calf serum containing 2 mM glutamine, and transfected using the DEAE-dextran procedure and allowed to grow for 2 d (Sambrook and Russel, 2001). Cells were washed briefly with PBS and treated with lysis buffer (50 mM Tris, pH 8.0, 150 mM NaCl, 1% Triton X-100, 2 mM EDTA (ethylenediaminetetraacetic acid DI-sodium salt), 1 mM benzamidine, 2 mM phenylmethylsulfonylfluoride, 2 μg/ml leupeptin, and 2 μg/ml aprotinin) for 2 h at 4°C. Lysates were centrifuged at 15,400 *g* for 10 min to obtain the Triton X-100–soluble supernatant which was analyzed by immunoblot analysis using antibodies to the specific tag, affinity-purified SHIP-NC sera, or antifilamin antibodies.

Intracellular localization of SHIP-2 in COS-7 cells

COS-7 cells were transiently transfected with GFP-SHIP-2, Myc-filamin, HA–SHIP-2, HA-SHIP-2ΔPRD, HA–SHIP-2ΔSH2, or HA-PRD truncation mutants (Table I), fixed/permeabilized, and stained. Alternatively, in some studies, 24 h after transfection, cells were placed in DME containing 0.1% FCS and 2 mM glutamate for a period of ~15 h and then stimulated with EGF (100 ng/ml). Cells expressing GFP-tagged proteins were gently washed with PBS and fixed with 3.7% formaldehyde. Cells expressing Myc and HA-tagged proteins were gently washed with PBS and then fixed and permeabilized for 10 min in PBS with 3.7% formaldehyde and 0.2% Triton X-100. Expression of Myc and HA-tagged proteins was localized using Myc and HA monoclonal antibodies and detected using tetramethylrhodamine isothiocyanate–conjugated TRITC anti-mouse IgG and fluorescein isothiocyanate–conjugated FITC anti–mouse IgG, respectively. Endogenous SHIP-2 was detected in nontransfected and Myc-filamin–transfected cells using the SHIP-2P antibody and FITC anti–rabbit IgG. Colocalization was performed using antibodies to filamin B detected with tetramethylrhodamine isothiocyanate–conjugated TRITC anti–rabbit IgG and specific actin markers, either phalloidin staining and/or antibodies to β-actin detected using TRITC anti–mouse IgG. Coverslips were mounted using SlowFade and visualized by confocal microscopy.

Immunoprecipitations

COS-7 cells were transfected via electroporation (Sambrook and Russel, 2001) and either harvested in lysis buffer 48 h posttransfection or EGF stimulated for 1 or 5 min as outlined above and harvested. Transfected and nontransfected cells were harvested and Triton X-100 extracted as outlined above. Triton X-100–soluble lysates were immunoprecipitated with either 10 μg of monoclonal FLAG or HA antibody, 5 μg of polyclonal anti–SHIP-2NC sera or preimmune sera and 60 μl of 50% slurry of protein A–Sepharose. Immunoprecipitates were immunoblotted with either FLAG, Myc, or filamin monoclonal antibodies.

Intracellular localization of SHIP-2 in A7 and M2 cells

Human filamin–deficient melanoma cell line (M2) and full-length filamin replete cell line (A7) were maintained as described (Cunningham et al., 1992; Ohta et al., 1999). Endogenous SHIP-2 was localized in resting and EGF-treated A7 and M2 cells as described above for COS-7 cells.

Assessment of β-actin, phalloidin, or GFP-PH/ARNO staining

COS-7 cells were transiently transfected via DEAE dextran-chloroquine with HA–SHIP-2 or HA-PRD, stimulated for 5 min with EGF (100 ng/ml), and costained with HA- and β-actin–specific antibodies, as outlined above. Cells were assessed for β-actin staining at the plasma membrane as a percentage of the total transfected cells. COS-7 cells were transiently transfected with HA–SHIP-2 or empty vector HA, stimulated for 5 min with EGF (100 ng/ml), and costained with HA antibodies and phalloidin. Cells were scored for phalloidin staining. COS-7 cells were transiently cotransfected with HA–SHIP-2, HA-SHIP2ΔPRD, or HA-PRD, or myc-filamin and GFP fused to the PH domain of ARNO, (GFP-PH/ARNO), or empty vector HA and GFP-PH/ARNO, stimulated for 5 min with EGF (100 ng/ml), and stained with HA antibody as outlined above. Cells were assessed for GFP-PH/ARNO expression at the plasma membrane. Approximately 40 cells were scored by an independent observer for each experiment.

Generation of FLNC truncation mutants

A PCR-based strategy was employed to generate FLNC truncation mutants which were subcloned into the EcoRI site of pGADT7, creating HA-tagged GAL4 recombinant proteins. The oligonucleotide and construct descriptions are given in Table II. Nucleotides 2,434–3,252 of FLNC was subcloned into the XbaI site and MluI site of pCGN and pEFBOS-Myc tagged, respectively. Fidelity of all PCR products and the final constructs were confirmed by dideoxy sequencing.

Localization of SHIP-2 and filamin in murine heart and soleus muscle

Mice were killed humanely following National Health and Medical Research Council guidelines, Monash University animal ethics number BAM/B/2000/17. Murine heart and soleus were dissected from 12-wk-old male mice, C57B/6. Organs were snap frozen in isopentane chilled with liquid nitrogen and blocked in OCT (10.24% wt/wt polyvinyl alcohol, 4.26% wt/wt polyethylene glycol, and 85.5% wt/wt nonreactive ingredients) compound and stored at −70°C until used. Blocks were equilibrated to −20°C before sectioning. Cross-sections and longitudinal sections were cut 7-μm thick and placed on superfrost plus slides before staining. They were then fixed in PBS/4% paraformaldehyde for 5 min at room temperature, washed with PBS, then blocked and permeablized with PBS, 10% horse serum, and 0.1% Triton X-100 for 15 min at room temperature. Slides were washed and stained with anti–SHIP-2NC sera, and detected with FITC anti–rabbit IgG. Antifilamin was detected with TRITC anti–goat IgG and anti-α-actinin was detected with TRITC anti–rabbit IgG; overnight incubation at 4°C. Sections were washed with PBS, mounted using SlowFade, and visualized by confocal microscopy.

We thank Drs. Tony Tiganis, Raju Gurung, and Susan Brown (Monash University, Clayton, Australia) for advice and helpful discussions; and Meagan McGrath and all members of the Mitchell laboratory for technical advice. Confocal images were obtained at the Biomedical Confocal Imaging Facility of Monash University.

Cindy O'Malley was funded by an Anti-Cancer Council of Victoria scholarship. This work was funded by the National Health and Medical Research Council of Australia.

Submitted: 2 April 2001
Revised: 28 September 2001
Accepted: 19 October 2001

References

Aman, M.J., S.F. Walk, M.E. March, H.P. Su, D.J. Carver, and K.S. Ravichandran. 2000. Essential role for the C-terminal noncatalytic region of SHIP in FcγRIIB1-mediated inhibitory signaling. *Mol. Cell. Biol.* 20:3576–3589.

Ausubel, F.M., R. Brent, R.E. Kingston, D.D. Moore, J.G. Seidman, J.A. Smith, and K. Struhl. 1991. Current protocols in molecular biology. John Wiley and Sons, Inc., New York.

Balla, T., T. Bondeva, and P. Varnai. 2000. How accurately can we image inositol lipids in living cells? *Trends Pharmacol. Sci.* 21:238–241.

Blero, D., F. De Smedt, X. Pesesse, N. Paternotte, C. Moreau, B. Payrastre, and C. Erneux. 2001. The SH2 domain containing inositol 5-phosphatase SHIP2 controls phosphatidylinositol 3,4,5-trisphosphate levels in CHO-IR cells stimulated by insulin. *Biochem. Biophys. Res. Commun.* 282:839–843.

Blomberg, N., E. Baraldi, M. Nilges, and M. Saraste. 1999. The PH superfold: a structural scaffold for multiple functions. *Trends Biochem Sci.* 24:441–445.

Cantley, L.C., and B.G. Neel. 1999. New insights into tumor suppression: PTEN suppresses tumor formation by restraining the phosphoinositide 3-kinase/AKT pathway. *Proc. Natl. Acad. Sci. USA.* 96:4240–4245.

Clement, S., U. Krause, F. Desmedt, J.-F. Tanti, J. Behrends, X. Pesesse, T. Sasaki, J. Penninger, M. Doherty, W. Malaisse, et al. 2001. The lipid phosphatase SHIP2 controls insulin sensitivity. *Nature.* 409:92–97.

Corvera, S., A. D'Arrigo, and H. Stenmark. 1999. Phosphoinositides in membrane traffic. *Curr. Opin. Cell Biol.* 11:460–465.

Cunningham, C.C., J.B. Gorlin, D.J. Kwiatkowski, J.H. Hartwig, P.A. Janmey, H.R. Byers, and T.P. Stossel. 1992. Actin-binding protein requirement for cortical stability and efficient locomotion. *Science.* 255:325–327.

Damen, J.E., M.D. Ware, J. Kalesnikoff, M.R. Hughes, and G. Krystal. 2001. SHIP's C-terminus is essential for its hydrolysis of PIP3 and inhibition of mast cell degranulation. *Blood.* 97:1343–1351.

Datta, S.R., A. Brunet, and M.E. Greenberg. 1999. Cellular survival: a play in three Akts. *Genes Dev.* 13:2905–2927.

Fedorov, A.A., E. Fedorov, F. Gertler, and S.C. Almo. 1999. Structure of EVH1, a novel proline-rich ligand-binding module involved in cytoskeletal dynamics and neural function. *Nat. Struct. Biol.* 6:661–665.

Gorlin, J.B., R. Yamin, S. Egan, M. Stewart, T.P. Stossel, D.J. Kwiatkowski, and J.H. Hartwig. 1990. Human endothelial actin-binding protein (ABP-280, nonmuscle filamin): a molecular leaf spring. *J. Cell Biol.* 111:1089–1105.

Habib, T., J.A. Hejna, R.E. Moses, and S.J. Decker. 1998. Growth factors and insulin stimulate tyrosine phosphorylation of the 51C/SHIP2 protein. *J. Biol Chem.* 273:18605–18609.

Hejna, J.A., H. Saito, L.S. Merkens, T.V. Tittle, P.M. Jakobs, M.A. Whitney, M. Grompe, A.S. Friedberg, and R.E. Moses. 1995. Cloning and characterization of a human cDNA (INPPL1) sharing homology with inositol polyphosphate phosphatases. *Genomics.* 29:285–287.

Hughes, W.E., F.T. Cooke, and P.J. Parker. 2000. Sac phosphatase domain proteins. *Biochem. J.* 350:337–352.

Ijuin, T., Y. Mochizuki, K. Fukami, M. Funaki, T. Asano, and T. Takenawa. 2000. Identification and characterization of a novel inositol polyphosphate 5-phosphatase. *J. Biol. Chem.* 275:10870–10875.

Ishihara, H., T. Sasaoka, H. Hori, T. Wada, H. Hirai, T. Haruta, W.J. Langlois, and M. Kobayashi. 1999. Molecular cloning of rat SH2-containing inositol phosphatase 2 (SHIP2) and its role in the regulation of insulin signaling. *Biochem. Biophys. Res. Commun.* 260:265–272.

Khan, A.H., D.C. Thurmond, C. Yang, B.P. Ceresa, and J.E. Pessin. 2000. Munc18c regulates insulin-stimulated GLUT4 translocation to the transverse tubules in skeletal muscle. *J. Biol. Chem.* 38:12.

Khayat, Z.A., P. Tong, K. Yaworsky, R.J. Bloch, and A. Klip. 2000. Insulin-induced actin filament remodeling colocalizes actin with phosphatidylinositol 3-kinase and GLUT4 in L6 myotubes. *J. Cell Sci.* 113:279–290.

Kisseleva, M.V., M.P. Wilson, and P.W. Majerus. 2000. The isolation and characterization of a cDNA encoding phospholipid-specific inositol polyphosphate 5-phosphatase. *J. Biol. Chem.* 275:20110–20116.

Maestrini, E., C. Patrosso, M. Mancini, S. Rivella, M. Rocchi, M. Repetto, A. Villa, A. Frattini, M. Zoppe, P. Verzoni, et al. 1993. Mapping of two genes encoding isoforms of the actin binding protein ABP-280, a dystrophin like protein, to Xq28 and to chromosome 7. *Hum. Mol. Genet.* 2:761–766.

Majerus, P.W. 1996. Inositols do it all. *Genes Dev.* 10:1051–1053.

Malecz, N., P.C. McCabe, C. Spaargaren, R. Qiu, Y. Chuang, and M. Symons. 2000. Synaptojanin 2, a novel rac1 effector that regulates clathrin-mediated endocytosis. *Curr. Biol.* 10:1383–1386.

Martin, T.F. 1997. Phosphoinositides as spatial regulators of membrane traffic. *Curr. Opin. Neurobiol.* 7:331–338.

Mochizuki, Y., and T. Takenawa. 1999. Novel inositol polyphosphate 5-phosphatase localizes at membrane ruffles. *J. Biol. Chem.* 274:36790–36795.

Ohta, Y., N. Suzuki, S. Nakamura, J.H. Hartwig, and T.P. Stossel. 1999. The small GTPase RalA targets filamin to induce filopodia. *Proc. Natl. Acad. Sci. USA.* 96:2122–2128.

Ooms, L.M., B.K. McColl, F. Wiradjaja, A.P. Wijayaratnam, P. Gleeson, M.J. Gething, J. Sambrook, and C.A. Mitchell. 2000. The yeast inositol polyphosphate 5-phosphatases np52p and np53p translocate to actin patches following hyperosmotic stress: mechanism for regulating phosphatidylinositol 4,5-bisphosphate at plasma membrane invaginations. *Mol. Cell. Biol.* 20:9376–9390.

Pesesse, X., S. Deleu, F. De Smedt, L. Drayer, and C. Erneux. 1997. Identification of a second SH2-domain-containing protein closely related to the phosphatidylinositol polyphosphate 5-phosphatase SHIP. *Biochem. Biophys. Res. Commun.* 239:697–700.

Pesesse, X., V. Dewaste, F. De Smedt, M. Laffargue, S. Giuriato, C. Moreau, B. Payrastre, and C. Erneux. 2001. The SH2 domain containing inositol 5-phosphatase SHIP2 is recruited to the EGF receptor and dephosphorylates phosphatidylinositol 3,4,5-trisphosphate in EGF stimulated COS-7 cells. *J. Biol. Chem.* 10:10.

Phee, H., A. Jacob, and K.M. Coggeshall. 2000. Enzymatic activity of the Src homology 2 domain-containing inositol phosphatase is regulated by a plasma membrane location. *J. Biol. Chem.* 275:19090–19097.

Prasad, N., R.S. Topping, and S.J. Decker. 2001. SH2-containing inositol 5′-phosphatase SHIP2 associates with the p130(Cas) adapter protein and regulates cellular adhesion and spreading. *Mol. Cell. Biol.* 21:1416–1428.

Rickert, P., O.D. Weiner, F. Wang, H.R. Bourne, and G. Servant. 2000. Leukocytes navigate by compass: roles of PI3Kgamma and its lipid products. *Trends Cell Biol.* 10:466–473.

Sakisaka, T., T. Itoh, K. Miura, and T. Takenawa. 1997. Phosphatidylinositol 4,5-bisphosphate phosphatase regulates the rearrangement of actin filaments. *Mol. Cell. Biol.* 17:3841–3849.

Sambrook, J., and D.W. Russel. 2001. Molecular Cloning: A Laboratory Manual. Cold Spring Harbor Laboratory Press, Cold Spring Harbor, NY.

Servant, G., O.D. Weiner, P. Herzmark, T. Balla, J.W. Sedat, and H.R. Bourne. 2000. Polarization of chemoattractant receptor signaling during neutrophil chemotaxis. *Science.* 287:1037–1040.

Stossel, T.P., J. Condeelis, L. Cooley, J.H. Hartwig, A. Noegel, M. Schleicher, S. Shapiro. 2001. Filamin as integrators of cell mechanics and signalling. *Nat. Rev.* 2:138–145.

Takafuta, T., G. Wu, G.F. Murphy, and S.S. Shapiro. 1998. Human beta-filamin is a new protein that interacts with the cytoplasmic tail of glycoprotein Ibalpha. *J. Biol. Chem.* 273:17531–17538.

Taylor, V., M. Wong, C. Brandts, L. Reilly, N.M. Dean, L.M. Cowsert, S. Moodie, and D. Stokoe. 2000. 5′ phospholipid phosphatase SHIP-2 causes protein kinase B inactivation and cell cycle arrest in glioblastoma cells. *Mol. Cell. Biol.* 20:6860–6871.

Tsujishita, Y., S. Guo, L.E. Stolz, J.D. York, and J.H. Hurley. 2001. Specificity determinants in phosphoinositide dephosphorylation: crystal structure of an archetypal inositol polyphosphate 5-phosphatase. *Cell.* 105:379–389.

van der Ven, P.F., W.M. Obermann, B. Lemke, M. Gautel, K. Weber, and D.O. Furst. 2000. Characterization of muscle filamin isoforms suggests a possible role of gamma-filamin/ABP-L in sarcomeric Z-disc formation. *Cell Motil. Cytoskeleton.* 45:149–162.

Wada, T., T. Sasaoka, M. Funaki, H. Hori, S. Murakami, M. Ishiki, T. Haruta, T. Asano, W. Ogawa, H. Ishihara, and M. Kobayashi. 2001. Overexpression of SH2-containing inositol phosphatase 2 results in negative regulation of insulin-induced metabolic actions in 3T3-L1 adipocytes via its 5′-phosphatase catalytic activity. *Mol. Cell. Biol.* 21:1633–1646.

Warton, S.J., and J. Downward. 1999. Akt/PKB localisation and 3' phosphoinositide generation at sites of epithelial cell-matrix and cell-cell interaction. *Curr. Biol.* 9:433–436.

Whisstock, J.C., S. Romero, R. Gurung, H. Nandurkar, L.M. Ooms, S.P. Bottomley, and C.A. Mitchell. 2000. The inositol polyphosphate 5-phosphatases and the Apurinic/Apyrimidinic base excision repair endonucleases share a common mechanism for catalysis. *J. Biol. Chem.* 275:37055–37061.

Wisniewski, D., A. Strife, S. Swendeman, H. Erdjument-Bromage, S. Geromanos, W.M. Kavanaugh, P. Tempst, and B. Clarkson. 1999. A novel SH2-containing phosphatidylinositol 3,4,5-trisphosphate 5-phosphatase (SHIP2) is constitutively tyrosine phosphorylated and associated with src homologous and collagen gene (SHC) in chronic myelogenous leukemia progenitor cells. *Blood.* 93:2707–2720.

Xie, Z., W. Xu, E.W. Davie, and D.W. Chung. 1998. Molecular cloning of human ABPL, an actin-binding protein homologue. *Biochem Biophys. Res. Commun.* 251:914–919.

Xu, W., Z. Xie, D.W. Chung, and E.W. Davie. 1998. A novel human actin-binding protein homologue that binds to platelet glycoprotein Ibalpha. *Blood.* 92:1268–1276.

IUBMB *Life*, 53: 25–36, 2002

1521-6543/02 $12.00 + .00

Review Article

Inositol Polyphosphate 5-Phosphatases: Lipid Phosphatases With Flair

Christina A. Mitchell, Rajendra Gurung, Anne M. Kong, Jennifer M. Dyson, April Tan, and Lisa M. Ooms

Department of Biochemistry and Molecular Biology, Monash University, Victoria, 3800, Australia

Summary

Recent studies have identified the inositol polyphosphate 5-phosphatases as a large family of signal modifying enzymes comprising 10 mammalian and 4 yeast family members. A number of investigations including gene-targeted deletion of 5-phosphatases in mice have demonstrated that these enzymes regulate many important cellular events including hematopoietic cell proliferation and activation, insulin signaling, endocytosis, and actin polymerization.
IUBMB *Life*, 53: 25–36, 2002

Keywords Actin cytoskeleton; B cell proliferation; calcium signaling; inositol 5-phosphatase; insulin signaling; vesicle trafficking.

CELLULAR FUNCTIONS OF INOSITOL POLYPHOSPHATE 5-PHOSPHATASES

The phosphatidylinositols are phospholipids present in all mammalian cells, both on the inner wall of the plasma membrane and in various discrete subcellular compartments such as the Golgi, endoplasmic reticulum, endosomes, and nuclear membrane. In response to agonist stimulation by growth factors, neurotransmitters, hormones, and peptide agonists, phosphatidylinositols are phosphorylated by specific kinases and thereby generate multiple intracellular signals that include [1]PtdIns(4,5)P_2, PtdIns(3,4,5)P_3, and PtdIns(3,5)P_2. These signaling molecules induce a vast number of significant cellular events mediated by recruiting various effector proteins to the membrane and thereby contributing to their activation (Fig. 1; *1–7*). PtdIns(4,5)P_2 regulates actin polymerization, vesicular recycling, and serves as a precursor for Ins(1,4,5)P_3 mediated-intracellular calcium release. PtdIns(3,4,5)P_3 regulates cell proliferation, cell death, differentiation, actin polymerization, vesicular trafficking, insulin signaling, cell migration, and secretion. The inositol polyphosphate 5-phosphatases (5-phosphatases) dephosphorylate 5-position phosphoinositide and inositol phosphate messenger molecules resulting in either the generation of potentially new signaling molecules such as PtdIns(3,4)P_2, PtdIns 4-P, and PtdIns 3-P (Figs. 1 and 2), or molecules such as Ins(1,4)P_2 or Ins(1,3,4)P_3, which no longer mobilize intracellular calcium but may lead to other signaling pathways (Fig. 3). Therefore, the 5-phosphatases may act as signal generating, or signal terminating enzymes (*8, 9*).

The investigation of 5-phosphatase enzyme cellular function is complicated by the vast number of agonists that generate phosphoinositide synthesis; the diverse roles these various phosphoinositide signaling molecules play in cellular activation; the significant number of 5-phosphatases that have recently been identified, many of which are expressed in the same cell; the distinct subcellular localization of the various isoforms; the diverse number of potential substrates; and the difficulties in discriminating between the results of 5-phosphatase substrate specificity shown by in vitro enzyme assays using recombinant 5-phosphatases, versus the results shown by in vivo cellular models in which 5-phosphatases have been either overexpressed or underexpressed by gene-targeted deletion in mice, or by antisense studies in cell lines. This review focuses on recent studies that reveal the distinct functional roles specific 5-phosphatases play in regulating intracellular calcium release, synaptic vesicle recycling, actin polymerization, cell proliferation, and insulin signaling.

CALCIUM SIGNALING: REGULATION OF Ins(1,4,5)P_3 AND Ins(1,3,4,5)P_4

In nonexcitable cells Ins(1,4,5)P_3 stimulates calcium release from intracellular stores, followed by calcium influx across the

Received 24 October 2001; accepted 24 October 2001.

Address correspondence to Christina Mitchell, Dept. of Biochemistry and Molecular Biology, Monash University, P.O. Box 13D, Victoria 3800, Australia. E-mail: Christina.Mitchell@med.monash.edu.au

[1]Abbreviations: PtdIns, phosphatidylinositol; PI 3-kinase, phosphoinositide 3-kinase; SHIP, SH2-containing inositol 5-phosphatase; OCRL, oculocerebrorenal syndrome of Lowe; SKIP, skeletal muscle and kidney-enriched inositol 5-phosphatase; PtPP, proline-rich inositol polyphosphate 5-phosphatase; BCR, B cell receptor; ITIM, immunoreceptor tyrosine-based inhibition motif.

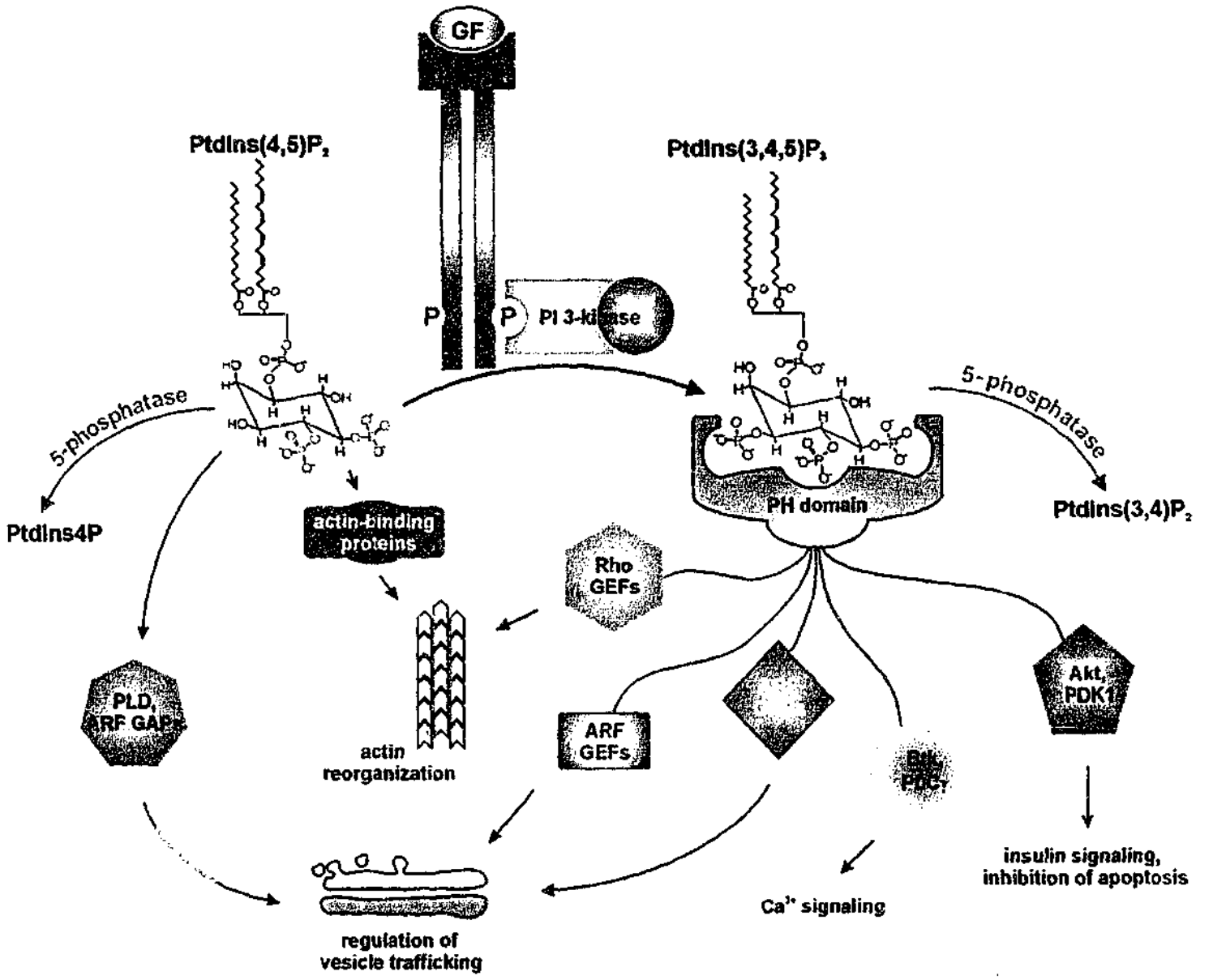

Figure 1. PtdIns(4,5)P_2 and PtdIns(3,4,5)P_3 signaling pathways. Growth factor (GF)-mediated activation of receptor tyrosine kinases (RTKs) leads to the activation of phosphoinositide 3-kinase (PI3-kinase) resulting in the synthesis of PtdIns(3,4,5)P_3 from PtdIns(4,5)P_2. Both PtdIns(3,4,5)P_3 and PtdIns(4,5)P_2 are involved in many intracellular signaling pathways. PtdIns(4,5)P_2 interacts with a number of actin-binding proteins and promotes actin polymerization. It is also involved in the regulation of a number of proteins required for vesicle trafficking. PtdIns(3,4,5)P_3 interacts with and modulates the activities and localizations of a number of PH domain-containing proteins, which regulate anti-apoptotic, B-cell proliferation, insulin signaling, membrane trafficking, and actin reorganization.

plasma membrane via store operated channels (SOCs). Intracellular calcium regulates a wide range of cellular processes including gene transcription, contraction, secretion, and cell proliferation (*10*, *11*). Ins(1,4,5)P_3 is rapidly metabolized, either by phosphorylation by a specific 3-kinase to Ins(1,3,4,5)P_4, which facilitates calcium entry at the plasma membrane; or Ins(1,4,5)P_3 is dephosphorylated by the 5-phosphatases to form inositol 1,4-bisphosphate (Ins(1,4)P_2), which does not release intracellular calcium (Fig. 3).

The 43-kDa 5-phosphatase (5-phosphatase I) is a widely expressed enzyme that hydrolyzes Ins(1,4,5)P_3 and Ins(1,3,4,5)P_4 forming Ins(1,4)P_2 and inositol 1,3,4-trisphosphate (Ins(1,3,4)P_3), respectively (*12*). This enzyme contains a central 5-phosphatase domain with a *C*-terminal CAAX motif that mediates localization of the enzyme to the inner wall of the plasma membrane, the site of Ins(1,4,5)P_3 production. Overexpression of the 43-kDa enzyme in CHO cells abrogates ATP-induced calcium oscillations (*13*). In contrast, underexpression of the 5-phosphatase using an anti-sense strategy results in increased Ins(1,4,5)P_3 levels, leading to increased sensitivity and amplitude of the calcium oscillations in response to both low- and high-dose agonist stimulation (*14*). Calcium oscillations regulate both activation of specific transcription factors and cell cycle progression. Cells underexpressing the 43-kDa 5-phosphatase

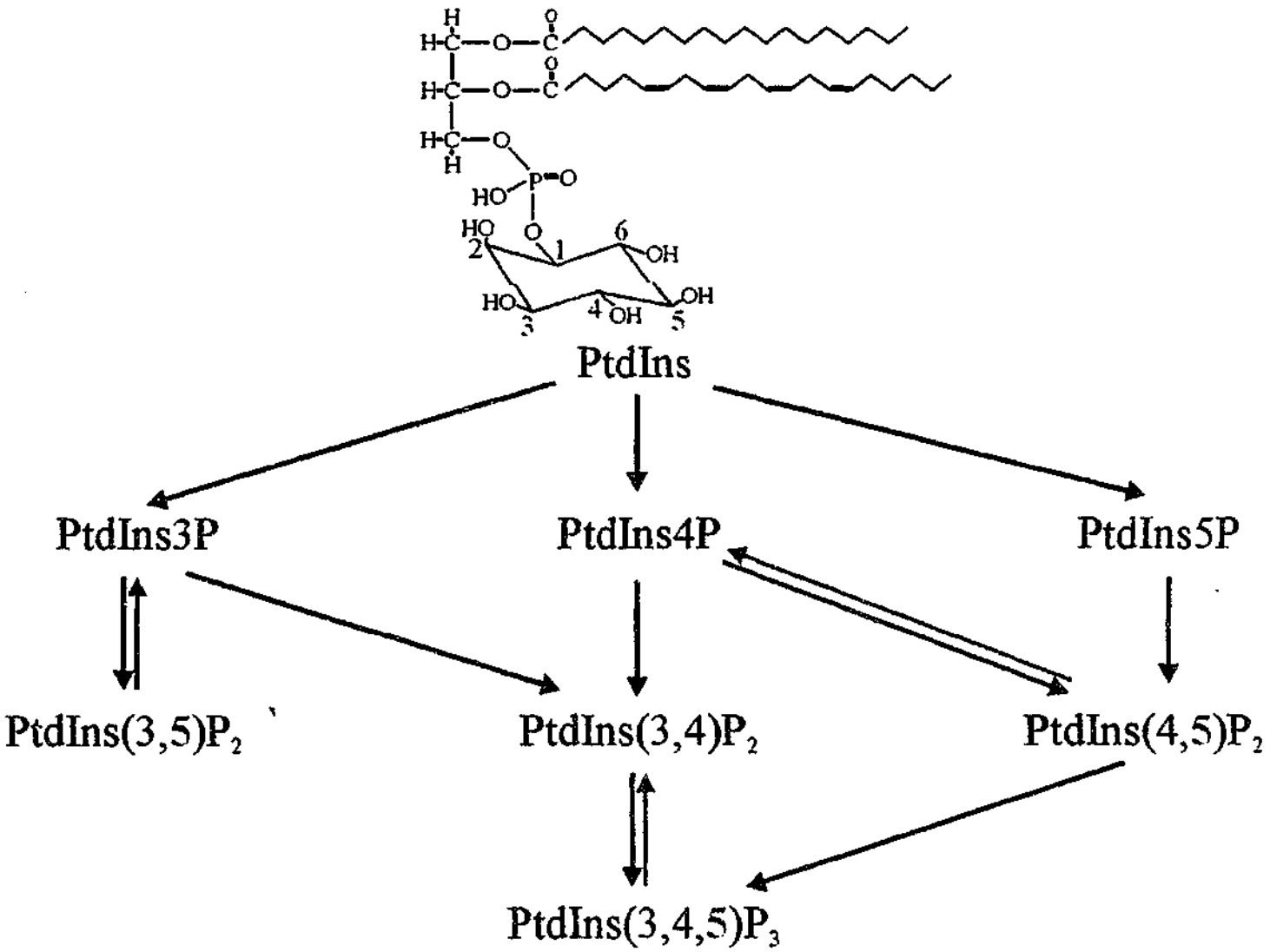

Figure 2. 5-Phosphatase metabolites. Phosphatidylinositol (PtdIns) consists of two acyl groups and an inositol ring attached to a glycerol backbone. The free hydroxyl groups of the inositol ring can be phosphorylated at positions 3, 4, and/or 5 by distinct kinases (black arrows) to generate various phosphoinositides. The action of 5-phosphatases (red arrows) modulates the signaling functions of these molecules. Inositol phosphates are not shown.

form tumors in nude mice (*15*). These studies demonstrate the critical role the 43-kDa 5-phosphatase plays in regulating intracellular calcium and thereby cell growth.

Recent exciting studies have shown $Ins(1,3,4,5)P_4$ inhibits the actions of the 43-kDa 5-phosphatase in hydrolyzing $Ins(1,4,5)P_3$ (*16*). The 43-kDa 5-phosphatase has a 10-fold higher affinity for $Ins(1,3,4,5)P_4$ than $Ins(1,4,5)P_3$ and a 100-fold lower V_{max} for $Ins(1,3,4,5)P_4$, compared to $Ins(1,4,5)P_3$. Following agonist stimulation, $Ins(1,3,4,5)P_4$ has a much longer half-life than $Ins(1,4,5)P_3$. $Ins(1,3,4,5)P_4$ inhibits $Ins(1,4,5)P_3$ metabolism by the 43-kDa 5-phosphatase and thereby facilitates calcium entry via activation of the store-operated Ca^{2+} current (Fig. 3).

The 43-kDa 5-phosphatase forms a complex with the major platelet phosphoprotein pleckstrin following platelet activation. The association between these species results in enhanced 5-phosphatase activity (*17*). The 43-kDa 5-phosphatase also forms a complex in vitro, with the signaling adapter protein 14-3-3, resulting in increased $Ins(1,4,5)P_3$ 5-phosphatase activity. The 43-kDa 5-phosphatase possesses a 14-3-3 binding site ^{363}RSESEE located at the *C*-terminus of the protein that mediates the interaction with 14-3-3 (*18*).

Synaptic Vesicle Recycling

$PtdIns(4,5)P_2$ regulates the molecular events that govern endocytosis by mediating the recruitment of AP-2, AP180, dynamin, and epsin to the plasma membrane (*7*, *19*), which leads to the formation of clathrin-coated pits and thereby initiates coated vesicle formation. The 5-phosphatase synaptojanin-1 plays a significant role in regulating synaptic vesicle endocytosis (*20*). Cortical neurons from synaptojanin-1-deficient mice demonstrate increased levels of $PtdIns(4,5)P_2$ and accumulate clathrin-coated vesicles. Electrophysiological studies of synaptojanin-1-deficient mice are consistent with impaired synaptic vesicle recycling (*21*). The *Caenorhabditis elegans* synaptojanin ortholog is encoded by the *UNC-26* gene. *Unc-26* mutants display defects in trafficking, vesicle budding, and uncoating, not

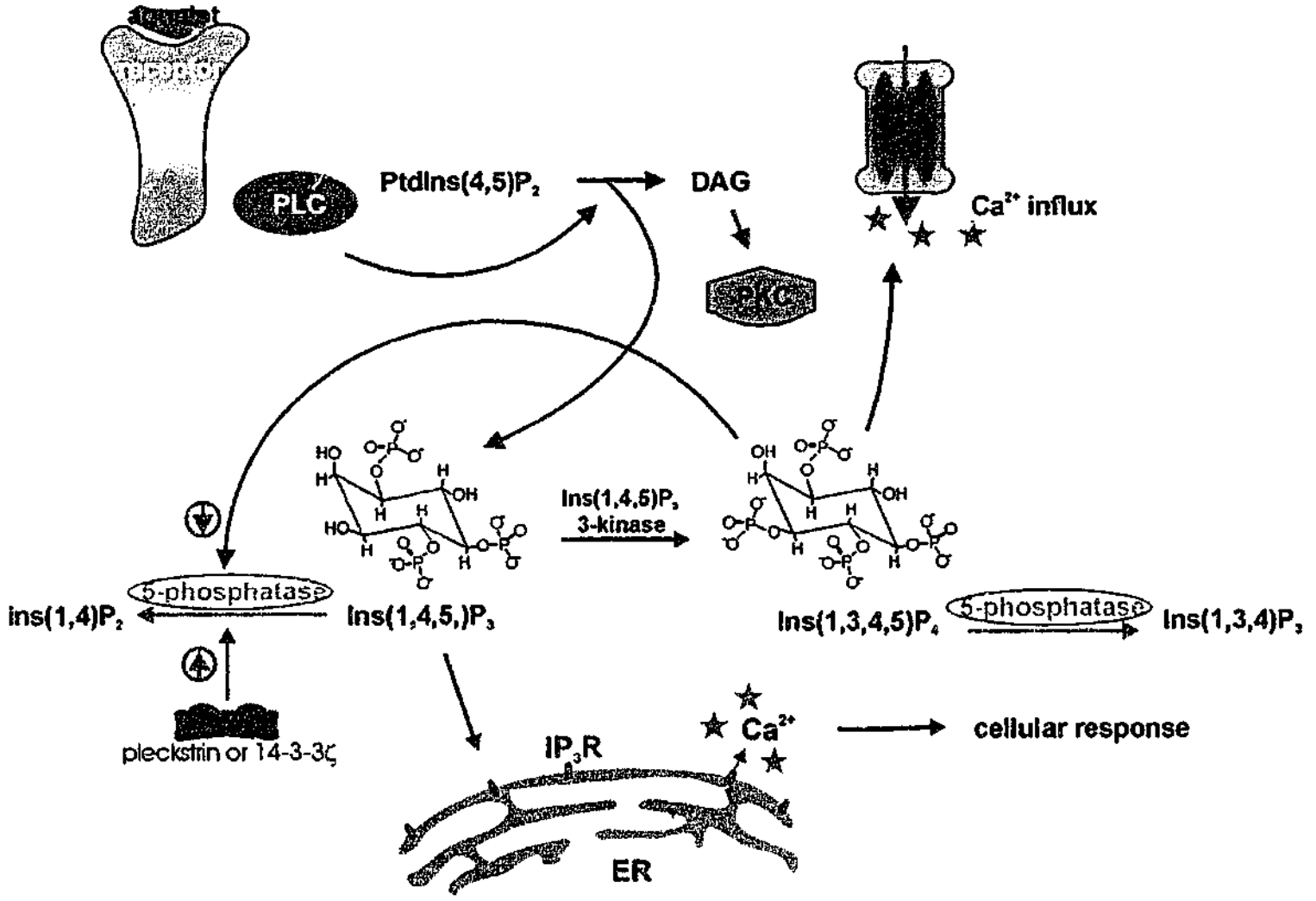

Figure 3. Role of the 43-kDa 5-phosphatase in regulating intracellular calcium release. The agonist stimulated hydrolysis of $PtdIns(4,5)P_2$ by phospholipase C (PLC) generates the second messengers $Ins(1,4,5)P_3$ and diacylglycerol (DAG). DAG activates protein kinase C (PKC), whereas $Ins(1,4,5)P_3$ binds $Ins(1,4,5)P_3$-receptors (IP_3R) on the endoplasmic reticulum (ER) and mobilizes Ca^{2+}. Specific kinases can convert $Ins(1,4,5)P_3$ into $Ins(1,3,4,5)P_4$, which is associated with extracellular Ca^{2+} influx. $Ins(1,3,4,5)P_4$ inhibits the activity of the 43-kDa 5-phosphatase leading to sustained $Ins(1,4,5)P_3$ signal (32). Thus, 43-kDa 5-phosphatase enzyme activity may be increased via complex formation with either pleckstrin or 14-3-3. In contrast, $Ins(1,3,4,5)P_4$ inhibits the activity of the 43-kDa 5-phosphatase resulting in prolongation of the $Ins(1,4,5)P_3$ signal.

confined to the nervous system (22). Collectively, these studies suggest synaptojanin regulates the uncoating of clathrin-coated vesicles. The proposed mechanism for this effect is via metabolism of $PtdIns(4,5)P_2$, which is essential for the recruitment of AP-2 and hence clathrin.

Two synaptojanin isoforms (1 and 2) have been cloned and characterized. Both have a similar domain structure containing an *N*-terminal Sac1 domain, a central 5-phosphatase domain and diverged *C*-terminal proline-rich domains. Synaptojanin-1 and -2 are expressed as 140- or 170-kDa isoforms and both isoforms demonstrate extensive splice variations in the *C*-terminal domains. Synaptojanin-1 is highly expressed in the brain, specifically in nerve termini; synaptojanin-2 is more widely expressed (*23*). Although in vitro synaptojanin-1 and -2, via the 5-phosphatase domain, hydrolyze $PtdIns(4,5)P_2$, $PtdIns(3,4,5)P_3$, $Ins(1,4,5)P_3$, and $Ins(1,3,4,5)P_4$, and the Sac1 domain serves as a polyphosphoinositide phosphatase, in vivo studies have shown synaptojanin-1 regulates $PtdIns(4,5)P_2$ (*24*, *25*). However, these studies must be interpreted with caution as there are significant difficulties in labeling phosphoinositides in cells, in particular $PtdIns(3,4,5)P_3$, and secondly, $PtdIns(4,5)P_2$ is generated in vast excess of $PtdIns(3,4,5)P_3$. It is of interest to note that in vitro phosphatase assays have demonstrated pronounced differences in $PtdIns(3,4,5)P_3$ 5-phosphatase activity in synaptojanin-deficient mice compared to normal litter mate controls (*21*).

Synaptojanin-1 hydrolyzes $PtdIns(4,5)P_2$ bound to the actin regulatory proteins α-actinin, vinculin, gelsolin, and profilin, and decreases the number of stress fibers in the cell (*26*). Synaptojanin-1 has been shown in vitro to interact with the SH3 domain of the dynamin-binding protein: synapin I. The latter also binds to N-WASP (neuronal Wiskott-Aldrich syndrome protein), a $PtdIns(4,5)P_2$-binding protein enriched in nerve terminals, which promotes actin polymerization (*27*).

The synaptojanin-1 *C*-terminal proline-rich domain mediates interactions with numerous SH3 domain-containing proteins including amphiphysin, and the low molecular weight small SH3 domain-containing proteins SH3p4, SH3p8, and SH3p13, also known as endophilins (*28*, *29*). Binding of synaptojanin with the nerve terminal proteins intersectin and synapin has been shown in vitro but not in vivo (*27*, *30*). The 170-kDa synaptojanin isoform also complexes with the clathrin adapter AP-2 and with the Epsin15 homology (EH) domain of the clathrin-associated protein Eps15 (*31*, *32*).

Synaptojanin-1, dynamin, amphiphysin, epsin, Eps15, and AP180 are phosphorylated in resting nerve terminals and are coordinately dephosphorylated upon endocytosis of synaptic vesicles. Phosphorylation may regulate protein-protein interactions during synaptic vesicle recycling (*33*, *34*).

Synaptojanin-2 may also play a role in regulating endocytosis. The activated small GTPase Rac1 binds synaptojanin-2. Synaptojanin-2 directly interacts with Rac1 in a GTP-dependent manner, resulting in translocation of the 5-phosphatase to membrane ruffles and inhibition of endocytosis (*35*). Catalytically active synaptojanin-2, which is localized to the plasma membrane, inhibits endocytosis of the EGF receptor, suggesting synaptojanin-2 mediates Rac1 inhibition of endocytosis. However, membrane-targeted synaptojanin-2 had no effect on lamellipodia, which is regulated by PI 3-kinase and Rac1 activity (*35*). One of the splice variants of synaptojanin-2 is localized to the outer mitochondrial membrane, whereby the 5-phosphatase forms a complex with a novel integral mitochondrial membrane protein designated OMP25. This interaction regulates the intracellular distribution of the organelle (*36*).

Regulation of Hemopoietic Cell Activation and Proliferation

The SH2 domain-containing 5-phosphatase-1 (SHIP-1) suppresses PI 3-kinase-dependent pathways following recruitment to immunoreceptor tyrosine-based inhibition motif (ITIM)-containing proteins (Fig. 4). Targeted disruption of murine SHIP-1 results in a myeloproliferative-like syndrome characterized by a massive increase in granulocyte macrophage progenitor cells in the bone marrow and spleen, leading to dramatic myeloid infiltration of the lungs, wasting and shortened life span (*37*, *38*). Progenitor cells from SHIP-$1^{-/-}$ mice demonstrate hyperresponsiveness to many hematopoietic growth factors and cytokines, compared to SHIP-$1^{+/+}$ littermates (*37*). Collectively, these findings are consistent with a model in which SHIP-1 acts as a negative regulator of hematopoietic cell proliferation and survival.

SHIP-1 hydrolyzes PtdIns(3,4,5)P_3 and Ins(1,3,4,5)P_4, forming PtdIns(3,4)P_2 and Ins(1,3,4)P_3, respectively. The *C*-terminal proline-rich domain is essential for full enzyme activity, presumably by regulating membrane association (*39*, *40*). More recent studies have demonstrated SHIP-1 also hydrolyzes PtdIns(4,5)P_2, forming PtdIns 4-P. However, its principal in vivo phosphoinositide substrate is likely to be PtdIns(3,4,5)P_3 (*41*). SHIP-1 is composed of multiple domains including an *N*-terminal SH2 domain, central catalytic 5-phosphatase domain, two NPXY motifs that mediate binding to phosphotyrosine binding (PTB) domain-containing proteins, and proline-rich regions in the *C*-terminus (*42*, *43*). SHIP-1 is expressed exclusively in cells of hematopoietic origin and has been shown to play a significant functional role in regulating B cell, mast cell, and phagocytic cell activation (*44*).

Engagement of antigen receptors such as the B cell receptor (BCR), T cell receptor, FcγRIII, and FcεRI results in synthesis of PtdIns(3,4,5)P_3, which activates Bruton's tyrosine kinase and phospholipase C leading to intracellular calcium release. In B cells, coligation of the B cell antigen receptor with FcγRIIB initiates phosphorylation of the FcγRIIB ITIM, which results in the recruitment of SHIP-1 leading to PtdIns(3,4,5)P_3 hydrolysis and attenuation of downstream signaling (*56*). SHIP-1 also recruits the RasGAP-binding protein $p62^{dok}$ to the FcγRIIB-BCR-complex, resulting in its phosphorylation and increased binding to RasGAP. This association is critical for inhibition of BCR-mediated activation of the Ras signaling pathway (*45*) (Fig. 4).

In mast cells, SHIP-1 plays a significant role in regulating mast cell degranulation by limiting IgE-induced degranulation and preventing Steel Factor-induced intracellular signaling from initiating degranulation (*46*). In mast cells, SHIP-1 is recruited to the ITIM of the FcεRI/ FcγRIIB complex (*47*). The mechanism of SHIP-1 action appears to be the same in both mast and B cells and functions to regulate cytokine- or antigen-induced stimulation of PtdIns(3,4,5)P_3 synthesis and thereby extracellular calcium entry and activation of the survival factor, serine-threonine kinase Akt. The SHIP-1 *C*-terminal proline-rich domain plays an important functional role in mediating these responses, as intact SHIP-1 but not SHIP-1 truncation mutants that lack the *C*-terminal proline-rich domain, rescue SHIP-$1^{-/-}$ bone marrow-derived mast cell hyperresponsive phenotype (*40*).

In phagocytic cells such as macrophages, SHIP-1 regulates phagocytosis. Macrophages overexpressing SHIP-1 show impaired CR3-mediated phagocytosis, and cells from SHIP-$1^{-/-}$ mice demonstrated 2.5-fold enhanced phagocytosis (*48*). SHIP-1 is expressed as 145-, 135-, 125-, and 110-kDa isoforms resulting from *C*-terminal truncation, with the expression of the different isoforms correlating with the stage of hematopoietic differentiation and leukemogenesis (*49*, *50*). In addition, the cytokine hyperresponsive phenotype of the SHIP-$1^{-/-}$ mice is similar to that detected following Bcr-Abl transformation in mice (*51*, *52*). The Bcr-Abl oncogene causes a clonal expansion of hematopoietic progenitor cells and granulocyte lineage cells, resulting in chronic myeloid leukemia (CML). An inverse correlation between the expression of the oncogenic fusion protein Bcr-Abl and SHIP-1 in chronic myeloid leukemia has been detected, suggesting decreased SHIP-1 activity may contribute to the proliferative advantage of these leukemic cells (*53*). SHIP-1 expression may be regulated by the Bcr-Abl oncogenic fusion protein, as treatment of CML cells with the specific tyrosine kinase inhibitor STI571 results in re-expression of SHIP-1. It

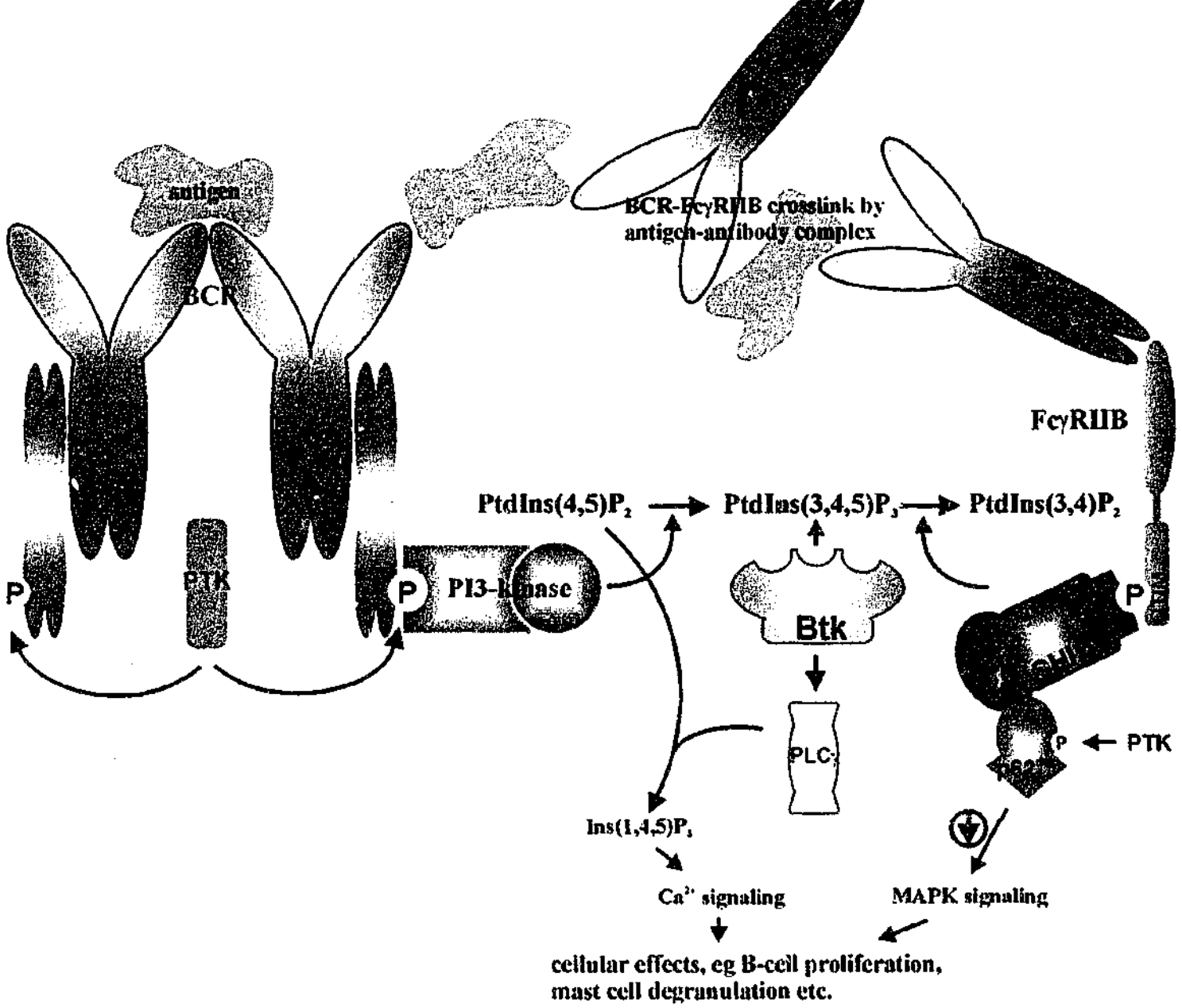

Figure 4. SHIP-1 regulation of B-cell negative signalling. Activation of PI3-kinase triggered by B-cell receptor (BCR) cross-linking with antigens leads to PtdIns(3,4,5)P_3 synthesis. Membrane recruitment of Bruton's tyrosine kinase (Btk) via its PH domain results in activation of phospholipase C-(PLC), subsequent PtdIns(4,5)P_2 hydrolysis and intracellular Ca^{2+} release, and B-cell proliferation. Co-engagement of FcγRIIB with BCR by specific antibodies leads to recruitment of SHIP-1 to the phosphorylated ITIM of FcγRIIB, PtdIns(3,4,5)P_3 hydrolysis, and attenuation of the proliferative signaling. The recruitment of $p62^{dok}$ to ITIM-bound SHIP-1 also leads to phosphorylation by tyrosine kinases (PTK) of $p62^{dok}$ and down-regulation of MAPK signaling.

is noteworthy that the more widely expressed and homologous 5-phosphatase SHIP-2 interacts with the Bcr-Abl oncogene product. In addition, SHIP-2 is constitutively tyrosine phosphorylated and associated with Shc in chronic myeloid leukemic progenitor cells, suggesting a role for SHIP-2 in $210^{bcr/abl}$-mediated myeloid expansion (*54*). Both SHIP-1 and SHIP-2 are constitutively tyrosine phosphorylated in Bcr-Abl-expressing cells. SHIP-2 specifically binds the SH3 domain of Abl, but not Grb2, whereas SHIP-1 binds the SH3 domains of Src and Grb2.

Finally, an intriguing study has demonstrated the gene *DSHP* (Duncan's disease SH2 domain protein) is responsible for X-linked lymphoproliferative syndrome, which is characterized by increased susceptibility to Epstein–Barr virus infection, leading to high-grade lymphoma. DSHP comprises a single SH2 domain that demonstrates extensive sequence homology with the SH2 domain of SHIP-1. The results of this study suggest that DSHP may compete with SHIP-1 binding to sites of activated receptors and thereby enhance lymphocyte activation and proliferation (*55*).

Regulation of Insulin Signaling

SHIP-2 is a widely expressed 5-phosphatase that plays a significant role in negatively regulating insulin signaling (*56, 57*). SHIP-2 was originally cloned and named "inositol polyphosphate 5-phosphatase-like protein 1" (INPPL1) in the search for functional complementation of Fanconi's anemia (*58*). Subsequent studies have suggested the diversity within the *N*-terminal SH2 domains of SHIP-2 and INNPL1 probably relate to a cloning artefact (*59*). SHIP-2 contains an amino-terminal SH2 domain, a central 5-phosphatase domain, and a carboxyl-terminal proline-rich domain and bears significant sequence identity with the 5-phosphatase, SHIP-1, except in the proline-rich domain. SHIP-2 *C*-terminal domain predicts for a PDZ-binding domain as well as sites for tyrosine phosphorylation and a SAM domain (sterile-alpha module). Unlike SHIP-1, SHIP-2 is widely expressed in many tissues and cells. SHIP-2 hydrolyzes the 5-position phosphate from PtdIns(3,4,5)P_3 and PtdIns(4,5)P_2 and in some, but not all studies, has been shown to hydrolyze the soluble inositol phosphate Ins(1,3,4,5)P_4 (*54, 60, 61*). SHIP-2 undergoes cytokine-, growth factor-, and insulin-stimulated phosphorylation in a number of cell lines (*54, 62*). SHIP-2 localizes to focal contacts of adherent cells, as well as lamellipodia of EGF-stimulated cells. Membrane association is in part mediated via SHIP-2 association with the $p130^{Cas}$ adapter protein at focal adhesions, regulating cell spreading. Association between these species is dependent on the SHIP-2 SH2 domain and is enhanced by tyrosine phosphorylation and cell adhesion (*63*). In addition SHIP-2, like PTEN, regulates both PtdIns(3,4,5)P_3-mediated Akt activation and induces cell cycle arrest, associated with increased stability of expression of the cell cycle inhibitor $p27^{KIP1}$ (*61*).

Recent studies have demonstrated SHIP-2 negatively regulates insulin signaling. Insulin-activated Akt activation and translocation of the glucose transporter GLUT4 in both skeletal muscle and adipocytes are largely dependent on PI 3-kinase activation and subsequent production of PtdIns(3,4,5)P_3 and PtdIns(3,4)P_2 (*64, 65*). Microinjection of recombinant SHIP-1 into 3T3-L1 adipocytes inhibited insulin-induced GLUT4 translocation, DNA synthesis, and membrane ruffling responses and in addition inhibited downstream signaling pathways from the insulin receptor (*66*). Because SHIP-1, in contrast to SHIP-2, is not expressed in either skeletal muscle or fat, subsequent studies have concentrated on investigating the role SHIP-2 plays in regulating insulin signaling. Both endogenous and recombinant SHIP-2 are tyrosine phosphorylated in response to insulin stimulation, associated with a reduction in mitogen-activated protein kinase (MAPK) activation (*56*). Overexpression of wild-type or dominant-negative SHIP-2 in fibroblasts, or 3T3-L1 adipocytes, does not affect early signaling events following insulin stimulation such as insulin receptor substrate (IRS) phosphorylation, or PI 3-kinase activation. However, PtdIns(3,4,5)P_3 levels are significantly increased in cells expressing dominant-negative SHIP-2 compared to cells expressing the wild-type enzyme (*67*). In addition, overexpression of SHIP-2, but not catalytically inactive SHIP-2, in 3T3-L1 adipocytes results in negative regulation of insulin-induced signaling. Cells expressing dominant-negative SHIP-2 are unable to down-regulate responses downstream of PI 3-kinase including Akt and PKCλ activation, GLUT4 translocation, glucose uptake, and glycogen synthase kinase 3β phosphorylation (*67*).

Newborn homozygous mice lacking SHIP-2 exhibit severe hypoglycemia, show aberrant expression of genes involved in gluconeogenesis in the liver, and die in the neonatal period from respiratory failure (*57*). SHIP-2 $^{+/-}$ and $^{+/+}$ mice exhibit similar blood glucose levels under both feeding and fasting conditions and produce comparable levels of insulin in response to glucose. However, adult SHIP-2 heterozygous mutant mice demonstrate insulin sensitivity associated with increased translocation of GLUT4 to the plasma membrane, in response to insulin treatment (*57*). Although the signaling pathways mediating the phenotype of insulin-hypersensitivity have yet to be fully determined, insulin-stimulated GLUT4 translocation to the plasma membrane appears to be enhanced in mice lacking SHIP-2.

Ocular Cerebrorenal Syndrome of Lowe (OCRL)

Lowe's syndrome is an X–chromosome-linked disorder characterized by a pleiotropic phenotype that includes mental retardation, congenital cataracts and renal tubular acidosis (*68*). The gene locus disrupted in this syndrome was mapped to Xq25-q26 and subsequently found to encode a 5-phosphatase with a predicted molecular weight of 112 kDa. The OCRL (oculocerebrorenal syndrome of Lowe) gene product is most closely related to the 75-kDa 5-phosphatase (5-phosphatase II), sharing 71% amino acid sequence similarity (*69*). The recombinant enzyme preferentially hydrolyzes PtdIns(4,5)P_2, but activity towards PtdIns(3,4,5)P_3, Ins(1,4,5)P_3, and Ins(1,3,4,5)P_4 has been demonstrated (*70, 71*). Cell lines from patients with Lowe's syndrome accumulate PtdIns(4,5)P_2, consistent with the enzyme acting predominantly as a PtdIns(4,5)P_2 5-phosphatase (*71*). However, it is noteworthy that although other 5-phosphatases are expressed in these cells, they appear unable to compensate for the loss of the OCRL 5-phosphatase. Surprisingly, mice that lack Lowe's protein demonstrate no phenotype (*72*). The localization of the OCRL protein has been proposed to be in either the Golgi (human fibroblasts), or the lysosomes (human kidney proximal tubules) (*71, 73*). The lysosomal localization of the protein is supported by the intriguing observation that several lysosomal enzymes are increased in the plasma of OCRL patients, presumably as the result of abnormal lysosomal trafficking (*74*).

Lowe's syndrome is the first and only known inborn error of phosphatidylinositol metabolism. The relationship between the defective enzyme and the clinical phenotype of the disease is not well understood. Mutations in the *OCRL* gene in these patients are heterogeneous. Deletions, frame shifts, nonsense, and missense mutations throughout the coding sequence, including outside the 5-phosphatase catalytic domain have been reported (*75–78*).

5-Phosphatases of Unknown Function

Recent studies in the last 2 years have resulted in the cloning of three new mammalian 5-phosphatases, a 52-kDa enzyme designated "SKIP" (for skeletal muscle and kidney enriched 5-phosphatase), a 72-kDa protein called "pharbin," and 107-kDa 5-phosphatase called "PIPP" (for proline-rich inositol polyphosphate 5-phosphatase). The latter 5-phosphatase has extensive proline-rich regions within both the *N*- and *C*-terminal domains. Within these regions, six putative 14-3-3 binding sites have been identified, suggesting this isoform, like the 43-kDa 5-phosphatase, complexes with this signaling adapter protein. PIPP is widely expressed and recombinant PIPP demonstrates activity towards Ins(1,4,5)P_3, Ins(1,3,4,5)P_4, and PtdIns(4,5)P_2; however, metabolism of PtdIns(3,4,5)P_3 and PtdIns(3,5)P_2 have not been reported (*79*). The 107-kDa enzyme may undergo posttranslational modification such as serine/threonine phosphorylation. This enzyme localizes at membrane ruffles, which requires the presence of both the *N*- and *C*-terminal proline-rich domains. However, this enzyme localization does not affect membrane ruffling.

SKIP is expressed as three splice variants, the largest of which is 52 kDa. Although the 5-phosphatase is highly expressed in both kidney and skeletal muscle, the enzyme appears to be widely expressed at similar levels in many tissues. Recombinant SKIP hydrolyzes both soluble inositol phosphates Ins(1,4,5)P_3 and Ins(1,3,4,5)P_4, and phosphoinositides PtdIns(4,5)P_2 and PtdIns(3,4,5)P_3. Recombinant and endogenous SKIP localize in a cytosolic distribution and concentrate in a perinuclear area. Overexpression of SKIP results in reduced actin stress fiber formation in these areas (*80*).

Cloning and characterization of human, mouse, and rat isoforms of a 72-kDa 5-phosphatase designated "pharbin" for phosphatase that induces arborization (*81*) have been reported by three groups. The human isoform has been designated the "Type IV 5-phosphatase," due to its unique substrate specificity (*41*) and we have designated the mouse isoform the 72-kDa 5-phosphatase (*82*). The pharbin sequence bears 88% amino acid sequence identity with the mouse 72-kDa 5-phosphatase, whereas the human Type IV enzyme recently identified by Kisseleva et al. (*41*) demonstrates 76% amino acid identity over 649 amino acids with the mouse enzyme, suggesting it may represent either the human homolog, or a spliced variant. Considerable sequence diversity occurs within the *N*-terminal proline-rich domain, with the human isoform containing a greater content of prolines (19% compared to 13% in the mouse ortholog). Amino acid sequence analysis has demonstrated that in addition to an *N*-terminal proline-rich domain, the sequence predicts for a *C*-terminal CAAX motif, and a putative ITAM (immunoreceptor tyrosine-based activation motif). The latter is commonly found in the cytoplasmic region of many immune receptors and functions as a link between activated cell surface receptors and their effector molecules in the cytosol. Whether this motif plays a functional role for this 5-phosphatase has yet to be shown. The mouse 72-kDa enzyme is highly expressed in brain and testis, with the human enzyme demonstrating in addition high expression in heart, with lower levels in liver and kidney (*41*, *82*). The 72-kDa 5-phosphatase localizes to the cytoplasmic surface of the Golgi, mediated by the *N*-terminal proline-rich domain (*82*). In contrast, pharbin localizes to the plasma membrane of neural cells and promotes arborization (*81*). Different substrate specificities have been reported for the mouse, rat, and human 72-kDa 5-phosphatases. Studies using the recombinant rat isoform suggest the enzyme hydrolyzes Ins(1,4,5)P_3, Ins(1,3,4,5)P_4, and PtdIns(4,5)P_2, yet in contrast neither the mouse nor human 5-phosphatase were shown to hydrolyze the soluble inositol phosphates (*81*), and demonstrate greatest activity towards PtdIns(3,4,5)P_3 (*41*, *82*). In a detailed kinetic analysis, Majerus and colleagues have shown the human type IV enzyme has the greatest activity towards PtdIns(3,4,5)P_3 of any mammalian 5-phosphatase including SHIP-1, with a K_m of 0.65 M versus 5.95 M, respectively. In these studies, both SHIP-1 and 72-kDa 5-phosphatase enzyme activity was shown to be highly sensitive to the presence of specific detergents in the assay, which may in part explain some discrepancies in the literature about the distinct substrate specificity of various 5-phosphatase isoforms (*41*).

Insights From the Analysis of Yeast 5-Phosphatases

The yeast *Saccharomyces cerevisiae* has been utilized by several investigators as a model organism to study 5-phosphatase cellular function. Four 5-phosphatases have been identified and partially characterized in yeast. Three enzymes designated Inp51p, Inp52p, and Inp53p contain an *N*-terminal Sac1 domain, a central 5-phosphatase domain, and a *C*-terminal proline-rich domain. Inp54p contains a 5-phosphatase domain and a *C*-terminal hydrophobic tail (*83*). All of these 5-phosphatases hydrolyze PtdIns(4,5)P_2 (*84–87*). Inp52p also demonstrates 5-phosphatase activity towards PtdIns(3,5)P_2 (*87*). Null mutation of any one of the Sac1 domain-containing 5-phosphatases results in little phenotype (*88*), suggesting that these 5-phosphatases have overlapping functions. However, disruption of any two of the Sac1 domain-containing 5-phosphatases results in marked phenotypic changes characterized by cell wall thickening and actin depolymerization defects, yet deletion of all three is lethal (*84*, *88*, *89*).

In yeast, the actin cytoskeleton appears to be linked to endocytosis [reviewed by (*90*)] and null mutation of *inp51 inp52* results in defects of the actin cytoskeleton as well as severe defects in fluid-phase and receptor-mediated endocytosis (*84*, *89*). Deletion of any two yeast Sac1 domain-containing 5-phosphatases results in a phenotype that includes disorganization of polymerized actin and delocalization of actin patches from the growing yeast bud to the daughter cell [reviewed by Hughes et al. (*91*)]. It is noteworthy the yeast 5-phosphatases, Inp52p and Inp53p, translocate to actin patches upon osmotic stress, the site of plasma membrane invaginations. In addition, overexpression of Inp52p and Inp53p, but not catalytically inactive Inp52p, results in a significant reduction in the repolarization

time of actin patches following osmotic stress (*87*). Deletion of *inp51 inp52* results in massive plasma membrane invaginations that may reflect an imbalance between endocytosis and exocytosis (*89*). However, exocytosis appears normal in all Sac1 5-phosphatase mutant strains, as secretion of invertase or a reporter protein is not impaired (*83*, *89*). The *inp51 inp53* and *inp52 inp53* null mutants also display impairment of endocytosis and plasma membrane invaginations; however, the phenotype is less marked than that observed in the *inp51 inp52* null mutant strain (*88*, *89*).

Defects in endocytosis and the actin cytoskeleton appear to correlate with abnormalities in cell polarity in the *inp51 inp52* and *inp52 inp53* disrupted strains, which demonstrate abnormal bud site selection (*89*). All three double null mutants also show thickened cell walls, compromised growth on hyperosmotic media, and fragmented vacuoles (*84*, *87*, *88*).

Yeast 5-phosphatases have been shown to display genetic interactions with several other proteins. Deletion of *inp51* is capable of partially suppressing the growth defect of a *sac6* null mutant. *SAC6* encodes the yeast homolog of fimbrin, an actin bundling protein, suggesting that Inp51p and Sac6p have opposing effects on the actin cytoskeleton (*89*). Double deletion of *inp51* together with *pan1*, the yeast homolog of eps15, is lethal (92). Pan1p is required for both endocytosis and organization of the actin cytoskeleton (*93*, *94*).

Genetic screening for suppressors of *pma1* that divert mutant Pma1p from delivery to the vacuole have identified Inp53p (Sop2) (*95*). Results from this study have implicated Inp53p in the regulation of trafficking between the endosome and Golgi. Inp53p has also been predicted to play a role in clathrin-coated vesicle trafficking from the *trans* Golgi network, based on the demonstration of the 5-phosphatase's genetic interaction with the clathrin heavy chain gene *CHC1* (*96*).

Although the Sac1 domain-containing 5-phosphatases appear to play a significant role in regulating organization of the actin cytoskeleton and thereby endocytosis, the yeast 5-phosphatase Inp54p, is localized to the endoplasmic reticulum and regulates secretion from this compartment. Inp54p localizes to the endoplasmic reticulum by its *C*-terminal hydrophobic tail, which is consistent with a tail-anchored protein. Deletion of *inp54* leads to a 2- to 3-fold increase in secretion of a reporter protein, compared to wild-type cells or *inp51*, *inp52*, or *inp53* null mutants (*83*). Consistent with its localization to the endoplasmic reticulum, loss of *inp54* does not affect the actin cytoskeleton, cell polarity, or the morphology of the cell (*83*).

To date, few proteins that physically interact in vivo with the yeast 5-phosphatases have been identified. High-throughput yeast two-hybrid screens have identified Gtt1p and the uncharacterized Ydl204p as potential binding partners for Inp54p (*97*). Gtt1p is a glutathione S-transferase protein localized to the endoplasmic reticulum (*98*) placing it in proximity to Inp54p. Glutathione S-transferases are thought to play a role in cellular detoxification, although Gtt1p is not required for protection against oxidative stress (*98*).

CONCLUSIONS

The 5-phosphatases demonstrate a regulatory function in many cellular processes, and although the potential role these enzymes play in human diseases is only recently emerging, results of many recent studies have demonstrated the critical role 5-phosphatase-mediated hydrolysis of both inositol phosphate and phosphoinositide signaling molecules plays in the regulation of cellular activation and proliferation.

REFERENCES

1. Martin, T. F. (1998) Phosphoinositide lipids as signaling molecules: common themes for signal transduction, cytoskeletal regulation, and membrane trafficking. *Annu. Rev. Cell Dev. Biol.* **14**, 231–264.
2. Vanhaesebroeck, B., Leevers, S. J., Ahmadi, K., Timms, J., Katso, R., Driscoll, P. C., Woscholski, R., Parker, P. J., and Waterfield, M. D. (2001) Synthesis and function of 3-phosphorylated inositol lipids. *Annu. Rev. Biochem.* **70**, 535–602.
3. Raucher, D., Stauffer, T., Chen, W., Shen, K., Guo, S., York, J. D., Sheetz, M. P., and Meyer, T. (2000) Phosphatidylinositol 4,5-bisphosphate functions as a second messenger that regulates cytoskeleton-plasma membrane adhesion. *Cell* **100**(2), 221–228.
4. Czech, M. P. (2000) PIP2 and PIP3: complex roles at the cell surface. *Cell* **100**(6), 603–606.
5. Janmey, P. A. (1994) Phosphoinositides and calcium as regulators of cellular actin assembly and disassembly. *Annu. Rev. Physiol.* **56**, 169–191.
6. Janmey, P. A., Xian, W., and Flanagan, L. A. (1999) Controlling cytoskeleton structure by phosphoinositide-protein interactions: phosphoinositide binding protein domains and effects of lipid packing. *Chem. Phys. Lipids* **101**(1), 93–107.
7. Corvera, S., D'Arrigo, A., and Stenmark, H. (1999) Phosphoinositides in membrane traffic. *Curr. Opin. Cell. Biol.* **11**(4), 460–465.
8. Erneux, C., Govaerts, C., Communi, D., and Pesesse, X. (1998) The diversity and possible functions of the inositol polyphosphate 5-phosphatases. *Biochim. Biophys. Acta* **1436**(1–2), 185–199.
9. Majerus, P. W., Kisseleva, M. V., and Norris, F. A. (1999) The role of phosphatases in inositol signaling reactions. *J. Biol. Chem.* **274**(16), 10669–10672.
10. Berridge, M., Lipp, P., and Bootman, M. (1999) Calcium signalling. *Curr. Biol.* **9**(5), R157–159.
11. Bootman, M. D., Collins, T. J., Peppiatt, C. M., Prothero, L. S., MacKenzie, L., De Smet, P., Travers, M., Tovoy, S. C., Seo, J. T., Berridge, M. J., Ciccolini, F., and Lipp, P. (2001) Calcium signalling—an overview. *Semin. Cell. Dev. Biol.* **12**(1), 3–10.
12. Laxminarayan, K. M., Matzaris, M., Speed, C. J., and Mitchell, C. A. (1993) Purification and characterization of a 43-kDa membrane-associated inositol polyphosphate 5-phosphatase from human placenta. *J. Biol. Chem.* **268**(7), 4968–4974.
13. De Smedt, F., Missiaen, L., Parys, J. B., Vanweyenberg, V., De Smedt, H., and Erneux, C. (1997) Isoprenylated human brain type I inositol 1,4,5-trisphosphate 5-phosphatase controls Ca^{2+} oscillations induced by ATP in Chinese hamster ovary cells. *J. Biol. Chem.* **272**(28), 17367–17375.
14. Speed, C. J., Neylon, C. B., Little, P. J., and Mitchell, C. A. (1999) Underexpression of the 43 kDa inositol polyphosphate 5-phosphatase is associated with spontaneous calcium oscillations and enhanced calcium responses following endothelin-1 stimulation. *J. Cell. Sci.* **112**(Pt. 5), 669–679.
15. Speed, C. J., Little, P. J., Hayman, J. A., and Mitchell, C. A. (1996) Underexpression of the 43 kDa inositol polyphosphate 5-phosphatase is associated with cellular transformation. *EMBO J.* **15**(18), 4852–4861.
16. Hermosura, M. C., Takeuchi, H., Fleig, A., Riley, A. M., Potter, B. V., Hirata, M., and Penner, R. (2000) InsP4 facilitates store-operated calcium influx by inhibition of InsP3 5-phosphatase. *Nature* **408**(6813), 735–740.

17. Auethavekiat, V., Abrams, C. S., and Majerus, P. W. (1997) Phosphorylation of platelet pleckstrin activates inositol polyphosphate 5-phosphatase I. *J. Biol. Chem.* **272**(3), 1786–1790.
18. Campbell, J. K., Gurung, R., Romero, S., Speed, C. J., Andrews, R. K., Berndt, M. C., and Mitchell, C. A. (1997) Activation of the 43 kDa inositol polyphosphate 5-phosphatase by 14-3-3zeta. *Biochemistry* **36**(49), 15363–15370.
19. Simonsen, A., Wurmser, A. E., Emr, S. D., and Stenmark, H. (2001) The role of phosphoinositides in membrane transport. *Curr. Opin. Cell. Biol.* **13**(4), 485–492.
20. Cremona, O., and De Camilli, P. (2001) Phosphoinositides in membrane traffic at the synapse. *J. Cell. Sci.* **114**(Pt. 6), 1041–1052.
21. Cremona, O., Di Paolo, G., Wenk, M. R., Luthi, A., Kim, W. T., Takei, K., Daniell, L., Nemoto, Y., Shears, S. B., Flavell, R. A., McCormick, D. A., and De Camilli, P. (1999) Essential role of phosphoinositide metabolism in synaptic vesicle recycling. *Cell* **99**(2), 179–188.
22. Harris, T. W., Hartwieg, E., Horvitz, H. R., and Jorgensen, E. M. (2000) Mutations in synaptojanin disrupt synaptic vesicle recycling. *J. Cell. Biol.* **2000 150**(3), 589–600.
23. Ramjaun, A. R., and McPherson, P. S. (1996) Tissue-specific alternative splicing generates two synaptojanin isoforms with differential membrane binding properties. *J. Biol. Chem.* **271**(40), 24856–24861.
24. McPherson, P. S., Garcia, E. P., Slepnev, V. I., David, C., Zhang, X., Grabs, D., Sossin, W. S., Bauerfeind, R., Nemoto, Y., and De Camilli, P. (1996) A presynaptic inositol-5-phosphatase. *Nature* **379**(6563), 353–357.
25. Woscholski, R., Finan, P. M., Radley, E., Totty, N. F., Sterling, A. E., Hsuan, J. J., Waterfield, M. D., and Parker, P. J. (1997) Synaptojanin is the major constitutively active phosphatidylinositol-3,4,5-trisphosphate 5-phosphatase in rodent brain. *J. Biol. Chem.* **272**(15), 9625–9628.
26. Sakisaka, T., Itoh, T., Miura, K., and Takenawa, T. (1997) Phosphatidylinositol 4,5-bisphosphate phosphatase regulates the rearrangement of actin filaments. *Mol. Cell. Biol.* **17**(7), 3841–3849.
27. Qualmann, B., Roos, J., DiGregorio, P. J., and Kelly, R. B. (1999) Syndapin I, a synaptic dynamin-binding protein that associates with the neural Wiskott-Aldrich syndrome protein. *Mol. Biol. Cell* **10**(2), 501–513.
28. de Heuvel, E., Bell, A. W., Ramjaun, A. R., Wong, K., Sossin, W. S., and McPherson, P. S. (1997) Identification of the major synaptojanin-binding proteins in brain. *J. Biol. Chem.* **272**(13), 8710–8716.
29. Micheva, K. D., Kay, B. K., and McPherson, P. S. (1997) Synaptojanin forms two separate complexes in the nerve terminal. Interactions with endophilin and amphiphysin. *J. Biol. Chem.* **272**(43), 27239–27245.
30. Yamabhai, M., Hoffman, N. G., Hardison, N. L., McPherson, P. S., Castagnoli, L., Cesareni, G., and Kay, B. K. (1998) Intersectin, a novel adaptor protein with two Eps15 homology and five Src homology 3 domains. *J. Biol.Chem.* **273**(47), 31401–31407.
31. Haffner, C., Takei, K., Chen, H., Ringstad, N., Hudson, A., Butler, M. H., Salcini, A. E., Di Fiore, P. P., and De Camilli, P. (1997) Synaptojanin 1: localization on coated endocytic intermediates in nerve terminals and interaction of its 170 kDa isoform with Eps15. *FEBS Lett.* **419**(2–3), 175–180.
32. Haffner, C., Paolo, G. D., Rosenthal, J. A., and De Camilli, P. (2000) Direct interaction of the 170 kDa isoform of synaptojanin 1 with clathrin and with the clathrin adaptor AP-2. *Curr. Biol.* **10**(8), 471–474.
33. Turner, K. M., Burgoyne, R. D., and Morgan, A. (1999) Protein phosphorylation and the regulation of synaptic membrane traffic. *Trends Neurosci.* **22**(10), 459–464.
34. Cousin, M. A., Tan, T. C., and Robinson, P. J. (2001) Protein phosphorylation is required for endocytosis in nerve terminals: potential role for the dephosphins dynamin I and synaptojanin, but not AP180 or amphiphysin. *J. Neurochem.* **76**(1), 105–116.
35. Malecz, N., McCabe, P. C., Spaargaren, C., Qiu, R., Chuang, Y., and Symons, M. (2000) Synaptojanin 2, a novel rac1 effector that regulates clathrin-mediated endocytosis. *Curr. Biol.* **10**(21), 1383–1386.
36. Nemoto, Y., and De Camilli, P. (1999) Recruitment of an alternatively spliced form of synaptojanin 2 to mitochondria by the interaction with the PDZ domain of a mitochondrial outer membrane protein. *EMBO J.* **18**(11), 2991–3006.
37. Helgason, C. D., Damen, J. E., Rosten, P., Grewal, R., Sorensen, P., Chappel, S. M., Borowski, A., Jirik, F., Krystal, G., and Humphries, R. K. (1998) Targeted disruption of SHIP leads to hemopoietic perturbations, lung pathology, and a shortened life span. *Genes Dev.* **12**(11), 1610–1620.
38. Liu, Q., Sasaki, T., Kozieradzki, I., Wakeham, A., Itie, A., Dumont, D. J., and Penninger, J. M. (1999) SHIP is a negative regulator of growth factor receptor-mediated PKB/Akt activation and myeloid cell survival. *Genes Dev.* **13**(7), 786–791.
39. Phee, H., Jacob, A., and Coggeshall, K. M. (2000) Enzymatic activity of the Src homology 2 domain-containing inositol phosphatase is regulated by a plasma membrane location. *J. Biol. Chem.* **275**(25), 19090–19097.
40. Damen, J. E., Ware, M. D., Kalesnikoff, J., Hughes, M. R., and Krystal, G. (2001) SHIP's C-terminus is essential for its hydrolysis of PIP(3) and inhibition of mast cell degranulation. *Blood* **97**(5), 1343–1351.
41. Kisseleva, M. V., Wilson, M. P., and Majerus, P. W. (2000) The isolation and characterization of a cDNA encoding phospholipid-specific inositol polyphosphate 5-phosphatase. *J. Biol. Chem.* **275**(26), 20110–20116.
42. Krystal, G., Damen, J. E., Helgason, C. D., Huber, M., Hughes, M. R., Kalesnikoff, J., Lam, V., Rosten, P., Ware, M. D., Yew, S., and Humphries, R. K. (1999) SHIPs ahoy. *Int. J. Biochem. Cell. Biol.* **31**(10), 1007–1010.
43. Rohrschneider, L. R., Fuller, J. F., Wolf, I., Liu, Y., and Lucas, D. M. (2000) Structure, function, and biology of SHIP proteins. *Genes Dev.* **14**(5), 505–520.
44. Krystal, G. (2000) Lipid phosphatases in the immune system. *Semin. Immunol.* **12**(4), 397–403.
45. Tamir, I., Stolpa, J. C., Helgason, C. D., Nakamura, K., Bruhns, P., Daeron, M., and Cambier, J. C. (2000) The RasGAP-binding protein p62dok is a mediator of inhibitory FcgammaRIIB signals in B cells. *Immunity* **12**(3), 347–358.
46. Huber, M., Helgason, C. D., Scheid, M. P., Duronio, V., Humphries, R. K., and Krystal, G. (1998) Targeted disruption of SHIP leads to Steel factor-induced degranulation of mast cells. *EMBO J.* **17**(24), 7311–7319.
47. Ono, M., Bolland, S., Tempst, P., and Ravetch, J. V. (1996) Role of the inositol phosphatase SHIP in negative regulation of the immune system by the receptor Fc(gamma)RIIB. *Nature* **383**(6597), 263–266.
48. Cox, D., Dale, B. M., Kashiwada, M., Helgason, C. D., and Greenberg, S. (2001) A regulatory role for Src homology 2 domain-containing inositol 5'-phosphatase (SHIP) in phagocytosis mediated by Fc gamma receptors and complement receptor 3 (alpha(M)beta(2); CD11b/CD18). *J. Exp. Med.* **193**(1), 61–71.
49. Geier, S. J., Algate, P. A., Carlberg, K., Flowers, D., Friedman, C., Trask, B., and Rohrschneider, L. R. (1997) The human SHIP gene is differentially expressed in cell lineages of the bone marrow and blood. *Blood* **89**(6), 1876–1885.
50. Damen, J. E., Liu, L., Ware, M. D., Ermolaeva, M., Majerus, P. W., and Krystal, G. (1998) Multiple forms of the SH2-containing inositol phosphatase, SHIP, are generated by C-terminal truncation. *Blood* **92**(4), 1199–1205.
51. Daley, G. Q., Van Etten, R. A., and Baltimore, D. (1990) Induction of chronic myelogenous leukemia in mice by the P210bcr/abl gene of the Philadelphia chromosome. *Science* **247**(4944), 824–830.
52. Elefanty, A. G., Hariharan, I. K., and Cory, S. (1990) bcr-abl, the hallmark of chronic myeloid leukaemia in man, induces multiple haemopoietic neoplasms in mice. *EMBO J.* **9**(4), 1069–1078.
53. Sattler, M., Verma, S., Byrne, C. H., Shrikhande, G., Winkler, T., Algate, P. A., Rohrschneider, L. R., and Griffin, J. D. (1999) BCR/ABL directly inhibits expression of SHIP, an SH2-containing polyinositol-5-phosphatase involved in the regulation of hematopoiesis. *Mol. Cell. Biol.* **19**(11), 7473–7480.
54. Wisniewski, D., Strife, A., Swendeman, S., Erdjument-Bromage, H., Geromanos, S., Kavanaugh, W. M., Tempst, P., and Clarkson, B. (1999) A novel SH2-containing phosphatidylinositol 3,4,5-trisphosphate

5-phosphatase (SHIP2) is constitutively tyrosine phosphorylated and associated with src homologous and collagen gene (SHC) in chronic myelogenous leukemia progenitor cells. *Blood* **93**(8) 2707–2720.

55. Nichols, K. E., Harkin, D. P., Levitz, S., Krainer, M., Kolquist, K. A., Genovese, C., Bernard, A., Ferguson, M., Zuo, L., Snyder, E., Buckler, A. J., Wise, C., Ashley, J., Lovett, M., Valentine, M. B., Look, A. T., Gerald, W., Housman, D. E., and Haber, D. A. (1998) Inactivating mutations in an SH2 domain-encoding gene in X-linked lymphoproliferative syndrome. *Proc. Natl. Acad. Sci. U.S.A.* **95**(23), 13765–13770.
56. Ishihara, H., Sasaoka, T., Hori, H., Wada, T., Hirai, H., Haruta, T., Langlois, W. J., and Kobayashi, M. (1999) Molecular cloning of rat SH2-containing inositol phosphatase 2 (SHIP2) and its role in the regulation of insulin signaling. *Biochem. Biophys. Res. Commun.* **260**(1), 265–272.
57. Clement, S., Krause, U., De Smedt, F., Tanti, J., Behrends, J., Pesesse, X., Sasaki, T., Penninger, J., Doherty, M., Malaisse, W., Dumont, J. E., Le Marchand-Brustel, Y., Erneux, C., Hue, L., and Schurmans, S. (2001) The lipid phosphatase SHIP2 controls insulin sensitivity. *Nature* **409**, 92–97.
58. Hejna, J. A., Saito, H., Merkers, L. S., Tittle, T. V., Jakobs, P. M., Whitney, M. A., Grompe, M., Friedberg, A. S., and Moses, R. E. (1995) Cloning and characterization of a human cDNA (INPPL1) sharing homology with inositol polyphosphate phosphatases. *Genomics* **29**(1), 285–287.
59. Pesesse, X., Deleu, S., De Smedt, F., Drayer, L., and Erneux, C. (1997) Identification of a second SH2-domain-containing protein closely related to the phosphatidylinositol polyphosphate 5-phosphatase SHIP. *Biochem. Biophys. Res. Commun.* **239**(3), 697–700.
60. Pesesse, X., Moreau, C., Drayer, A. L., Woscholski, R., Parker, P., and Erneux, C. (1998) The SH2 domain containing inositol 5-phosphatase SHIP2 displays phosphatidylinositol 3,4,5-trisphosphate and inositol 1,3,4,5-tetrakisphosphate 5-phosphatase activity. *FEBS Lett.* **437**(3), 301–303.
61. Taylor, V., Wong, M., Brandts, C., Reilly, L., Dean, N. M., Cowsert, L. M., Moodie, S., and Stokoe, D. (2000) 5′ Phospholipid phosphatase SHIP-2 causes protein kinase B inactivation and cell cycle arrest in glioblastoma cells. *Mol. Cell. Biol.* **20**(18), 6860–6871.
62. Habib, T., Hejna, J. A., Moses, R. E., and Decker, S. J. (1998) Growth factors and insulin stimulate tyrosine phosphorylation of the 51C/SHIP2 protein. *J. Biol. Chem.* **273**(29), 18605–18609.
63. Prasad, N., Topping, R. S., and Decker, S. J. (2001) SH2-containing inositol 5′-phosphatase SHIP2 associates with the p130(Cas) adapter protein and regulates cellular adhesion and spreading. *Mol. Cell. Biol.* **21**(4), 1416–1428.
64. Cheatham, B., Vlahos, C. J., Cheatham, L., Wang, L., Blenis, J., and Kahn, C. R. (1994) Phosphatidylinositol 3-kinase activation is required for insulin stimulation of pp70 S6 kinase, DNA synthesis, and glucose transporter translocation. *Mol. Cell. Biol.* **14**(7), 4902–4911.
65. Kotani, K., Carozzi, A. J., Sakaue, H., Hara, K., Robinson, L. J., Clark, S. F., Yonezawa, K., James, D. E., and Kasuga, M. (1995) Requirement for phosphoinositide 3-kinase in insulin-stimulated GLUT4 translocation in 3T3-L1 adipocytes. *Biochem. Biophys. Res. Commun.* **209**(1), 343–348.
66. Vollenweider, P., Clodi, M., Martin, S. S., Imamura, T., Kavanaugh, W. M., and Olefsky, J. M. (1999) An SH2 domain-containing 5′ inositolphosphatase inhibits insulin-induced GLUT4 translocation and growth factor-induced actin filament rearrangement. *Mol. Cell. Biol.* **19**(2), 1081–1091.
67. Wada, T., Sasaoka, T., Funaki, M., Hori, H., Murakami, S., Ishiki, M., Haruta, T., Asano, T., Ogawa, W., Ishihara, H., and Kobayashi, M. (2001) Overexpression of SH2-containing inositol phosphatase 2 results in negative regulation of insulin-induced metabolic actions in 3T3-L1 adipocytes via its 5′-phosphatase catalytic activity. *Mol. Cell. Biol.* **21**(5), 1633–1646.
68. Chamas, L. R., and Gahl, W. A. (1991) The oculocerebrorenal syndrome of Lowe. *Adv. Pediatr.* **38**, 75–107.
69. Attree, O., Olivos, I. M., Okabe, I., Bailey, L. C., Nelson, D. L., Lewis, R. A., McInnes, R. R., and Nussbaum, R. L. (1992) The Lowe's oculocerebrorenal syndrome gene encodes a protein highly homologous to inositol polyphosphate-5-phosphatase. *Nature* **358**(6383), 239–242.
70. Zhang, X., Jefferson, A. B., Auethavekiat, V., and Majerus, P. W. (1995) The protein deficient in Lowe syndrome is a phosphatidylinositol-4,5-bisphosphate 5-phosphatase. *Proc. Natl. Acad. Sci. U.S.A.* **92**(11), 4853–4856.
71. Zhang, X., Hartz, P. A., Philip, E., Racusen, L. C., and Majerus, P. W. (1998) Cell lines from kidney proximal tubules of a patient with Lowe syndrome lack OCRL inositol polyphosphate 5-phosphatase and accumulate phosphatidylinositol 4,5-bisphosphate. *J. Biol. Chem.* **273**(3), 1574–1582.
72. Janne, P. A., Suchy, S. F., Bernard, D., MacDonald, M., Crawley, J., Grinberg, A., Wynshaw-Boris, A., Westphal, H., and Nussbaum, R. L. (1998) Functional overlap between murine Inpp5b and Ocrl1 may explain why deficiency of the murine ortholog for OCRL1 does not cause Lowe syndrome in mice. *J. Clin. Invest.* **101**(10), 2042–2053.
73. Olivos-Glander, I. M., Janne, P. A., and Nussbaum, R. L. (1995) The oculocerebrorenal syndrome gene product is a 105-kD protein localized to the Golgi complex. *Am. J. Hum. Genet.* **57**(4), 817–823.
74. Ungewickell, A. J., and Majerus, P. W. (1999) Increased levels of plasma lysosomal enzymes in patients with Lowe syndrome. *Proc. Natl. Acad. Sci. U.S.A.* **96**(23), 13342–13344.
75. Kawano, T., Indo, Y., Nakazato, H. Shimadzu, M., and Matsuda, I. (1998) Oculocerebrorenal syndrome of Lowe: three mutations in the OCRL1 gene derived from three patients with different phenotypes. *Am. J. Med. Genet.* **77**(5), 348–355.
76. Lin, T., Orrison, B. M., Leahey, A. M., Suchy, S. F., Bernard, D. J., Lewis, R. A., and Nussbaum, R. L. (1997) Spectrum of mutations in the OCRL1 gene in the Lowe oculocerebrorenal syndrome. *Am. J. Hum. Genet.* **60**(6) 1384–1388.
77. Kubota, T., Sakurai, A., Arakawa, K., Shimazu, M., Wakui, K., Furihata, K., and Fukushima, Y. (1998) Identification of two novel mutations in the OCRL1 gene in Japanese families with Lowe syndrome. *Clin. Genet.* **54**(3), 199–202.
78. Satre, V., Monnier, N., Berthoin, F., Ayuso, C., Joannard, A., Jouk, P. S., Lopez-Pajares, I., Megabarne, A., Philippe, H. J., Plauchu, H., Torres, M. L., and Lunardi, J. (1999) Characterization of a germline mosaicism in families with Lowe syndrome, and identification of seven novel mutations in the OCRL1 gene. *Am. J. Hum. Genet.* **65**(1), 68–76.
79. Mochizuki, Y., and Takenawa, T. (1999) Novel inositol polyphosphate 5-phosphatase localizes at membrane ruffles. *J. Biol. Chem.* **274**(51), 36790–36795.
80. Ijuin, T., Mochizuki, Y., Fukami, K., Funaki, M., Asano, T., and Takenawa, T. (2000) Identification and characterization of a novel inositol polyphosphate 5-phosphatase. *J. Biol. Chem.* **275**(15), 10879–10875.
81. Asano, T., Mochizuki, Y., Matsumoto, K., Takenawa, T., and Endo, T. (1999) Pharbin, a novel inositol polyphosphate 5-phosphatase, induces dendritic appearances in fibroblasts. *Biochem. Biophys. Res. Commun.* **261**(1), 188–195.
82. Kong, A. M., Speed, C. J., O'Malley, C. J., Layton, M. J., Meehan, T., Loveland, K. L., Cheema, S., Ooms, L. M., and Mitchell, C. A. (2000) Cloning and characterization of a 72-kDa inositol-polyphosphate 5-phosphatase localized to the Golgi network. *J. Biol. Chem.* **275**(31), 24052–24064.
83. Wiradjaja, F., Ooms, L. M., Whisstock, J. C., McColl, B. K., Helfenbaum, L., Sambrook, J. F., Gething, M. J., and Mitchell, C. A. (2000) The yeast inositol polyphosphate 5-phosphatase Inp54p localizes to the endoplasmic reticulum via a C-terminal hydrophobic anchoring-tail. Regulation of secretion from the endoplasmic reticulum. *J. Biol. Chem.* **14**, 14.
84. Srinivasan, S., Seaman, M., Nemoto, Y., Daniell, L., Suchy, S. F., Emr, S., De Camilli, P., and Nussbaum, R. (1997) Disruption of three phosphatidylinositol-polyphosphate 5-phosphatase genes from *Saccharomyces cerevisiae* results in pleiotropic abnormalities of vacuole morphology, cell shape, and osmohomeostasis. *Eur. J. Cell. Biol.* **74**(4), 350–360.
85. Stolz, L. E., Kuo, W. J., Longehamps, J., Sekhon, M. K., and York, J. D. (1998) INP51, a yeast inositol polyphosphate 5-phosphatase required for

phosphatidylinositol 4,5-bisphosphate homeostasis and whose absence confers a cold-resistant phenotype. *J. Biol. Chem.* **273**(19), 11852–11861.

86. Guo, S., Stolz, L. E., Lemrow, S. M., and York, J. D. (1999) SAC1-like domains of yeast SAC1, INP52, and INP53 and of human synaptojanin encode polyphosphoinositide phosphatases. *J. Biol. Chem.* **274**(19), 12990–12995.
87. Ooms, L. M., McColl, B. K., Wiradjaja, F., Wijayaratnam, A. P., Gleeson, P., Gething, M. J., Sambrook, J., and Mitchell, C. A. (2000) The yeast inositol polyphosphate 5-phosphatases inp52p and inp53p translocate to actin patches following hyperosmotic stress: mechanism for regulating phosphatidylinositol 4,5-bisphosphate at plasma membrane invaginations. *Mol. Cell. Biol.* **20**(24), 9376–9390.
88. Stolz, L. E., Huynh, C. V., Thorner, J., and York, J. D. (1998) Identification and characterization of an essential family of inositol polyphosphate 5-phosphatases (INP51, INP52 and INP53 gene products) in the yeast Saccharomyces cerevisiae. *Genetics* **148**(4), 1715–1729.
89. Singer-Kruger, B., Nemoto, Y., Daniell, L., Ferro-Novick, S., and De Camilli, P. (1998) Synaptojanin family members are implicated in endocytic membrane traffic in yeast. *J. Cell. Sci.* **111**(Pt. 22)(47), 3347–3356.
90. Qualmann, B., Kessels, M. M., and Kelly, R. B. (2000) Molecular links between endocytosis and the actin cytoskeleton. *J. Cell. Biol.* **150**(5), F111–F116.
91. Hughes, W. E., Cooke, F. T., and Parker, P. J. (2000) Sac phosphatase domain proteins. *Biochem. J.* **350**(Pt. 2), 337–352.
92. Wendland, B., and Emr, S. D. (1998) Pan1p, yeast eps15, functions as a multivalent adaptor that coordinates protein-protein interactions essential for endocytosis. *J. Cell. Biol.* **141**(1), 71–84.
93. Tang, H. Y., and Cai, M. (1996) The EH-domain-containing protein Pan1 is required for normal organization of the actin cytoskeleton in *Saccharomyces cerevisiae*. *Mol. Cell. Biol.* **16**(9), 4897–4914.
94. Wendland, B., McCaffery, J. M., Xiao, Q., and Emr, S. D. (1996) A novel fluorescence-activated cell sorter-based screen for yeast endocytosis mutants identifies a yeast homologue of mammalian eps15. *J. Cell. Biol.* **135**(6 Pt. 1), 1485–1500.
95. Luo, W., and Chang, A. (1997) Novel genes involved in endosomal traffic in yeast revealed by suppression of a targeting-defective plasma membrane ATPase mutant. *J. Cell. Biol.* **138**(4), 731–746.
96. Bensen, E. S., Costaguta, G., and Payne, G. S. (2000) Synthetic genetic interactions with temperature-sensitive clathrin in *Saccharomyces cerevisiae*. Roles for synaptojanin-like Inp53p and dynamin-related Vps1p in clathrin-dependent protein sorting at the trans-Golgi network. *Genetics* **154**(1), 83–97.
97. Ito, T., Chiba, T., Ozawa, R., Yoshida, M., Harrori, M., and Sakaki, Y. (2001) A comprehensive two-hybrid analysis to explore the yeast protein interactome. *Proc. Natl. Acad. Sci. U.S.A.* **98**(8), 4569–4574.
98. Choi, J. H., Lou, W., and Vancura, A. (1998) A novel membrane-bound glutathione S-transferase functions in the stationary phase of the yeast *Saccharomyces cerevisiae*. *J. Biol. Chem.* **273**(45), 29915–29922.